Université de Bourgogne- Franche-Comté
UFR Sciences de la Vie
UFR Sciences de Santé

UMR 1231 INSERM-Université de Bourgogne-AgroSup Dijon
Centre de Recherche « Lipides, Nutrition, Cancer » (LNC)
Labex Lipstic (Lipoprotéines et santé : prévention et traitement des maladies inflammatoires non vasculaires et du cancer)

THESE

Pour obtenir le grade de Docteur de l'Université de Bourgogne-Franche Comté
Discipline: Biochimie, Biologie Cellulaire et Moléculaire (Sciences de la Vie)
Spécialités: Immunologie, Biochimie, Biologie Cellulaire et Moléculaire, pharmacologie moléculaire

---

"MITOPHAGY IN MYELOID CELLS: ROLE IN INFECTION WITH GRAM-

NEGATIVE BACTERIA"

Par

Danish PATOLI

Soutenue publiquement le 29 Juin 2017

Professeur David MASSON, PU-PH……………………………………..……………………**Président du Jury**
Université de Bourgogne, UMR1231, Dijon
Docteur Catherine DESRUMAUX, Chargée de Recherche INSERM …………………………......**Rapporteur**
INSERM U1198, Université de Montpellier, Montpellier
Docteur Jean BASTIN, Directeur de Recherche INSERM……………………………………......**Rapporteur**
UMRS 1124, Université Paris Descartes, Paris
Docteur Maryse GUERIN, Directrice de Recherche INSERM………………………………….**Examinatrice**
INSERM UMRS 1166 – ICAN, Faculté de Médecine Pitié-Salpêtrière, Paris
Docteur Charles THOMAS, Maître de Conférences………………………………….**Co-encadrant de thèse**
Université de Bourgogne, UMR1231, Dijon
Docteur Laurent LAGROST, Directeur de Recherche INSERM …………………...……………**Directeur de thèse**
INSERM, UMR1231, Dijon

ACKNOWLEDGEMENT

I would like to express my sincere gratitude to my Ph.D. advisor Dr. Laurent LAGROST for his continuous support during my Ph.D. study and related research, for his patience, motivation, and immense knowledge. His guidance helped me all the time of my research and writing of this thesis. I would also like to thank my Ph.D. co-supervisor Dr. Charles THOMAS for all his guidance, for always being there whenever I needed and giving me all theoretical and technical support. The work presented in this thesis would not be possible without the support of my two Ph.D. supervisors.

Besides my advisors, I would like to thank the Jury members Pr. David MASSON and Dr. Maryse GUERIN for their precious time to judge my thesis. I would like to particularly thank my thesis reviewers Dr. Catherine DESRUMAUX, and Dr. Jean BASTIN, for their insightful comments and encouragement during the review process.

I would also like to thank Dr. Thomas GAUTIER for his all support and guidance starting from my arrival in Dijon, and during all ups and downs during my thesis work. It was a great experience to work under your guidance.

I would like to specially thank Dr. Aziz HICHAMI for opening new area of research and for his enormous support throughout the period of my Ph.D. He always remained at my back to support me and guide me whenever needed.

I would also like to also thank Dr. Naim KHAN for his great moral support and help.

My sincere gratitude goes to Dr. Jacques GROBER for his support and efforts to get this Ph.D. position. I am profoundly thankful to him for trusting me and allowing to avail this wonderful opportunity to work in an excellent scientific environment under the supervision of Dr. Laurent LAGROST.

I would like to acknowledge:

- Franck MIGNOTTE, who is sadly no longer in between us. I would like to thank him for his initial contribution to this topic,

Summary

Sepsis and related organ dysfunctions remain a leading cause of mortality in intensive care units. Increasing evidences have shed light on an unexpected link between mitochondria and immune cell functions. Alterations in mitochondrial functions have been reported in peripheral blood cells in sepsis. We hypothesize here that mitophagy might impact on phagocyte functions in the context of bacterial infection. Mitophagy is a mitochondria-dedicated autophagy that governs the elimination of dysfunctional mitochondria. We demonstrated here *in vivo* and *in vitro* that macrophages exposed to Gram-negative bacteria or their cell wall component LPS display a marked inhibition of mitophagy that constitutes a protective mechanism against sepsis. LPS/IFNγ-driven macrophage activation results in early inhibition of PINK1-dependent mitophagy through a STAT1-Caspase 4/11 pathway. This inhibition of mitophagy contributes to explain the metabolic reprogramming observed in classically activated macrophages and leads to a rise in mitochondrial ROS (mROS) production. As signaling molecules, mROS lead to macrophages activation in a HIF-1α- and NF-κB-dependent manner. Furthermore, these molecules contribute to bacterial clearance in activated phagocytes. Interestingly, we demonstrated *in vitro* and *in vivo* that pharmacological modulation of mitophagy allows either mimicking or repressing the effects of LPS on macrophages polarization, cytokine release and bactericidal activity. To conclude, this work demonstrates that inhibition of mitophagy is a feature of LPS-dependent macrophage activation and a protective mechanism against Gram-negative bacteria. This study also highlights an unknown relationship between IFNγ-signaling, inflammatory caspases and mitophagy. Finally, our work point out the impact of pharmacological modulators of mitophagy on macrophage function and open new opportunities for the development of novel strategies to boost host defense.

Keywords: sepsis, mitophagy, macrophages, STAT1, caspase 4/11.

Contents

List of figures (Scientific Background)

List of figures (Experimental Results)

PART I

Chapter 1:

Chapter 2:

Chapter 3:

PART II

PART III

List of figures (Conclusion)

Curriculum Vitae

Qualification

2006 – 2010

Doctor of Pharmacy (Pharm-D), five years, with GPA 3.9 out of 4.0.

From: University of Sindh, Jamshoro, Pakistan.

Trainings and work experience:

- Worked as a Diabetes Educator for Eli Lilly Pakistan (Private) Limited (In Mercury Division, which is also part of Ali Gohar & Company Private Ltd) from 15th June 2011 to 8th oct 2012.

- Two months Internship/Training Program at Agha khan Maternity and child care centre Hyderabad from 20th March 2011 to 20th May 2011.

- Three hundred (300) hours Internship/Training Program at Liaquat University of Medical & Health Sciences (LUMHS) Hospital Hyderabad from 8th January 2011 to 18th February 2011 in the Medicine Unit II.

- Three hundred (300) hours Internship Training Program at NOVARTIS, Pakistan from 21st June 2010 to 31st July 2010 in the following sections:
  - **Pharmaceutical Production Section**
  - **Pharmaceutical Quality Assurance Section**
  - **Pharmaceutical Ware-House Section**

Trainings attended during PhD

1. 06th April 2017: "Transmission Electron Microscopy and Scanning Electron Microscopy" at Dimacell Platform (Centre of microscopy INRA/uB), organized by doctoral school, Université de Bourgogne- Franche-Comté, Dijon, France.

2. 16th February 2017: "Confocal Microscopy" at Dimacell Platform (Centre of microscopy INRA/uB), organized by doctoral school, Université de Bourgogne- Franche-Comté, Dijon, France.

3. 03rd February 2015-2016: 6 hours of training on "redaction of scientific article", organized by doctoral school, Université de Bourgogne- Franche-Comté, Dijon, France.

4. 29th -30th January 2015: 14 hours of training on "monitor and manage a thesis project", organized by doctoral school, Université de Bourgogne- Franche-Comté, Dijon, France.

5. 25th August to 5th September 2014: 50 hours of French culture and language course (2B level) at "Centre International d'Etudes Françaises (CIEF)", Université de Bourgogne- Franche-Comté, Dijon, France

6. 28th July to 22nd August 2014: 100 hours of French culture and language course (A2 level) at "Centre International d'Etudes Françaises (CIEF)", Université de Bourgogne- Franche-Comté, Dijon, France

7. 6th February to 11th April 2014: 15 hours of French language course at "Centre International d'Etudes Françaises (CIEF)", Université de Bourgogne- Franche-Comté, Dijon, France.

8. 7th-11th July 2014: 50 hours of training course on "Functional Cytometry: understanding and applying cytomic assays" at university of Valencia, Valencia, Spain.

Publications (peer-reviewed):

1. **Danish Patoli**, Franck Mignotte, Thomas Gautier, Valérie Deckert, Adélie Dumont, Aurélie Rieu, Charlène Magnani, Naig Le Guerin, Stéphane Mandard, Jean Bastin, Fatima Djouadi, Michel Narce, Mickael Rialland, David Masson, Laurent Lagrost, Charles Thomas. "STAT1-dependent inhibition of mitophagy in macrophages protects against sepsis". **In preparation**.

2. Wahib Sali, **Danish Patoli**, Jean Paul Pais de Barros, Jerome Labbé, Valerie Deckert, Vincent Duhéron, Lil Proukhnitzky, Naig Le Guern, Denis Blache, Charles Thomas, Denis Chaumont, Eric Lesniewska Benoit Gasquet, Laurent Lagrost and Thomas Gautier. "Polysaccharide chain length of lipopolysaccharides from *Salmonella minnesota* is a determinant of aggregate stability, plasma residence time and proinflammatory propensity". **In preparation**.

3. Charles Thomas, Charlène Magnani, Minako Ishibashi, Thibaut Bourgeois, Antoine Jalil, Victoria Bergas, Louise Ménégaut, **Danish Patoli**, Naig Le Guern, Jérôme Labbé, Thomas Gautier, Jean Paul Pais de Barros, Laurent Lagrost and David Masson. "LPCAT3 deficiency in macrophages alters cholesterol and plasmalogen homeostasis and promotes atherosclerosis". **In preparation**.

4. Thomas Gautier, Valérie Deckert, Virginie Aires, Naig Le Guern, Lil Proukhnitzky, **Danish Patoli**, Stéphanie Lemaire, Guillaume Maquart, Amandine Bataille, Charlène Magnani, David Masson, Geneviève Jolivet, Louis-Marie Houdebine, Laurent Lagrost. "Human apoC1: a natural CETP inhibitor to reduce atherosclerosis in transgenic hypercholesterolemic rabbits". **In preparation**.

5. Fatima Zahra Ghanemi, Meriem Belarbi, Aurélie Fluckiger, Abdelhafid Nani, Charlotte De Rosny, Ikram Aboura, Amira Sayed Khan, Babar Murtaza, Adélie Dumont, Chahid Benammar, Boucif Farid Lahfa, **Danish Patoli**, Dominique Delmas, Cédric Rébé, Naim Akhtar Khan, François Ghringhelli, Mickael Rialland, Lionel Apétoh, Aziz Hichami. "Carob leaf polyphenols trigger intrinsic apoptotic pathway and induce cell cycle arrest in colon cancer cells". *Journal of Functional Foods*, *33*, 112-121. (2017)

6. Wafa Zeriouh , Abdelhafid Nani , Meriem Belarbi, Adélie Dumont, Charlotte de Rosny, Ikram Aboura, Fatima Zahra Ghanemi, Babar Murtaza, **Danish Patoli**, Charles Thomas, Lionel Apetoh, Cédric Rébé, Dominique Delmas,Naim Akhtar Khan, François Ghiringhelli, Mickael Rialland, Aziz Hichami. "Phenolic extract from oleaster (Olea europaea var. Sylvestris) leaves reduces colon cancer growth and induces caspase-dependent apoptosis in colon cancer cells via the mitochondrial apoptotic pathway". *PloS one*, *12***(2), e0170823. (2017)**

Presentations:

1. 18th-19th June 2015: Oral presentation in 21st edition of "Forum des Jeunes Chercheurs", Université de Bourgogne- Franche-Comté, Dijon, France

2. 21st-22nd September 2015: Oral presentation in "Mitochondria at the Cross road (MitoCross) symposium", University of Strasbourg, Strasbourg, France.

3. 5th -7th October 2015: Oral presentation in " The Francophone Autophagy Club (CFATG) 5th Annual scientific days", Lille, France.

List of Abbreviations

2,4-DNP: 2,4-dinitrophenol

2-DG :   2-deoxyglucose

3-MA :   3-methyladenine

AD :   alzheimer's disease

ADP :   adenosine diphosphate

AMP :   adenosine monophosphate

AMPK :   AMP activated protein kinase

ANT :   adenine nucleotide translocase

AP-1 :   activator protein-1

APC :   antigen presenting cell

ASC :   apoptosis-associated speck like protein containing CARD

ATP :   adenosine triphosphate

BMDMs :   Bone marrow derived macrophages

CASP :   Colon ascendes stent peritonitis

CCCP :   carbonyl cyanide m-chlorophenylhydrazone

CD :   cluster of differentiation

CK2 :   caseine kinase-2

CLP :   cecal ligation and puncture

CLR :   c-type lectin receptor

DAMPs: danger associated molecular Patterns

dMfn :   mitochondrial fusion promoting factor

Drp1 :   dynamin-related protein 1

ECSIT :   evolutionarily conserved signaling intermediate in Toll pathway

ERRs :   estrogen-related receptors

ETC :   electron transport chain

Fc :   fragment crystallizable

FUNDC1 :   FUN14 domain containing 1

GAS :   gamma associated sequence

GBP2 :   guanine binding protein-2

HIF1α :   hypoxia-inducible factor 1-alpha

ICE :   IL-1β converting enzyme

IFN: interferon

IFNGR1:   interferon gamma receptor 1

IFNGR2:   interferon gamma receptor 2

IFNγ: interferon gamma

IKB :   inhibitor of K light chain gene enhancer in B cells

IL-1β :   interleukin 1 beta

IL-4 :   interleukin-4

IMS :   intermembrane space

iNOS :   inducible nitric oxide synthase

iP :   inorganic phosphate

IRAK1 :   interleukin-1 receptor associated kinase 1

IRAK4 :   interleukin-1 receptor associated kinase 4

ITAM :   immunoreceptor tyrosine-based activation motif

JAK1 :   janus kinase 1

KDO :   2-keto-3-deoxyoctonic acid

LBP : lipopolysaccharide binding protein

LC3B : light chain 3

LIR : light chain 3 interacting region

LPS : lipopolysaccharides

LTA : lipoteichoic acid

MAM : Mitochondrial associated membrane

MAPK : mitogen activated protein Kinase

MAVS : mitochondria antiviral signaling

mCD14 : membrane CD14

MCP: monocyte chemoattractant Protein

MD2: myeloid Differentiation protein 2

Mdivi1 : mitochondrial-division inhibitor-1

MEFs : mouse embryonic fibroblasts

Mfn1 : mitofusin 1

Mfn2 : mitofusin 2

MPP : mitochondrial processing peptidase

MPTP : mitochondrial permeability Transition Pore

mROS : mitochondrial Reactive Oxygen Species

mTOR : mammalian target of rapamycin

MTS : mitochondrial targeting sequence

MyD88: myeloid differentiation factor 88

NAC : N-acetyl cysteine

NADPH : nicotinamide adenine dinucleotide phosphate-oxidase

NF-kB: nuclear factor-kappa B

NLR : nucleotide binding oligomerization domain like receptor

NLRP3: nucleotide-binding oligomerization gomain, leucine rich repeat and pyrin domain containing 3

NO : nitric oxide

NRF: nuclear respiratory factor

OMVs : outer membrane vesicles

OPA1 : optic atrophy type 1

OPTN : optineurin

PAMPs: pathogen associated molecular patterns

PARL : persenilins-associated rhomboid-like protein

PD : parkinson's disease

PFK2 : 6-phospho-fructo-2-kinase

PGC1-α : peroxisome proliferator-activated receptor gamma co-activator 1-alpha

PGC-1β : peroxisome proliferator-activated receptor (PPAR)γ-coactivator-1β

PI3K : phosphoinositide-3-kinase

Pink1: PTEN induced putative kinase

PKA : protein kinase A

PMN : polymophonuclear leukocytes

PRRs: pattern recognition receptors

RCCs :   respiratory chain complexes

RLR :   RIG-1(retinoic acid inducible gene 1) like receptor

RNS :   reactive nitrogen species

ROS :   reactive oxygen species

sCD14 :   soluble form of CD 14

SH2 :   src homology 2

SOCS1 :   suppressor of sytokine signaling 1

STAT1 :   signal transducer and activator of transcription 1

STAT6 :   signal transducer and activator of transcription 6

TBB :   4,5,6,7-tetrabromobenzotriazole

TFAM :   mitochondrial transcription factor A

TFBs :   transcription factor B proteins

TIR :   toll/IL-1R like receptor

TLRs :   toll like receptors

TNFα: tumor necrosis factor-α

TRAF6 :   tumor necrosis factor receptor associated factor 6

TYK2 :   tyrosine kinase 2

ULK1 :   unc-51-like autophagy activating kinase 1

VDAC :   voltage dependent anion channels

Introduction

All pathogens encounter several barriers at the time of invasion into the host. Pathogens that cross the physical barriers like epithelium, mucous membrane and skin are dealt by body immune system. The presence of any pathogen in the host body or any tissue injury initiates the release of chemical mediators which attract and recruit different immune cells in order to remove the pathogens and perform tissue repair to maintain tissue integrity (Medzhitov, 2008).

These immune cells are equipped with different germline encoded receptors known as Pattern Recognition Receptors (PRRs) (Akira et al., 2006; Mogensen, 2009). PRRs detect or sense the specific molecular patterns that are harmful to the body. These molecular patterns can originate from exogenous sources (pathogens) as well as from endogenous sources (tissue damages, signals from apoptotic and dying cells). These exogenous and endogenous molecular patterns are named Pathogen Associated Molecular Patterns (PAMPs) and Danger Associated Molecular Patterns (DAMPs), respectively (Akira et al., 2006; Mogensen, 2009). PAMPs are structural components of pathogens. They include Lipopolysaccharides (LPS) (from Gram-negative bacteria), Lipoteichoic acid (LTA) (from Gram-positive bacteria), single or double stranded RNA (from virus) and zymosan (from Fungi). PAMPs are detected by PRRs and initiate specific immune (Akira et al., 2006; Hellman et al., 2000; Mogensen, 2009; Rietschel et al., 1994). Infections with Gram-negative bacteria remain a major health concern and are one of the major causes of death in intensive care units. LPS is a ligand of the Toll-like receptor 4 (TLR4) (Chow et al., 1999; Poltorak et al., 1998a). Binding of LPS to this membrane bound receptor contributes to the activation of macrophages, also referred as classical activation or M1 polarization (Biswas et al., 2012; Biswas and Mantovani, 2010; Gordon and Taylor, 2005; Mantovani et al., 2013; Martinez and Gordon, 2014).

Macrophages are key players in innate immunity. They are primary effectors of body defense mechanism along with neutrophils. Macrophages can reside in the tissues or arise from circulatory monocytes and can then differentiate into different subsets of macrophages (Geissmann et al., 2010; Murray and Wynn, 2011). Macrophages are endowed with the ability to detect environmental cues and cytokine environment. According to these surrounding signals,

they can acquire a dedicated phenotype in a process known as macrophage polarization (Biswas et al., 2012; Mantovani et al., 2013; Murray and Wynn, 2011). The two main phenotypes of macrophages are M1 macrophages (classically activated macrophages) and M2 macrophages (alternatively activated macrophages). M1 macrophages are known for their pro-inflammatory, bactericidal, and tumoricidal activity; whereas M2 macrophages are characterized by an anti-inflammatory, anti-parasitic and pro-tumor activity (Biswas et al., 2012; Biswas and Mantovani, 2010; Mantovani et al., 2013; Murray and Wynn, 2011).

LPS and interferon-gamma (IFN-γ), a Th1 cytokine, lead to the M1 phenotype, whereas IL-4, a Th2 cytokine, induces the M2 phenotype. The M1 phenotype is associated with metabolic reprogramming towards glycolysis whereas the metabolism of M2 macrophages mainly relies on oxidative phosphorylation (OXPHOS) (Biswas and Mantovani, 2012; Mills et al., 2017). The role of mitochondria in macrophage polarization is becoming clearer with time with special reference to the metabolic reprogramming in different phenotypes of macrophages (Biswas and Mantovani, 2012; Mills et al., 2017).

Mitochondria, the "power house of the cells", play key roles in energy production (Speakman, 2003). They are also involved in calcium signaling, cell cycle, and apoptosis (Danial and Korsmeyer, 2004; Jacobson and Duchen, 2004). Mitochondria are a major source of adenosine triphosphate (ATP) through oxidative phosphorylation (OXPHOS) from the respiratory chain complexes (RCCs) located in the inner membrane of mitochondria (Scheffler, 2011). Along with the production of ATP, mitochondria also produce ample amounts of reactive oxygen species (mROS) (Di Meo et al., 2016). In activated macrophages (M1), the enhanced mROS production is associated with a metabolic switch toward glycolysis (Mills et al., 2016). It has been proposed that this metabolic switch would allow taking fatty acids away from oxidative phosphorylation and redirect them to fulfill the structural requirements of the cells such as membrane synthesis which is crucial for phagocytosis (Mills et al., 2016). The role of increased mROS production was addressed only recently. Two recent studies highlighted that mROS, beyond their signaling roles, actively participates in the bactericidal activity of M1 macrophages (Garaude et al., 2016; West et al., 2011a). The origin of this rise in mROS production in M1 macrophages is still unclear. Nevertheless, several mechanisms have been proposed. First, LPS-activated macrophages exhibit

higher expression of inducible nitric oxide synthase (iNOS) and increased nitric oxide (NO) production (Biswas and Mantovani, 2012; Corraliza et al., 1995; Munder et al., 1998). This participates in bactericidal activity of the macrophages. Additionally, this elevated NO production was shown to inhibit mitochondrial respiration by nitrosylation iron-sulfur-containing proteins, including complex I, complex II and complex IV of the ETC, thereby inhibiting electron transport and subsequent ATP production. This event could contribute to increasing mROS production in M1 macrophages. (Beltran et al., 2000; Corraliza et al., 1995; Mills et al., 2017; Munder et al., 1998). Indeed, it has long been appreciated that inhibition of respiratory chain complexes (RCC), especially this of complex I and III is a critical source of mROS in the cells. The concept that mROS may participate to bactericidal activity came from the work of West *et al.* The authors proposed that TLR signaling (TLR1-2-4) increases mROS production through TRAF6-dependent destabilization of the complex I (West et al., 2011a). This mechanism was recently debated in several articles (Mills et al., 2016; Mills et al., 2017; Tannahill et al., 2013; Van den Bossche et al., 2017). More recently, the contribution of complex II in pathogen clearance and mROS-mediated release of the pro-inflammatory IL-1β was recently highlighted. The detection of Gram-negative bacteria by macrophages modulates ETC-super complexes assembly and increases complex II (succinate dehydrogenase, SDH) activity to trigger antibacterial defense (Garaude et al., 2016). Conversely, Mills *et al.* showed that LPS-mediated drop in mitochondrial membrane potential coupled to oxidation of succinate by SDH significantly augments mROS production. This results in the stabilization and activation of Hypoxia-inducible factor 1 alpha (HIF1α) and the subsequent release of IL-1β (Mills et al., 2016; Tannahill et al., 2013). HIF1α is not the sole inflammatory pathway activated by mROS. nuclear factor-kappa B (NF-κB) and Nucleotide-Binding Oligomerization Domain, Leucine Rich Repeat and Pyrin Domain Containing 3 (NLRP3) were also shown to be mROS targets (Asehnoune et al., 2004; Tschopp and Schroder, 2010; Zhou et al., 2011). A *princeps* study from the Tschopp's group demonstrated that 3-MA-driven inhibition of mitophagy leads to the enhancement of mROS production and activation of the NLRP3 inflammasome (Tschopp and Schroder, 2010).

Mitochondria are now recognized as central hubs for immunity (Arnoult et al., 2011; Mills et al., 2017; Weinberg et al., 2015), nevertheless the role of mitochondrial dynamics and mitophagy in innate immunity remains poorly understood.

M1 macrophages play a major role in anti-bacterial defense. In the context of bacterial infection, prolonged or uncontrolled activation of M1 macrophages can contribute to release of high amounts of inflammatory cytokines also referred as "cytokine storm". Ultimately, it leads to sepsis and septic shock. Sepsis is often associated with multiple organ failure (Carré et al., 2010; Japiassu et al., 2011). Mitochondrial dysfunctions have been linked to this organ failure and have been negatively correlated to survival during sepsis (Carré et al., 2010; Japiassu et al., 2011). Altered mitochondrial functions and dynamics were observed in peripheral blood monocytes of septic patients (Adrie et al., 2001; Garrabou et al., 2012; Japiassu et al., 2011; Santos et al., 2016). This may lead to a modulation of mROS production and of related signaling pathways during sepsis. Recently, three mouse lines deficient for the genes encoding proteins (PINK, Parkin and DJ-1) that have a major impact on mitophagy were studied in the context of sepsis. PTEN-induced putative kinase 1- (PINK1, a serine/threonine-protein kinase) and Parkin- (an E3 ubiquitin ligase) deficient mice were resistant to septic shock whereas DJ-1-knock-out mice appeared to be more sensitive (Amatullah et al., 2016; Kang et al., 2016; Mannam et al., 2014). Recently, two studies established a link between mitophagy and immunity. Zhong *et al*. showed that NF-κB restricts mROS-induced inflammasome activation by promoting mitochondrial clearance through mitophagy (Zhong et al., 2016). In macrophages, inhibition of mitophagy subsequent to the invalidation of PINK1 contributes to mitochondrial antigen presentation by major histocompatibility complex class I (MHCI) (Matheoud et al., 2016).

Objectives

These recent evidence suggests that the modulation of mitophagy may impact on macrophage function and immunity. Since the inhibition of mitophagy is a major source of mROS within the cells and because changes are observed in mitochondrial function and mitochondrial dynamics in monocytes and macrophages upon LPS-mediated activation as well as during sepsis, we hypothesized that LPS and Gram-negative bacteria may alter mitochondrial function and mROS

production in macrophages through the inhibition of mitophagy. The objectives of this work have been to investigate mitophagy *in vitro* and *in vivo* in myeloid cells exposed to LPS or in a context of sepsis, to decipher the role of this modulation of mitophagy in activated macrophages and to unravel the underlying molecular mechanisms.

Organization of the Thesis

This thesis is organized into three parts. The first part gives the general scientific background. The second part presents the experimental results. The third part is devoted to discussion about the findings and the results obtained, with reference to previously published data and results. The fourth part is dealing with conclusion and future perspectives.

In the first part, a scientific background is divided into four main chapters. The first chapter introduces the inflammatory conditions with special reference to sepsis and septic shock. The second chapter gives a general overview of the immune system, with specific emphasis on macrophages, their functions and phenotypes (including a special focus on classically activated macrophages). In the third and fourth chapters, background knowledge about mitochondria, mitochondrial dynamics, and the role of mitochondria in immunity is provided. It includes mitochondrial quality control process, with detailed information about mitophagy.

Scientific Background

Chapter 1: Inflammation and sepsis

Inflammation

Inflammation is a response to tissue injury or infection. Inflammation was initially characterized by swelling, redness, burns and pain. The signs are initiated by accumulation of fluid exudate containing blood leukocytes and plasma to the site of infection or injury. The goal is to clear off harmful insults and to restore homeostasis (Medzhitov, 2008). Short term inflammation is known as acute inflammation. When inflammation persists for longer periods of time, it is known as chronic inflammation. Based on the type of stimuli (infectious or not), the inflammation can be divided into two main types known as sterile or septic inflammation. **Sterile inflammation** is initiated in the absence of infectious agents (Chen and Nuñez, 2010b; Erridge, 2010; Rubartelli et al., 2013). It can be induced in response to tissue injuries, burns, nutrient or oxidative stress or due to detection of DAMPs (Erridge, 2010). The recruitment and activation of macrophages in atherosclerosis (Chen and Nuñez, 2010a; Ross, 1999), the inflammatory response to the tissue injury caused by increased ROS production in context of ischemia-reperfusion (Chen and Nuñez, 2010a) or the activation of microglial cells associated β-amyloid plaque in Alzheimer's disease (Chen and Nuñez, 2010a) are a few examples of sterile inflammation.

The inflammation initiated in response to infectious agents (bacteria, virus, fungi etc..) or endotoxins (LPS) is referred as **septic inflammation** (Chen and Nuñez, 2010b; Erridge, 2010; Rubartelli et al., 2013).

Invasion of pathogens into tissue is detected by tissue resident macrophages and mast cells via the PRRs (Medzhitov, 2008). These immune cells later release chemokines and cytokines leading to the recruitment and activation of other innate immune cells such as neutrophils and monocytes (Medzhitov, 2008). In the context of bacterial infection, blood neutrophils and monocytes infiltrate the site of infection and eradicate pathogens through phagocytosis. They release inflammatory cytokines and reactive species (Reactive Oxygen Species (ROS) & Reactive Nitrogen Species (RNS) which originates from NADPH oxidase and iNOS, respectively) to fight against the pathogenic insult. This initial response is followed by activation of adaptive immune cells.

Pathogens recognition by immune cells

Immune cells are equipped with specialized cell surface and intracellular proteins that sense and detect specific molecular structure from endogenous and exogenous origin also referred as Pattern Recognition Receptors (PRR). PRRs are germ-line encoded receptors and represent as an essential component of the immune system (Akira et al., 2006).

Exogenous molecular structures can be of microbial origin (bacteria, virus, fungi…), referred as Pathogen-Associated Molecular Patterns (PAMPs). Conversely, the endogenous signals sensed by PRR are referred as Damage-Associated Molecular Patterns (DAMPs).

DAMPs are host-derived molecular structures released subsequently to tissue damages. DAMP-mediated activation of PRRs induces an immune response which can lead to the worsening of the pathology. Activation of NLRP3 is a good example of the inflammatory response induced by DAMPs (NLRP3 inflammasome assembly and function is discussed below). Activation of the NALP3/NLRP3 inflammasome by β-Amyloid protein contributes to the inflammation and worsening of Alzheimer's disease (AD) (Halle et al., 2008). Similarly, uric acid, the causative agent of gout, also contributes to the NALP3 inflammasome-dependent inflammatory response (Martinon et al., 2006).

PAMPs are usually components of microbial structure and are often essential for their survival and functions (Van Amersfoort et al., 2003). These specific molecular structures are recognized by a number of PRRs. Detection of these antigenic structures acts as a stimulant for the immune cells leading to their activation (Van Amersfoort et al., 2003). **Four main pattern recognition receptors are known and have been widely studied**: 1) the C-Type Lectin receptors (CLR), 2) the nucleotide binding oligomerization domain receptors (NLR), 3) the RIG-1 (retinoic acid inducible gene-1)-like receptor (RLR), and 4) the toll-like receptors (TLR). Figure 1 depicts the main PAMPs and their related PRRs.
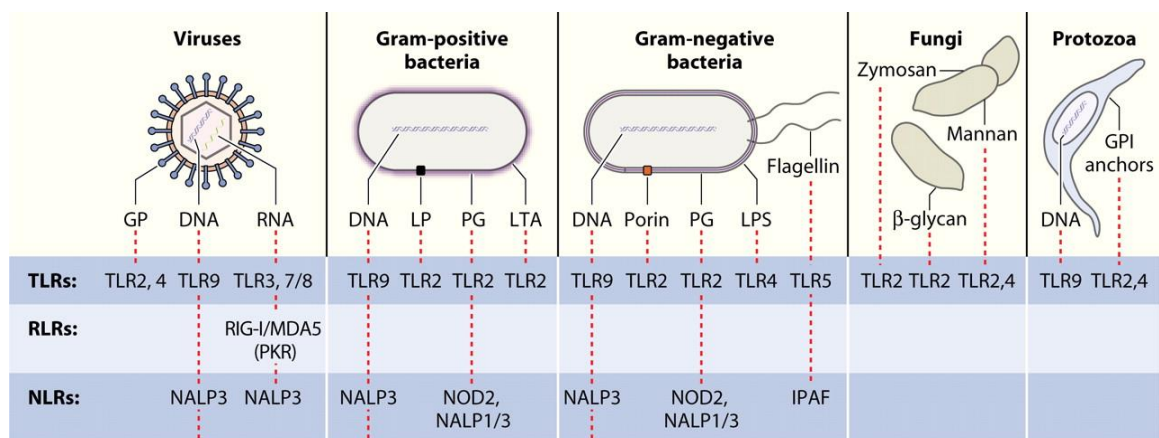
Figure 1: PAMPs from different pathogens and their recognition by PRRs (Mogensen, 2009)

(1) C-Type lectin receptors (CTL) are a large family of metazoan proteins, containing C-Type lectin-like domains (CTLDs) (Zelensky and Gready, 2005). They were named on the basis of their function. The Ca^{2+}-dependent (C-type) carbohydrate-binding (lectin) proteins are also abbreviated as C-type lectin (Zelensky and Gready, 2005). Lectin proteins recognize and bind to specific carbohydrate structures (Sharon and Lis, 1972). The inflammatory response can be produced through the direct interaction with CLRs such as dectin-1 (Rogers et al., 2005; Sato et al., 2006). Dectin-1, type-1 transmembrane glycoprotein, is a pathogen recognition receptor (Brown and Gordon, 2005). Dectin-1 is known to recognize β-Glucans (Brown and Gordon, 2005). β-glucans are polysaccharides primarily found in fungi but also in some yeasts, plants and bacteria (Brown and Gordon, 2005). Dectin-1 is predominantly expressed on monocytes/macrophages, neutrophils and dendritic cells. (Reid et al., 2004).

(2) RLRs are RNA helicase enzymes and constitute another family of intracellular PRRs (Gitlin et al., 2006; Venkataraman et al., 2007; Yoneyama et al., 2004). The RLR family includes three members: RIG-1, MDA-5 and LGP2 (Gitlin et al., 2006; Venkataraman et al., 2007; Yoneyama et al., 2004). Different members of RLRs recognize viral RNA based on their size and length (Kato et al., 2008; Kato et al., 2006; Loo et al., 2008). Detection of single or double stranded RNA by RLRs induce an antiviral response (Kato et al., 2008; Kato et al., 2006; Loo et al., 2008; Mogensen, 2009). The structures and domains are shown in figure 2.
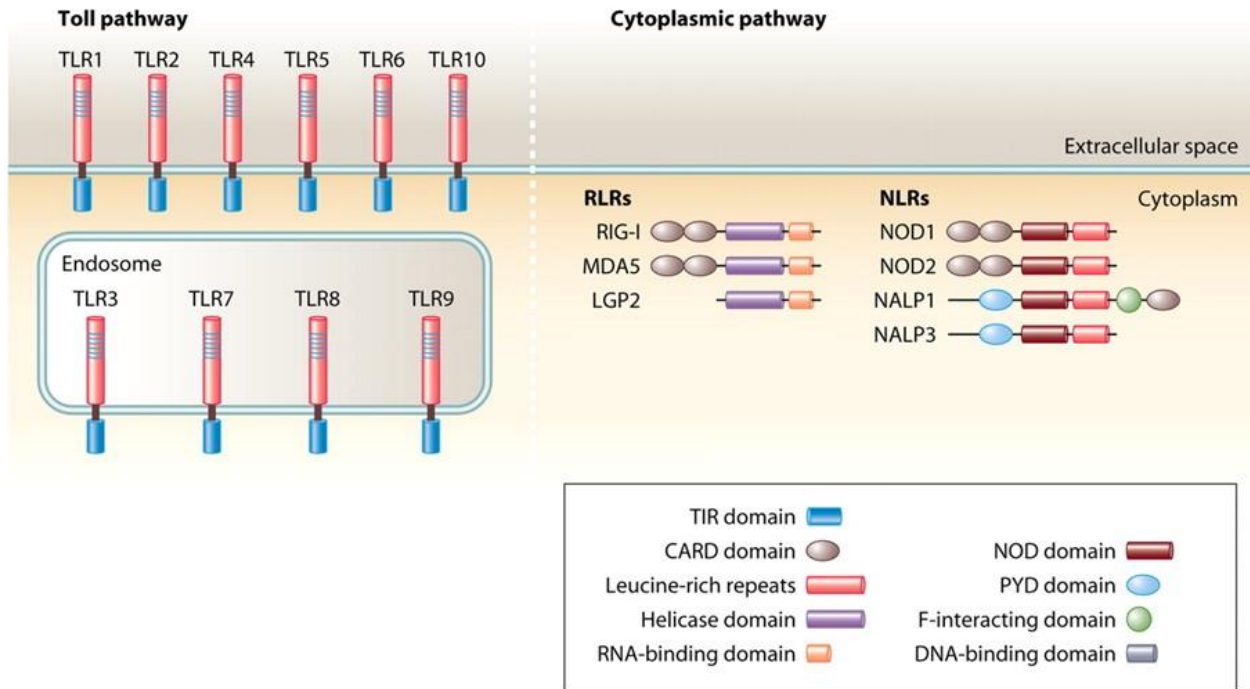
Figure 2: Localization of different PRRs (Mogensen, 2009)

(3) The NLR receptor family comprises 22 members in Humans and 34 members in the mouse (Ting et al., 2008). All members of NLR family contain a common nucleotide oligomerization binding (NACHT) domain, a C-terminal leucine rich repeat (LRR) domain, and an N-terminal effector domain (Martinon et al., 2009). The NLR subfamilies vary in N-terminal effector domain (Martinon et al., 2009). Based on the type of effector domain attached to the N-terminal, they are named as NLRP and NLRC containing pyrin domain and caspase activation and recruitment domain (CARD), respectively (Martinon et al., 2009). Their localization and structure are described in figure 2.

In NLRs, NACHT domain is considered as a central domain. The activation of NLRs depends on the oligomerization of NACHT domain forming a complex molecule (Faustin et al., 2007; Martinon and Tschopp, 2004). Like other PRRs, different members of the NLR family respond to various pathogen signals that initiate an immune response. Detection of ligands by NLRs leads to the activation of either NFκB or a multiprotein complex known as inflammasome (Kumar et al., 2009). Amongst different NLRs, the better characterized are NOD1, NOD2 and NLRP3.

Both NOD1 and NOD2 members of the NLRs family contain a CARD domain. NOD1 can sense γ-D-glutamyl-meso-diaminopimelic acid (iE-DAP), whereas NOD2 detects Muramyl dipeptide (MDP) (Chamaillard et al., 2003; Girardin et al., 2003). iE-DAP and MDP are components of bacterial peptidoglycan (Chamaillard et al., 2003; Girardin et al., 2003). Upon activation both NOD1 and NOD2 activate NFκB and initiate an immune response (Akira et al., 2006).

NLRs are cytoplasmic receptors. They do not only detect and respond to the pathogenic signals but also work in coordination with other PRRs (like TLRs) and promote the inflammatory response through detection of endogenous signals released in response to other PRRs stimulation. Coordinated activation of the NLRP3 (Nucleotide-Binding Oligomerization Domain, Leucine Rich Repeat and Pyrin Domain Containing 3) inflammasome is a good illustration of the mechanism of NLR activation. NLRP3 inflammasome is a multimeric protein complex which acts as a platform for the maturation and release of inflammatory cytokines (IL-1β and IL-18), as well as regulation of pyroptosis, an inflammatory cell death (He et al., 2016; Schroder and Tschopp, 2010; Tschopp and Schroder, 2010). Both IL-1β and IL-18 cytokines play important roles in the regulation of the inflammatory response. More specifically, IL-1β is involved in the recruitment of innate immune cells to the site of infection. It is also involved in activation of adaptive immune cells. In contrast, IL-18 plays a role in the regulation of the production of IFNγ, and it potentiates the cytolytic activity of natural killer cells and T cells (He et al., 2016). This multimeric protein complex is made of NLRP3, apoptosis-associated speck-like protein containing a CARD domain (ASC), and caspase 1 (He et al., 2016). In macrophages, NLRP3 inflammasome activation requires two signals. The former/priming signal from microbial or a cytokine stimulus leads to NFκB-mediated induction of pro-IL-1β, pro-IL-18 as well as NLRP3. The following/second step is activation per se (He et al., 2016; Mogensen, 2009). NLRP3 is known to be activated by a number of stimuli including ATP, uric acid crystal, ROS, viral RNA and bacterial DNA (He et al., 2016; Mogensen, 2009). It was also reported that NLRP3 inflammasome gets activated in response to mROS and mitochondrial DNA (mtDNA) (Saitoh et al., 2008; Zhou et al., 2011). Activation of NLRP3 inflammasome leads to cleavage of caspase-1 and release of IL-1β and IL-18. Such activation pathway is also known as canonical inflammasome activation which is described in figure 3. Recent studies have shown the

existence of a non-canonical activation pathway that may require caspase 4/11 which is described below in the caspase 4/11 section (Kayagaki et al., 2011; Kayagaki et al., 2013).
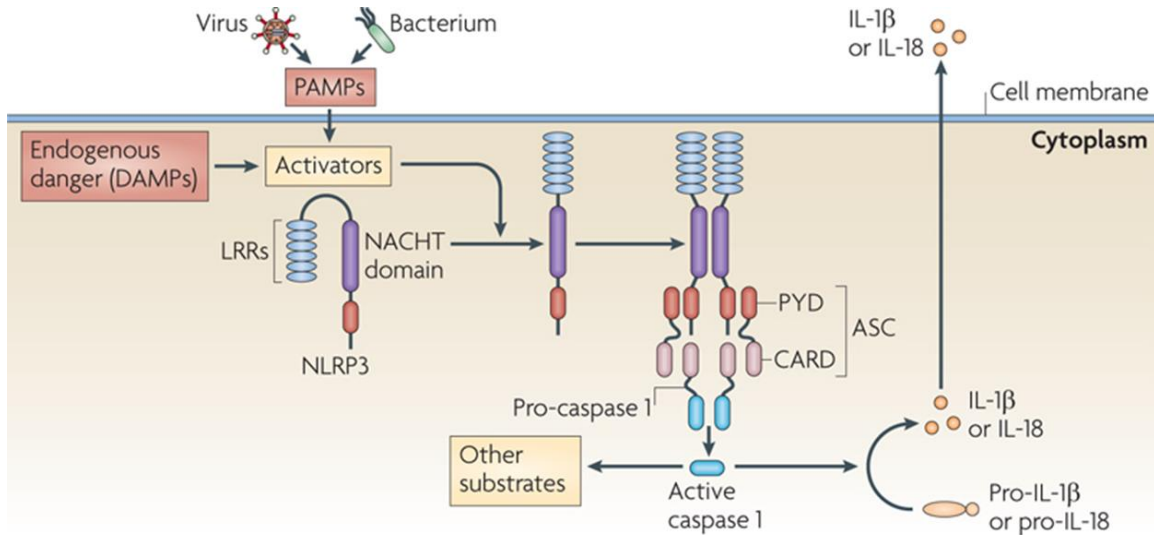
Figure 3: Mechanism of canonical inflammasome activation (Tschopp and Schroder, 2010)

 (4) TLRs are membrane-bound glycoproteins, expressed on different cells including immune cells (like antigen presenting cells (APCs)) as well as on epithelial cells and fibroblasts. Expression levels of TLRs may vary from one cell type to another, and can be affected and modulated by different stimuli and environmental factors (Akira et al., 2006). In mammals, the family of TLRs can be grouped on the basis of their subcellular localization (Figure 2). TLR1, TLR2, TLR4, TLR5, TLR6, and TLR10 are found on the surface of the cell, whereas TLR3, TLR7, TLR8 and TLR9 have an intracellular localization (Figure 2) (Akira et al., 2006; Mogensen, 2009). Detection of ligands to the respective TLRs leads to the hetero- or homo-dimerization of TLRs (Akira et al., 2006). Activation of the downstream signaling cascade finally leads to the commitment of different transcription factors (NFκB, AP-1, IRF3, IRF5, IRF7) that modulate gene expression of key inflammatory genes (Akira et al., 2006). The different TLRs along with their ligands are depicted in figure 1. Amongst different TLRs, TLR4 is widely studied. It recognizes lipopolysaccharides and plays a key role in immune response against Gram-negative bacteria.

Lipopolysaccharides

LPS is an important component of Gram-negative bacteria which is recognized by TLR4. During proliferation or death of bacteria, it is released from the bacterial cell wall and detected by immune cells (Hellman et al., 2000; Rietschel et al., 1994).

Structure and composition of Lipopolysaccharide

LPS is an amphipathic molecule (Lugtenberg and Van Alphen, 1983). There are four components in a molecule of LPS (Figure 4), including (1) the **Lipid-A**, the hydrophobic part of LPS which is considered as the toxic moiety responsible for initiating the immune response (Lugtenberg and Van Alphen, 1983; Raetz, 1990; Van Amersfoort et al., 2003); (2) the **inner core**, which is part of hydrophilic portion of LPS molecule; attached to the Lipid A, it comprises several sugar units (two or more 2-keto-3-deoxyoctonic acid (KDO) and two to three L-glycero-d-manno-heptose) (Figure 4) (Lugtenberg and Van Alphen, 1983; Van Amersfoort et al., 2003); (3) the **outer core** which is the third component and part of the hydrophilic portion of LPS molecule (Van Amersfoort et al., 2003); like the inner core, the outer core also consists of a few sugar unit chain, with one or more side chains (Van Amersfoort et al., 2003). This part is more variable as compared to inner core (Van Amersfoort et al., 2003). The outer core is attached to the last component of LPS molecule, called (4) **O-Antigen**. It is a polysaccharide portion and the outermost part of the cell wall, recognized by antibodies (Lugtenberg and Van Alphen, 1983; Raetz, 1990; Van Amersfoort et al., 2003). This is the most variable part which varies in size and structure from one bacterial strain to another (Rietschel et al., 1994; Van Amersfoort et al., 2003). This can be absent in some bacteria. The presence of O-antigen gives smooth appearance whereas absence gives rough appearance to bacteria. It can be referred as S and R LPS for smooth and rough form of LPS, respectively (Lugtenberg and Van Alphen, 1983; Raetz, 1990; Van Amersfoort et al., 2003).

The entire molecule of LPS containing Lipid A, inner core, outer core and O-Antigen is referred as smooth (S) LPS as produced by wild-type bacteria. There are other forms of LPS depending on the presence and size of many components. It includes Ra-LPS (containing all components except O-Antigen), Re-LPS which is the shortest form of LPS containing one or more KDO units along with Lipid A portion, Rd1-LPS with Lipid A and inner core, Rc-LPS which is Rd1 LPS with a small

portion of outer core (Lugtenberg and Van Alphen, 1983; Raetz, 1990; Van Amersfoort et al., 2003) (Figure 4).
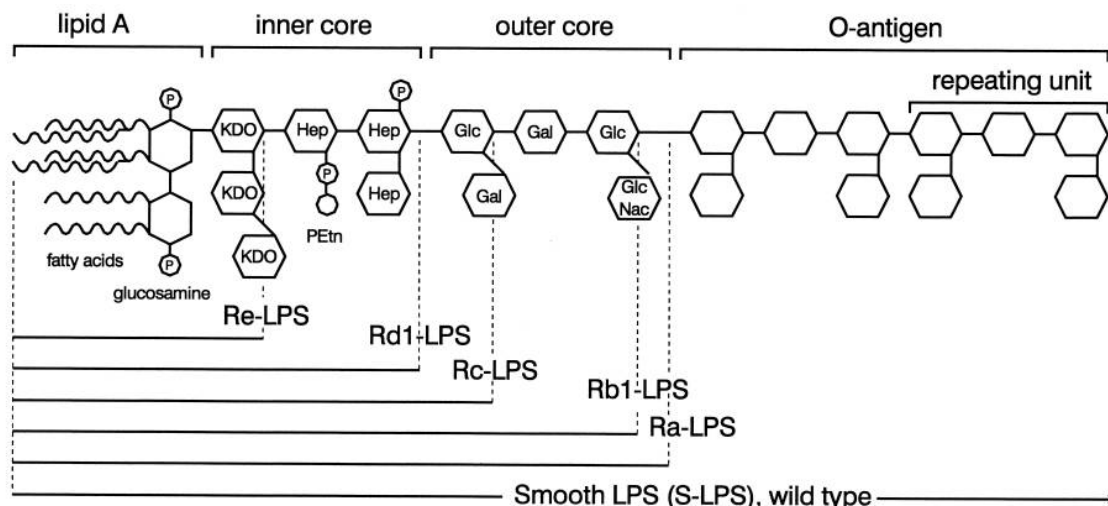
Figure 4: LPS structure from different serotypes (Van Amersfoort et al., 2003)

Detection and signaling pathway initiated by Lipopolysaccharides

Initially, TLR4 was recognized as a membrane receptor for LPS (Chow et al., 1999; Poltorak et al., 1998a). Recent studies have suggested a new intracellular sensor, caspase 4/11, in the detection of LPS (Aachoui et al., 2013; Akhter et al., 2012; Broz et al., 2012; Case et al., 2013; Kayagaki et al., 2011; Shi et al., 2014a). Both receptors along with downstream signaling cascade are discussed in details in chapter 2.

Gram-negative bacteria represent a major risk and etiological agent for many life threating diseases including SIRS, sepsis and septic shock (Morrison and Ryan, 1987).

SIRS, sepsis and septic shock

Inflammation is a protective mechanism against infectious agents. It contributes to tissue repair and homeostasis function (Kotas and Medzhitov, 2015; Medzhitov, 2008). Uncontrolled and dysregulated inflammatory response can be hazardous to the host. It can ultimately lead to dramatic clinical conditions like Systemic Inflammatory Response Syndrome (SIRS), sepsis, severe

sepsis and septic shock (Bone et al., 1992; Medzhitov, 2008). These medical conditions, if not managed and treated properly, are associated with a high mortality rate (Medzhitov, 2008).

SIRS is a cluster of signs and symptoms associated with infection or non-infectious causes. SIRS can be simply defined as the presence of any of the two of the following conditions: altered body temperature, tachypnea, tachycardia and alteration in normal blood leukocyte count (Bone et al., 1992). When SIRS is associated with the presence of infection, it is referred as sepsis (Bone et al., 1992). Worsening of sepsis leads to reduced blood supply and decreased blood pressure. Ultimately, it leads to organ dysfunction, *i.e.* the condition termed as severe sepsis (Bone et al., 1992). Hypovolemic shock in the condition of sepsis is referred as septic shock (Bone et al., 1992; Levy et al., 2003).

The systemic inflammatory response involves the release of inflammatory cytokines and ROS to fight against infection and infectious agents in the early stage of sepsis. This early inflammatory response is followed by anti-inflammatory response where the decrease in functional status of different immune cells is observed, making the host predisposed to other opportunist pathogens. This compensated state of inflammation is referred as compensatory anti-inflammatory response syndrome (CARS) (Bone et al., 1992; Levy et al., 2003; Ward et al., 2008).

Etiology of Sepsis

An increasing number of case of sepsis due to Gram-positive bacteria has been reported over the last years. Nevertheless, Gram-negative bacteria remain a major cause of sepsis (Bosenberg et al., 1988; Lira et al., 2010; Parrillo et al., 1990; Ramachandran, 2014). The most commonly observed Gram-negative bacteria found in septic patients include *Escherichia Coli, Klebsiella species* and *Pseudomonas species* (*P. aureginosa*) (Opal et al., 2003). *Staphylococcus Aureus* and *Streptococcus pyogenes* are the most frequently isolated Gram-positive bacterial strains in sepsis (Opal et al., 2003).

Epidemiology of Sepsis

Sepsis and septic syndrome is a major health and financial concern for the physicians and health care professionals. It remains one of the main causes of death in the intensive care units all over

the world (Poeze et al., 2004). A study conducted in 2001 and based on 1995 data from different hospitals of United States showed 3 cases of severe sepsis out of 1000 population individuals, with the average cost of $ 22,100 per case (Angus et al., 2001). In France, a three years follow-up study conducted on 1698 patients in 6 distinct intensive care units, shows that 42% of the patients were admitted with severe sepsis, with an average cost of 22,800 € (Adrie et al., 2005). Sepsis, severe sepsis, and septic shock are associated with high mortality and morbidity rates.

Sepsis in human and its relevance to animal models of sepsis

Animal models are crucial to investigate the pathophysiology of sepsis. Nevertheless, it should be stressed here that differences exist between sepsis condition observed in Humans and in animal models. This is namely the case for the hemodynamic changes that occur during progression of sepsis (Buras et al., 2005). The progression of sepsis in mouse models differs from humans with regards to the time to develop co-morbidities, multi-organ failure and predisposition to opportunist pathogens. In clinical settings, patients with septic condition receive several supportive therapies like fluid resuscitation, oxygen and drugs to restore normal hemodynamics including vasopressors, as well as pharmacological agents such as antibiotics, anti-inflammatory drugs and diuretics. It depends on the actual state of individuals (Buras et al., 2005). Septic patients in a hospital or clinical settings often encounter many surgical interventions which make them susceptible to pathogenic infections. These differences need to be kept in mind while extrapolating the results obtained from animal studies to human sepsis.

None of the animal models of sepsis used in the laboratory can exactly mimic the human sepsis. However, animal models have significantly contributed to the understanding and deciphering of the inflammatory and anti-inflammatory response that occur during the course of sepsis.

Animal models of sepsis and endotoxemia

A number of strategies and models of sepsis are available, using different animal species such as dogs, pigs, baboons, monkeys, rabbits, rats and mice (Greenfield et al., 1974; Pappova et al., 1971; REYNOLDS, 1972; Swan and Jacobson, 1967; Willerson et al., 1970). Each of them has

different advantages and pitfalls. These models can be divided into three main groups as described below.

1) Administration of TLR ligands

Administration of PAMPs to animals enables to investigate the physiological and pathological modulations occurring in response to inflammatory stimuli (Buras et al., 2005; Parker and Watkins, 2001; Wichterman et al., 1980). LPS (also known as endotoxin) is widely used (Buras et al., 2005; Parker and Watkins, 2001; Wichterman et al., 1980). Using endotoxins as a tool to study sepsis has advantages over other strategies as well as some drawbacks. Firstly, endotoxins can be purified and can produce a specific response that needs to be investigated (Buras et al., 2005; Fink and Heard, 1990). Secondly, endotoxins can be quantified and injected in absolute amounts. Hence, they are more easily reproducible and reliable as compared to administration of live bacteria which are difficult to control and may grow rapidly (Buras et al., 2005). Thirdly, the rate of administration of endotoxins can be controlled and modulated accordingly to mimic the pathological state to the extent that is needed for the investigation (Buras et al., 2005; Fink and Heard, 1990). In contrast, using endotoxins to induce sepsis has some important drawbacks as it differs from sepsis which involves invasion of live bacteria. Furthermore, endotoxin-infused models of sepsis do not rely on the disruption of physiological barriers. Nevertheless, it has been reported that LPS injection may lead to a secondary increase in the gut permeability to gut bacteria (Guo et al., 2013; Guo et al., 2015). So far, administration of pure endotoxins to induce pro-inflammatory cytokine release remains an important tool to evaluate the role of different cytokines in the induction and progression of sepsis as well as to assess new therapeutic strategies (Remick and Ward, 2005).

The extent of response to the administration of endotoxins depends upon the dose, rate, and route of administration as well as the prior-exposure to endotoxins. One single dose of LPS injected intraperitoneally / intravenously to induce sepsis in laboratory animals is considered as a good strategy to carry out survival experiments (Fink and Heard, 1990). Alternatively, continuous administration of LPS by using osmotic pumps can be used as a model of chronic endotoxemia (Fish and Spitzer, 1984). In rats and rabbits, high and low intravenous doses of LPS

were found to induce hypodynamic and hyperdynamic circulatory state, respectively (Brackett et al., 1985; Fink et al., 1988; Law and Ferguson, 1988; Wyler et al., 1970).

Other TLR ligands have also been used to induce an inflammatory response. The stimulation of TLR9 with bacterial DNA can induce sepsis (Sparwasser et al., 1997). In addition, co-stimulation of TLR4 and TLR9 with LPS and bacterial DNA, respectively, can synergize the effect on proinflammatory cytokine release (Sparwasser et al., 1997). Similar synergism can be obtained by the use of D-galactosamine with LPS (Galanos and Freudenberg, 1993). Purified lipoteichoic acid (LTA), a component of the cell wall of Gram-positive bacteria, is used to study the inflammatory response to Gram-positive infection.

2) Intestinal barrier disruption models

The gut contains a large amount of Gram-negative bacteria. An increase in the permeability of the gut leads to the circulation in the blood as well as infiltration of surrounding tissues of these guts bacteria. In such setting, gut bacteria become harmful for the host, namely because of the release of endotoxins. Several factors can affect the permeability of gut including inflammatory bowel diseases, high fat diet and stress (Caradonna et al., 2000). This is associated with increased plasma levels of LPS (Amar et al., 2008; Brock-Utne et al., 1988). Disruption of intestinal barrier represents a good strategy to induce sepsis by allowing the entry of bacteria and endotoxins into peritoneal cavity and bloodstream. Mainly, two surgical intestinal barrier disruption models have been described in the literature: cecal ligation and puncture model of sepsis (CLP) (Wichterman et al., 1980), and colon ascendens stent peritonitis (CASP) (Zantl et al., 1998). Both are mouse models of polymicrobial infection and sepsis.

CASP is a standard model of peritonitis and sepsis (Traeger et al., 2010). The procedure involves laparotomy and isolation of the ascending colon. A stent is placed in the ascending colon stabilized by suture. The colon is milked off to release its content and placed back to the abdominal cavity allowing it to release the content for the desired period of time. Fluid resuscitation is performed with 0.5 mL of saline before stitching up the abdominal wall with the suture. The severity and mortality can be controlled by changing the diameter of the stent (Buras et al., 2005; Traeger et al., 2010). The CASP model has the advantage to allow removal of the

stent by carrying out second surgery. This last setting is referred as CASP with intervention (CASPI) (Traeger et al., 2010). The CASP model is reliable but requires technical skills. Elevation of pro-inflammatory cytokines (such as TNFα and IL-1) was reported after three hours of stent insertion mimicking the clinical sepsis (Maier et al., 2004; Zantl et al., 1998). The CASP model of sepsis is a standard model but requires more time as compared to CLP.
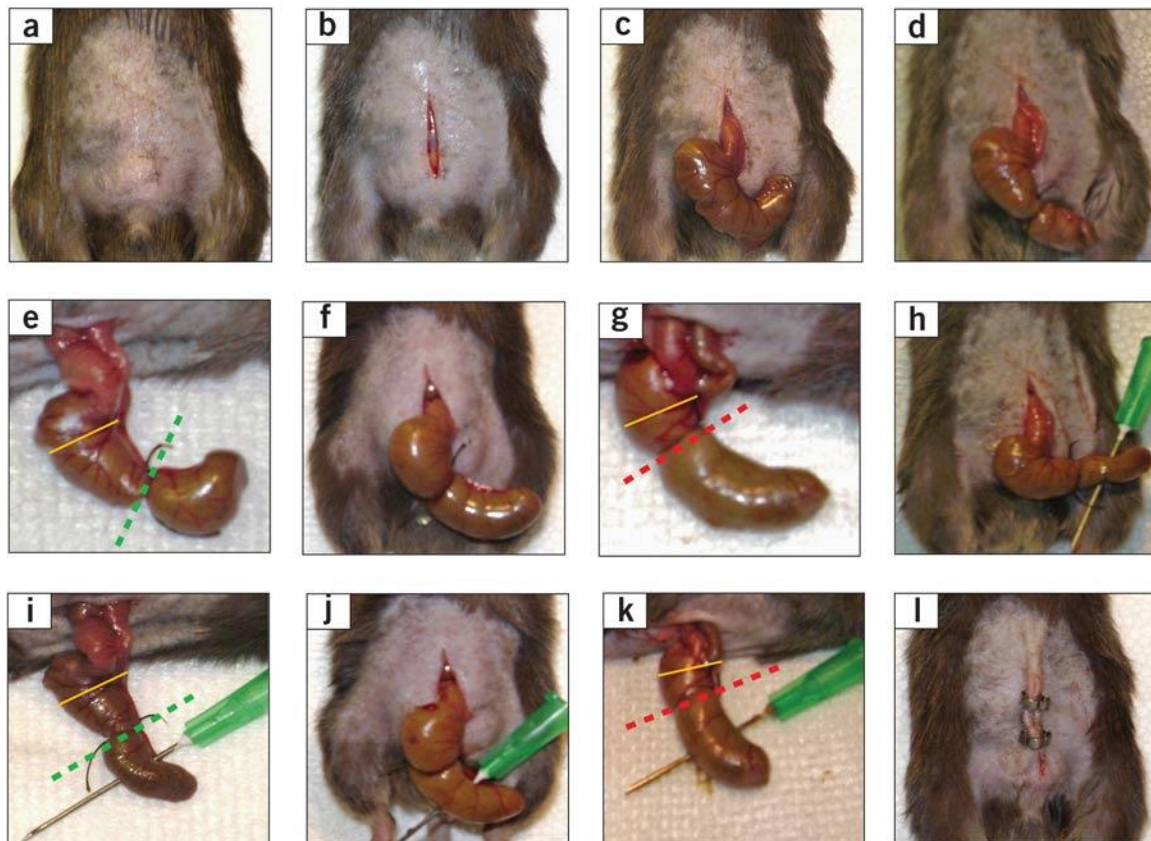
Figure 5: Procedure for Cecal Ligation and Puncture (CLP) (Rittirsch et al., 2008)

(a-b) Shave, disinfect and make a midline incision to the abdomen, (c-g) take the lower portion of the cecum out of the abdominal cavity and ligate at the indicated position (h-k) puncture the cecum "through and through" (I) place back the cecum to the abdominal cavity and ligate the abdomen with suture and metallic clips

The CLP model is considered as the gold standard model of sepsis which mimics "appendicitis and perforated diverticulitis" in Humans (Chen et al., 2014; Parker and Watkins, 2001; Wichterman et al., 1980). The procedure of CLP is described in figure 5. It involves surgically opening of the abdominal wall to reach the cecum, ligating it just below the ileocecal valve,

making a puncture with a standard size needle, milking it off gently to extrude its content, then placing it back to the abdominal section to allow the cecal content and microorganisms entering the peritoneal cavity and thereby into systemic circulation (Buras et al., 2005; Chen et al., 2014). Maier *et al.,* compared CASP and CLP models of sepsis (Maier et al., 2004). The bacterial contents and overall levels of serum cytokines (TNF-alpha, IL-1β, and IL-10) were increased in a time-depended manner in both models, with a greater magnitude after the CASP procedure in mice. The mortality rate was independent of the number of punctures in CLP mice whereas in the CASP model the rate of mortality was proportional to the diameter of the inserted stent (Maier et al., 2004). Both models are widely used in different laboratories depending on study criteria as well as on available technical skills.

Mitochondrial dysfunction in the context of sepsis

Sepsis has been associated with mitochondrial dysfunction in many organs which leads to organ dysfunctions. Mitochondria are vital organelles in cells. They are the main source of ATP, and also play a critical role in calcium signaling, cell death and apoptosis (Scheffler, 2011). Mitochondrial functions (including metabolic status, oxygen consumption, activities of respiratory chain complexes, and production of mitochondrial reactive oxygen species (mROS) or mitochondrial dynamics) have been assessed in the context of sepsis and septic syndrome.

In muscle biopsies obtained from critically ill patients admitted to intensive care units, mitochondrial biogenesis was higher in survivors as compared to the non-survivors (Carré et al., 2010). This suggests that mitochondrial biogenesis is a compensatory mechanism to maintain the viable mitochondrial pool.

Peripheral blood leukocytes were more extensively studied as these cells are more easily accessible in ill patients. Blood leukocytes collected at the first week of admission in septic patients showed an early increase in respiration with increased mtDNA and cytochrome C contents along with enhanced citrate synthase (CS) activity (Sjövall et al., 2013). The same group has previously reported that platelets from septic patients showed increased mitochondrial respiration and cytochrome c contents as compared to control during the first week, whereas no differences were seen in mtDNA contents (Sjövall et al., 2010). Garrabou *et al.,* observed that peripheral blood monocytes isolated from septic patients had decreased activity of complex I, III

and IV of the respiratory chain without alteration in mitochondrial contents as measured by using CS activity (Garrabou et al., 2012). Another study showed a decreased respiratory capacity and reduced ATP production with lower activity of F1Fo ATP synthase in blood monocytes from septic patients (Japiassu et al., 2011). It was also reported that peripheral blood monocytes in early sepsis were associated with decreased mitochondrial membrane potential (Adrie et al., 2001). This increase in the percentage of depolarized mitochondria was higher in non-survivors as compared to the survivors (Adrie et al., 2001).

In animal models of sepsis, a study performed on hepatocytes in CLP mouse model of sepsis showed decreased oxidative phosphorylation and decreased mitochondrial density suggesting increased autophagy/mitophagy followed by an increase in mitochondrial biogenesis in a TLR9-dependent manner (Carchman et al., 2013). Similar results were obtained in primary hepatocytes treated *in vitro* with LPS (Carchman et al., 2013). Mitochondria isolated from skeletal muscles of LPS injected mice showed increased production of nitric oxide and decreased oxygen consumption as compared to control (Aguirre et al., 2012).

Altogether, these observations highlight that mitochondrial function is altered in various tissues, namely in immune cells, in the context of sepsis. Nevertheless, the origins of these changes of mitochondrial function and their consequences, especially on immune response, need to be unraveled. Understanding these aspects of sepsis may help to the development of alternative strategies to control the inflammatory response.

Chapter 2: Immune cells and pathogen clearance

Innate and adaptive immunity represent two components of the immune system in mammals. Both are important for the defense of host against pathogenic and hazardous insults. Innate immunity is mainly involved in acute reaction towards infectious agents but also play a role in modulating the adaptive immunity. Adaptive immunity is rather involved in late phase and long-term protection of the host against pathogens (Abbas et al., 2014; Medzhitov, 2008).

Both immune systems work in coordination to eradicate the pathogenic insults and to prevent subsequent infection. Invasion of bacteria or pathogens in tissue leads to the release of chemotactic substances from resident macrophages and mast cells that recruit neutrophils and later monocytes that differentiate into macrophages to kill the pathogen (Medzhitov, 2008). Pathogenic antigens are then processed and presented by antigen presenting cells (APC), like dendritic cells, to the T lymphocytes or are released by neutrophils which later get detected by B-cells (Abbas et al., 2014). Both lead to the activation of the adaptive immune system to deal with the subsequent infection.

Neutrophils are also known as polynuclear phagocytes. They are the most abundant leukocytes in the blood. They contain granules (lysosomal structures) in the cytoplasm and hence belong to the granulocytes. After rushing to the site of infection, they are activated in response to pathogenic stimuli or cytokines released. They have a shorter half-life as compared to monocytes which, after extravasation, differentiate into macrophages and can live for a longer period of time (Abbas et al., 2014; Medzhitov, 2008; Sadik et al., 2011). Macrophages constitute another line of defense against pathogens. Their activation greatly contributes to the success of the host defense against pathogen aggression (Mege et al., 2011).

Monocytes and Macrophages

Monocytes and macrophages are of the same lineage. They are referred as the mononuclear phagocyte system (Abbas et al., 2014). Monocyte-macrophage lineage cells are heterogeneous and found ubiquitously throughout the body (Gordon and Taylor, 2005). Monocytes originate from the myeloid progenitor cells from bone marrow, enter into the systemic circulation where

they constitute 5 to 10% of total leukocytes in humans (Geissmann et al., 2010; Gordon and Taylor, 2005; van Furth and Cohn, 1968). Monocytes remain in the systemic circulation for several days and then they enter into tissues where they differentiate into macrophages and dendritic cells (Geissmann et al., 2010; Gordon and Taylor, 2005; van Furth and Cohn, 1968). Any pathogenic or inflammatory signal is able to enhance the migration of monocytes towards the infected tissue (Geissmann et al., 2010; Gordon and Taylor, 2005; van Furth and Cohn, 1968). This migration and infiltration of the monocytes to the site of infection or injury is mediated by chemokine and adhesion receptors (Geissmann et al., 2010).

In humans, monocytes are classified on the basis of expression levels of CD14 and CD16 (FcγRIII). On the basis of differential expression of these two markers, monocytes are classified into classical ($CD14^{++} CD16^{-}$), intermediate ($CD14^{++} CD16^{+}$) or non-classical ($CD14^{+}CD16^{++}$) monocytes. Classical, intermediate and non-classical monocytes are associated with phagocytic, pro-inflammatory and patrolling properties, respectively (Ingersoll et al., 2011; Tacke and Randolph, 2006; Yang et al., 2014). Similarly, in mouse, on the basis of differential expression levels of Ly6C (lymphocyte antigen 6 complex), monocytes are classified into classical ($Ly6C^{hi}$), Intermediate ($Ly6C^{int}$) and non-classical ($Ly6C^{lo}$) monocytes. Both human and mouse monocytes classes are summarized in table 1 along with their functions and expression levels of chemokine receptors. Furthermore, CD115 (receptor for Macrophage colony stimulating factor (M-CSF)) is a widely used a marker for monocytes. CD11b can be concomitantly used to select pure monocyte populations. Monocytes can be further classified into different subsets, based on the expression level of their chemokine (Cx_3CR1 and CCR_2) and adhesion receptors (CD62L, adhesion receptor also called L-selectin) (Ingersoll et al., 2011; Tacke and Randolph, 2006; Yang et al., 2014).

Table 1: Human and mouse monocyte subsets (adapted from (Yang et al., 2014))

Species	Subsets	Surface markers	Chemokine receptors	Functions
Human	Classical	$CD14^{++}CD16^{-}$	$CCR2^{high}CX3CR1^{low}$	Phagocytosis
	Intermediate	$CD14^{++}CD16^{+}$	$CCR2^{mid}CX3CR1^{high}CCR5^{+}$	Pro-inflammatory
	Non-classical	$CD14^{+}CD16^{++}$	$CCR2^{low}CX3CR1^{high}$	Patrolling

Species	Subsets	Surface markers	Chemokine receptors	Functions
Mouse	Ly6C^{high} (Ly6C$^+$)	CD11b$^+$CD115$^+$Ly6C^{high}	CCR2^{high}CX3CR1^{low}	Phagocytosis & Pro-inflammatory
	Ly6C^{middle} (Ly6C$^+$)	CD11b$^+$CD115$^+$Ly6C^{middle}	CCR2^{high}CX3CR1^{low}	Pro-inflammatory
	Ly6C^{low} (Ly6C$^-$)	CD11b$^+$CD115 $^+$Ly6C^{low}	CCR2^{low}CX3CR1^{high}	Patrolling; tissue repair
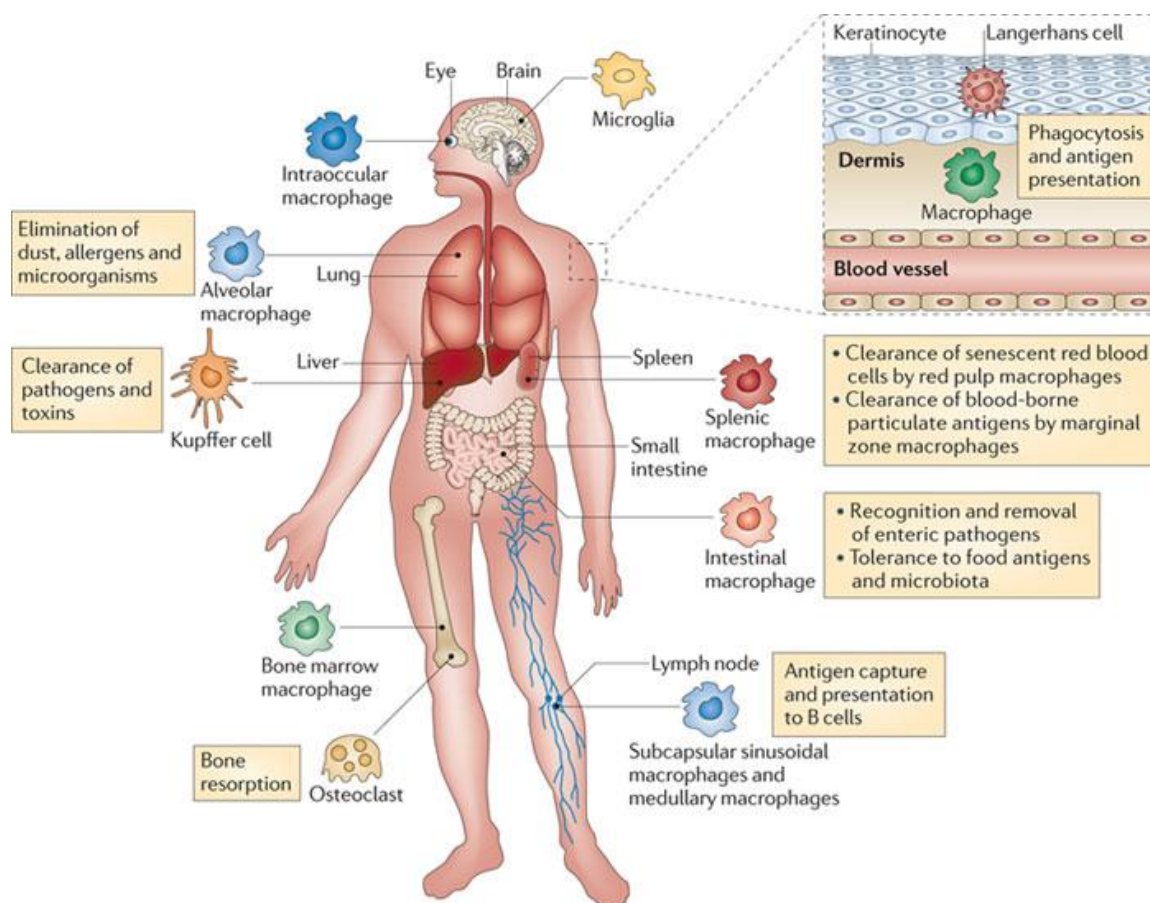
Figure 6: Tissue macrophages subtypes with their functions (Murray and Wynn, 2011)

Macrophages are found within tissues and endowed with pro-inflammatory or anti-inflammatory functions depending on their environment, namely the cytokine environment (Biswas and Mantovani, 2010; Geissmann et al., 2010). Like monocytes, macrophages also form a heterogeneous population (Biswas and Mantovani, 2010; Gordon and Taylor, 2005; Mantovani et al., 2013). Under normal conditions, tissue macrophages are continuously being renewed by

circulating monocytes which differentiate into macrophages when infiltrating tissues (Gordon and Taylor, 2005; van Furth and Cohn, 1968). It has been hypothesized that there is a role of circulating precursors cells along with circulating monocytes to replenish tissue-resident macrophages in the state of any injury or inflammatory stimuli (Gordon and Taylor, 2005; van Furth and Cohn, 1968). Different classes of tissue-resident macrophages based on their location are summarized along with their functions in a sketch from Murray et al.,2011 (Figure 6) (Gordon and Taylor, 2005; Murray and Wynn, 2011).

Macrophages are equipped with a number of PRRs for the recognition of endogenous and exogenous danger signals that switches them towards distinct phenotypes to better deal with and to eradicate the threat (Murray and Wynn, 2011). They are also equipped with scavenger receptors to internalize different negatively charged molecules like modified LDL as well as apoptotic cells (Gordon and Taylor, 2005; Mantovani et al., 2013). Tissue-resident macrophages have the ability to plasticize into distinct phenotypes, depending on the tissue environment or pathophysiological conditions. This property of macrophages to plasticize is known as macrophage polarization (Biswas et al., 2012).

Macrophages polarization

Macrophages are the key components of innate immunity and are antigen presenting cells (APC). Macrophages exhibit functional diversity. Depending upon the type of stimuli or environmental signal that they sense, macrophages have the ability to plasticize from one form to another (Biswas et al., 2012; Biswas and Mantovani, 2010; Gordon and Taylor, 2005; Mantovani et al., 2013; Martinez and Gordon, 2014). Macrophages can be classified into two main types: (1) classically activated macrophages (M1 macrophages) and (2) alternatively activated macrophages (M2 macrophages) (Biswas et al., 2012; Biswas and Mantovani, 2010; Gordon and Taylor, 2005; Mantovani et al., 2013; Martinez and Gordon, 2014).

M1 macrophages are the pro-inflammatory form of macrophages that play a key role in the eradication of pathogenic insults (Biswas et al., 2012). The M1 phenotype is associated with the bactericidal activity, pro-inflammatory, and anti-tumoral functions. M1 macrophages are characterized by the increased production of pro-inflammatory cytokines (IL-1β, IL-6, IL-12,

TNFα), ROS, reactive nitrogen oxygen species (RNS), increased expression of MHC-II, CD64 and CD80 (Gordon and Taylor, 2005; Mantovani et al., 2013). CD64 is the FcγRI receptor. FCγRs are receptors for the fragment crystallizable (Fc) region of immunoglobulin G (IgG) (Vogelpoel et al., 2015). CD80 and CD86, collectively called as B7, are costimulatory molecules for the activation of T lymphocytes expressed on APCs. Exposure of quiescent macrophages to LPS along with the Th1 cytokine IFN-gamma (IFN-γ) switches them toward an M1 phenotype (Biswas et al., 2012; Biswas and Mantovani, 2010; Gordon and Taylor, 2005; Mantovani et al., 2013; Martinez and Gordon, 2014).

Stimuli:
- Microbes(LPS)
- IFNγ
- GM-CSF

M1 Macrophages

Properties:
- Pro-inflammatory
- Anti-tumoral
- Microbicidal

Characterized by:
- Inflammatory cytokines (IL-1b, IL-6, IL-12),
- ROS
- High expression of CD64, CD80 and iNOS

- **Metabolic Profile:** Gylcolysis

Stimuli:
- Immune complex
- Cytokines (IL-4, IL-13)
- M-CSF

M2 Macrophages

Properties:
- Anti-inflammatory
- Pro-tumorol
- Tissue repair

Characterized by:
- Anti-inflammatory (IL-10, IL-1RA),
- High expression of scavenger receptors, Dectin1(Glycan) and CD206 (Mannose)

- **Metabolic Profile:** Fatty acid oxidation

Figure 7: Summary of two main Macrophage phenotypes with their characteristics

M2 macrophages are named like this with reference to Th2 response (Biswas et al., 2012; Stein et al., 1992). The Th2 cytokine Interleukin-4 (IL-4), as well as other anti-inflammatory cytokines (such as Interleukin-13 (IL-13) and Interleukin-10 (IL-10)) and immune complexes, switch macrophages towards M2 phenotype (Mantovani et al., 2004). M2 macrophages are endowed with anti-inflammatory properties, anti-parasitic activity and are associated with increased expression of the mannose receptor (CD206) (Gordon and Taylor, 2005; Mantovani et al., 2013; Stein et al., 1992). Furthermore, different subtypes of M2 macrophages have been observed depending on the stimuli used. IL-4 or IL-13 induces the M2a phenotype whereas immune complex along with TLR agonists and IL-1R ligands induce the M2b phenotype. IL-10 induces the

M2c phenotype (Mantovani et al., 2004). M2a and M2b are known to perform an immune-regulatory function and to promote Th2 response whereas M2c are known to suppress the immune response and to participate to tissue remodeling (Mantovani et al., 2004). M2 macrophages perform various functions including resolution of inflammation, tumor progression, tissue remodeling and repair as well as immune regulation (Biswas et al., 2012). Figure 7 depicts the main features of M1 and M2 phenotypes.

Signaling pathways involved in classical activation of macrophages (M1)

As presented in the previous section, the Th1 cytokine IFN-γ and LPS are considered as the initiators of the classical activation of macrophages (M1 Phenotype) (Akira et al., 2006; Nathan et al., 1983; Nathan et al., 1984). Recognition of LPS by TLR4 initiates a signaling cascade which subsequently leads to the activation of transcription factors that regulate the inflammatory response (Chow et al., 1999). Binding to IFN-γ to the IFN-γ Receptors (INFGRs) activate signal transducer and activator of transcription factor (STAT1) signaling pathway.

Toll-like receptor 4 signaling pathway

LPS is mainly sensed by surface receptor toll-like receptor 4 (TLR4) (Chow et al., 1999; Poltorak et al., 1998a; Poltorak et al., 1998b). TLR4 belongs to the TIR (toll/IL-1R like receptor) receptor superfamily, containing TIR domain (Bowie and O'Neill, 2000; Kawai and Akira, 2010). Initially, lipopolysaccharides binding protein (LBP), an acute phase protein produced by the liver, was believed to be involved in detection of LPS (Pålsson-McDermott and O'Neill, 2004; Schumann et al., 1990). LBP belongs to the family of lipid binding proteins. On the one hand, it is known to exhibit anti-inflammatory effect by promoting the transfer of LPS and LTA to HDL, thereby neutralizing the microbial ligands (Schumann et al., 1990; Tobias et al., 1995; Van Amersfoort et al., 2003). On the other hand, LBP facilitates the binding of LPS to CD14, a glycoprotein known as a response element for LPS (Schletter et al., 1995; Ulevitch and Tobias, 1995; Van Amersfoort et al., 2003). CD14 exists in two forms mCD14 (membrane CD14) and sCD14 (soluble CD14). The mCD14, which contains glycophosphatidylinositol tail, mediates LPS binding to TLR4 in myeloid cells. sCD14 mediates LPS response in endothelial and epithelial cells (Van Amersfoort et al., 2003). Because CD14 does not contain a transmembrane domain for the signal transduction, the

existence of another receptor was emphasized. Thus, TLR4 was identified as a receptor for LPS lately (Chow et al., 1999; Poltorak et al., 1998a; Poltorak et al., 1998b). TLR4 works in the coordination of membrane receptor CD14 and MD2 (also called as Lymphocyte antigen 96; LY96), and form a multi-receptor complex (da Silva Correia et al., 2001; Shimazu et al., 1999). It was observed that LPS crosslinks with TLR4 and MD2 in presence of CD14 (da Silva Correia et al., 2001). MD2 was shown to be an essential component of TLR4 signal transduction pathway in response to LPS (Shimazu et al., 1999). MD2$^{-/-}$ mice failed to respond to intraperitoneal injection of LPS (Nagai et al., 2002).
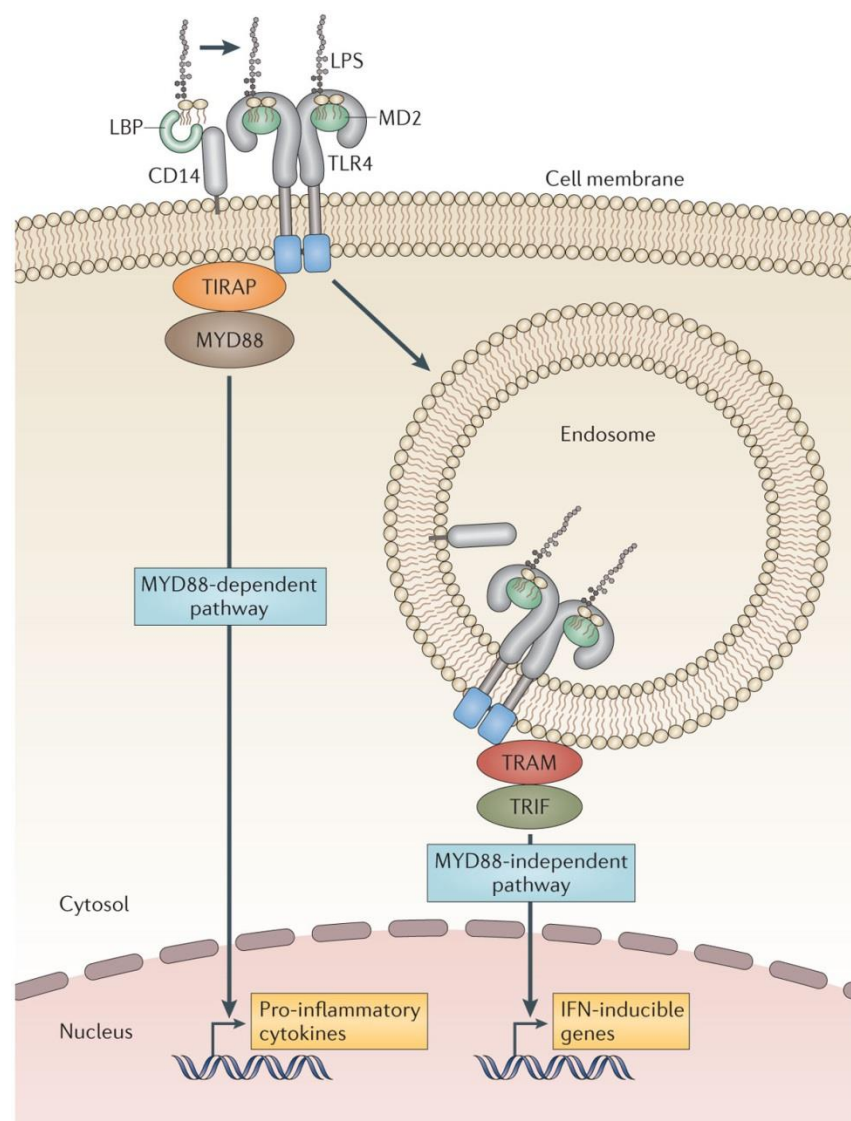
Figure 8: Initiation sites of Myd-88 dependent and Myd-88 independent TLR4 signaling pathway (Needham and Trent, 2013)

Activation of TLR4 by LPS leads to the oligomerization of the receptor (Lu et al., 2008). TLR4 then utilizes two adaptor proteins: Myd88(myeloid differentiation protein 88) or TRIF (TIR domain containing adaptor for inducing IFN-β), thereby initiating Myd88-dependent and Myd88-independent signaling pathways, respectively (Lu et al., 2008). Both adaptor molecules are recruited to the TLR4 receptor through interactions between their TIR domains. The Myd88-dependent pathway is activated upon the detection of LPS by TLR4 at the cell surface whereas LPS detection in endosomes containing TLR4 leads to the activation of the TRIF-dependent pathway (Figure 8). Myd88-dependent pathway is considered as pro-inflammatory and is associated with the production of pro-inflammatory cytokines such as TNFα, IL-6 and IL-12 whereas TRIF-dependent pathway is considered as less inflammatory and is associated with the production of IFNβ and interferon-inducible proteins (CXC chemokine ligand 10 (CXCL10 also called IP10), monocyte chemoattractant protein (MCP1), chemokine ligand 5 (CCL5) and granulocyte colony-stimulating factor (G-CSF)) (Needham and Trent, 2013).

Both pathways involve several downstream signaling cascades which converge in few points (Figure 9). Myd88-dependent pathway utilizes Interleukin-1 receptor-associated kinase 4 (IRAK4). Myd88 and IRAK4-deficient mice displayed a lack of response to LPS stimulation and abrogated production of inflammatory cytokines. These mice are resistant to septic shock induced by LPS (Kawai et al., 1999; Suzuki et al., 2002). IRAK1 is downstream of IRAK4 (Lu et al., 2008; Lye et al., 2004). In macrophages, the LPS-mediated cytokine release was not completely dependent on IRAK1 (Swantek et al., 2000). Another adaptor molecule that plays a critical role in the Myd88-dependent signaling cascade is Tumor necrosis factor receptor-associated factor 6 (TRAF6) (Gohda et al., 2004). TRAF6 exists downstream of IRAK4 and IRAK1 in the signaling cascade (Lu et al., 2008). TRAF6 forms a complex with two ubiquitin-conjugating enzymes (UBC13; ubiquitin-conjugating enzyme 13 and UEVIA; ubiquitin-conjugating enzyme E2 variant isoform A) to activate Tak1 kinase (transforming growth factor-β activated kinase) (Gohda et al., 2004; Lomaga et al., 1999; Lu et al., 2008). Tak1 then activates IKK (Ikβ kinase) (Sato et al., 2005) and leads to IKK-mediated phosphorylation of IκB (Inhibitor of κ light chain gene enhancer in B cells) which in turn is degraded and releases NFκB (Lu et al., 2008). NFκB translocates to the nucleus and initiates the transcription of pro-inflammatory genes (Lu et al., 2008). In addition,

Tak-1-mediated MAPK activation induces the activation of the Activator Protein-1 (AP-1) transcription factor which also participates to NFκB activation (Chang and Karin, 2001).
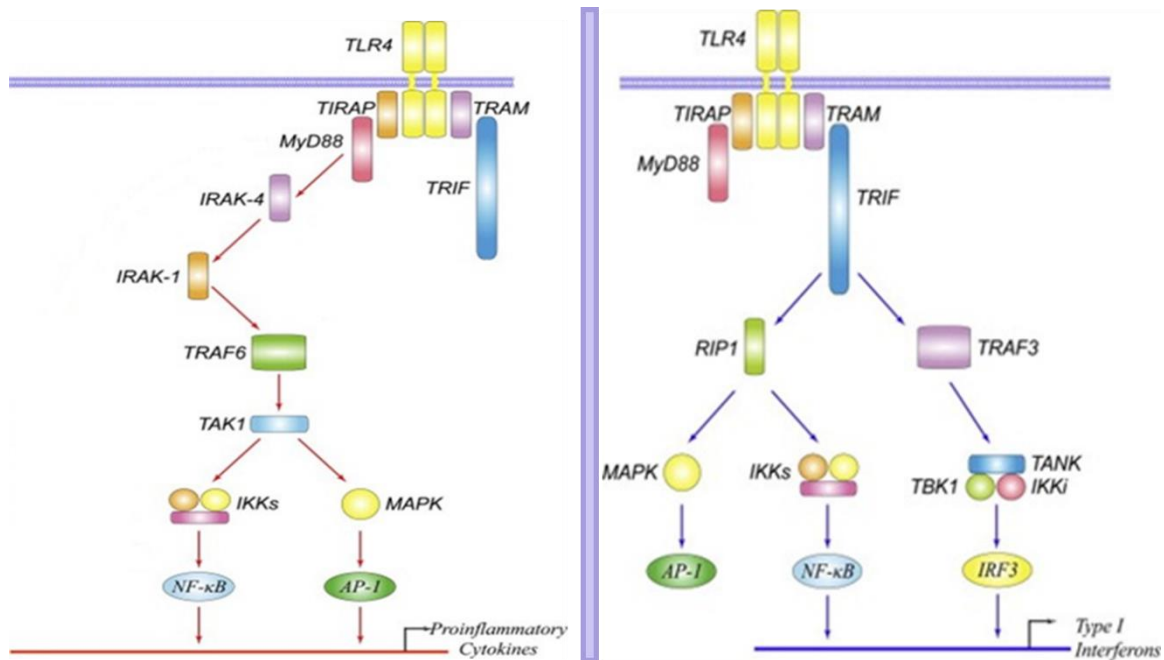
Figure 9: MyD88 dependent and MyD88 independent TLR4 signaling pathway (adapted from: (Lu et al., 2008)

Myd88-independent pathway requires alternative TIR containing adaptor protein TRIF (Lu et al., 2008). Activation of TRIF mediates the commitment of IRF3 transcription factor as well as NFκB (Lu et al., 2008). TRIF utilizes TRAF3 to activate IRF3. TRAF3 binds and activates TBK1 and IKK. It leads to the activation of IRF3 which then translocates to the nucleus and induces the transcription of interferon-inducible genes (Fitzgerald et al., 2003; Guo and Cheng, 2007; Hemmi et al., 2004; Lu et al., 2008). Therefore, the TRIF-dependent pathway also activates NFκB and AP-1 (Lu et al., 2008).

IFN-gamma Receptor Pathway

Interferons are cytokines involved in antiviral and antibacterial defense as well as anti-proliferative activity on normal and tumor cells (Platanias, 2005). Interferons are classified into three types on the basis of structural homology (Pestka et al., 2004). Type I interferons include

IFN-α, IFN-β, IFN-ε, IFN-τ, IFN-κ, IFN-ω, IFN-δ and IFN-ζ; Type II interferon family consists of only one interferon (IFN-γ); Type III interferon family consists of IL-29 (IFNλ1), IL-28A(IFNλ2) and IL-28B (IFNλ3) which has similar function to type I interferons (McNab et al., 2015).

Type I and III IFNs and their respective receptors have no direct role in classical activation of macrophages. We will only discuss here the role of type II interferon (IFN-γ).

Interferon-gamma is mainly produced by T cells and natural killer cells (NK). It acts on cells endowed with interferon gamma receptors (IFNGRs) which comprised of two chains of the IFNGR1 subunit and two chains of the IFNGR2 subunit. Both are glycoproteins with a molecular mass of 90 and 60 kDa, respectively (Schoenborn and Wilson, 2007; (Pestka et al., 1997). Binding of IFN-γ to the IFNGR1 (the ligand binding chain) and IFNGR2 (the accessory receptor chain) leads to the oligomerization of the receptor (Pestka et al., 1997) and leads to the phosphorylation of JAK1 and JAK2 associated with IFNGR1 and IFNGR2, respectively (Darnell et al., 1994). Sequentially, IFN-γ binds to the IFNGR1 that leads to the intracellular activation of JAK2 by auto-phosphorylation followed by trans-phosphorylation and activation of JAK1 (Briscoe et al., 1996). JAK1 phosphorylates the IFNGR1 at tyrosine 440, allowing the formation of two docking sites for SH2 (Src homology 2) domains (Boehm et al., 1997). STAT1 then binds to the docking sites through SH2 domain forming a dimer which is then phosphorylated at Tyrosine 701 by the JAK2 (Briscoe et al., 1996). STAT1 after phosphorylation forms homodimers and translocates to the nucleus where it binds to gamma associated sequence (GAS) element and initiates the transcription of inflammatory genes (Aaronson and Horvath, 2002; Boehm et al., 1997; Darnell, 1997; Stark et al., 1998). IFN-γ is a potent activator of macrophages and synergizes the effect of other cytokines and microbial products. This property to potentiate the response of other cytokines or ligands on the subsequent challenge is referred as "priming" (Hu et al., 2008; Schroder et al., 2004). Priming of macrophages with a low dose of IFN-γ has been shown to increase the transcription of STAT1, thereby enhancing its levels in the cytosol (Hu et al., 2008; Hu et al., 2002). Furthermore, the higher expression of STAT1 induced by IFN-γ priming allows the competitive inhibition of suppressor of cytokine signaling 1 (SOCS1) protein by STAT1 on docking sites on IFNGR1 and counteracts its anti-inflammatory effect (Hu et al., 2008). Therefore,

Interferon gamma receptors (IFNGRs) in association with their downstream cascade play a critical role in classical activation of macrophages.

STAT1

To date, seven STATs are known: STAT1, STAT2, STAT3, STAT4, STAT6, STAT5a and STAT5b. All present an SH2 (Src Homology 2) domain which helps to form homodimers or heterodimers (Shuai et al., 1994). After dimerization, STATs translocate to the nucleus and bind to DNA at promoter region (Figure 10). Phosphorylation of STAT1 at tyrosine 701 is a prerequisite for its activation and translocation to the nucleus. For maximum transcriptional activity, phosphorylation at serine 727 residue is also required (Wen et al., 1995).

Serine phosphorylation of STAT1 has been shown to be mediated by protein kinase C-δ (delta) in response to type II as well as type I IFNs (Deb et al., 2003; Ivaska et al., 2003; Uddin et al., 2002). IFN-γ-dependent phosphorylation STAT1 at serine (S727) by calcium / calmodulin-dependent protein kinase II has also been reported (Aaronson and Horvath, 2002; Boehm et al., 1997; Darnell, 1997; Stark et al., 1998). Transcription of interferon-responsive genes requires translocation of STAT1 to the nucleus. It is mediated by nuclear pore through the interaction of STAT1 homodimer with importin-α-1 (NPI-1) (Sekimoto et al., 1997). The complete STAT1 translocation into the nucleus takes place between 15 to 30 minutes of IFN-γ exposure (Sekimoto et al., 1997). STAT1-deficient mice are susceptible to viral and bacterial (*Listeria monocytogenes*) challenges, and have a reduced survival rate compared to wild-type counterparts (Meraz et al., 1996). Peritoneal macrophage from STAT1-deficient mice showed decreased nitric oxide production as compared to wild-type mice, supporting the idea of a reduced bactericidal activity and enhanced susceptibility to infection (Meraz et al., 1996). By contrast, STAT1-deficient mice appeared to be more resistance to septic shock induced when submitted to CLP surgery (Herzig et al., 2012; Kamezaki et al., 2004).

Interestingly, STAT1-mediated regulation of Caspase-4/11 gene expression established a linked between IFNγ signaling, non-canonical inflammasome pathway and pyroptosis (Schauvliege et al., 2002).
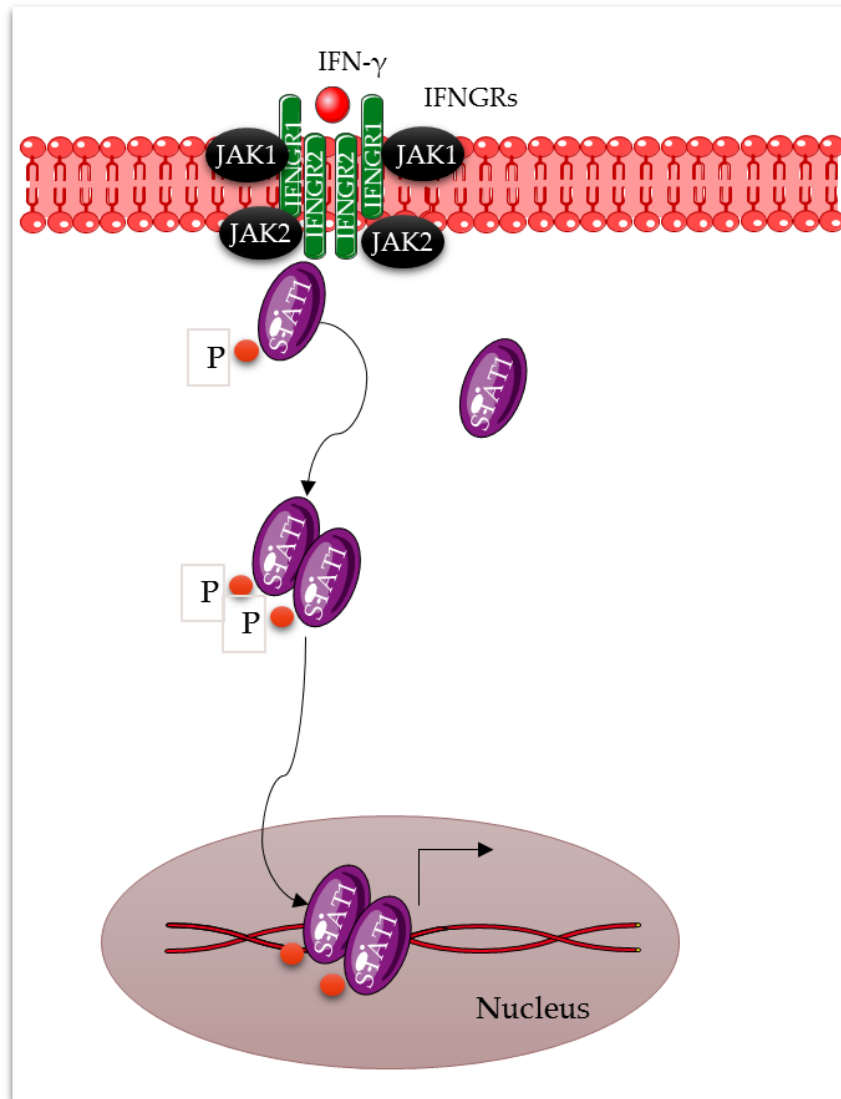
Figure 10: Simplified view of Interferon gamma signaling pathway (adapted from: (Gough et al., 2008))

Caspase 4/11

Mouse Caspase-11, the ortholog of human caspase 4/5, belongs to the family of inflammatory caspases (Martinon and Tschopp, 2004). Caspases are cysteine proteases. They have different functions in inflammation and cell death (Thornberry, 1999). Total Five murine and human inflammatory caspases are known to date and these include: caspase 1, 4, 5, 11, and 12. These caspases are involved in the release of inflammatory cytokine (IL-1β, and IL-18). Caspase-1 was the first caspase identified and, based on its function in the cleavage-dependent activation of IL-

1β, it was also termed IL-1β converting enzyme (ICE) (Thornberry, 1999; Thornberry et al., 1992). Caspase-1 exists in an inactive form which upon stimulation undergoes autoproteolytic activation within a multiprotein complex called inflammasome (such as NLRP3 inflammasome (Figure 3)) (Broz et al., 2010; Martinon and Tschopp, 2004; Thornberry et al., 1992). Upon activation, caspase-1 cleaves Pro-IL-1β and pro-IL-18 to their active forms IL-1β and IL-18, respectively (Broz et al., 2010; Martinon and Tschopp, 2004; Thornberry et al., 1992).

Recent studies revealed that caspase 4/11 acts as an intracellular LPS receptor. Murine caspase 11 has been reported to sense intracellular LPS and bacteria, independently of TLR4 (Hagar et al., 2013; Kayagaki et al., 2011; Kayagaki et al., 2013). Similar observations were made with the human orthologues caspase 4 and 5 (Shi et al., 2014b). In our study, we have mainly worked with murine cells and models but for better understading we have denoted caspase 11 as caspase 4/11 throughout the manuscript (in figure 11 it is denoted as casp11). Caspase 4/11 can be activated by intracellular LPS from released from invading bacteria (*Burkholderia* and *Shigella*) (Kayagaki et al., 2015; Kayagaki et al., 2011; Shi et al., 2015; Shi et al., 2014a). Gram-negative bacteria unable to reach the cytosol can trigger caspase 4/11 activation through bacterial outer membrane vesicles (OMVs)-mediated LPS delivery to the cytosol. By contrast, Gram-positive bacteria are inefficient for activating caspase 4/11 (Vanaja et al., 2016). This intracellular recognition of LPS by caspase 4/11 leads to the activation of the inflammasome and is therefore referred as non-canonical inflammasome activation (Kayagaki et al., 2011; Kayagaki et al., 2013). As previously mentioned, the inflammasome acts as a platform for the maturation and activation of inflammatory cytokines (IL-1β and IL-18) and induction of pyroptosis to eradicate the pathogenic insults (Schroder and Tschopp, 2010). Caspase 4/11-mediated pyroptosis is independent of caspase-1 but IL-1β release requires caspase-1 (Kayagaki et al., 2011; Kayagaki et al., 2013).

As depicted earlier in this document, the NLRP3 inflammasome comprises NLRP3, ASC, caspase 1. It can also bind caspase 4/11. The canonical activation of NLRP3 inflammasome utilizes NLRP3 sensing of pathogenic or nonpathogenic stimuli (Figure 3). By contrast, non-canonical activation of NLRP3 inflammasome requires the detection of the pathogenic signal by caspase 4/11 (Hagar et al., 2013; Kayagaki et al., 2013) (Figure 11).
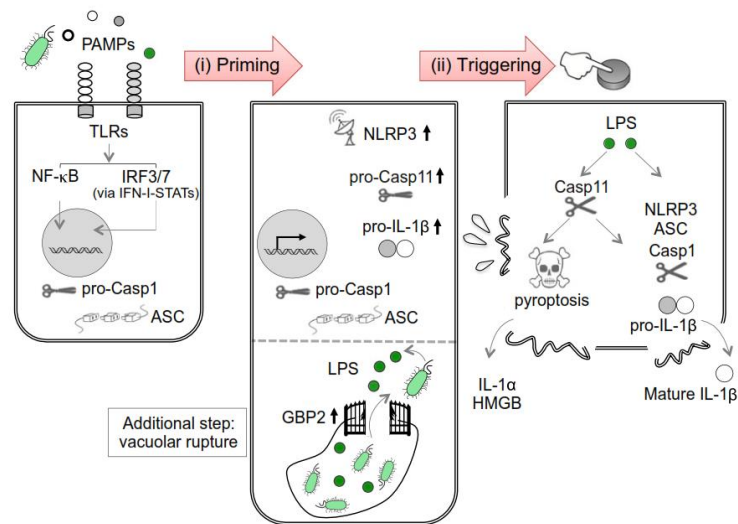
Figure 11: Non-canonical activation of inflammasome

Activation of the inflammasome by non-canonical pathway is composed of several steps, which include:

1. Priming is mediated by TLR ligands or cytokines and enhances the expression of inflammasome machinery (NLRP3 and ASC), pro-caspase-11 (non-canonical) as well as inflammatory cytokines (pro-IL-1β).

2. Then, a triggering signal will lead to the activation of the inflammasome. Activation of the non-canonical inflammasome involves the sensing of intracellular LPS by caspase 4/11 (Bauernfeind et al., 2009; Hagar et al., 2013; Kayagaki et al., 2011; Kayagaki et al., 2013). The canonical inflammasome is commonly activated by ATP and nigericin (He et al., 2016).

3. In the presence of whole bacteria, LPS-mediated activation of caspase 4/11 relies on the rupture of the endosomal membrane by entrapped bacteria. LPS is then released into the cytosol to be sensed by caspase-11. Vacuolar rupture is mediated by guanine-binding protein 2 (GBP2). GBP2 is a GTPase induced by IFNs. It is recruited to the pathogen coating vacuoles and ruptures them to release vacuolar pathogen components into the cytosol (Kayagaki et al., 2013; MacMicking, 2004; Meunier et al., 2014; Pilla et al., 2014).

The mechanism of activation non-canonical inflammasome and signals required are summarized in the sketch from kayagaki et al, 2015 (Stowe et al., 2015)

Both TLR4 and caspase 4/11 activation leads to the release of inflammatory cytokines. Contrary to LPS-mediated activation of TLR4, it is currently unknown whether LPS-mediated caspase 4/11 activation contributes to M1 polarization.

Metabolic reprogramming during macrophage polarization

Immunometabolism encountered a considerable increase of interest during the last decade. It is now well appreciated that M1 and M2 phenotypes exhibit very distinct metabolic profiles. Metabolic changes associated with macrophage polarization greatly contribute to specific functions of M1 and M2 macrophages. Mechanisms leading to this metabolic switch during macrophage polarization was only started to be investigated recently.

M1 Phenotype of macrophage is known to rely on anaerobic glycolysis for ATP production and present decreased oxygen consumption even in the presence of ample amount of oxygen (Haschemi et al., 2012; Rodriguez-Prados et al., 2010). The enzymes involved in glycolysis were shown to be upregulated in classically activated macrophages, favoring further the metabolic switch towards glycolysis (Rodriguez-Prados et al., 2010). For example, PFK2 (6-phospho-fructo-2-kinase) was shown to be converted from L-PFK2 into more active isoform uPFK2 (ubiquitous PFK2) (Rodriguez-Prados et al., 2010). Interestingly, inducible Nitric Oxide Synthase (iNOS), an enzyme involved in arginine metabolism, was shown to be augmented in classically activated macrophages (Corraliza et al., 1995; Munder et al., 1998). iNOS catalyzes the conversion of arginine to citrulline and nitric oxide (NO) and plays an important role in bactericidal activity (Biswas and Mantovani, 2012).

Hypoxia inducible factors, HIF1α and HIF2α, are master regulators of cell response to hypoxic stress (Taylor et al., 2016). HIF1 comprises of two subunits, HIF1α and HIF1β. HIF1β is constantly expressed whereas HIF1α is unstable and undergoes degradation. In resting cells, HIF1α is hydroxylated by pyrolyle hydroxylase (PHD) which is later ubiquitinated by E3 ubiquitin ligase followed by proteasomal degradation. Therefore, in normoxia, HIF1α is only present at very low

levels. During hypoxia, PHD activity is inhibited, leading to stabilization of HIF1α. HIF1α is then translocated to the nucleus and binds to hypoxia response elements (HRE) and initiates transcription of inflammatory genes (Corcoran and O'Neill, 2016; Taylor et al., 2016). HIF1α has been shown to be significantly increased during M1 polarization. (Corcoran and O'Neill, 2016; Mills et al., 2016). LPS-activated macrophages have increased levels of succinate, an intermediate of TCA cycle. Tannahill *et al.* demonstrated that this accumulation of succinate leads to the stabilization of HIF1-α and subsequently triggers the increased expression and release of IL-1β (Tannahill et al., 2013). Inhibiting glycolysis by treating LPS-activated macrophages with 2-deoxyglucose (2-DG) inhibited the LPS-mediated stabilization of HIF1-α in BMDMs (Tannahill et al., 2013). Interestingly, the LPS-mediated release of TNF-α remained unchanged with 2-DG, indicating the specificity of the pathway to IL-1β (Tannahill et al., 2013). More recently, the same group showed that LPS-activated macrophages present an increase in succinate oxidation by succinate dehydrogenase (SDH) (complex II of RC). The authors proposed that in the context of decrease oxygen consumption, this increased succinate oxidation contributes to explain the rise in the mitochondrial membrane potential and the enhanced mROS production, which then leads to HIF1-α stabilization and IL-1β release. The authors suggested that upon exposure to LPS, macrophage produces mROS at complex I through reverse electron transport (RET). Additionally, it was shown in this study that dimethyl malonate (DMM), an inhibitor of succinate oxidation, promotes an anti-inflammatory outcome in macrophages. Furthermore, dissipation of mitochondrial membrane potential with the mitochondrial uncoupler CCCP counteracts the effect of LPS on mROS and IL-1β production (Mills et al., 2016).

The metabolic phenotype of M2 macrophages is drastically different from this of M1 macrophages. M2 macrophages display increase oxidative phosphorylation, increased fatty acid oxidation associated with an increase in oxygen consumption (Biswas and Mantovani, 2012; Galván-Peña and O'Neill, 2014). Alternatively activated macrophages possess anti-inflammatory and tissue repair properties, hence relying on oxidative phosphorylation to fulfill their long term energy demand. IL-4 induces M2 polarization namely through the activation of STAT6. STAT6 was shown to regulate PGC-1β (Peroxisome proliferator-activated receptor (PPAR) γ-coactivator-1β)

a cofactor known for promoting mitochondrial biogenesis and fatty acid oxidation (Galván-Peña and O'Neill, 2014; Vats et al., 2006).

Altogether, these studies suggest that macrophage function and specialization are tightly related to the modulation of the metabolism and mitochondrial function in macrophages.

Chapter 3: Mitochondria

Mitochondria are the metabolic hubs of the cells and are frequently designated as "power house of the cells". They vary in number and morphology (size and shape) from one cell to another, and even within the same cell type. Initially, two structures were observed with the light microscope: filaments (mito) and grains (chondria) that they thought to be different structures with different functions. Later, with the development of technology, they were found to be the same functional organelles (Scheffler, 2011). Apart from the production of energy, mitochondria also play a role in calcium signaling and homeostasis (Jacobson and Duchen, 2004), cell cycle as well as apoptosis (Danial and Korsmeyer, 2004). Recent studies have shed light on a novel role of mitochondria in immunity (Weinberg et al., 2015). Therefore, knowledge of the basic structural components of mitochondria is important to better understand the molecular mechanism involved in the contribution of mitochondria to immunity.
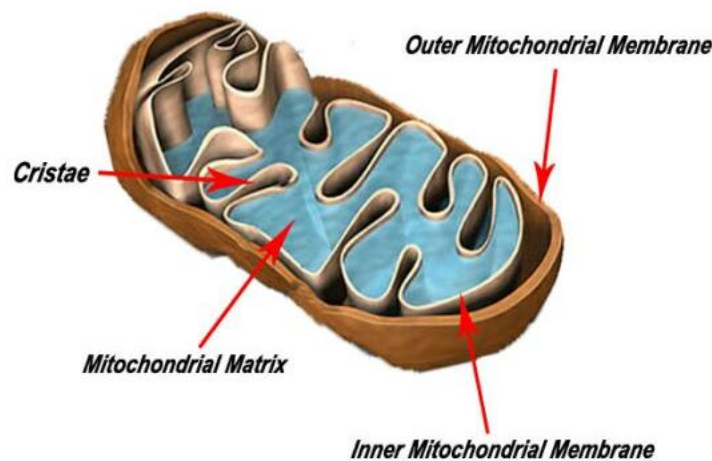
Figure 12: The structure of Mitochondrion

Structure of mitochondria

The typical mitochondria are made of an outer membrane, an inner membrane (cristae), an intermembrane space, a mitochondrial matrix and mtDNA. (Figure: 12).

The outer mitochondrial membrane

The outer membrane is enriched with numerous integral proteins called porins which act as membrane channels and allow the free movement of molecules up to the size of 5000 Da (including nutrients, ions, ATP and ADP). The voltage-dependent anion channels (VDAC) are channels found on the outer mitochondrial membrane which allow the movement of small hydrophilic molecules (Shoshan-Barmatz et al., 2006). VDAC in association with adenine nucleotide translocase (ANT) (a component of the inner mitochondrial membrane) and cyclophilin-D (from the mitochondrial matrix) forms a multiprotein complex called mitochondrial permeability transition pore (MPTP) (Crompton, 1999; Halestrap and Brenner, 2003). VDACs are also known as targets of pro- and anti-apoptotic proteins, and allow the release of apoptosis inducing proteins from the outer mitochondrial membrane through MPTP opening into the cytosol (Crompton, 1999; Shoshan-Barmatz et al., 2006).

Inner Membrane of Mitochondria (IMM)

The inner membrane of mitochondria contains a number of invaginations/convolutions known as cristae. They are much more complex in structure than outer membrane. These invaginations or cristae provide a larger surface area and more complexity, depending upon the energy demand of the cells (Scheffler, 2011). Large, highly folded and lamellar cristae are found in muscle and neurons where the rate of respiration and energy demand is high (Scheffler, 2011). The morphology and structural arrangement of the cristae are controlled by mitofilin (John et al., 2005). The inner membrane contains multiprotein complexes that are the main source of adenosine triphosphate (ATP) production. These multiprotein complexes are known as respiratory chain complexes (RCC). RCC comprise four complexes (from I to IV) and the F_1F_0 ATP synthase (also called complex V). RCC utilizes the electrons from by NADH, H^+ and FADH2, produced by glycolysis, β-oxidation and Krebs cycle. These electrons are transferred through different complexes to the complex IV where molecular oxygen (O_2) is reduced to water (H_2O). RCC also utilizes two electron transporters including ubiquinone (coenzyme Q) and cytochrome c. Ubiquinone and cytochrome c transfer electrons from complex I/II to complex III and complex III to complex IV, respectively. Concomitantly with electron transfer, the protons are continuously

pumped from the inner mitochondrial matrix into the intermembrane space (IMS) through proton pumping enzymes (Complex I, II, & IV). It creates a proton motive force, also referred as mitochondrial membrane potential. This proton gradient is later utilized to run the ATP synthase machinery and to produce ATP from ADP and inorganic phosphate (iP) (Figure 13). The complete process is termed as oxidative phosphorylation (Speakman, 2003). The inner mitochondrial membrane also contains adenine nucleotide translocase (ANT), which acts as a transporter for ADP across the inner membrane. It also forms an important component of mitochondrial permeability transition pore (MPTP) and plays an important role in programmed cell death (Halestrap and Brenner, 2003).
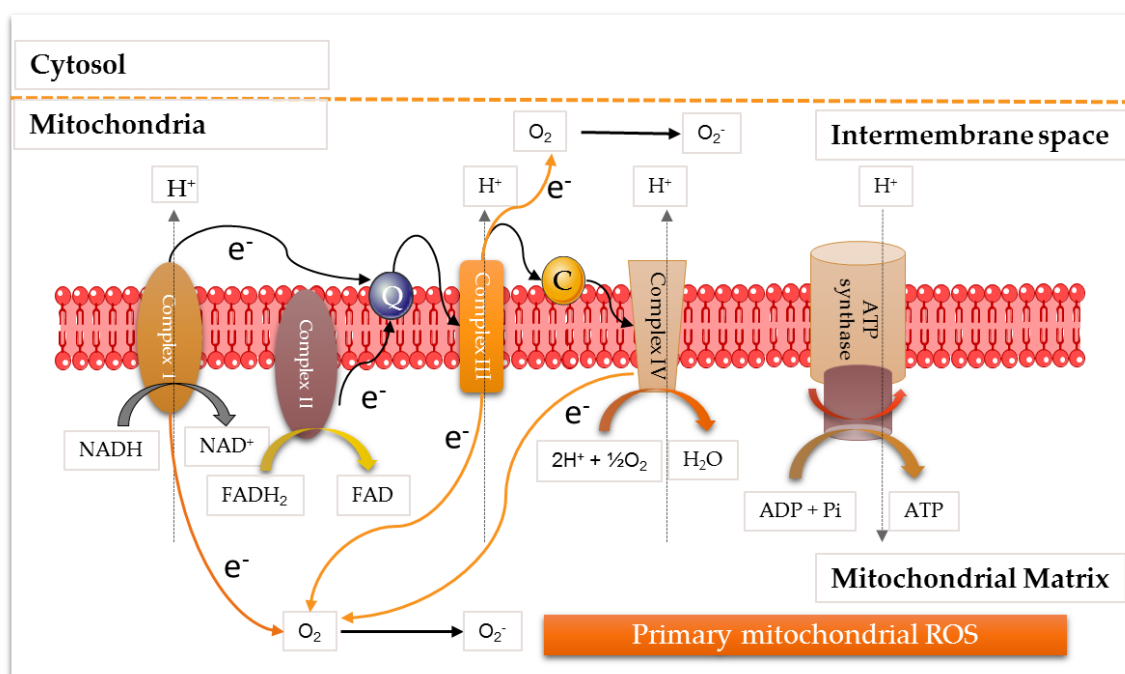
Figure 13: Respiratory chain complexes and site of ROS generation

Mitochondrial ROS Production

During the whole process of electron transport and ATP generation, there is continuous leakage of electrons from respiratory chain complexes which react with molecular oxygen (O_2) in the mitochondrial matrix and causes incomplete reduction of molecular oxygen. It produces superoxide anions ($\bullet O_2^-$) (Turrens, 2003) which later react with other molecules and act as

precursors of other ROS (Turrens, 2003). Main sites of mROS generation are depicted in figure 13.

The three major ROS produced in cells are hydrogen peroxide (H_2O_2), superoxide anion (O_2^-) and Hydroxyl Radical (•OH). Among these ROS, H_2O_2 is more stable and is considered as a secondary messenger in various cell signaling. •OH is the strongest oxidant in nature (Turrens, 2003). The chain reaction as given below (Macdonald et al., 2003; Scheffler, 2011).

$$O_2^- \longrightarrow {}^{\cdot}O_2^- \longrightarrow H_2O_2 \longrightarrow {}^{\cdot}OH \longrightarrow H_2O$$

| Molecular oxygen | Superoxide anion Radical | Hydrogen peroxide | Hydroxyl Radical | Water |
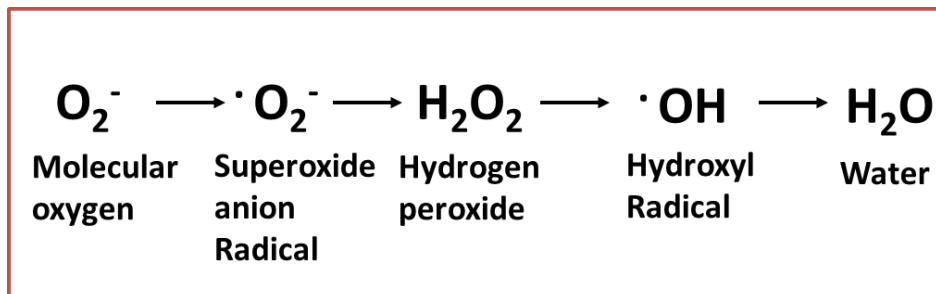
Under normal physiological conditions, ROS remain at normal levels whereas superfluous ROS is neutralized by the cellular antioxidant system. Intracellular ROS levels are controlled by various antioxidants, including catalase, superoxide dismutase (SOD) and glutathione peroxidase and glutathione reductase. ROS play an important role in cellular physiology and act as signaling molecules (Ray et al., 2012). Under some pathophysiological conditions, the imbalance between ROS and antioxidant system leads to higher levels of cellular ROS (a condition referred as oxidative stress). High level of ROS can damage intracellular lipids, proteins, polysaccharides and nucleic acids (DNA) (Speakman, 2003). Apart from mROS, there are various other sources of ROS in the cell. NADPH oxidase enzyme located on the plasma membrane or on the membrane of phagosome also produces ROS (Nauseef, 2004). NADPH oxidase utilizes molecular oxygen as an electron acceptor for the oxidation of NADPH and produces superoxide anions ($O_2^-•$) (Nauseef, 2004). NADPH oxidase also produces ROS inside the phagosome containing microbes where it helps to kill invading microbes.

West *et al.* have recently shown a role of mROS in bactericidal activity of macrophages (West et al., 2011a). They proposed that, apart from ROS produced by NADPH oxidase inside the phagosome, mROS also contributes to the killing of intracellular bacteria (West et al., 2011a). They proposed that the mechanism involves an interaction between TRAF6 and ECSIT proteins

which leads to the destabilization of complex I of RCC and increased production of mROS (West et al., 2011a). Nevertheless, its mechanism is controversial and has been debated in few recent publications from O'Neill group. In mitochondria, mROS are mainly released from complex I and complex III of respiratory chain complexes (RCC) (Drose and Brandt, 2012). Inhibition of these complexes by pharmacological agents like Rotenone (inhibitor of complex I) and antimycin A (inhibitor of complex III) are known to induce mROS production (Koopman et al., 2010). Furthermore, the accumulation of damaged and dysfunctional mitochondria is also considered as an important source of ROS. It was shown that increase in mROS can lead to the activation of the NLRP3 inflammasome and initiate an immune response (Zhou et al., 2011).

These observations strengthen the hypothesis of a key role of mitochondria in host defense namely through the increase in mROS production in macrophages.

Mitochondrial DNA

Apart from the genomic DNA in the nucleus, mitochondria are the only organelles which contain its own DNA. DNA in the mitochondria is arranged into protein-DNA complex called nucleoids (Spelbrink, 2010). Each nucleoid comprises of several copy numbers of mtDNA (Spelbrink, 2010). The number of the nucleoid in the cells varies from one cell to another, from one species to another, and is dependent on growth conditions (Spelbrink, 2010). In mammals, mtDNA is circular and comprises of 16.5 kilo base pairs (Kbps). The mtDNA encodes 13 peptides for the different components of respiratory chain complexes, 2 ribosomal RNA (rRNA) and 22 tRNA (Scarpulla, 2008; Scheffler, 2011). The replication and transcription of mtDNA is regulated by mitochondrial transcription factor A (TFAM) (Scarpulla, 2008) and it acts as a limiting factor for mtDNA copy number and proteins encoded by the mitochondrial genome (Scarpulla, 2008) .

Mitochondrial dynamics and its regulation

Mitochondria are dynamic organelles. They are endowed with the abilities to move within cell, to divide, proliferate and fuse with other mitochondria to form a mitochondrial network. They vary in size and shape and can be found as interconnected filamentous or elongated network. They can also appear as fragmented pieces. Mitochondrial dynamics is the result of a balance

between two key processes: fission and fusion. Both processes are tightly regulated by a number of dynamin related proteins as discussed below and as summarized in figure 14.
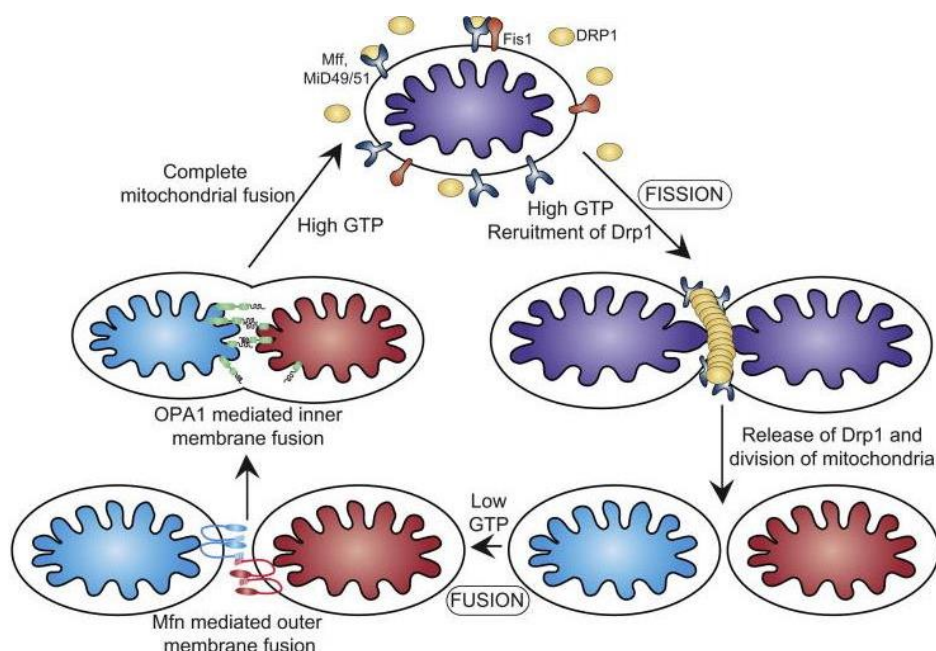
Figure 14: Mitochondrial dynamics

On the left-hand side, mitochondrial fusion is described. It requires fusion of outer mitochondrial membrane that is mediated by mitofusin 1/2 followed by tethering and merging of the inner mitochondrial membrane that requires OPA1. On the right-hand side, mitochondrial morphology relies on the balance between mitochondrial fission and fusion. Mitochondrial fission is mediated by Drp1 which is distributed on mitochondria and cytosol and becomes oligomerized at the site of fission and induce fission (Osellame et al., 2012)

Mitochondrial Fission

Mitochondrial fission is a process of mitochondrial division that occurs as one of the major events at the time of cell proliferation. Microscopy analysis has suggested that mitochondrial stretching is followed by fission. Interestingly, studies have suggested that mitochondria share the components of division machinery with peroxisomes (Scheffler, 2011). The mechanism of fission was initially studied in yeast. There is a limited amount of knowledge available on fission-related proteins in mammals. In yeast, the mitochondrial fission involves the interaction of three outer mitochondrial membrane proteins Fis1p, Mdv1p and Dnp1p (Hoppins et al., 2007). Fis1p is

distributed on the outer mitochondrial membrane. It is anchored to the membrane through its C-terminus, while the N-terminal faces the cytosol (Hoppins et al., 2007). Fis1p interacts with another outer mitochondrial membrane protein: Mdv1p. Mdv1p later facilitates the recruitment of Dnp1p, a dynamin-related GTPase, to form a complex of three proteins: Fis1p-Mdv1p-Dnm1p (Hoppins et al., 2007; Scheffler, 2011). The exact mechanism of fission remains unknown. In humans, Drp1 (also called DNM1L) and hFis1 are known to regulate mitochondrial fission and are orthologs of yeast Dnm1 and Fis1, respectively (Hoppins et al., 2007).

Dynamic related protein1 (Drp1) was found to regulate mitochondrial division in *Caenorhabditis elegans* (Labrousse et al., 1999) as well as in mammalian cells (Smirnova et al., 2001). Drp1 in mammals and Dnm1 in yeasts are both considered as master regulators of mitochondrial fission (Hoppins et al., 2007). Drp1/Dnm1 is distributed in the cytosol as well as on the outer mitochondrial membrane (Labrousse et al., 1999; Smirnova et al., 2001). Mutation in Drp1 gene has been associated with increased mitochondrial network whereas its overexpression induced mitochondrial fragmentation (Labrousse et al., 1999). Similarly to Drp1, Fis1 is also considered as an essential component of mitochondrial fission machinery in humans. Fis1 is a low molecular weight protein (18 kDa) anchored at the outer mitochondrial membrane through its C-terminal (Stojanovski et al., 2004; Yoon et al., 2003). Like Drp1, Fis1 overexpression has been shown to induce mitochondrial fragmentation whereas genetic knockdown or silencing was shown to be associated with a tubular mitochondrial network (Hoppins et al., 2007; Stojanovski et al., 2004; Yoon et al., 2003).

Apart from its role in morphology and mitochondrial division, mitochondrial fission is also considered as a major event during mitochondrial autophagy (mitophagy). It will be described in details in the next chapter. Mitochondrial fission events are summarized in Figure 14.

Mitochondrial Fusion

The collision between mitochondria leads to the fusion that requires contact between membranes of mitochondria (Scheffler, 2011). The fusion of mitochondria leads to the formation of elongated and tubular mitochondrial networks. Mitochondrial morphology relies on a balance between mitochondrial fusion and fission (Figure 14). Mitochondrial fusion is regulated by a family of GTPase which are considered as fusion machinery of mitochondria. In Drosophila

spermatogenesis, proteins encoded by fuzzy onions (Fzo) genes were recognized as the founding members of the mitochondrial fusion process (Hales and Fuller, 1997). It should be stressed here that mitochondria are double membrane organelles and that the fusion requires merging of both outer and inner mitochondrial membranes. GTPase proteins that mediate fusion of inner and outer mitochondrial membrane belong to the family of dynamin superfamily of proteins. In mammals, it includes mitofusin (Mfn) 1 and 2 (mammalian homologue of fzo genes that mediate fusion of outer membrane) and optic atrophy type 1 (OPA1) which mediate fusion of inner mitochondrial membrane (Hoppins et al., 2007). These proteins are important for maintaining overall health and functions of mitochondria. Mice deficient in one of the mitofusin proteins failed to survive at an embryonic stage. Mouse embryonic fibroblasts (MEFs) from Mfn1- or Mfn2-deficient mice showed fragmented mitochondria and decreased fusion (Chen et al., 2003). Mfn double mutant (Mfn-dm) cells showed almost no mitochondrial fusion (Chen et al., 2005). Cells from Mfn1- or Mfn2-deficient mice showed variation in mitochondrial membrane potential and reduced respiration (Chen et al., 2005).

The inner mitochondrial membrane fusion is mediated by OPA1 (Mgm1 in yeast). Invalidation of OPA1 by RNA interference experiments resulted in fragmented mitochondria and lack of mitochondrial fusion (Chen et al., 2005; Cipolat et al., 2004). It was suggested that OPA1 requires Mfn1 (but not Mfn2) for inner mitochondrial membrane fusion (Cipolat et al., 2004). The mutation in OPA1 gene is known to be associated with autosomal dominant optic atrophy, loss of visual acuity in human (Alexander et al., 2000; Delettre et al., 2000). Like yeast Mgm1, the OPA1 human homologue of Mgm1 is also cleaved by proteolytic enzymes to produce isoforms of OPA1 (Hoppins et al., 2007). Because there are different splice variants for OPA1, processing of OPA1 might vary from a tissue to another (Delettre et al., 2001; Hoppins et al., 2007). Although the exact mechanism of OPA1 processing is still unknown, it involves the mitochondrial proteases PARL (Presenilins-Associated Rhomboid-Like protein) and paraplegin (Cipolat et al.; Hoppins et al., 2007; Ishihara et al., 2006). PARL-deficient mice were shown to possess fewer amounts of short and soluble isoforms of OPA1 (Cipolat et al.; Hoppins et al., 2007; Ishihara et al., 2006).

Mitochondrial dynamic-related proteins Mfn1, Mfn2 and OPA1 not only regulate mitochondrial morphology and fusion but are also involved in other functions of mitochondria. Apart from the

inner mitochondrial membrane fusion, OPA1 was found to regulate the structure of cristae (Olichon et al., 2003; Smirnova et al., 2001).

Mitochondrial biogenesis

Damaged and dysfunctional mitochondria are removed through the process of mitochondrial autophagy (mitophagy) and replaced by newly formed mitochondria through mitochondrial biogenesis. Mitochondrial biogenesis takes place at the basal level and can even increase in order to fulfill the energy demand and to maintain the viable pool of mitochondria.

Mitochondrial biogenesis is a complex process as it involves the transcription, translation and recruitment of translated proteins into mitochondria from two different sources. As mtDNA encodes only 13 proteins that are essential for the function of respiratory chain complexes, all other proteins are encoded by nuclear DNA (Dominy and Puigserver, 2013; Scarpulla, 2008). Mitochondrial biogenesis is regulated by different transcription factors and co-activators including Peroxisome proliferator-activated receptor gamma co-activator 1-alpha (PGC1-α), mitochondrial transcription factor A (TFAM), nuclear respiratory factors (NRFs), and estrogen-related receptors (ERRs) (Palikaras and Tavernarakis, 2014). PGC1-α is considered as a master regulator of mitochondrial biogenesis. It belongs to the family of co-activators of Peroxisome proliferator activated receptor (PPARs) (Dominy and Puigserver, 2013). Transcription co-activators do not bind directly to the DNA but they promote the transcriptional activity of other transcription factors (Dominy and Puigserver, 2013). The PGC-1 family of proteins (mainly PGC-1α and PGC-1β) are known to regulate mitochondrial density, components of RCC, enzymes, components of metabolic pathways, protein import complexes and proteins involved in mitochondrial fission and fusion (Dominy and Puigserver, 2013). They regulate mitochondrial biogenesis and other processes through the regulation of the activity of other transcription factors involved in mitochondrial biogenesis. It includes ERRs, NRFs (Nuclear Respiratory factors) and YY1 (Dominy and Puigserver, 2013).

NRF1 and NRF2 regulate the transcription of a number of mitochondrial genes encoded by the nuclear genome. It includes the mitochondrial transcription factor A (TFAM) and the transcription factor B proteins (TFBs). In turn, TFAM acts as a limiting factor for the replication and transcription of mtDNA (Scarpulla, 2008).

Estrogen-related receptors (ERRs) constitute a family of nuclear hormone receptors. It includes ERR-α, ERR-β and ERR-γ. ERRs induce the biogenesis of different components of mitochondria in response to hormones. ERR-α has been known to regulate transcription of mitochondrial genes encoded by the nuclear genome, such as components involved in oxidative phosphorylation, fatty acid oxidation, TCA cycle, and factors regulating mitochondrial fusion and fission (Dominy and Puigserver, 2013; Palikaras and Tavernarakis, 2014).

Different signals regulate mitochondrial biogenesis. One of the important pathways involves activation of AMP activated protein kinase (AMPK) (Jager et al., 2007). AMPK is activated in response to a high AMP/ATP ratio, either due to low ATP level or high ATP demand (Hardie, 2007). AMPK induces mitochondrial biogenesis through regulation of nuclear-encoded mitochondrial genes (Palikaras and Tavernarakis, 2014). It has been shown that mitochondrial biogenesis is stimulated by AMPK through direct phosphorylation of PGC1-α (Jager et al., 2007). PGC1-α activity is also modulated by several other mediators including p38 mitogen activated protein kinase and calcium/ calmodulin-dependent protein kinase (CaMK) and in response to calcium signaling (Palikaras and Tavernarakis, 2014; Wright et al., 2007; Wu et al., 2002). Mitochondrial biogenesis is also stimulated by deacetylation of PGC1α mediated by SIRT1 (Cantó et al., 2009). AMPK activation leads to the increased concentration of NAD^+, which in turn activates SIRT1 and thereby increases mitochondrial biogenesis (Cantó et al., 2009).

Mitochondrial biogenesis along with mitophagy constitutes the quality control process of mitochondria. Mitophagy and autophagy are closely related processes. Understanding the mechanism of autophagy is helpful to decipher the mechanisms of mitophagy.

Chapter 4: Autophagy and Mitophagy

Autophagy

Autophagy (self-eating) is considered as a housekeeping and quality control process of cells in which cytoplasmic contents are degraded into simpler forms either for clearance or to fulfill energy demand of the cell. There are three different types of autophagy processes: (I) microautophagy, (II) chaperone-mediated autophagy, and (III) macroautophagy (Mizushima et al., 2008). These are described in Figure 15 (Schneider and Cuervo, 2014).

(I) In microautophagy, cytoplasmic contents are directly delivered to lysosomes and degraded by lysosomal enzymes (Boya et al., 2013). (II) Chaperone-mediated autophagy involves direct recognition of targeted proteins by a molecular chaperone (Hsp70), which is later delivered directly to the lysosome. The delivery of the protein to the lysosome requires its interaction with lysosomal membrane protein LAMP-2A (Boya et al., 2013). (III) Macroautophagy involves engulfment and degradation of the bulk cytoplasmic contents including bulk proteins and organelles (Boya et al., 2013; Komatsu and Ichimura, 2010). This thesis focuses on macroautophagy only which will be referred hereafter as autophagy. Figure 15 depicts the autophagic pathways involved in hepatocytes (Schneider and Cuervo, 2014).

Autophagy is a process in which cytoplasmic contents (macromolecules like proteins and lipids) or even cellular organelles are captured by double membrane structures called autophagosomes. They are globular organelles with a diameter of approximately 1 µm (Komatsu and Ichimura, 2010). Autophagosome later fuses with lysosome, giving rise to a single membrane structure called autophagolysosome (autolysosome) which in turn leads to degradation of the contents of autophagosome by lysosomal enzymes (Mizushima et al., 2008).

Autophagy, as a catabolic process, provides amino acids after the degradation of macromolecular structures, thereby acting as a source for energy production and protein synthesis (especially in the condition of starvation) (Komatsu and Ichimura, 2010). Mutations in autophagy genes in *Saccharomyces cerevisiae* were found to be associated with defective protein degradation in response to nitrogen starvation (Tsukada and Ohsumi, 1993). Similarly, autophagy in mammals

was found to be a survival mechanism in response to the early cut-off of placental nutrition at the time of birth in neonates (Kuma et al., 2004). Beyond the role of autophagy in starvation, and under normal conditions, basal autophagy is known to play a role in cellular homeostasis and to act as housekeeping process. It removes unnecessary and dysfunctional proteins to maintain the cellular integrity and health (Komatsu et al., 2007).
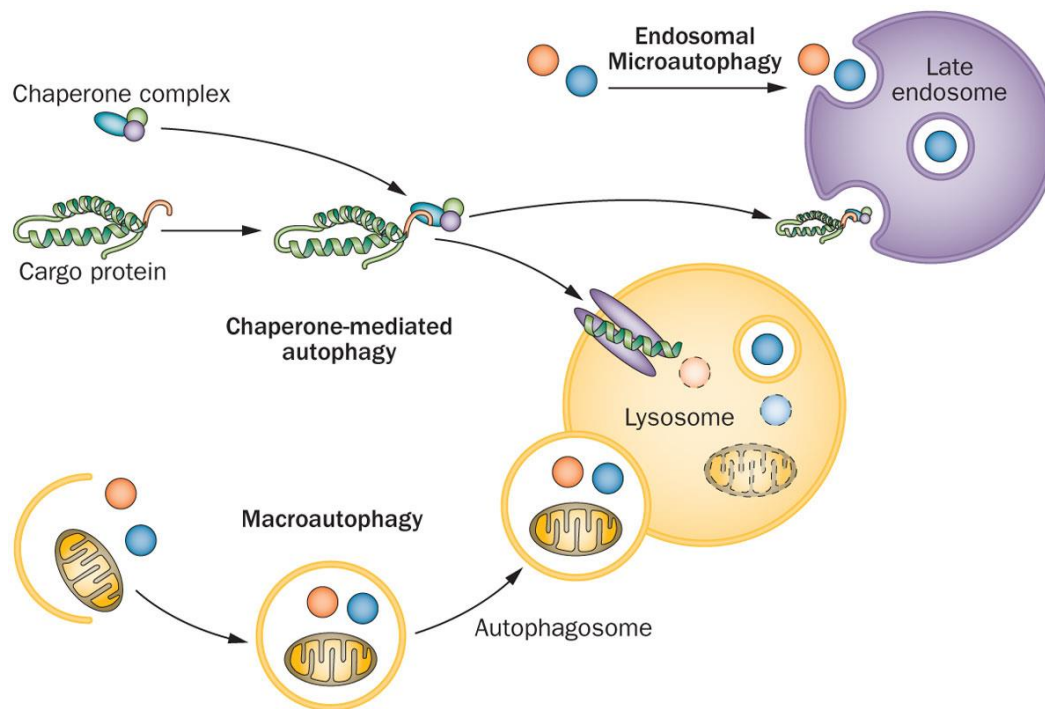
Figure 15: Pathways of autophagy (Schneider and Cuervo, 2014)

The defects in autophagy or genetic ablation of autophagy-related proteins were shown to be associated with neurodegenerative diseases, cancer, infections, and aging (Mizushima et al., 2008). Autophagy is a survival mechanism for the cells and it protects them from a different kind of cellular stress. It also plays an important role in apoptosis and cell death (Mizushima et al., 2008). Under some pathological conditions like cancer, autophagy can act as a protective mechanism for tumor cells, with chemotherapeutic-induced cellular stress leading to the resistance to chemotherapeutic agents and worsening of a pathological condition (Levine and Kroemer, 2008). Therefore understanding the underlying molecular mechanism of autophagy should enable to improve outcomes of different therapeutic agents.

Mechanism of autophagy

The mechanism of autophagy can be primarily divided into several main steps as follows: (1) formation of double-membrane isolation membrane, (2) elongation of phagophore, (3) sequestration of cargo and formation of autophagosome, (4) Maturation to autolysosome (fusion of autophagosome with lysosome to form autophagolysosome (autolysosome)) (5) lysosomal degradation of entrapped cargo. The schematic representation of mechanism of autophagy is depicted in Figure 16.
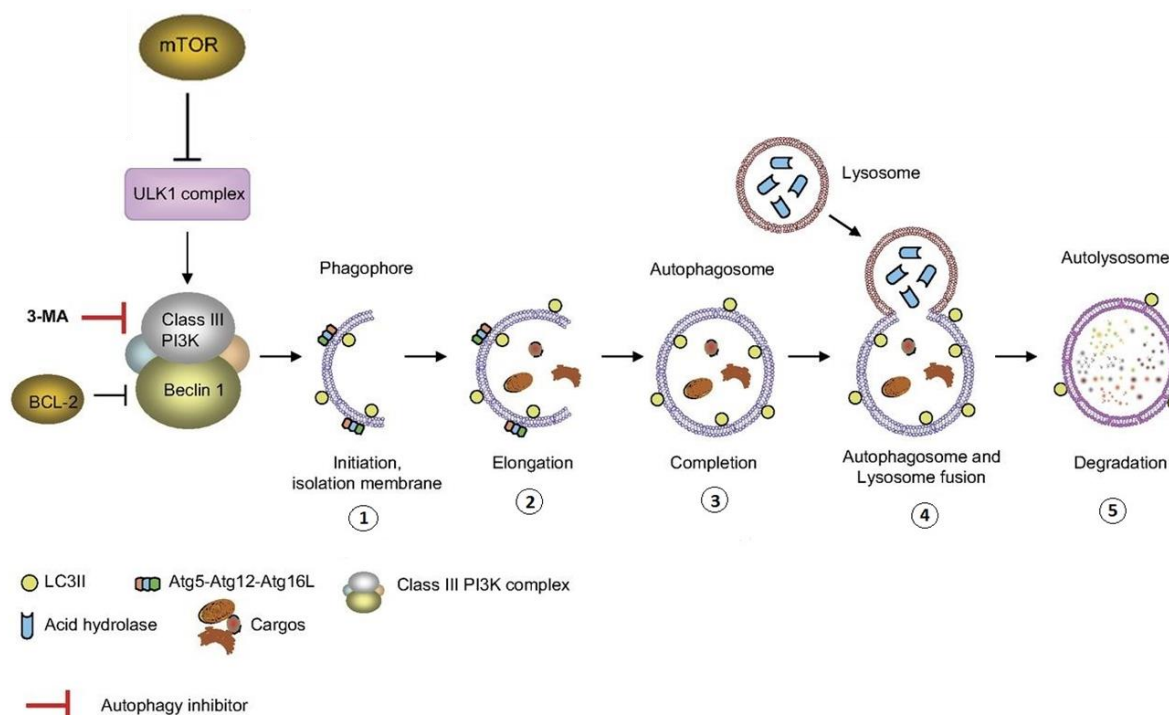
Figure 16: Mechanism of autophagy (adapted from (Nakahira and Choi, 2013))

Initiation of autophagy requires inhibition of mammalian target of rapamycin (mTOR). mTOR is a serine/threonine protein kinase. Under normal conditions, mTOR inhibits the activity of two kinase proteins including unc-51-like kinase 1 and 2 (ULK 1/2). ULK 1/2 are the mammalian homologs of yeast Atg1 protein. The activity of mTOR is inhibited in starvation or with mTOR inhibitor (rapamycin). Inhibition of mTOR leads to the activation ULK 1/2. Activation of the

ULK1/2 complex, in turn, activates the formation of PI3 kinase complex and initiates the phagophore formation (Glick et al., 2010; Nakahira and Choi, 2013).

mTOR is activated in response to MAPK and Akt signaling pathway. PI3K inhibitors like 3-methyl adenine have also been shown to activate mTOR and to inhibit autophagy. At the opposite, starvation and increased concentration of AMP leads to the activation of AMPK, which in turn inhibits mTOR thereby inducing autophagy. P53 signaling also inhibits mTOR and induces autophagy.

The elongation of the phagophore to form a mature autophagosome involves two ubiquitin-like conjugation systems (Glick et al., 2010). Firstly, the elongation of the phagophore requires the incorporation of multimeric protein complexes of Atg16L-Atg5-Atg12 into the phagophore. The second step required for the formation of autophagosomes. It involves processing of microtubule-associated protein light chain 3 (LC3B) protein and its incorporation into autophagosomes (Glick et al., 2010). Pro-LC3B is cleaved by Atg4 to form LC3B-I which then gets conjugated with phosphatidylethanolamine (PE) and forms LC3B-II (Glick et al., 2010). Later, LC3B-II is incorporated into the phagophore with the help of Atg5-Atg12. LC3-II is present on the both surfaces of autophagosome and contributes to the recognition of the cargo as well as fusion of the membranes (Glick et al., 2010). LC3B-II is widely used as an indicator of autophagy flow in the cells (Barth et al., 2010).

During the elongation process, a cargo is engulfed through a selective or a non-selective pathway. The selective pathway of autophagy may require an additional adaptor protein which may be p62/SQSTM1, NBR1, NDP52 or optineurin (Boya et al., 2013). These adaptor proteins contain ubiquitin-associated domain (UBA) through which they recognize the ubiquitinated cargo. They also contain an LC3 interacting region (LIR) which helps to facilitate the interaction with LC3B-II and engulfment by autophagosome (Boya et al., 2013). Mature double membrane autophagosome then fuses with the lysosome to form a single membrane structure called autophagolysosome. The entrapped cargo (cytosolic protein or organelles) are degraded by lysosomal hydrolases and delivered back to the cytoplasm for recycling.

The selective form of autophagy can target specific cellular organelles. It is named differently such as autophagy targeting peroxisome or mitochondria which are referred as pexophagy (Kim et al., 2008) or mitophagy (Geisler et al., 2010; Novak and Dikic, 2011), respectively. The autophagy also plays a role in the removal of invading microorganism like bacteria and viruses and is referred as xenophagy (Orvedahl et al., 2010; Thurston et al., 2009). Since mitochondria are vital organelles, autophagy dedicated to mitochondria plays a critical role in health and diseases. This will be discussed in details in the next section.

Mitophagy

Introduction to Mitophagy

Mitophagy is a selective form of autophagy dedicated to mitochondria. It is a part of quality control process. In total, three different pathways of mitochondrial quality control are known: (1) Degradation of unfolded proteins by AAA protease of mitochondria, (2) degradation of oxidized mitochondrial proteins by lysosome delivered by mitochondrial derived vesicle (MDVs), and (3) degradation of whole mitochondria by selective autophagy referred as mitophagy (Ashrafi and Schwarz, 2013). These three pathways are depicted in figure 17. Mitophagy involves detection of damages or mitochondrial dysfunction, entrapment of dysfunctional mitochondria by the autophagosomal assembly, and finally degradation of mitochondria by lysosomal enzymes.

Mitochondria are dynamic organelles that continuously undergo the processes of fission and fusion. These both processes affect mitochondrial clearance (Twig and Shirihai, 2011). Mitophagy occurs at a basal level to maintain a healthy and functional mitochondrial pool. Mitochondria constitute a main source of ROS. Thus, damaged or nonfunctional mitochondria could alter ROS production. Increased mROS may also contribute to damage the mitochondrial components and may also cause the release of pro-apoptotic proteins (cytochrome-c and apoptosis inducing factors), leading to the cell death (Scherz-Shouval and Elazar, 2011; Twig and Shirihai, 2011). mROS can oxidize cellular and mitochondrial lipids, proteins and DNA (Scherz-Shouval and Elazar, 2011). Therefore, the removal of ROS producing mitochondria is an important process to maintain the cellular integrity and health (Scherz-Shouval and Elazar, 2011).
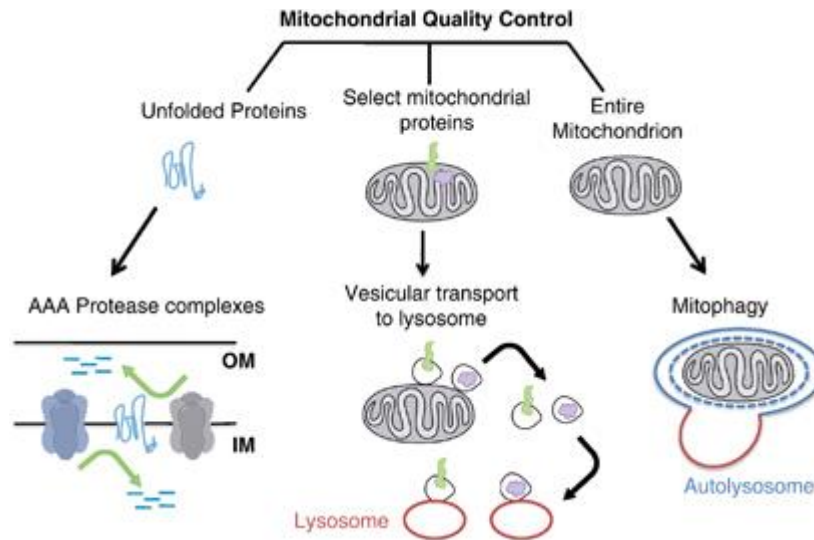
Figure 17: Pathways of mitophagy (Ashrafi and Schwarz, 2013)

Mechanism of the mitophagy process

Mitophagy is mainly regulated by three key proteins along with the contribution of mitochondrial proteins involved in dynamics of mitochondria. These three key proteins include PINK1, Parkin, and DJ-1. Mutations in the genes encoding these proteins have been associated with the autosomal recessive form of Parkinson's disease (Bonifati et al., 2003; Dodson and Guo, 2007; Kitada et al., 1998; Valente et al., 2004). Defects in different mitochondrial functions are known to contribute to the development neurodegenerative diseases including Parkinson's disease (Exner et al., 2012). The three proteins were shown to physically interact and to form an E3 ubiquitin ligase complex. This protein complex regulates the degradation of proteins mediated by the ubiquitin proteasome system (Xiong et al., 2009). It is should be noted here that the exact mechanism of DJ-1 in the ubiquitin ligase activity of the complex is not known yet. Therefore, it will be discussed separately and in details in the next section dedicated to DJ-1.

PINK1 (PTEN-induced putative kinase 1) is a serine/threonine kinase that continuously senses the mitochondrial health (Nguyen et al., 2016). Therefore, a classical method used to promote mitophagy is to trigger a drop in the mitochondrial membrane potential through the use of respiratory chain uncouplers such as carbonyl cyanide m-chlorophenyl hydrazine (CCCP) or 2,4

dinitrophenol (2,4DNP). CCCP is the most commonly used. Mitochondrial dysfunction leads to the PINK1-mediated phosphorylation and recruitment of Parkin to the mitochondria, thus initiating mitophagy (Nguyen et al., 2016). The structure of mammalian PINK1 comprises a mitochondrial targeting sequence (MTS), a transmembrane helix and a serine/threonine kinase domain (Figure 18.A) (Trempe and Fon, 2013). Stability of PINK1 on mitochondrial membrane depends on mitochondrial membrane potential. PINK1 is imported to the outer mitochondrial membrane (OMM) and thereby to the inner mitochondrial membrane (IMM) via translocase proteins (TOM and TIM, respectively). The import of PINK1 to the OMM and IMM is driven by transmembrane potential (Greene et al., 2012; Jin et al., 2010). In healthy mitochondria with high mitochondrial membrane potential, PINK1 is first cleaved by matrix processing peptidase (MPP) at IMM to remove mitochondrial targeting sequence (MTS) (Greene et al., 2012). Then PINK1 is cleaved a second time at the position A103 by another inner mitochondrial membrane protease: presenilin-associated rhomboid-like protein (PARL) (Deas et al., 2011; Jin et al., 2010; Meissner et al., 2011). This second cleavage of PINK1 leads to the release of the cleaved form of PINK1 with exposed N-end into the cytosol. Cytosolic cleaved PINK1 is later recognized by E3 ubiquitin enzyme by N-end rule and is degraded by the proteasome (Yamano and Youle, 2013).

The 52 kDa cleaved form of PINK1 that translocates from the mitochondrial membrane to the cytosol in a soluble form that has two fates. Either it is degraded by the ubiquitin proteasome system through N-end rule (Greene et al., 2012; Lin and Kang, 2008; Narendra et al., 2010; Yamano and Youle, 2013) or it binds to the Parkin and inhibits its translocation to the mitochondria, thereby act as a negative regulator of mitophagy as recently shown (Fedorowicz et al., 2014). The corresponding mechanism is depicted in figure 18 (B).

By contrast, damaged or dysfunctional mitochondria displaying a decrease in their membrane potential fail to import PINK1 to the IMM, which spares it from MPP/PARL-mediated cleavage (Deas et al., 2011; Greene et al., 2012; Jin et al., 2010; Meissner et al., 2011). In this case, PINK1 accumulates on the outer mitochondrial membrane (OMM) forming a multimeric, large protein complex with TOM (Figure 19) (Becker et al., 2012; Lazarou et al., 2012).
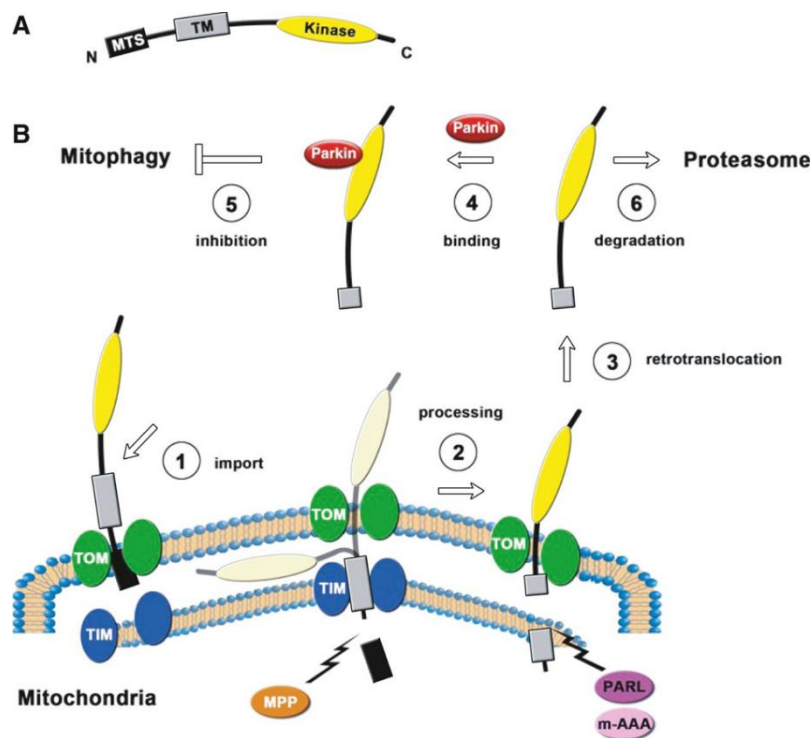
Figure 18: Structure, import and processing of PINK1 (Fedorowicz et al., 2014)

A. Structure of PINK1 comprises three main domains. 1- MTS: Mitochondrial targeting sequence, 2-TM: Transmembrane domain 3- Kinase: kinase domain
B. Import and processing of PINK1
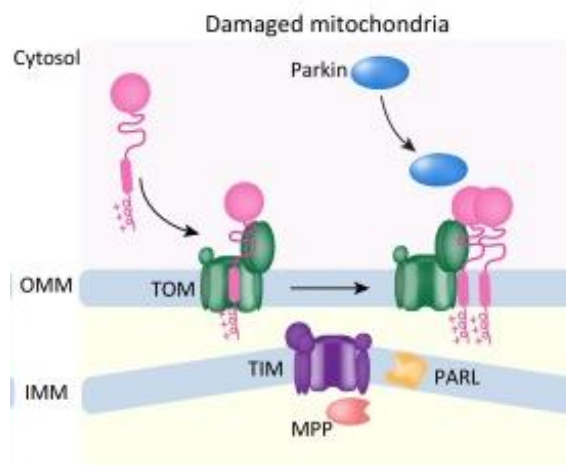
Figure 19: Mechanism of recruitment of PINK1 damaged mitochondria (adapted from (Nguyen et al., 2016)

It was recently shown that the autophosphorylation of PINK1 at ser228 and the ser402 residue is a prerequisite for its kinase activity (Okatsu et al., 2012). PINK1 accumulates on mitochondria and is activated through auto-phosphorylation, with the subsequent phosphorylation and recruitment of Parkin to the damaged mitochondria, thus initiating mitophagy (Okatsu et al., 2012).

Parkin is phosphorylated at position s65 of the ubiquitin-like domain. It was initially considered as mandatory for its activation and recruitment to the mitochondria (Kondapalli et al., 2012; Shiba-Fukushima et al., 2012). However, recent studies have shown that PINK1 also phosphorylates ubiquitin at s65 on OMM which acts as a recruitment site for Parkin (Kazlauskaite et al., 2014; Okatsu et al., 2015; Ordureau et al., 2014; Shiba-Fukushima et al., 2014). Mitofusin 2, a regulator of mitochondrial fusion, is also known to be phosphorylated by PINK1. It was reported that phosphorylated Mitofusin 2 acts as a recruitment site for Parkin. Ablation of Mfn2 prevents the translocation of PARKIN to the mitochondria (Chen and Dorn, 2013). However, previous studies have shown normal Parkin recruitment and mitochondrial degradation in MEFs from Mfn 1/2 double-knock-out mice as compared to controls (Chan et al., 2011; Narendra et al., 2008).

Parkin is a 52 kDa protein comprising 465 amino acids and encoded by the PARK2 gene (Kitada et al., 1998). Parkin is an E3 ubiquitin enzyme (Narendra et al., 2008). E3 ubiquitin ligase enzyme transfers ubiquitin moieties from the E2 ubiquitin-conjugating enzyme to the targeted proteins. Parkin recruitment to damaged mitochondria leads to the ubiquitination of different mitochondrial proteins. VDAC1 was found to be a substrate of Parkin-mediated ubiquitination in CCCP-induced mitophagy (Geisler et al., 2010). Ubiquitination of proteins on the outer mitochondrial membrane allows recognition and engulfment of depolarized mitochondria by autophagosome thanks to autophagy adaptor proteins (Lazarou et al., 2015). Later, the autophagosome-containing mitochondria fuse with lysosomes, leading to the degradation of mitochondrial proteins by lysosomal enzymes. In yeast, the mitophagy receptor Atg32 (a mitochondrial membrane protein), was found to be essential for induction of mitophagy (Kanki et al., 2009; Okamoto et al., 2009). Atg32 interacts with Atg8 and Atg11, and facilitates the encapsulation of mitochondria by the isolation membrane (Kanki et al., 2009; Okamoto et al.,

2009). Recently, Bcl2-L-13 has been reported as a mammalian homologue of Atg32 in yeast (Murakawa et al., 2015). Bcl2-L-13 was found to restore mitophagy in Atg32-deficient yeasts (Murakawa et al., 2015). In HEK293 cells, the silencing of Bcl2-L-13 attenuates the mitochondrial fragmentation and mitophagy in response to the CCCP-mediated uncoupling treatment. It indicates the importance of Bcl2-L-13, an integral mitochondrial membrane protein, in the mitochondrial dynamics and mitophagy (Murakawa et al., 2015). The Bcl2-L-13-mediated mitophagy is independent of Parkin/PINK1, as suggested by the knockdown of Parkin in HEK293 cells which showed a similar level of mitophagy as compared to the control (Murakawa et al., 2015).

In mammals, different receptors for mitophagy have been recognized. All of them are found on the mitochondrial membrane and contain an LC3 interaction region (LIR) motif. These receptors include Bcl-2 homology domain 3 (BH3) family members, BNIP3 and BNIP3L/NIX (NIP3-like protein X) (Stotland and Gottlieb, 2015). BNIP3L/NIX was found to be important for mitophagy during reticulocyte maturation (Schweers et al., 2007). The FUN14 domain containing 1 (FUNDC1) is another adaptor protein for mitophagy, which is essential for the hypoxia-induced mitophagy (Liu et al., 2012). Hypoxia induces dephosphorylation of FUNDC1 in Hela cells. It leads to the induction of mitophagy that is mediated through the interaction between the LIR domain of FUNDC1 and LC3 (Liu et al., 2012). These mitophagy processes which do not utilize PARKIN/ PINK1 are also known as Parkin/PINK1-independent mitophagy (Georgakopoulos et al., 2017). Recently, Optineurin (OPTN) and Nuclear dot protein 52 (NDP52), have been reported as receptors for Parkin/PINK1-mediated mitophagy. OPTN and NDP52 are recruited to the depolarized ubiquitinated mitochondria, which in turn induce formation of phagophore by recruiting autophagy initiating factors: ULK1 (unc-51-like autophagy activating kinase 1), DFCP1(double FYVE-domain containing protein 1) and WIPI1 (WD repeat domain, phosphoinositide interacting 1) (Georgakopoulos et al., 2017; Lazarou et al., 2015).
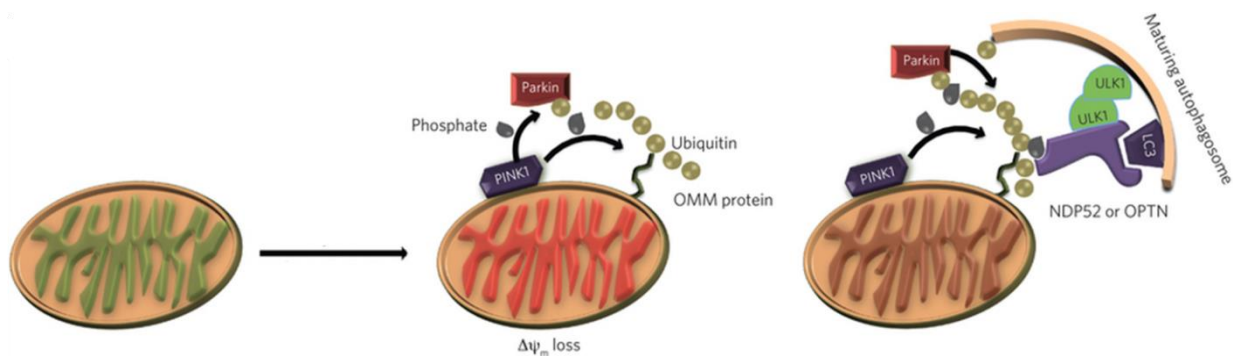
Figure 20: Model of Parkin/PINK1-mediated mitophagy (adapted from (Georgakopoulos et al., 2017))

Figure 20 depicts the model of mitochondrial uncouplers (CCCP) mediated Parkin/PINK1-dependent autophagy, which can be summed-up as follow:

1) Decreased mitochondrial membrane potential leads to the stabilization of PINK1 on mitochondria.

2) PINK1 phosphorylates ubiquitin and recruits Parkin to the depolarized mitochondria.

3) Parkin ubiquitinates mitochondrial targeted proteins and provides ubiquitin substrate for PINK1 to phosphorylate, thereby enhancing the activity of PINK1.

4) Autophagy adaptor proteins (NDP52 and OPTN) are recruited to mitochondria, which in turn recruit autophagy initiating factors (ULK1, DFCP1 and WIPI1) and initiate phagophore formation.

Together, Parkin and PINK1 act as key regulators of mitochondrial quality control system that works in coordination with other mitophagy-related proteins like DJ-1 and mitochondrial dynamic related protein.

DJ-1

DJ-1 is encoded by PARK7 gene. Several mutations in this gene have been associated with the early onset of an autosomal recessive form of Parkinson's disease (Bonifati et al., 2003). It is a small molecular weight (20 kDa) cytosolic protein. It translocates to the mitochondria during oxidative stress and exerts neuroprotective effect (Bonifati et al., 2003; Canet-Avilés et al., 2004). Furthermore, oxidation of cysteine 106 and formation of cysteine sulfinic acid in DJ-1 is a prerequisite for its translocation to mitochondria and neuroprotective activity (Blackinton et al., 2009; Canet-Avilés et al., 2004).

DJ-1 primarily acts as a ROS scavenger and protects cells from oxidative stress. DJ-1 plays important role in mitochondrial functions and stability. However, the exact role of DJ-1 in Parkin/PINK1-mediated mitophagy is not really known. DJ-1 was reported to form a complex with two other mitophagy-related proteins, Parkin and PINK1 (Xiong et al., 2009). This complex of proteins was suggested to promote ubiquitination and degradation of Parkin and synphilin-1 in neuroblastoma cells and human brain lysates (Xiong et al., 2009). It was shown that DJ-1 regulates the stabilization of PINK1 (Tang et al., 2006). Further, PINK1 and DJ-1 are known to protect cells against oxidative stress and pathogenesis of different neurodegenerative diseases like PD and AD, which are associated with increased ROS production (Yan et al., 2013). Loss of DJ-1 in dopaminergic neurons was shown to produce a mitochondrial phenotype similar to that produced by loss of PINK1 (Dagda et al., 2009; Thomas et al., 2011). Loss of DJ-1 and PINK1 was associated with altered mitochondrial morphology (Irrcher et al., 2010), increased mitochondrial fragmentation and oxidative stress (Dagda et al., 2009; Thomas et al., 2011). Loss of DJ-1 resulted in an increased ROS production and decreased mitochondrial membrane potential while the activity of respiratory chain complexes remained unchanged (Giaime et al., 2012; Thomas et al., 2011). It was recently reported that PINK1-mediated Parkin translocation to the mitochondria was negatively regulated by DJ-1 in a ROS-dependent manner (Joselin et al., 2012). Pretreatment of MEF with ROS scavenger significantly reduced translocation of Parkin to the CCCP-mediated depolarized mitochondria (Joselin et al., 2012). These studies suggest that DJ-1 acts as a negative regulator of Parkin/PINK1-mediated mitophagy in neurons (Joselin et al., 2012).

Role of Mitochondrial Dynamics in mitophagy

Mitophagy is tightly linked to modulation of mitochondrial dynamics (Kubli and Gustafsson, 2012). Mitochondria are known as dynamic organelles, which continuously move and undergo fusion and fission processes, depending on the energy requirement and cellular conditions. Mitochondrial fission produces smaller daughter mitochondria. Mitophagy process requires isolating damaged or non-functional parts of the mitochondria to eliminate them in order to maintain a functional mitochondrial network. The isolation of these damaged parts of the

mitochondria relies on the commitment of fission machinery. Isolated parts of the mitochondria are then engulfed through autophagy process (Figure 21).
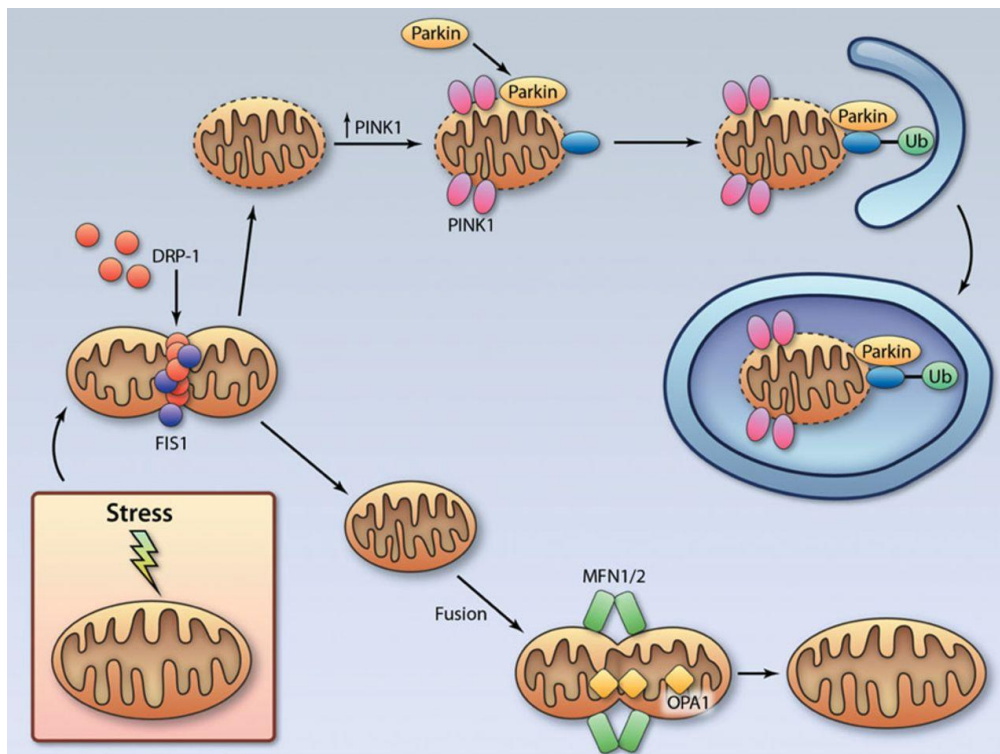
Figure 21: Mitochondrial Dynamics and Mitophagy

Mitophagy process involves DRP1-mediated fission of damaged part of mitochondria from the healthy part. Damaged mitochondria have decreased mitochondrial membrane potential, which allows the stabilization of PINK1. This, in turn, recruits cytosolic Parkin. Recruitment of Parkin leads to the ubiquitination of different proteins on mitochondrial membrane. Ubiquitinated mitochondria are entrapped by the autophagosomal assembly, followed by fusion with lysosome and degradation. Alternatively, healthy mitochondria fuse to form an elongated mitochondrial network that is mediated by mitofusin 1/2 and OPA1. (Kubli and Gustafsson, 2012)

Mitochondria can reach the size up to 5 µm (Cereghetti and Scorrano, 2006), while the diameter of autophagosome is approximately 1 µm (Komatsu and Ichimura, 2010). Encapsulation of such a large mitochondrial network by autophagosomal assembly looks impractical, reflecting the need for mitochondrial fragmentation preceding mitophagy. This idea was further strengthened and supported by several studies showing the role of key mitophagy-related proteins in the regulation of mitochondrial dynamics. Mitochondrial fusion promoting proteins (mitofusin-1 and

mitofusin-2) were shown to be ubiquitinated and degraded by proteasomes in a Parkin/PINK1-dependent manner (Gegg et al., 2010; Glauser et al., 2011; Poole et al., 2010). Moreover, mitochondria are motile organelles equipped with motor proteins (kinesin). Kinesin is attached to the mitochondrial outer membrane by mitochondrial RHO1 (MIRO). It was observed that Parkin/PINK1-mediated mitophagy was associated with the phosphorylation and degradation of MIRO, thereby blocking its motility and fusion with other mitochondria (Wang et al., 2011).

DRP1 was seen to be phosphorylated by protein kinase A (PKA) at ser637 during starvation, thereby inhibiting its translocation to the mitochondria and favoring elongation of the mitochondrial network (Gomes et al., 2011; Rambold et al., 2011). This elongation of mitochondria acts as a protective mechanism from starvation-induced autophagy (Gomes et al., 2011; Rambold et al., 2011). Increased mitochondrial network, due to the unopposed fusion of mitochondria, allows the sufficient production of ATP and better survival (Gomes et al., 2011; Rambold et al., 2011).

All these studies highlight the importance of mitochondrial fragmentation and inhibition of fusion with other mitochondrial network that precedes mitophagy.

Pharmacological modulation of mitophagy/Autophagy

There are no known fully specific inhibitors of mitophagy. Different studies have reported the use pharmacological agents that inhibit autophagy or mitochondrial division, thereby indirectly inhibiting mitophagy. 3-methyl adenine (3-MA) is an inhibitor of phosphoinositide-3-kinase (PI3K), an enzyme essential for the induction of autophagy under starvation or nutrient deficiency (Glick et al., 2010). It inhibits autophagy by inhibiting the formation of autophagosome. It was used as an autophagy inhibitor for the first time in 1982 by Seglan *et al.* (Seglen and Gordon, 1982). Zhou *et al.*, later showed that 3-MA also inhibits mitophagy and induces ROS production (Zhou et al., 2011). Mdivi-1 is an inhibitor of mitochondrial division and it was shown to inhibit mitophagy as well as mitochondrial membrane permeabilization (Cassidy-Stone et al., 2008). Mdivi-1 is the inhibitor of Drp1. Inhibition of Drp1 is known to induce elongation of mitochondrial network and to protect mitochondria from mitophagy (Gomes et al., 2011; Rambold et al., 2011). Casein kinase-2 (CK2) was reported to be essential for mitophagy as it phosphorylates Atg32 to induce mitophagy in yeast (Kanki et al., 2013). The invalidation of CK2 gene by RNA interference

leads to the inhibition of mitophagy. Therefore, we can assume that 4,5,6,7-Tetrabromobenzotriazole (TBB) and apigenin could be efficient pharmacological mitophagy inhibitors.

At the opposite, the mitochondrial uncouplers, carbonyl cyanide m-chlorophenyl hydrazine (CCCP) and 2,4-dinitrophenol (2,4-DNP) are typically used to induce mitophagy, especially CCCP (Narendra et al., 2008). Mitochondrial uncouplers dissipate the mitochondrial membrane potential and induce recruitment of Parkin to the mitochondria (Narendra et al., 2008).

Mitochondria in immunity and inflammation

Increasing number of studies are showing a role of mitochondria in the regulation of immune system through different pathways. Mitochondria contribute to antiviral as well as anti-bacterial response of immune cells through following pathways including; the direct detection of PAMPs, the release of mitochondrial molecular patterns, metabolic reprogramming, reactive oxygen species production and/or modulation of mitophagy.

Detection of PAMPs

The contribution of mitochondria in immunity was initially observed in antiviral signaling. The major breakthrough in the understanding of antiviral signaling mediated by members of RLRs family was the discovery of mitochondrial antiviral signaling (MAVS) proteins (Weinberg et al., 2015). MAVS proteins were found on mitochondria in association with the mitochondrial-associated membrane (MAM). MAMs are connections between the mitochondrial membrane and endoplasmic reticulum (Horner et al., 2011). MAVS are also found on peroxisomes. Activation of both the mitochondrial and peroxisome-associated MAVS are required for the maximum antiviral signaling (Weinberg et al., 2015).

Mitochondrial molecular patterns

Another pathway through which mitochondria contribute to the immune response is the release of mitochondrial molecular patterns. These mainly include mtDNA and N-formyl peptide.

Mitochondrial DNA can be released in response to injury and infection. It induces an inflammatory response by acting as damage-associated molecular patterns (DAMPs) (Zhang et al., 2010a; Zhang et al., 2010b). Mitochondrial DNA has structural similarity with the bacterial DNA and has been shown to induce an inflammatory response *in vivo* (Weinberg et al., 2015; West et al., 2011b). Similar to bacterial DNA, mtDNA also contain CpG motifs and are recognized by TLR9 (Weinberg et al., 2015; West et al., 2011b). Interestingly, intra-articular injection of human as well as murine mtDNA induced arthritis in mice through inflammation mediated by monocytes and macrophages (Collins et al., 2004). It was also reported that mtDNA, more specifically oxidized mtDNA, can activate NLRP3 (Nakahira et al., 2011; Shimada et al., 2012). Mitochondrial DNA is also known to be released in response to infection as well as injury and initiate an immune response (Zhang et al., 2010a; Zhang et al., 2010b). Another well-known host mitochondria-derived DAMP is N-Formyl peptide. Similarly to the bacterial N-formyl peptide, host-derived mitochondrial N-formyl peptide also acts as a chemo attractant for polymophonuclear leukoytes (PMN) and stimulator of the immune system (1982; Rabiet et al., 2007; Zhang et al., 2010b).

Metabolic reprogramming

The role of mitochondria in innate and adaptive immunity is receiving increasing attention by the immunologists. The contribution of metabolic pathways to the regulation of immune cell functions and phenotypes has led to the development of a new field of investigation called "immuno-metabolism". Mitochondria and mitochondrial functions are known to contribute in switching the phenotypes of different immune cells, with functional consequences. A classical example of a metabolic switch between two functionally distinct phenotypes of macrophages has already been discussed in chapter 2 (see the section: Metabolic reprogramming during macrophage polarization).

Mitochondrial ROS production

Production of ROS and endogenous ROS scavengers plays a key role in maintaining the inflammatory status of immune cells. Several studies have shown that the regulation of

inflammatory pathways is mediated by ROS. However, there are number of sources of ROS present in the cells. One of the major sources is mitochondria. Under the normal physiological conditions only a small amount of ROS is produced through complex I and III of RCC of mitochondria. In the context of immune cells, especially macrophages, activities of RCCs as well as ROS production play important roles. Recently, it was reported that stimulation of macrophages with different TLRs agonists elicited mROS production, primarily through complex I. However, the mechanism of increased ROS production remains controversial. It was proposed that the increased ROS production was due to destabilization of complex I through TRAF6-mediated ubiquitination and destabilization of Evolutionary Conserved Signaling Intermediate of Toll pathway (ECSIT), a component of complex I assembly (West et al., 2011a). This destabilization of complex I contributes to the bactericidal activity of macrophages through enhanced mROS production (West et al., 2011a). This was the first study which showed the contribution of mROS to the bactericidal activity of macrophages (West et al., 2011a). Moreover, NDUFS4 (NADH ubiquinone oxidoreductase iron sulphur protein) was shown to be critical for TLR4-mediated release of ROS and inflammation (Jin et al., 2014). NDUFS4 is a subunit of complex I of RCCs. Interestingly, macrophages from NDUFS4$^{-/-}$ mice presented an M1 phenotype (Jin et al., 2014). Furthermore, the LPS-mediated release of IL-1β was shown to be counteracted by the inhibition of complex I with metformin and rotenone (Kelly et al., 2015). Interestingly, mROS scavenging abrogated the effect of the LPS-mediated release of IL-1β whereas TNFα remained unaffected (Kelly et al., 2015).

NFκB, which is one of the key transcription factor for inflammatory genes, was shown to be activated and translocated to the nucleus in a ROS-dependent manner. ROS scavengers, like N-acetyl cysteine (NAC) and α-tocopherol, inhibited the LPS-mediated activation and translocation of NFκB to the nucleus in neutrophils as well as in macrophages (Asehnoune et al., 2004; Fox et al., 1997; Macdonald et al., 2003). Antioxidants prevented the expression of pro-inflammatory genes and exerted a protective effect to inflammatory stimuli *in vitro* (Asehnoune et al., 2004; Fox et al., 1997; Macdonald et al., 2003) and *in vivo* (Zhang et al., 1994). Furthermore, mROS was shown to induce activation of NLRP3 inflammasome and to release of inflammatory cytokines (Saitoh et al., 2008; Zhou et al., 2011).

Therefore, mROS might play an important role in innate immunity through a number of signaling pathways.

Mitochondrial autophagy in immunity

The role of mitophagy in innate immunity is not well known. Recent studies have highlighted the role of mitophagy in repressing mitochondrial antigen presentation by MHC-I in macrophages (Matheoud et al., 2016). Moreover, recent reports have suggested that PINK1, Parkin and DJ-1 deficiency may have an impact on the severity of sepsis in animal models. It was reported that PINK1 $^{-/-}$ and Park2 $^{-/-}$ mice were more sensitive to polymicrobial infection model of sepsis as compared to the wild-type mice (Kang et al., 2016). Heterozygous PINK1$^{-/+}$ mice were also reported to be more susceptible to a lethal dose of LPS. However, the mechanism by which PINK1 contributed to LPS-induced death remains obscure (Mannam et al., 2014). Conversely, DJ-1 knock-out mice appeared to be more sensitive to polymicrobial infection model of sepsis (Amatullah et al., 2016).

Inhibition of autophagy and mitophagy leads to the accumulation of damaged mitochondria that produce ROS and increase the activation of inflammasome (Zhou et al., 2011). Recently, activation of NLRP3 inflammasome has been shown to be restricted by NFκB through induction of mitophagy (Zhong et al., 2016). Whether NLRP3 activation is secondary to inhibition of mitophagy or whether mitophagy inhibition is mediated by NLRP3 activation remains elusive.

These studies indicate that mitophagy might be involved in the regulation of immune response. Further investigations are required to decipher the contribution of mitophagy in immunity and immune cell functions.

Materials and Methods

Materials and Methods:

Animals

C57BL/6 mice were purchased from Charles River (France). SV129 wild-type (WT) and STAT1-knock-out (STAT1KO) mice were purchased from Taconic (Denmark). All animals were housed in a temperature- and humidity-controlled facility (University of Burgundy), with a 12-hour/12-hour light/dark cycle. They were fed a standard chow diet and bred according to the local guidelines. Animals used were between 8 to 10 weeks old. Only female mice were used in *in-vivo* experiments. All experiments were approved by the local experimental animal ethics committee, University of Burgundy, Dijon, France.

Sampling methods for in vivo experiment

Blood samples from WT and/or STAT1 KO mice were collected either by retro-orbital puncture or by intra-cardiac puncture. Collection tubes were containing heparin sodium. Plasma was prepared by centrifugation (500 g for 10 minutes). For flow cytometry experiment, 100 μL of whole blood was hemolyzed with red blood cell (RBC) lysis buffer for 10 min at room temperature. Antibodies used for flow cytometry are listed in table 7.

Peritoneal leukocytes were obtained by injecting 10 mL of sterile PBS into the peritoneal cavity. PBS was allowed to stand for several seconds, while mice were shaken subsequently. PBS-containing leukocytes were recovered from the peritoneal cavity. Cells were incubated with RBCs lysis buffer for 10 min at room temperature to remove RBC contamination in peritoneal leukocytes. Leukocytes were washed three times by adding PBS and subsequently centrifuged at 500 g for 10 min. Peritoneal cells were then processed for flow cytometry or cell culture.

Endotoxemia in mice

Lipopolysaccharide from *Salmonella enterica* serotype *Typhimurium* (Sigma Aldrich) was resuspended in sterile PBS and was shaken vigorously before intraperitoneal injection (0.5 mg/kg or 10 mg/kg). Blood samples and peritoneal washings were collected at different time points. For survival studies, mice were checked twice a day.

Polymicrobial infection in mice

Cecal ligation and puncture (CLP) operations were carried out as previously described (Rittirsch et al., 2008). Briefly, mice were submitted to surgery upon anesthesia with isoflurane on a heat-controlled pad (37°C). A midline laparotomy was made to get access to the cecum. Cecum was exteriorized and ligated with sterile 4-0 suture just below the ileocecal valve without obstructing the bowel. A single puncture was made with the 21 gauge needle. A small quantity fecal content was extruded out of the cecum. The cecum was placed back into the abdomen and the incision was closed by stitching with a 6-0 suture followed by clipping of the skin. The fluid loss that occurred during laparotomy was compensated by resuscitation with 0.4 mL of saline injected subcutaneously. Blood samples were collected by an intra-orbital puncture after 2, 6 and 24 hours of laparotomy. For survival studies, mice were checked twice a day for 7 days.

Injection of pharmacological modulators of mitophagy

To assess the impact of mitophagy induction in monocytes and macrophages *in vivo*, mitophagy inducers (CCCP or DNP) were suspended in sterile PBS. PBS or mitophagy inducers were injected intraperitoneally 24 hours prior to the injection (LPS or saline) or surgery (CLP or sham). To assess the impact of mitophagy inhibition *in vivo*, Mdivi1 was suspended in PBS (DMSO) and injected intraperitoneally.

Measurement of bacterial load:

Peritoneal lavage fluid, liver homogenates, and blood were subjected to serial 10-fold dilutions and cultured on 5% sheep blood agar (Oxoid) plates. Colony forming units (CFUs) were quantified after 24h of incubation at 37°C in anaerobic conditions.

Cell Culture:

Table 2: Material for cell culture

Product	Purchased from
Roswell Park Memorial Institute (RPMI 1640) w/ L-Glutamine	Dominique dutscher

Minimum essential medium (MEM) w/o L-Glutamine	Dominique dutscher
Antibiotics (ATBs)	PAN biotech
Fetal Bovine serum	PAN biotech
Horse serum	PAN biotech
Phosphate-buffered saline	Dominique dutscher
Trypsin-EDTA	Dominique dutscher

Raw 264.7 cells

Raw 264.7 is a murine macrophage cell line established by producing tumor (ascites) by intraperitoneal injection of Abselon Leukaemia Virus in BALB/C mice. Raw 264.7 macrophage cell line was purchased from American Type Culture Collection (ATCC) (TIB-71). Cells were cultured in RPMI 1640 medium with 2mM L-glutamine supplemented with 10 % fetal bovine serum and 1 % antibiotics (Penicillin, Streptomycin and Amphotericin B (Fungizone)) in T75 flasks. Cells were cultured in the humidified incubator supplied with 5% CO_2 maintained at 37°C. Cells were passaged 3 times per week and batch was renewed after 20 passages. Cells were treated with different molecules mentioned in table 3. We used this cell line to conduct all the preliminary experiments in our study because this cell line was easy to culture and results were reproducible. However, most of the results were varrified either with primary cell line like bone marrow derived macrophages and peritoneal macrophages or with mouse models.

L929 cells

L929 mouse fibroblast cell line was purchased from ATCC. Cells were cultured in minimum essential media (MEM) supplemented with 10% horse serum and 1 % antibiotics (Penicillin, Streptomycin and Amphotericin B (Fungizone)). Cells were cultured in T75 flasks with the passage frequency of 2 times per week.

Preparation of L929 condition medium

L929 condition medium was prepared as described before (Weischenfeldt and Porse, 2008). Shortly, L929 cells (4.7 x 10^5) were plated in T75 flasks with 55 mL of medium. Cells were incubated for 7 days in a humidified incubator supplied with 5% CO_2 and maintained at 37°C

temperature. After 7 days of incubation, the medium (L929 condition) was collected, filtered and used for culturing bone marrow-derived macrophages (BMDMs) by following the previously-described guidelines (Weischenfeldt and Porse, 2008).

Bone marrow-derived macrophages (BMDMs)

Mice were anesthetized with isoflurane and were killed by cervical dislocation. Bones were recovered from lower limbs (tibia and femur). Bones were flushed with PBS supplemented with 1% antibiotic and antifungal drugs (Penicillin, Streptomycin and Amphotericin B (Fungizone)) under sterile conditions to isolate bone marrow cells. Cells were strained through 70 μM filter into 50 mL falcon tube. The cell suspension was centrifuged to pellet the cells. The supernatant was discarded and RBC lysis buffer (10 mL per tube) was added to the cell pellets. Cells were vortexed and incubated for 10 minutes at room temperature. PBS was added, cells were centrifuged and RBC lysis buffer was removed. Cells were washed with three repetitive times with PBS followed by centrifugation. After third washing, PBS was removed and cells were suspended in RPMI 1640 medium with L-glutamine supplemented with 10% fetal bovine serum, 1% antibiotics (Penicillin, Streptomycin and Amphotericin B (Fungizone)) and 20% L929 preconditioned medium. Cells were counted and seeded into 100 mm Petri dishes. Cells were allowed for 7 days to differentiate into macrophages. The medium was replaced periodically after every 48 hours. BMDMs were then treated and analyzed accordingly.

Peritoneal macrophages

Mice were anesthetized with isoflurane and euthanized by cervical dislocation. A midline incision was made into abdominal-wall to remove the skin without cutting the peritoneal lining. Peritoneal cells were recovered after lavage of the peritoneal cavity with 10 mL sterile PBS supplemented with 2mM EDTA. Cells were washed with PBS three times with repetitive centrifugation for 10 minutes at 500 g. After third washing, cells were suspended in RPMI 1640 supplemented with 10% fetal bovine serum and 1% Antibiotics (Penicillin, Streptomycin and Amphotericin B (Fungizone)). Cells were counted, seeded either in 24 well plates or in 100 mm dishes (10x 10^6 cells per dish) and cultured for 24 hours before treatment.

Molecule/Product	Purchased from
Lipopolysaccharides from salmonella enterica serotype typhimurium,	Sigma Aldrich
Recombinent mouse IFN-γ (carrier-free)	Biolegend
mitoTEMPOL (chemical name: 2,2,6,6-Tetramethyl-4-[[5-(triphenylphosphonio)pentyl]oxy]-1-piperidinyloxy bromide	Abcam
Apigenin	Tocris
TBB	Tocris
Mdivi 1	Tocris
Pam3CSK4	InvivoGen
R848	InvivoGen
Pam2CSK4	InvivoGen
Poly(I:C) (LMW)	InvivoGen
ODN D-SL01	InvivoGen
Antimycin A	Sigma Aldrich
N-Acetyl-L-Cysteine	Sigma Aldrich
2,4-Dinitrophenol	Merck
Z-VAD-FMK	rndsystems

Transfection with siRNA

Raw 264.7 cells were transfected with different siRNA (table 4) by using GenMute siRNA transfection reagent for Raw 264.7 (SignaGen) according to the manufacturer's instructions. All siRNA used in experiments were purchased and were validated from Ambion, Life technology. The silencing efficiencies of all the siRNA were verified and were between 60% to 80%. Shortly, cells were seeded into 24 well plates (0.83×10^5 cells per well), 24 hours before transfection. The medium was changed 30-60 min before transfection. Transfection buffer was prepared, siRNA was added to the transfection buffer and mixed by pipetting. Genemute transfection reagent was added to the mix and mixed by pipetting. The mix was incubated at room temperature for 15 min (not more than 30 min) to form a complex. The transfection mix was added dropwise to the cells to have a final concentration of 30 nM siRNA per well. Cells were incubated for further 24 hours before treatment.

Table 4: List of siRNA

siRNA	Source	Catalogue number	Ref - ID
siRNA STAT1	Life Technology	4390771	s74444
siRNA Casp-4/11	Life Technology	4390771	s63374
siRNA TLR4	Life Technology	4390771	s75206
siRNA IRAK4	Life Technology	4390771	s113931
siRNA Traf6	Life Technology	4390771	n430201
siRNA Irf3	Life Technology	4390771	s79432
siRNA Nfkb1	Life Technology	4390771	s70544
siRNA Hif1a	Life Technology	4390771	s67531
siRNA NLRP3	Life Technology	4390771	S103710
siRNA IFNGR1	Life Technology	4390771	S68097
siRNA IFNGR2	Life Technology	4390771	S68100

Western blot analysis

Cells were cultured and treated in 100 mm dishes. Culture medium was removed and cells were rinsed with PBS. Proteins were extracted by adding 300 µL of Radioimmunoprecipitation assay (RIPA) buffer. Proteins were quantified with Pierce BCA protein assay kit (Pierce). Lysates were denatured in Laemmli buffer by heating at 95 °C for 5 min. Proteins were migrated on 4 to 20 % SDS-PAGE gels (BioRad) and were transferred to polyvinylidene difluoride (PVDF) membranes by using transblot (BioRad) semi dry system . Membranes were blocked either by 5% BSA or 5% semi-skimmed milk in TBS-T (Tris-buffered saline with 0.01% tween) at room temperature for the duration of 1 hour. Incubation with primary antibodies (table 5) were carried out at 4°C overnight followed by one-hour incubation with appropriate secondary antibody conjugated with horseradish peroxidase (HRP). Chemiluminescence was revealed by incubating the membranes in ECL substrate (BioRad) and visualized with ChemiDoc imager (BioRad). Images were analysed with the Image Lab 5.1 software (BioRad). All the immunoblots presented in this study are the reperesentatives of atleat 2- 4 independent experiments.

Table 5: Antibodies for immunofluorescence and western blotting analysis

Antibody	Source	Clone
PARKIN	Abcam	Rabbit Polyclonal to PARKIN
PINK1	Abcam	Mouse monoclonal [38CT18.7] to PINK1
Caspase-11	Novusbio	Monoclonal (17D9)
TFAM	Cell Signaling Technology	Rabbit monoclonal (D5C8)
DRP1	Cell Signaling Technology	Rabbit monoclonal (D6C7)
VDAC	Cell Signaling Technology	Rabbit monoclonal (D73D12)
DJ-1	Cell Signaling Technology	Rabbit monoclonal (D29E5) XP®
Stat1	Cell Signaling Technology	Rabbit Polyclonal
Phospho-Stat1 (Ser727)	Cell Signaling Technology	Rabbit monoclonal (D3B7)
Phospho-Stat1 (Tyr701)	Cell Signaling Technology	Rabbit monoclonal (D4A7)
Lamin A/C (4C11)	Cell Signaling Technology	mouse monoclonal (4C11)
Tom20 Antibody (FL-145)	Senta cruz biotechnology, INC	Rabbit polyclonal

Fluorescence microscopy and electron microscopy

Cells were washed once with PBS to remove the culture medium. Cells were fixed with 4% paraformaldehyde by incubating for 10 minutes at 4°C. Cells were then permeabilized by incubating with PBS containing 0.1% Triton X-100. Blocking was carried out with PBS-T (PBS + 0.1% Tween 20) supplemented with 1% BSA and 10% Goat serum at 4°C for 30 min. Cells were then incubated with primary antibody (see table 5) at 4°C overnight in a humidified chamber. Cells were then washed and incubated with specific secondary antibody conjugated with a fluorophore for 1 hour under humidified chamber in the dark. Preparations were finally analyzed with Axio imager 2 (Carl zeiss Microscopy GmbH, Jena, Germany) and Image J software.

For transmission electron microscopy experiment, cells were fixed for 1 h in 4% formaldehyde/2.5% glutaraldehyde in 0.1 M Sörensen phosphate buffer, then washed in the same buffer at room temperature, and post-fixed for 1 h in 1% osmium tetroxide. The samples were dehydrated in increasing concentrations of ethanol (30%, 50%, 70%;95%; 100%) and were embedded in Epon 812 (EMS). Contrasted ultrathin sections (produced with an ultramicrotome (Reichert UltracutE)) were observed at 80 kV on a transmission electron microscope (Hitachi, H75500).

Real-time PCR

RNA isolation from cells was carried out by using Trizol reagent (Life Technologies), following the manufacturer's instructions. The amounts of RNA was measured by using Nanodrop ND-100 spectrophotometer. The complementary DNA (cDNA) was prepared from 500 to 1000 ng of RNA by using iScript Reverse Transcription Supermix (BioRad). Quantitative polymerase chain reaction was performed using 5 ng of cDNA and 5 µM of both (R+F) primers (table 6). The amplification was measured by using SYBR green reagent (Applied Biosystems, Foster City, USA) on a "XXXX" RT-QPCR system (Applied Biosystems). Data was analyzed using stepOne software V2.2.2. Expression level of each gene was normalized with mRNA levels of housekeeping genes and expression levels were measured by using $2^{-\Delta\Delta CT}$ method.

Primers used in this study along with their sequence and validation summary are given in the table 6.

Table 6: Primer sequence

Primer		Sequence
PINK1	mPINK1_R	ATATGCTGCCCCCACACTAC
	mPINK1_F	CAACTGCAAGGTCATCATGG
PARK7	mPARK7_R	AACACACCCACTGGCTAAGG
	mPARK7_F	CTCCACAATGGCTAGTGCAA
mDRP1	mDRP1_R	ATGCCTGTGGGCTAATGAAC
	mDRP1_F	AGTTGCCTGTTGTTGGTTCC
mCASP4	mCASP4_R	GGTGGGCATCTGGGAATGAA
	mCASP4_F	CCGAGACAAAACAGGAGGCT
TNFa	TNFa_R	ACATTCGAGCCAGTGAATTCGG
	TNFa_F	GGCAGGTCTACTTTGGAGTCATTGC

iNOS	iNOS_R	TCGCTCAAGTTCAGCTTGGT
	iNOS_F	GGCAAACCCAAGGTCTACGTT
IL-1β	IL-1β_R	TGCCCATCAGAGGCAAGGAGGA
	IL-1β_F	CCTCGGCCAAGACAGGTCGC
18s	18S_R	GCGAGACAGTCAAACCACG
	18s_F	GTGTGGGGAGTGAATGGTG
TLR4IL-12a	IL-12a_R	TTTCTCTGGCCGTCTTCACC
	IL-12a_F	CTCAGTTTGGCCAGGGTCAT
IL-6	IL-6_R	GTCACCAGCATCAGTCCCAA
	IL-6_F	GGAGCCCACCAAGAACGATA

Mitochondria isolation

Mitochondria were isolated with a mitochondria isolation kit (Miltenyi Biotec) using anti-Tom22 antibodies coupled with magnetic microbeads, according to manufacturer's instructions. In summary, the culture medium was removed and cells were washed once with PBS. Lysis buffer containing protease and phosphatase inhibitors was added and cells were scrapped. Cell suspension was then transferred to a dounce homogenizer and submitted to 40 strokes. Cell homogenates were then filtered with 70 µm filter and transferred into falcon tubes and the volume was adjusted to 10 mL with separation buffer. Fifty microliter of anti-tom22 antibodies coupled with magnetic micro-beads were added to the cell lysates and incubated at 4°C for 1 hour with continuous gentle shaking. Lysates were passed through the columns, mounted on the magnet. The retained mitochondria were washed three times with 3 mL of separation buffer. Columns were removed from the magnet and bound mitochondria were eluted out from the column with 1.5 mL of separation buffer. The eluate was centrifuged at 13,000 g to pellet the isolated mitochondria, which was subsequently washed three times with PBS. Finally, 150 µl of RIPA buffer was added to the mitochondrial pellet to lyse mitochondria.

Flow Cytometry

Macrophage polarization

Cells were suspended in 90 µl of PBS and 10 µl of FcR blocking agent (Miltenyi Biotec) was added. Cells suspension was then mixed vigorously by vortexing prior to a 10 min incubation at 4°C. Cells were then submitted to staining with CD64-APC, CD80-PE antibodies according to the

manufacturer's instruction (Mitenyi Biotec). Shortly, recommended quantities of antibodies were dispensed in each FACS tube containing cells already blocked with Fc receptor blocking agent. Cells were mixed vigorously by vortexing and incubated at 4 °C for 20 minutes. The volume of cells suspension was made up to 250 - 300 μl with PBS (2mM EDTA). Cells were then analyzed, by using LSRII flow cytometer (BD bioscience) and Flowjo V10.0 software (Tree Star).

Table 7: Antibodies for the Cytometry

Antibody	Source	Clone
CD80-PE	Miltenyi Biotec	mouse (clone: 16-10A1)
CD64 (FcγRI)-APC	Miltenyi Biotec	mouse (clone: REA286)
CD86-VioBlue	Miltenyi Biotec	mouse (clone: PO3.3)
Anti-F4/80-PerCP-Vio700	Miltenyi Biotec	mouse (clone: REA126)
CD11b-APC-Vio770	Miltenyi Biotec	human and mouse (clone: M1/70.15.11.5)
Anti-Ly-6C-APC	Miltenyi Biotec	mouse (clone: 1G7.G10)
Anti-Ly-6G-VioBlue	Miltenyi Biotec	mouse (clone: 1A8)
CD115-PE	Miltenyi Biotec	mouse (clone: AFS98)
FcR Blocking Reagent	Miltenyi Biotec	Mouse

Measurement of mitochondrial density

For measuring the mitochondrial density, cells were stained with mitotracker green FM (molecular probes) according to the manufacturer's instruction. Precisely, cells were rinsed three times with PBS (with Ca^{+2} and Mg^{+2}). Mitotracker green FM was added at a final concentration of 200 nM and the cells were incubated at 37°C in a humidified incubator supplied with 5 % CO_2. Cells were subsequently washed thrice with PBS and cells were then scrapped in 250 μL of PBS (2mM EDTA). Cell suspension was finally analyzed by using LSRII flow cytometer (BD bioscience) and Flowjo V10.0 software (Tree Star). The concentration of mitotracker green FM used was

selected by titrating with the different concentrations of mitotracker green FM and the same concentration was used throughout all experiments.

Measurement of mitochondrial ROS production

Mitochondrial ROS production was measured using Mitosox red (Molecular Probes), a probe to detect mitochondrial superoxide anion, primary ROS produce by mitochondria. Staining was carried out according to the manufacturer's instructions. In summary, cells were washed with PBS, incubated with Mitosox red 2.5 $\mu mol.L^{-1}$ in PBS for 20 min in a humidified incubator at 37 °C supplied with 5% CO_2. Cells were then washed thrice with PBS, scrapped in 250 μl of PBS (2mM EDTA) and were transferred to the FACS tubes. Cells were analyzed by using LSR-II flow cytometer (BD Bioscience) and data was analyzed by Flowjo V10.0 software (Tree Star). The Mitosox Red was used at the same concentration throughout all the experiments and concentration was selected after titration.

Mitochondrial membrane Potential

Mitochondrial membrane potential ($\Delta\psi$m) was measured by staining cells either with tetramethylrhodamine methyl ester perchlorate (TMRM, Molecular Probes) or JC-1 (Molecular Probes). The concentrations of both probs used in all experiments were selected after titration with different doses.

For TMRM staining, cells were washed with PBS and incubated in a medium containing 50 nM TMRM for 30 minutes at 37°C in a humidified incubator with 5% CO_2. The TMRM was removed from the cells and subsequently washed thrice with PBS. Cells were finally scrapped in PBS (2mM EDTA) and analyzed with the LSRII flow cytometer (BD bioscience) and the Flowjo V10.0 software (Tree Star).

For JC-1 staining, cells were incubated in a medium containing 5 μM of JC-1 for 30 minutes at 37°C in a humidified incubator with 5% CO_2. JC-1 is a probe used to measure mitochondrial membrane potential and mitochondrial density. JC-1 accumulates in mitochondria as monomers and forms aggregates proportionally to mitochondrial membrane potential. The fluorescence intensity of monomers and aggregates can be used to measure mitochondrial density and

membrane potential, respectively. Cells were then analyzed by either by flow cytometry or fluorescence microscopy.

Measurement of Autophagy

Raw 264.7 macrophages were plated on 24 well plates. Cells were treated with LPS (100 ng.mL^{-1}) and IFNγ (20 ng.mL^{-1}) for 6hours and 24 hours or with rapamycin (500 nM) for 24 hours. Cells were stained with cyto-ID autophagy detection kit (Enzo lifesciences) according to the manufacturer's instructions. Shortly, medium was removed and cells were washed once with 1X assay buffer. About 250 µl of medium (without indicator: Phenol red) containing cyto-ID green (1/1000 dilution) was added to the cells and incubated in dark at 37°C for 30 min. Cells were washed, scrapped in 1X assay buffer and were analyzed by BD LSR-II flow cytometer and Flowjo software.

Gentamycin Protection assay (Bactericidal activity)

The gentamycin protection assay was adapted to be analyzed by flow cytometry. *Escherichia coli* K12 and *Bacillus subtilis* CIP 52.65 were grown in tryptic soy broth (TSB; Biokar Diagnostics) for 24 h at 37°C. *E. coli* K12-GFP was grown aerobically in TSB with ampicillin, 100 µg.mL^{-1} (Sigma) for 24 h at 37°C. Bacterial cells were washed twice in sterile PBS and resuspended at 10^9 CFU per mL in PBS. Macrophages were infected with *E. coli* K12-GFP at multiplicity of infection (MOI: 10 bacteria per macrophage). Cells were washed three times with PBS containing Gentamycin (20ng.mL^{-1}). Cells were scraped and analyzed by BD LSR-II flow cytometer and flowjo software using decrease in fluorescence intensity of GFP (green fluorescence protein) as an indicator of bactericidal activity.

Measurement of Internalization of LPS

Fluorescent label (DOTA-Bodipy-NCS, "Bodipy") was a kind gift from Claire Bernhard, Mathieu Moreau and Franck Denat (ICMUB, Molecular Chemistry Institute of the University of Burgundy, Dijon, France) and synthesized as previously described (Bernhard C et al. Chem. Commun. 2010;46:8267–8269) and dissolved in DMSO. LPS from Escherichia coli O55:B5 (Sigma-Aldrich) was dissolved (final concentration, 20mg/mL) in sodium bicarbonate buffer (pH 9). One molar

equivalent of Bodipy was added prior to incubation for 1 h at 37 °C with gentle shaking. Labeled LPS was separated from free fluorescent label by FPLC using a Superdex 75 column (GE Healthcare). Bodipy-LPS were concentrated and dialyzed against pyrogen-free LPS with Nanosep MWCO 3 kDa (Pall) and filtered at 0.22 μm.

Raw 264.7 macrophages and peritoneal macrophages were incubated with Bodipy-LPS (100 ng.mL^{-1}) in the presence of IFNγ (20ng.mL^{-1}) for 24 h. Cells were washed with PBS and analyzed by flow cytometry measuring Bodipy fluorescence intensity as an indicator of internalized LPS.

Oxygen consumption

Raw 264.7 macrophages were treated with LPS/IFNγ for 24 hour. Cells were washed with PBS and recovered afterward. Cells were counted and diluted to get 4 x 10^6 cell.mL^{-1}. Oxygen consumption was measured by Clark's electrodes.

Measurement of mitochondrial enzyme activities in macrophages

Macrophages were pelleted and stored at -80°C until analysis, and resuspended in PBS buffer just before the enzyme assays. Measurements of respiratory chain (RC) complex I activity were performed spectrophotometrically at 614 nanometers in 1 ml of 25 mM potassium phosphate buffer pH 7.8 at 37°C, containing 3.5 mg/mL BSA, 60 μM DCIP, 70μM decylubiquinone, and 0,2 mM NADH. After addition of macrophages, CI activity was determined by addition of 1μM rotenone, and expressed as nanomol DCIP reduced/min/mg protein, as described in Janssen 2007 (Janssen et al., 2007). RC complex III activity was measured at 37°C by monitoring the reduction of cytochrome c at 550 nanometers in 1 mL of 10 mM potassium phosphate buffer pH 7.8 containing 2mM EDTA, 1mg/mL BSA, 240 μM KCN, 5 μM rotenone, 0.4 mM Lauryl maltoside, and 40 μM oxidized cytochrome c (Barrientos, 2002). After addition of macrophages, the reaction was initiated by addition of 80μM decylubiquinol, and the activity was expressed as nanomol cyt c reduced /min/mg proteins. Cytochrome c oxidase activity was measured at 37°C in 1mL of 10mM potassium phosphate buffer pH 7.8 containing 1mg/mL BSA, 13.6μM reduced cytochrome c, and 2.4mM lauryl maltoside) according to Barrientos 2002 (Barrientos, 2002).

Experimental Results

PART I

Inhibition of mitophagy in myeloid cells

Introduction

Myeloid cells (monocytes, macrophages and neutrophils) are major components of the innate immune system and are involved in the primary response to infection. The contribution of mitochondria to immunity is under investigation since the recent decades but still remains not fully understood. Mitochondrial dysfunctions contribute to organ failure and impair survival in sepsis (Carré et al., 2010; Japiassu et al., 2011); (Amatullah et al., 2016; Mannam et al., 2014). Changes in mitochondrial functions and dynamics were observed in peripheral blood monocytes in septic patients (Adrie et al., 2001; Garrabou et al., 2012; Japiassu et al., 2011; Santos et al., 2016). Recent studies have suggested a link between mitophagy and immunity. DJ-1-deficient mice showed higher resistance whereas PINK1- and Parkin-deficient mice showed higher susceptibility to septic shock (Amatullah et al., 2016; Kang et al., 2016; Mannam et al., 2014). We hypothesized that mitophagy and mitochondrial dynamics play role in functions and antibacterial mechanism of myeloid cells. The role of mitochondrial dynamics and mitophagy in myeloid cells is not known yet.

Chapter 1

Increased mitochondrial density is a hallmark of activated monocytes and macrophages

1.1 Increased mitochondrial density in macrophages is a specific response to Gram-negative bacteria and LPS

To assess the effect of bacterial infection on mitochondria in macrophages, Raw 264.7 macrophages were exposed to Gram-positive (*Bacillus subtilis*) and Gram-negative (*Escherichia coli*) bacteria at a multiplicity of infection (MOI) of 10 for different durations (20, 40 and 120 min) (Figure 1.1.A). Cells were stained with Mitotracker green FM, a mitochondrial dye used to measure mitochondrial density, which is insensitive to changes in mitochondrial membrane potential. The mitochondrial density was measured by flow cytometry. We observed that mitochondrial density in macrophages was increased in a time-dependent manner after the exposure to Gram-negative bacteria. Increase in mitochondrial density was drastically less pronounced in macrophages exposed to Gram-positive bacteria (Figure 5.1.A). These results showed that exposure of macrophages to bacteria impacts on their mitochondrial density. Macrophages are equipped with different PPRs and have the ability to sense different PAMPs and DAMPs. Amongst these PRRs, TLRs play a key role in immunity. In order to define which bacterial component and through which TLR bacteria impact on mitochondrial density, we stimulated macrophages with different TLR agonists and assessed mitochondrial density through flow cytometry using mitotracker green FM.

Raw 264.7 macrophages were treated for 24 hours with different doses of TLR agonists: Pam3CSK4 (TLR2/1 agonist) , a synthetic triacylated lipopeptide; Pam2CSK4 (TLR2/6 agonist), a synthetic diacylated lipopeptide; Polyinosinic-polycytidylic acid (Poli(I:C)) (TLR3 agonist), a synthetic analogue of dsRNA; R848 (resiquimod) (TLR7/8 agonist), an imidazoquinoline compound; CpG oligodeoxynucleotide (CpG ODN) (TLR9 agonist), a short synthetic DNA molecule with CpG motif; Lipoteichoic acid (LTA) (TLR2 agonist), a cell wall component of Gram-positive

bacteria; and Lipopolysaccharides (LPS) (TLR4 agonist), component cell wall of Gram-negative bacteria. The cells were stained with mitotracker green FM and were analyzed by flow cytometry to assess mitochondrial density. Strikingly, increase in mitochondrial density in macrophages was only observed for LPS (Figure 1.1.B). As LPS is a prototypical component Gram-negative bacteria, this observation argues in favor of our hypothesis that mitochondrial density increases in macrophages upon exposure to Gram-negative bacteria.
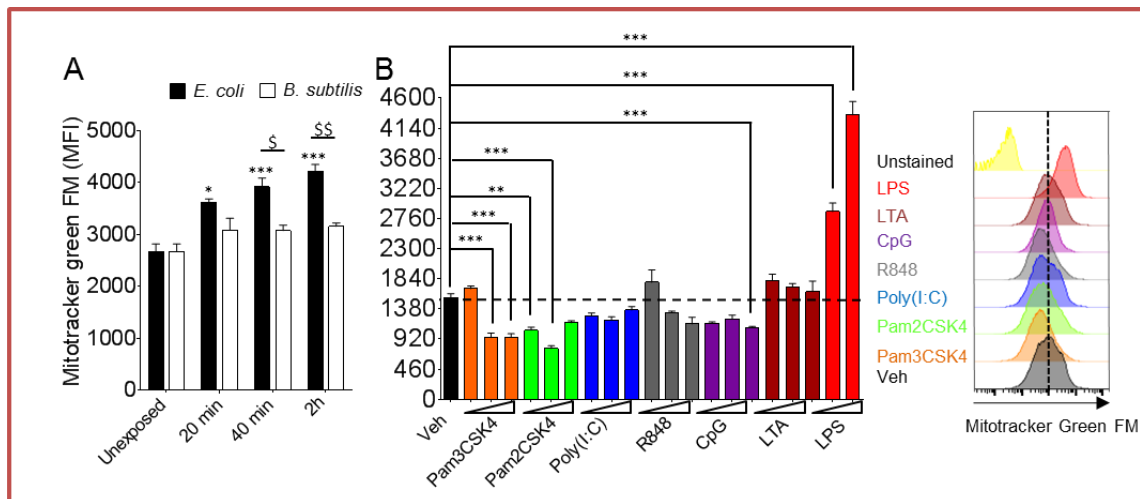
Figure 1.1: Increased mitochondrial density in macrophages is a specific response to gram negative bacteria and LPS

(A-B) Raw 264.7 macrophages were exposed to alive bacteria (MOI=10 for indicated duration) or various concentration of PAMPs (Pam3CSK4: 1-100ng/mL; Pam2CSK4: 1-100ng/mL; Poly(I:C): 0.1-10µg/mL; R848: 1-50µg/mL; CpG: 10-1000nmol/L; LTA: 10-1000ng/mL; LPS: 100-500ng/mL) for 24h. Mitochondrial density was assessed by flow cytometry using mitotracker green FM. Data represents mean ±SEM, n=3 per group (A-B) and significance levels were assessed by either one-way ANOVA (B) or two-way ANOVA followed by post hoc Bonferroni's test (A); * = comparison between *E.coli* infected versus unexposed control, *p <0.05, **p <0.01, ***p <0.001. $ = comparison between *E.coli* infected versus *B. subtitis* infected, $ p <0.05, $$ p <0.01, $$$ p <0.001.

1.2 LPS-induced mitochondrial density in macrophages in a dose-dependent manner

To further confirm that LPS impacts on mitochondria in macrophages we conducted dose studies with LPS on the Raw 264.7 macrophage cell line. Macrophages were treated with increasing doses of LPS (50,100 and 250 ng.mL^{-1}) for 24 hours. Mitochondrial density was assessed by flow cytometry. As depicted in Figure 1.2, LPS treatment leads to a dose-dependent increase in mitochondrial density in macrophages.
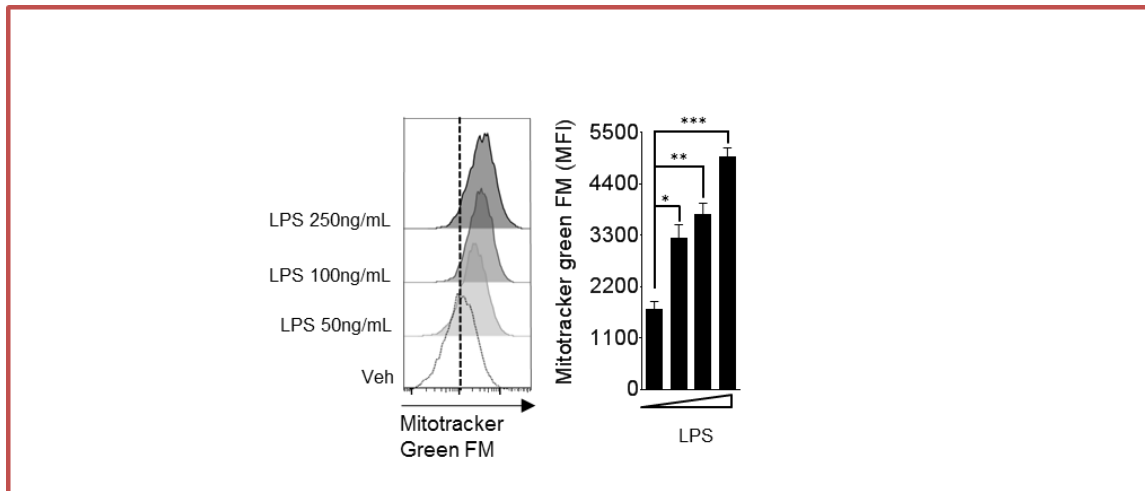
Figure 1.2: LPS-induced increase in mitochondrial density in macrophages in a dose-dependent manner

LPS was used at 50-250ng/mL for dose effect on Raw 264.7 macrophages and mitochondrial density was assessed by flow cytometry.

Data represents mean ±SEM, n=3 per group and significance levels were assessed by one-way ANOVA followed by post hoc Bonferroni's test; * = comparison between treated versus untreated control, *p <0.05, **p <0.01 or ***p <0.001.

1.3 Interferon-γ potentiates the effect of LPS on increase in mitochondrial density in macrophages

LPS contributes to classical activation of macrophages, namely through the activation of the TLR4 signaling pathway. As reported in the literature, classical activation of macrophages also relies on the presence of IFNγ, a Th1 cytokine, which activates IFNGR signaling pathway (Biswas and Mantovani, 2012; Galván-Peña and O'Neill, 2014). Therefore, mitochondrial density was assessed in experimental settings corresponding to physiologically relevant macrophage activation. Raw 264.7 cells were treated with LPS and IFNγ alone or in combination with different doses of both agonists. Mitochondrial density was assessed by flow cytometry using mitotracker green FM (Figure 1.3).

Macrophages were treated with LPS (50ng.mL^{-1}) and IFNγ (20ng.mL^{-1}) alone or in combination. Both LPS- and IFNγ-treated macrophages exhibited increased mitochondrial density. Interestingly, the combination of TLR4 and IFNGR agonists resulted in a dramatic increase in mitochondrial density as compared to both agonists separately (Figure 1.3.A). Therefore, TLR4 and IFNGR pathways seem to potentiate each other with regards to mitochondrial density

modulation, which appeared to be a feature of M1 macrophages. In LPS/IFNγ-treated macrophages, increased mitochondrial density was observed as soon as 1 hour time point and was further increased at 24 hours (Figure 1.3.B). The combination of different doses of LPS and IFNγ for 1h further confirmed that LPS and IFNγ potentiate their effect in a dose-dependent manner (Figure 1.3.C).

Together these results indicated that enhancement of mitochondrial density is a hallmark of classically activated macrophage (M1). Moreover, we have shown here the existence of the synergistic effect of LPS and IFNγ on mitochondrial density in activated macrophages. The relevance of these *in vitro* data was then tested *in vivo* in an animal model of sepsis and endotoxemia.
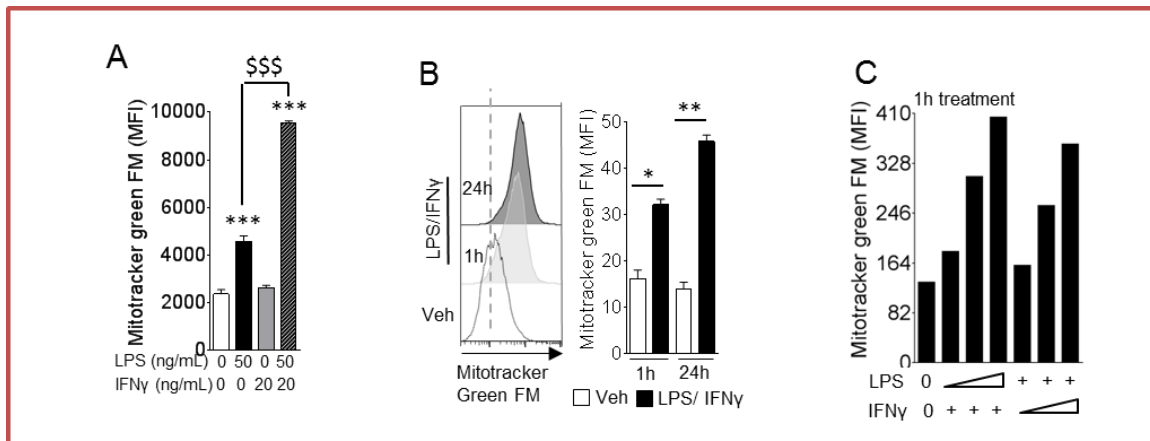
Figure 1.3: Interferon (IFN)-γ potentiates the effect of LPS on increase in mitochondrial density in macrophages

Mitochondrial density was assessed in (A) Raw 264.7 macrophages exposed to LPS (50 ng.mL^{-1}) and IFNγ (20 ng.mL^{-1}), alone or in combination for 24h with indicated concentrations. (B) Raw 264.7 macrophages treated with LPS/IFNγ (100.20 ng.mL^{-1}) for 1h or 24h. (C) Raw 264.7 macrophages exposed to different dosses LPS and IFNγ in combination for 1 hours, LPS was used at 50-250 ng.mL^{-1} for dose effect and 100ng.mL^{-1} for fixed dose and IFNγ was used at 10-50ng.mL^{-1} for dose effect and 20ng.mL^{-1} for fixed dose

(A-B) Data represents mean ±SEM, n=3 per group, and significance levels were assessed by either one-way ANOVA followed by post hoc Bonferroni's test (A and B) or t test (B); * = comparison between treated versus untreated group, *p <0.05, **p <0.01 or ***p <0.001. $ = comparison between LPS treated versus LPS and IFNγ co-treated group, $$$ p <0.001.

1.4 Assessment of mitochondrial density in peritoneal myeloid cells in the context of polymicrobial infection or endotoxemia

Cecal puncture Ligation (CLP) surgery is a standard model of polymicrobial infection mainly represented by Gram-negative bacteria (Merx et al., 2004). C57BL/6J mice were submitted to CLP or sham surgery. To assess the effect of polymicrobial infection on mitochondrial density in myeloid cells, peritoneal fluids were collected from CLP and sham-operated mice 2, 6 and 24H after surgery. Peritoneal macrophages were identified by flow cytometry according to the gating strategy depicted in Figure 1.4.A. Macrophages were defined as $CD11b^{Hi}$-$F4/80^{Hi}$ population among $CD45^{+}$ cells (leucocytes). Neutrophils were defined as $F4/80^{Lo}$-$Ly6G^{Hi}$ population among $CD45^{+}$ cells (Figure 1.5). It is noteworthy that we set up an original experimental procedure to measure mitochondrial density in freshly isolated white blood cells (WBC). Isolated WBCs, from the peritoneal cavity (after peritoneal washing) or from the blood, underwent a mild hemolysis. WBCs were then incubated with Mitotracker Green FM at the time of saturation of the Fc receptor with IgGs. This procedure was performed for 10 min at room temperature. WBCs were rinsed once with PBS and were then immunostained for further identification by flow cytometry using specific fluorochrome-coupled IgG. Immunostaining was performed on ice. WBCs were maintained on ice until flow cytometry analysis in order to maintain mitochondrial integrity. We observed that peritoneal macrophages ($CD45^{+}$ $CD11b^{Hi}$ $F4/80^{Hi}$) from CLP-operated mice exhibited higher mitochondrial density as compared to sham-operated mice after 2 hours and 6 hours of surgery (Figure 1.4.B). We observed that mitochondrial density in macrophages was increased after 24 hours of surgery in sham-operated mice. This could be related to release of DAMPs as a consequence of surgery-mediated injuries. This may ultimately lead to macrophage activation and subsequent increase in mitochondrial density in macrophages compared to earlier time points. This would need further investigation to be clarified.

After having assessed mitochondrial density in the whole population of peritoneal macrophages, we underwent to assess mitochondrial density in activated macrophages. First, we assessed the expression of two classically used macrophage activation markers: CD64 (FCγRI) and CD80 (Figure 1.4.D-E). As expected, both were significantly increased in the context of sepsis compared to sham-operated animals. Nevertheless, sepsis-mediated increase in CD64 appeared to be
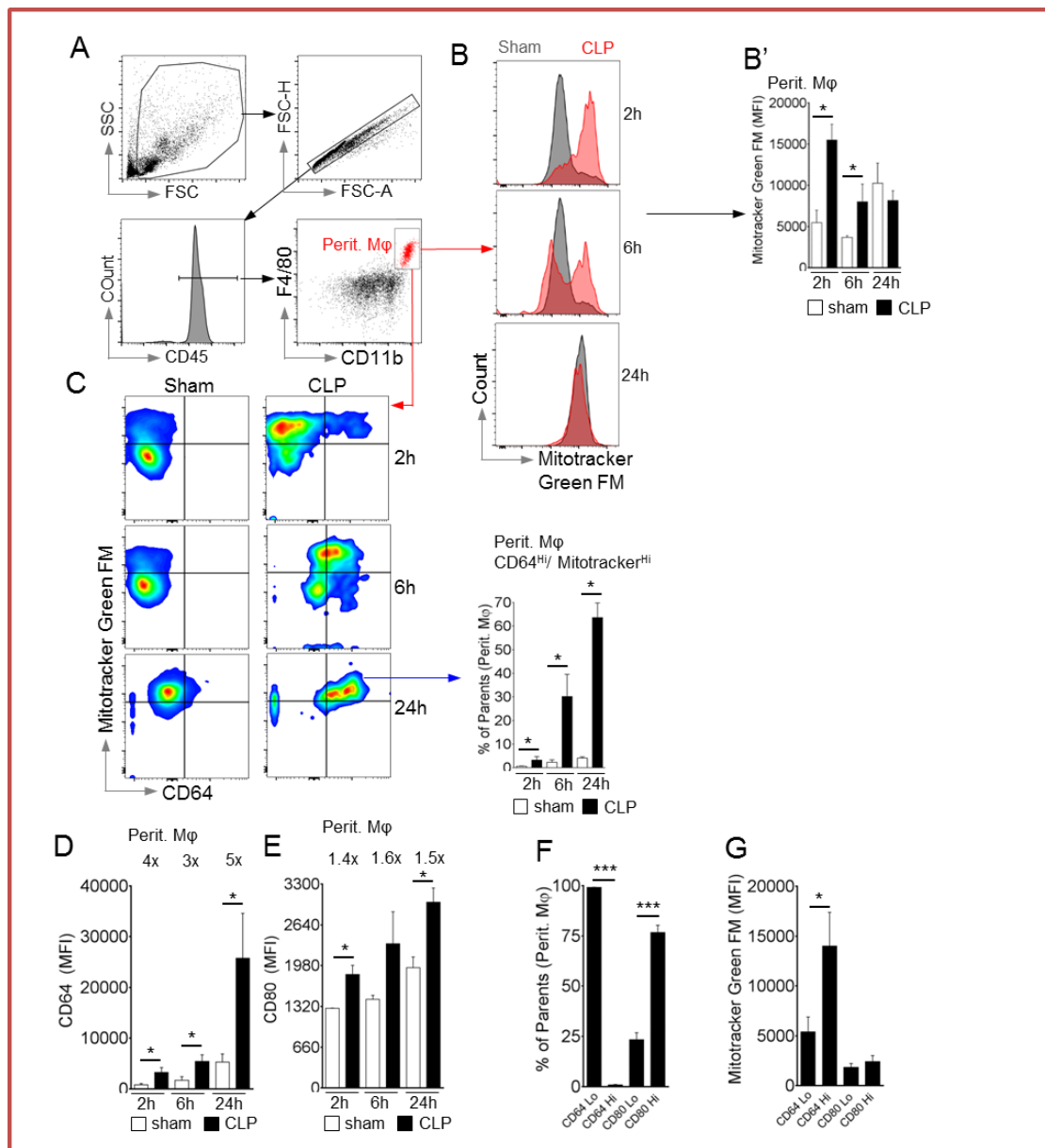
Figure 1.4 : Assessment of mitochondrial density in Peritoneal macrophages in the context of polymicrobial infection

(A-G) C57BL6/J mice underwent CLP or sham surgery. Peritoneal fluid were collected at indicated time points. Mitochondrial density was analyzed by flow cytometry using mitotracker green FM on peritoneal macrophages (A-C). (A) Peritoneal macrophages were defined using the depicted gating strategies. (D-E) CD64 MFI (D) and CD80 MFI (E) in peritoneal macrophages were determined by flow cytometry in peritoneal fluids of CLP- or sham-operated animals at indicated time points. (F-G) Percentage of CD64$^{Lo\&Hi}$ and CD80 $^{Lo\&Hi}$ peritoneal macrophages subpopulations (F) and their respective mitochondrial density (G) were determined by flow cytometry in peritoneal fluids collected after 2h in sham-operated animals.

The data in (A-G) represent mean ± SEM, n=5 per group (A-G) and significance levels were assessed by Mann-Whitney test; * = comparison between sham- and CLP-operated mice at different individual time points, * p <0.05, ** p <0.01, *** p <0.001.

striking more pronounced compared to CD80 in peritoneal macrophages. We observed a 5-fold increase in CLP-operated animals compared to control for CD64 whereas the increase was of 1.5-fold for CD80 (Figure 1.4.D-E).

Therefore, we focused on CD64^{Hi} macrophages and identified a new subpopulation of macrophages with a high level of CD64 along with an increased mitochondrial density (Mitotracker Green FM^{Hi}). This population referred as CD64^{Hi} Mitotracker^{Hi} macrophages appeared to be dramatically increased in a time-dependent manner in mice that underwent CLP compared to sham-operated animals (Figure 1.4.C). This *in vivo* data confirmed our *in vitro* observation that increased mitochondrial density is a feature of macrophage exposed to Gram-negative bacteria. Interestingly, at a basal level, in sham-operated animals, we noticed that the level of CD64^{Hi} macrophages was extremely low (Figure 1.4.F). This confirmed that CD64 is a good indicator of macrophage activation. More interestingly, we observed that even at a basal level, CD64^{Hi} macrophage subpopulation displayed a high mitochondrial density compared to CD80^{Hi} macrophages (Figure 1.4.G). This further confirms our assumption that high mitochondrial density is a hallmark of macrophage activation.

Neutrophils are phagocytes endowed with phagocytic and bactericidal activity. They are abundant in peripheral blood, respond quickly to pathogenic stimuli, and reach the site of infection upon activation (Abbas et al., 2014; Sadik et al., 2011). We observed that the percentage of neutrophils population (Ly6G^{Hi} F4/80^{lo}) in total peritoneal leukocytes (CD45^{+}) was increased in a time-dependent manner after CLP surgery (Figure 1.7.A). This corresponds to the infiltration of neutrophils to the peritoneum due to polymicrobial infection. Interestingly, the levels of CD64 and CD80 markers were increased in neutrophils population especially after 24 hours of CLP surgery (Figure 1.5.B-C). We checked the impact of polymicrobial infection on mitochondrial density in these cells and noticed that, similarly to peritoneal macrophages, the mitochondrial density was increased in peritoneal neutrophils (Figure 1.5.D). CLP-operated displayed a higher mitochondrial density in peritoneal neutrophils as well as a higher percentage of Mitotracker^{Hi} CD64^{Hi} neutrophils after 2 hours of surgery (Figure 1.5.D-E). After 24 hours of surgery, mitotracker green FM was high in neutrophils from both sham- and CLP-operated groups

compared to the 2 hour time point. The CD64^{Hi} Mitotracker^{Hi} subpopulation of neutrophils was higher in CLP-operated as compared to sham-operated (Figure 1.5.D-E).

Figure 1.5: Assessment of mitochondrial density in peritoneal neutrophils in the context of polymicrobial infection
(A-E) C57BL6/J mice underwent CLP or sham surgery. Peritoneal fluid was collected at indicated time points to analyze neutrophils (A-E). Neutrophils were defined as Ly6G^{Hi} and F4/80^{Lo} cells on the CD45+ subpopulation. Percentage of peritoneal neutrophils in CD45+ cells (A), CD64 MFI (B), CD80 MFI (C), mitochondrial density (D) and percentage of Mitotracker^{Hi} CD64^{Hi} subpopulation (E) of peritoneal neutrophils were determined by flow cytometry in peritoneal fluids of CLP- or sham-operated animals at indicated time points.
The data in (A-E) represent mean ± SEM, n=5 per group (A-E) and significance levels were assessed by Mann-Whitney test; * = comparison between sham- and CLP-operated mice at different individual time points, * p <0.05, ** p <0.05, *** p <0.05

In order to assess the impact of LPS on mitochondrial density in peritoneal macrophages, C57BL6/J mice were intraperitoneally injected with either a low (0.5 mg.kg^{-1}) or a high (15mg.kg^{-1}) dose of LPS or saline. Peritoneal fluids were collected after 1 hour and 24 hours. Samples were processed for cytometry as described before. We observed that mitochondrial density was increased in peritoneal macrophages from mice injected with high as well as low dose of LPS (Figure 1.6.A and C). Interestingly, the mitochondrial density in the inflammatory forms of macrophages (CD64^{Hi}), CD64^{Hi}Mitotracker^{Hi} population was increased after 1 hour for low dose (4.8%) and high dose (13.1%) as compared to control (0.44%). It was further increased after 24 hours for low dose (37.7%) and high dose (48.9%), reflecting dose- and time-dependent effects of LPS on mitochondrial density of peritoneal macrophages *in vivo* (Figure 1.6 (B and D)).
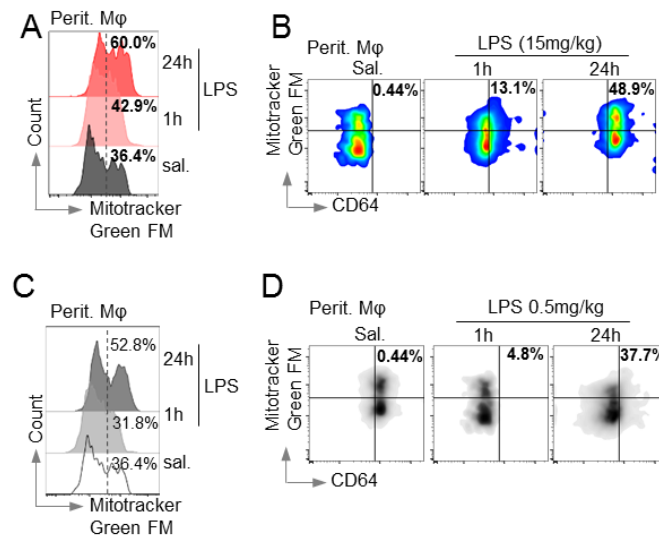
Figure 1.6: Assessment of mitochondrial density in peritoneal macrophages in the context of endotoxemia
(A-D) C57BL6/J mice received intraperitoneal injection high (15 mg/kg) (A-B) and low (0.5 mg/kg) (C-D) dose of LPS. Peritoneal washing were performed at indicated time point (1 hour and 24 hour) and mitochondrial density was assessed in peritoneal macrophages by flow cytometry using mitotracker green FM (A-D).

Interestingly, these results show that low and high doses of LPS produced a similar phenotype of peritoneal macrophages than the one observed in CLP-operated animals. Moreover, the mitochondrial density in peritoneal macrophages as well as the population (CD64[Hi] Mitotracker[Hi]) of peritoneal macrophages was increased, in a similar fashion, in both models of study. We next wondered whether similar changes in mitochondrial density could also be observed in blood monocytes.

1.5 Assessment of mitochondrial density in blood monocytes in the context of polymicrobial infection or endotoxemia

C57BL/6 mice were submitted to CLP or sham surgery and blood samples were collected after 2, 6 and 24 h of operation. Blood samples were collected at each time point before submitting the mice to euthanasia to collect the peritoneal fluids.

Figure 1.7 : Increased mitochondrial density in blood monocytes from CLP-operated mice
(A-C) C57BL6/J mice underwent CLP or sham surgery. Blood samples were collected at indicated time points. Mitochondrial density was analyzed by flow cytometry using mitotracker green FM on blood CD115+ monocytes (A-C).
(D-E) Monocytes were analyzed in blood by applying the gating strategy depicted on Fig. (A). Percentage of CD115+ monocytes (D) and CD115+ CD11h^{Hi} Ly6C^{Hi} inflammatory monocytes (E) were determined by flow cytometry in the blood from CLP- or sham-operated animals at indicated time points.
The data in (A-E) represent mean ± SEM, n=5 per group (A-E) and significance levels were assessed by Mann-Whitney test (B', C' and E); * p <0.05.

Blood monocytes were identified by flow cytometry according to the strategy depicted in Figure 1.7.A. Whole population of monocyte was identified as CD115$^+$ from CD45$^+$ cells (leucocytes) and the mitochondrial density was assessed. Interestingly, similarly to peritoneal macrophages, we observed an increase in mitochondrial density in CD115$^+$ blood monocytes in blood samples collected from CLP-operated mice as compared to sham-operated at 2 h as well as 24 h (Figure 1.7.B). Furthermore, CLP and sham-operated animals presented an increase in the percentage of

monocyte population (CD115$^+$) (Figure 1.7.D). This increase in monocyte population in sham-operated mice could be justified by the fact that injury induced by operation can also act as a signal for more recruitment of monocytes into the systemic circulation from myeloid progenitor cells located in the bone marrow (Geissmann et al., 2010; Gordon and Taylor, 2005; van Furth and Cohn, 1968). As expected, the percentage of inflammatory form of monocytes (CD115$^+$ CD11b$^+$ Ly6C$^+$), which are known to respond faster to inflammatory stimuli and are also known to be recruited to the site of infection (Sunderkotter et al., 2004; Yang et al., 2014), was increased time-dependently in blood samples collected from both CLP- and sham-operated mice (Figure 1.7.E). When assessing mitochondrial density in this population of monocytes, we observed that inflammatory forms of blood monocytes (CD115$^+$ CD11b$^+$ Ly6C$^+$) from CLP-operated mice exhibited higher increase in mitochondrial density as compared to sham-operated mice (Figure 1.7.C and C'). These results indicate that increased mitochondrial density is a hallmark of monocyte and macrophage activation in the context of sepsis.

Figure 1.8: Assessment of mitochondrial density in blood monocytes in the context of endotoxemia
C57BL6/J mice received an intraperitoneal injection low(0.5 mg/kg) and high (15 mg/kg) dose of LPS. Blood was collected 24h after the injection of LPS and mitochondrial density was assessed in CD115+ monocytes by flow cytometry using mitotracker green FM.
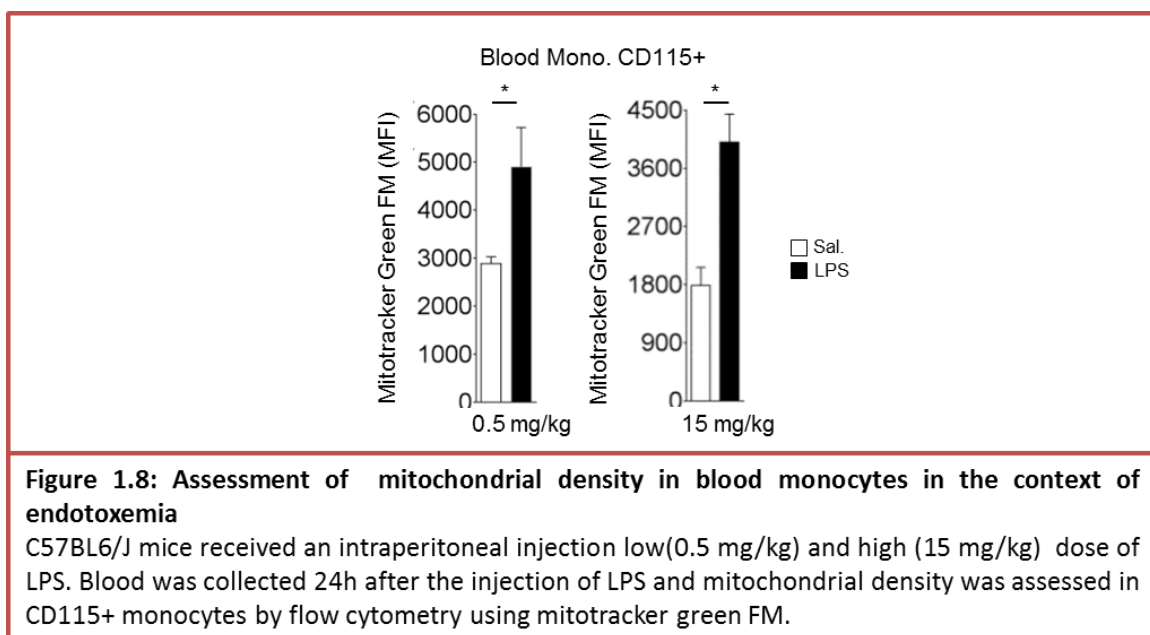
Altogether these data show that LPS is a major factor contributing to the observed effects on mitochondrial density in myeloid cells in the context of sepsis.

Chapter 2

Inhibition of mitophagy is an early feature of classical macrophage activation.

2.1 Increased mitochondrial density in macrophages indicates inhibition of mitophagy

As shown in the previous section, we observed that LPS/IFNγ-stimulated macrophages are associated with increased mitochondrial density. As the effects were observed at an early time point after exposure to Gram-negative bacteria or LPS *in vivo* and *in vitro*, we hypothesized that this increased mitochondrial density in macrophages as measured by mitotracker green FM could be due to the inhibition of mitophagy. First, to control that mitotracker green FM dye was suitable to assess mitophagy by flow cytometry, we assess the phenotype of macrophages exposed to pharmacological modulators of mitophagy. Raw 264.7 macrophages were treated with mitochondrial division inhibitor 1 (Mdivi1; inhibitor of DRP1) (Cassidy-Stone et al., 2008), 3-Methyladenine (3-MA; a PI3 kinase inhibitor, inhibitor of autophagy and mitophagy) (Zhou et al., 2011), TBB and Apigenin (Ruzzene et al., 2002). We checked their impact on mitochondrial density by using mitotracker green FM and flow cytometry strategy.

Mdivi1, 3-MA, TBB and Apigenin triggered a dose-dependent increase of the mitochondrial density in treated macrophages (Figure 2.1.A-D). Conversely, treatment of Raw 264.7 macrophages with CCCP (mitophagy inducer) at 100 and 250 µM for 24 hours lead to a drop in mitochondrial density (Figure 2.1.E). These results suggest that mitotracker green FM coupled to flow cytometry analysis is a valuable strategy to assess mitophagy with an increase reflecting an inhibition of mitophagy whereas a decrease being related to an induction of the mitophagy flux.

In order to further validate our hypothesis of inhibition of mitophagy in activated macrophages, we transfected Raw 264.7 macrophages with an expression vector encoding for the fusion protein mt-Keima (mito-keima). This fusion protein allows the expression of the Keima protein into mitochondria thanks to the fusion of Keima with a mitochondrial targeting signal (cytochrome C oxidase). Keima is a coral protein that is stable at acidic pH inside the lysosome. Keima exhibits different color signals at neutral and acidic pH (Figure 2.2) (Katayama et al., 2011).

This large Stokes shift in fluorescence exhibited by keima between neutral and acidic pH is used as an indicator of mitophagy flux. The higher ratio (550 nm /438 nm) fluorescence reflects increased mitochondrial entrapment by autophagosomal assembly and subsequent clearance.

Figure 2.1 : Increased mitochondrial density in macrophages indicates inhibition of mitophagy (A-D) Mitochondrial density was assessed by flow cytometry in raw 264.7 macrophages treated with Mdivi1 (10,25,50 μM, 24h) (A), 3-MA (500 and 1000 μM) (B), *apigenin* (25 and 50μM, 24h) (C) *4,5,6,7-tetrabromobenzotriazole* (TBB; 1, 10, 50 μM, 24h) (D) or CCCP (100, 250 nM, 24h) (E). Data represents mean ±SEM, n=3 per group and significance levels were assessed by one-way ANOVA followed by post hoc Bonferroni's test (A-E); * = comparison between treated versus untreated controls, ns: not significant, *p <0.05, **p <0.01 or ***p <0.001.

Figure 2. 2: Schematic representation of mechanism of Keima probe
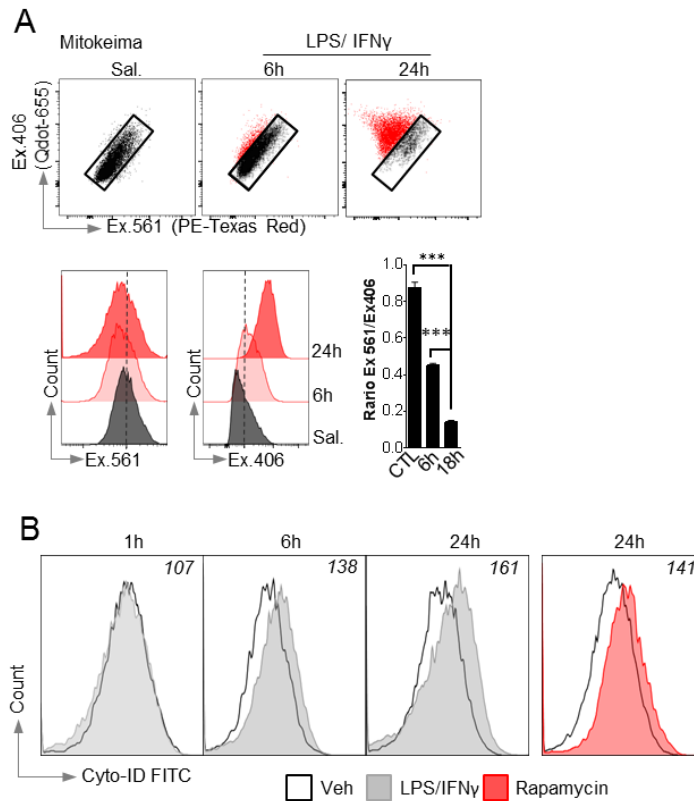
Figure 2.3: Classically activated macrophages exhibit inhibition of mitophagy (A) Mitophagy was assessed in Raw 264.7 macrophages by measuring mitokeima-derived fluorescence by flow cytometry. Cells were transfected with mitokeima expression vector and treated with LPS/IFNγ (100/20ng.mL^{-1}) for indicated duration. (B) Autophagy was assessed at indicated time point by flow cytometry with Cyto-ID autophagy detection kit in LPS/IFNγ (100/20ng.mL^{-1}) treated raw 264.7 macrophages. Rapamycin was used as a positive control. Data represents mean ±SEM, n=3 per group and significance levels were assessed by one-way ANOVA followed by post hoc Bonferroni's test (A); * = comparison between treated versus untreated controls, *p <0.05, **p <0.01 or ***p <0.001.

Katamaya et al., used microscopic technique and used the ratio (550 nm /438 nm) to measure the mitophagy (Figure 2.2) (Katayama et al., 2011). Here in our study, we used BD LSR II cytometer which is equipped with 406 nm and 561 nm laser. After 24 hours of transfection with mt-Keima, Raw 264.7 macrophages were treated with LPS (100ng.mL^{-1}) and IFNγ (20ng.mL^{-1}) for indicated periods of time and analyzed by cytometry. Cells were excited with 406 nm and 561 nm laser beams and excitation ratio (561 nm/406 nm) was used to assess mitophagy. We observed the ratio (561 nm/406 nm) was reduced time-dependently in LPS/IFNγ-treated macrophages, indicating an inhibition of mitophagy (Figure 2.3.A).

Autophagy has been shown to play an important role in immune response. It was reported that IFNγ, as several PAMPs, induces autophagy in macrophages (Delgado et al., 2008). It was also reported that autophagy is important in monocyte differentiation to macrophages in response to M-CSF (Jacquel et al., 2012). To confirm the effect of LPS and IFNγ on autophagy in macrophages, we treated Raw 264.7 macrophages with LPS/IFNγ for 6 hours and 24 hours. As a positive control macrophages were treated with Rapamycin. Rapamycin is a known inducer of autophagy which acts through inhibition of mTOR (Shimobayashi and Hall, 2014). Cells were stained with cyto-ID green dye according to the manufacturer's instructions and were analyzed by flow cytometry. Cyto-ID utilizes an amphiphilic cationic tracer (CAT) dye that selectively labels vacuoles associated with autophagy pathway. We observed that autophagy was induced with LPS/IFNγ-treated macrophages in a time-dependent manner (Figure 2.3.B), in accordance with reported studies (Delgado et al., 2008; Xu et al., 2007). Therefore, although autophagy is increased in LPS/IFNγ-activated macrophages, the dedicated mitochondrial autophagy (mitophagy) is reduced. Therefore inhibition of mitophagy is a specific feature of activated macrophages which role needs to be unraveled.

2.2 Classically activated macrophages exhibit increased mitochondrial network

Mitophagy and mitochondrial dynamics are closely related processes. It has been reported that mitochondrial fission precedes commitment to mitophagy. Moreover, increased mitochondrial network acts as a protective mechanism against autophagy (Gomes et al., 2011; Rambold et al., 2011). Therefore, to further confirm this inhibition of mitophagy in activated macrophages, we assessed the effect of LPS/IFNγ on mitochondrial dynamics and morphology in macrophages with fluorescence and electron microscopy. Mitochondrial density was assessed by microscopy in Raw 264.7 macrophages treated with LPS/IFNγ for 6 hours. Cells were stained with mitotracker green FM (200nM) and were observed under fluorescence microscopy (Figure 2.4.A). Increased mitochondrial density and network was observed in macrophages treated with LPS/IFNγ as compared to untreated controls as can be seen by the increase in green fluorescence intensity (Figure 2.4.A).
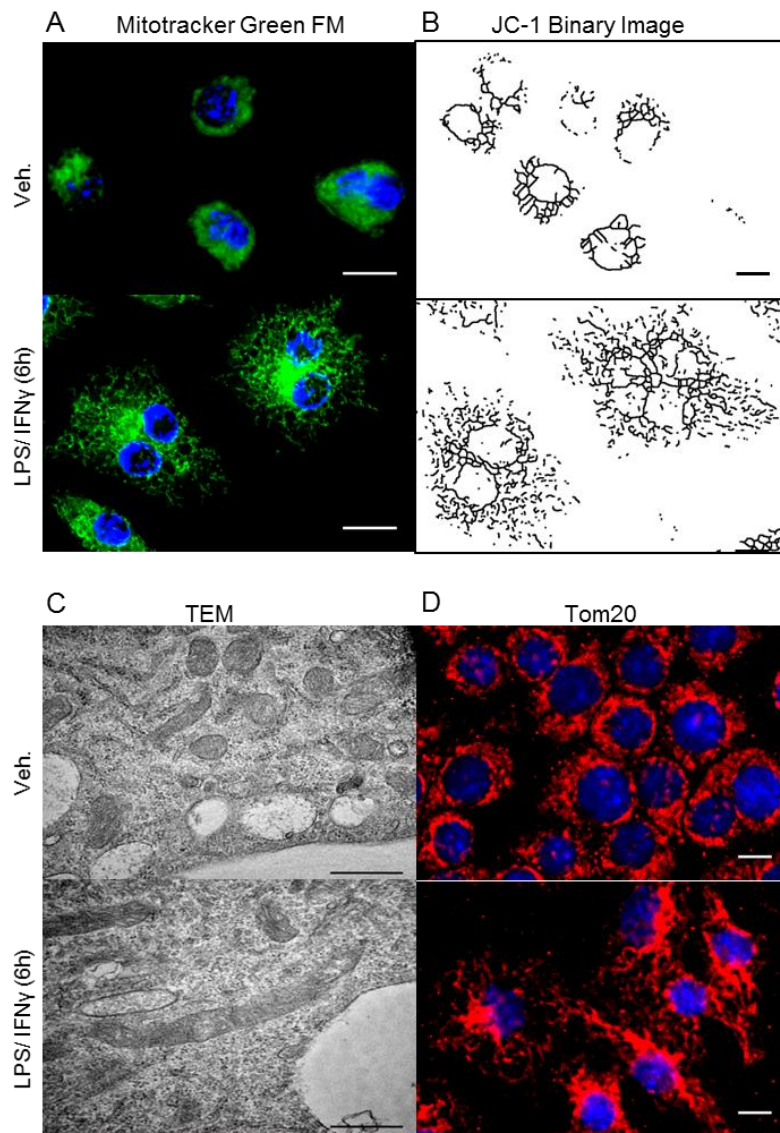
Figure 2.4: Classically activated macrophages exhibit increased mitochondrial network (A) Mitochondrial density and network was assessed 6h after LPS/IFNγ exposure (100/20ng.mL^{-1}) in Raw 264.7 macrophages by fluorescent microscopy (scale bar: 10µm) by staining macrophages with mitotracker green FM (A) or JC-1 - binary images (B). (C) Mitochondrial network was assessed 6h after LPS/IFNγ exposure (100/20ng.mL^{-1}) in Raw 264.7 macrophages by transmission electron microscopy (scale bar: 500nm) (D) Mitochondrial network was assessed by fluorescent microscopy 6h after LPS/IFNγ exposure (100/20ng.mL^{-1}) in peritoneal macrophages immune-stained for tom20 (scale bar: 10µm). Microscopy pictures (A-D) are representative of 3 separate experiments.

In another set of experiments, Raw 264.7 macrophages were stained with JC-1, a probe used to measure membrane potential and mitochondrial density. Cells were analyzed by fluorescence microscopy to assess mitochondrial density and network. To have a better understanding we

have converted images into binary form which allows a better visualization of the mitochondrial network (Figure 2.4.B). Image J software was used to convert images to binary form. These results showed that mitochondrial density and network was increased in LPS/IFNγ-treated macrophages compared to untreated control (Figure 2.4.B) (binary images).

Figure 2.5: Classically activated macrophages exhibit increased mitochondrial density (A-B) Raw 264.7 macrophages were transfected with MitoOrange expression vector and treated 24h after transfection with LPS/IFNγ (100ng.mL^{-1}/20ng.mL^{-1}) for 18h. Mitochondrial density was assessed by flow cytometry (A) or fluorescent microscopy (B). (B) Microscopy pictures are representative of 3 separate experiments (scale bar: 10μm). (A) Flow cytometry data represents mean ±SEM, n=3 per group and significance levels were assessed by t test; * = comparison between treated versus untreated controls; *p <0.05, **p <0.01 or ***p <0.001. (B) Microscopy pictures are representative of 3 separate experiments.

We repeated the treatment for 6 hours and processed cells for electron microscopy and assessed mitochondrial morphology. Interestingly, when macrophages were observed under transmission electron microscopy, the elongated mitochondrial network was seen in Raw 264.7 macrophages treated with LPS/IFNγ (Figure 2.4.C). It suggests increased mitochondrial fusion or decreased fission in macrophages with LPS/IFNγ treatment. Mouse peritoneal macrophages were treated for 6 hours with LPS/IFNγ and stained with anti-Tom 20 (Figure 2.4.D). In accordance with results obtained in Raw 264.6 macrophages, LPS/IFNγ-treated peritoneal macrophages showed increased mitochondrial network as compared to untreated control (Figure 2.4.D). Finally,

mitochondrial density was also assessed in Raw 264.7 macrophages by using another strategy. Raw 264.7 macrophages were transfected with MitoOrange expression vector designed to express a fluorescent protein fused with cytochrome C and therefore obtaining a fluorescence signal restricted to the mitochondria. After 24 hours of transfection, cells were treated with LPS/IFNγ for 18 hours and mitochondrial mass was measured by flow cytometry (Figure 2.5.A) and fluorescence microscopy (Figure 2.5.B). Again, we observed that an increased mitochondrial density and mitochondrial fusion in M1 macrophages (Figure 2.5.A-B).

Altogether these results demonstrated that LPS/IFNγ-activated macrophages display an increased mitochondrial network and density which is in accordance with the proposed inhibition of mitophagy.

2.3 Mitophagy checkpoints are down-regulated in macrophages upon classical activation

Mitophagy is a selective process and mainly relies on mitochondrial recruitment and activity of the key mitophagy-related proteins, PINK1, Parkin and DJ-1 (Dodson and Guo, 2007; Poole et al., 2008; Trempe and Fon, 2013). All three proteins have been recognized to form a E3 ubiquitin ligase complex and have also been associated with Parkinson's disease (Dodson and Guo, 2007; Exner et al., 2012; Hattori and Mizuno, 2004; Irrcher et al., 2010). Moreover, proteins involved in the modulation of mitochondrial dynamics especially Dynamin-related protein 1 (DRP1) also contribute to the regulation of mitophagy (Tanaka et al., 2010; Twig et al., 2008; Twig and Shirihai, 2011).

Mitochondrial uncouplers have been shown to dissipate mitochondrial membrane potential and to induce mitophagy (Narendra et al., 2008). We assessed the impact of LPS/IFNγ in Raw 264.7 macrophages on these key actors of mitophagy in the presence or in the absence of mitochondrial uncouplers (CCCP and 2,4-DNP). Interestingly, these four key proteins, PINK1, Parkin, DJ-1 and Drp1, were downregulated in LPS/IFNγ-treated Raw 264.7 macrophages (Figure 2.6.A-B). As expected, co-treatment of macrophages with mitophagy inducers CCCP and 2,4-DNP counteracted the effect of LPS/IFNγ on downregulation of all four proteins (Figure 2.6.A-B). Downregulation of these proteins strongly suggests that mitophagy is inhibited in classically

activated macrophages. A similar time-dependent downregulation of these proteins was seen in bone marrow-derived macrophages (BMDMs) treated with LPS/IFNγ (Figure 2.7.A).

Figure 2.6: Mitophagy checkpoints are downregulated in macrophages upon classical activation
(A) Immunoblots of PINK1, Parkin, DJ-1, DRP1 and β-actin on whole protein lysates from Raw 264.7 macrophages treated with LPS/IFNγ (100/20ng.mL^{-1}) alone or in combination with *carbonyl cyanide 3-chlorophenylhydrazone* (CCCP, 500nM) for 24h. Black arrow 63kDa, white arrow 52kDa. (B) Immunoblots of PINK1, Parkin, DJ-1, DRP1 and β-actin on whole protein lysates from raw 264.7 macrophages treated with LPS/IFNγ (100/20ng.mL^{-1}) alone or in combination with *2,4 dinitrophenol* (2,4-DNP, 1μM) for 24h.
Black arrow 63kDa, white arrow 52kDa, red arrow 45kDa.

Dissipation of mitochondrial membrane potential leads to stabilization of PINK1 on mitochondria. PINK1 activates and recruits Parkin to the mitochondria through its kinase activity. Parkin is known to ubiquitinate mitochondrial proteins in a PINK1-dependent manner. Ubiquitinated mitochondria are recognized by autophagy assembly and undergo mitophagy (Kazlauskaite et al., 2014; Kondapalli et al., 2012; Matsuda et al., 2010; Okatsu et al., 2012; Shiba-Fukushima et al., 2014; Shiba-Fukushima et al., 2012).

In contrast, on healthy mitochondria with stable membrane potential, full-length PINK1$_{63}$ (63 kDa) undergoes proteolysis processing and give rise to the cleaved form PINK1$_{53}$ (53 kDa) and the minor cleaved form PINK1$_{45}$ (45 kDa) (Fedorowicz et al., 2014; Kondapalli et al., 2012; Lin and Kang, 2008; Yamano and Youle, 2013). In our model, we observed that LPS/IFNγ-stimulated macrophages showed downregulation of Pink$_{63}$ and PINK1$_{53}$ form whereas PINK1$_{45}$ accumulated

in a time-dependent manner (Figure 2.7.B). Cleavage of PINK1 into the 53 kDa product and its subsequent translocation to cytosol has been reported to suppress Parkin translocation to the mitochondria (Fedorowicz et al., 2014). We have observed that in untreated macrophages, PINK1 was mainly localized on mitochondria whereas in LPS/IFNγ-stimulated macrophages it was distributed mainly in the cytosol (Data shown later, Figure 5.8). Interestingly, LPS/IFNγ-treated macrophages showed the disappearance of Parkin in mitochondrial fraction (Figure 2.7.B). Therefore, we can assume that cytosolic translocation of PINK1 represses the recruitment of Parkin to the mitochondria in LPS/IFNγ-treated animals. Furthermore, DJ-1 and DRP1 were also downregulated in mitochondrial fractions (Figure 2.7.B). Altogether these results further empower our hypothesis that LPS/IFNγ-activated macrophages display inhibition of mitophagy.

Figure 2.7: Mitophagy checkpoints are down-regulated in macrophages upon classical activation
(A-B) Mitophagy was assessed by western blotting. (A) Immunoblots of PINK1, Parkin, DJ-1, DRP1 and β-actin on whole protein lysates from BMDMs treated with LPS/IFNγ (100/20ng.mL^{-1}). (B) Immunoblots of PINK1, Parkin, DJ-1, VDAC and β-actin on mitochondrial lysates purified from Raw 264.7 macrophages treated with LPS/IFNγ (100/20ng.mL^{-1}).
Black arrow 63kDa, white arrow 52kDa, red arrow 45kDa.

2.4 Pharmacological modulation of mitophagy in myeloid cells

We have shown above that the population of peritoneal macrophages (CD64^{Hi} Mitotracker^{Hi}) was increased after CLP (Figure 1.4.C) as well as after intraperitoneal injection of LPS (Figure 1.6.B & D). By injecting mitophagy inhibitor, Mdivi1 (5 mg.kg^{-1}) intraperitoneally to C57BL6/J mice, we

observed that the same population of peritoneal macrophages (CD64^{Hi} Mitotracker^{Hi}) was increased with mitophagy inhibitor (Figure 2.8.A). Furthermore, the *in vitro* treatment of Raw 264.7 macrophages with LPS, LPS/IFNγ or Mdivi1 mimicked the *in vivo* observation (Figure 2.8.B-C). In contrast, the prior-injection of mitochondrial uncoupler (2,4-DNP) significantly reduced this population after LPS injection or CLP surgery (Figure 2.9.B & D). Mitochondrial density induced in peritoneal macrophages by LPS injection was significantly reduced in mice which received prior injection of 2,4-DNP (Figure 2.9.A). A similar reduction in mitochondrial density, induced after CLP, was observed in blood monocytes (CD115^{+}) as well as inflammatory blood monocytes (CD115^{+} CD11b^{Hi} Ly6C^{Hi}) from mice which received prior injection of 2,4-DNP (Figure 2.9.C).
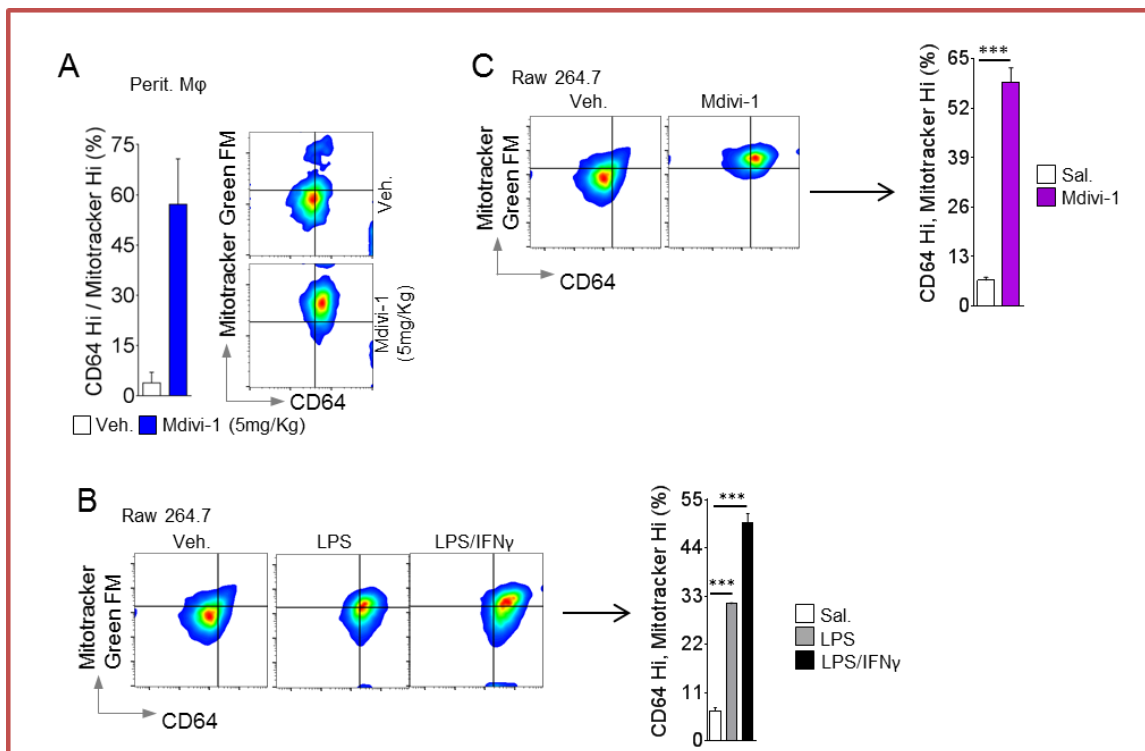
Figure 2.8: Increased mitochondrial density in myeloid cells (in vivo) indicates inhibition of mitophagy
(A) Mitochondrial density was assessed by flow cytometry in peritoneal macrophages of mice treated for 24h with *mitochondrial division inhibitor 1* (mdivi-1, 5mg/Kg) or vehicle (Veh., DMSO).
(B-C) Percentage of macrophage subpopulation (CD64^{Hi} Mitotracker^{Hi}) of was assessed in Raw 264.7 macrophages treated for 24 with LPS (100ng.mL^{-1}) or LPS/IFNγ (100/20ng.mL^{-1}) (B) or *mitochondrial division inhibitor 1* (mdivi-1, 50μM, 24h) (C).
Data represents mean ±SEM, n=3 per group and significance levels were assessed by t test (A,C) or one-way ANOVA followed by post hoc Bonferroni's test (B); * = comparison between treated versus untreated controls, *p <0.05, **p <0.01 or ***p <0.001.

Figure 2.9: Increased mitochondrial density in myeloid cells (*in vivo*) indicates inhibition of mitophagy

(A-D) Mitochondrial density was assessed by flow cytometry in peritoneal macrophages (A-B, D) and blood monocytes (C) of mice pre-treated for 24h with the mitophagy inducer *2,4 dinitrophenol* (2,4-DNP, 10mg/Kg) or saline (sal.) and then submitted to intraperitoneal LPS injection (10mg/kg) (A-B) or CLP surgery (C-D). Blood was collected 2h after CLP surgery (C) and peritoneal fluids were collected 24h after LPS injection (A-B) or CLP surgery (D).

The data in (A-D) represent mean ± SEM, n=6 (A-B), n=14 (C), and n=8 (D). Significance levels were assessed by Mann-Whitney test (A-D).

All flow cytometry histograms and dot plots are representative of 3-6 separate samples.

Altogether these results further show that increased mitochondrial density in peritoneal macrophages and blood monocytes observed *in vivo* after CLP as well as endotoxemia is a hallmark of mitophagy inhibition. Moreover, this data demonstrates that mitophagy can be modulated *in vivo* with these previously known mitophagy modulators in *in vitro* models.

Chapter 3

Inhibition of mitophagy in monocytes and macrophages protects mice against bacterial infection

3.1 Inhibition of mitophagy primes monocytes and macrophages against infection

In order to understand the role of mitophagy inhibition in macrophages and monocytes in immune defense against bacterial infection, we induced mitophagy *in vivo* with mitochondrial uncouplers and assessed the immune response by looking at several factors including survival to infection, cytokine release and bacterial burden. C57BL6/J mice received an intraperitoneal injection of 2,4-DNP (10 mg.Kg^{-1}) or saline. After 24 hours of injection, mice underwent CLP- or sham-surgery. Mice were observed for survival up to 10 days, blood samples were collected after 2 hours to assess mitochondrial density in blood monocytes and followed for survival. In an independent experiment, blood, peritoneal fluid and the liver were collected after 24 hours of CLP- or sham-surgery to assess bacterial load. Plasma cytokine levels were also measured in blood samples collected after at 24 hours of CLP- or sham-surgery. No death was observed in both sham-operated groups, 2,4-DNP- or saline-injected mice (Figure 3.1.A). This suggests that the dose of 2,4-DNP used was not toxic for mice. Survival studies revealed that mice which received 2,4-DNP prior to infection died more as compared to saline-injected mice. Indeed, mortality reached up to 92.3% in mice which received 2,4-DNP as compared to 71.41 % in saline-injected controls on day 10 after infection (Figure 3.1.A). We have previously shown that 2,4-DNP induced mitophagy in model of CLP, so we suspected that this higher mortality could be due to the reduced inhibition of mitophagy. Intriguingly, a correlation between mitochondrial density in blood monocytes (CD115+) as well as inflammatory blood monocytes (CD115+CD11b^{Hi}Ly6C^{Hi}) with the survival rate was observed, indicating that mice which survived more had higher mitochondrial density in these two populations (Figure 3.2.B-C). Furthermore, the correlation between the percentage of inflammatory monocytes and survival as well as the correlation between mitochondrial density and inflammatory monocytes were not significant (Figure 3.1.D-E). These observations suggest inhibition of mitophagy in monocytes (corresponding to higher mitochondrial density) is a predictive factor for survival.
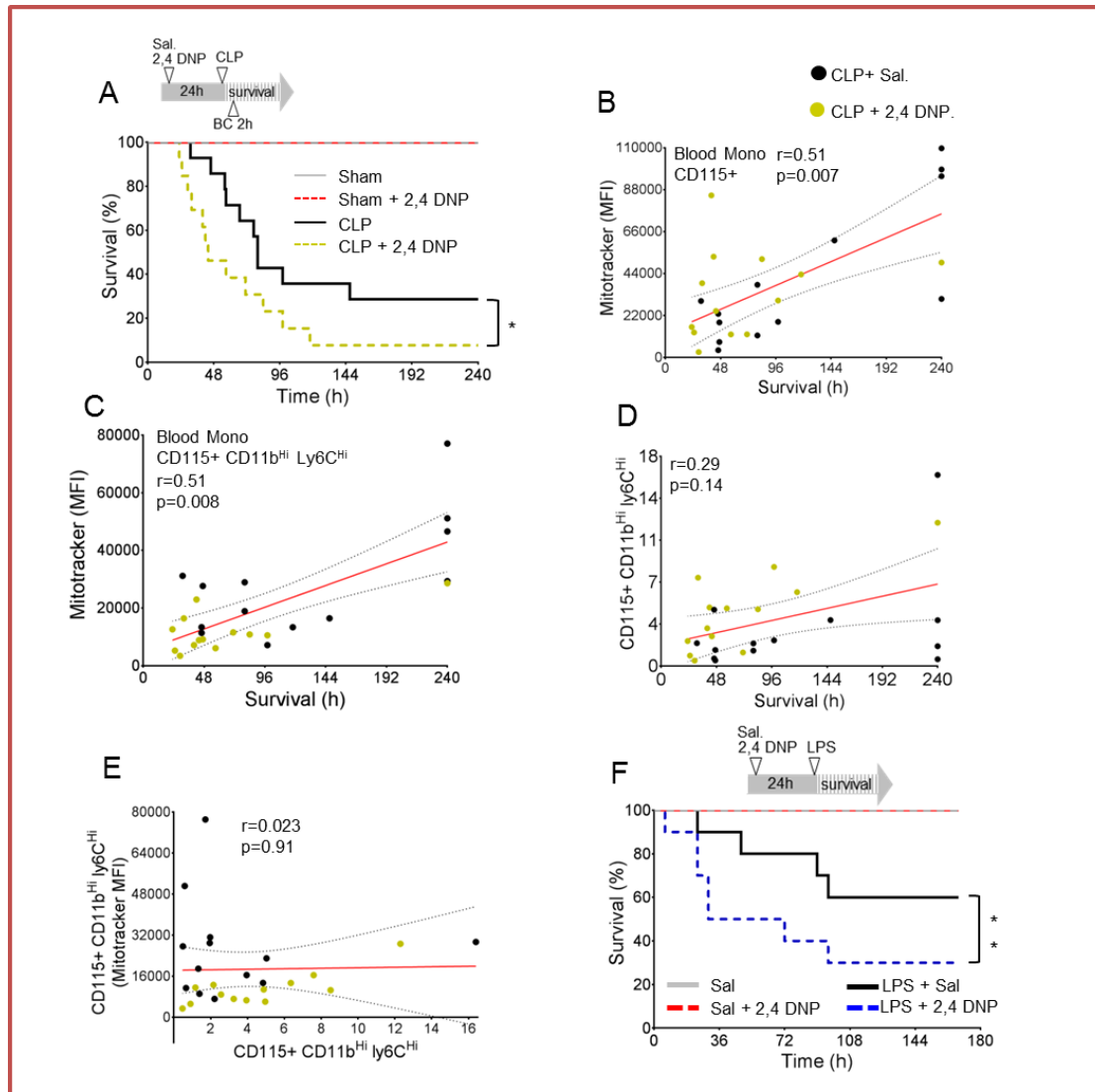
Figure 3.1: Mitophagy inhibition in monocytes is protective against infection

(A-E) C57BL6/J mice were pre-treated for 24h with 2,4-DNP (10mg/Kg) or saline (Sal.) and then underwent CLP. Survival was followed during 10 days (A-D). Blood was collected 2h after CLP and analyzed by flow cytometry. Correlation between survival and mitochondrial density in monocytes (CD115+) (B) or inflammatory monocytes population (CD115+CD11b^{Hi}Ly6C^{Hi}) (B-C) as well as correlation between inflammatory monocytes population (CD115+CD11b^{Hi}Ly6C^{Hi}) and survival (D) and their mitochondrial density (E) were examined .

(F) C57BL6/J (n=10) mice were pre-treated for 24h with *2,4 dinitrophenol* (2,4-DNP, 10mg/Kg) or saline (Sal.) and then received an intraperitoneal injection of LPS (15mg/Kg). Survival was followed during 7 days.

Survival was analyzed by Kaplan-Meier and significance levels were assessed by log-rank (Mantel-Cox) test (A, F); (A) Sham (n=5 per group) CLP (n=14 per group), (F) Sham (n=5 per group), LPS (n=10 per group). Correlation analysis was carried out with the parametric Pearson test (B-E).

*p <0.05, **p <0.01 or ***p <0.001.

Altogether these results gave rise to several new questions: How does this inhibition of mitophagy play role in monocytes and inflammatory monocytes? How does it contribute to survival against bacterial infection? How does modulation of mitophagy lead to higher death?

Figure 3.2: Mitophagy modulation impacts on inflammatory cytokine release in response to infection
C57BL6/J mice were pre-treated for 24h with 2,4-DNP (10 mg/Kg) or (15 mg/Kg) or saline (Sal.) and then underwent CLP. Blood samples were collected after 24 hours of CLP and Plasma inflammatory cytokines were measured.
The data in represent mean ± SEM, n=8 per group and significance levels were assessed by Mann-Whitney test; *p <0.05, **p <0.01 or ***p <0.001.

In order to answer these questions plasma cytokine levels in the blood and bacterial burden in peritoneal cavity, blood and liver were assessed in CLP-operated animals pre-treated with 2,4-DNP or saline. We observed that plasma cytokines, that are classically increased in sepsis (TNFα, IL-6, MCP-1 and IL-10), were at significantly lower levels in mice injected with 2,4-DNP as compared to saline-injected mice (Figure 3.2). Surprisingly, IL-1β levels in plasma were not significant but still higher in 2,4-DNP-injected as compared to saline-injected mice in their plasma after 24 hours of CLP surgery (Figure 3.2). When we assessed the bacterial load in the peritoneal cavity, mice pre-injected with 2,4-DNP, as compared to saline-preinjected, exhibited significantly higher bacterial load after CLP surgery (Figure 3.3.A), suggesting decreased bactericidal activity. No significant differences in bacterial load were observed in the liver and blood samples between both groups (Figure 3.3.B-C). Interestingly, peritoneal macrophages (CD64[Hi] CD80[Hi]) were significantly higher in mice which underwent CLP surgery and received a saline injection, compared to 2,4-DNP-injected mice (Figure 3.3.D). Furthermore, we found a significant correlation between macrophage-population (CD64[Hi]Mitotracker[Hi]) and bacterial load in the peritoneal cavity (Figure 3.3.E). This indicates that this population (CD64[Hi] Mitotracker[Hi]) of

macrophages that we have identified seems to be endowed with bactericidal activity. The mice that have a high percentage of these cells have also a lower bacterial load in the peritoneal cavity. Together, our data allow assuming that the reduction of the inhibition of mitophagy in CLP-operated animals (obtained with 2,4-DNP pretreatment) leads to a reduce activation of macrophages in the peritoneal cavity. This explains the reduced plasma level of inflammatory cytokines associated with the reduced anti-microbicidal activity. This contributes to the higher death rate observed in the CLP-operated animal treated with a mitophagy inducer. Therefore, inhibition of mitophagy in myeloid cells seems to be a protective mechanism in the context of bacterial infection.
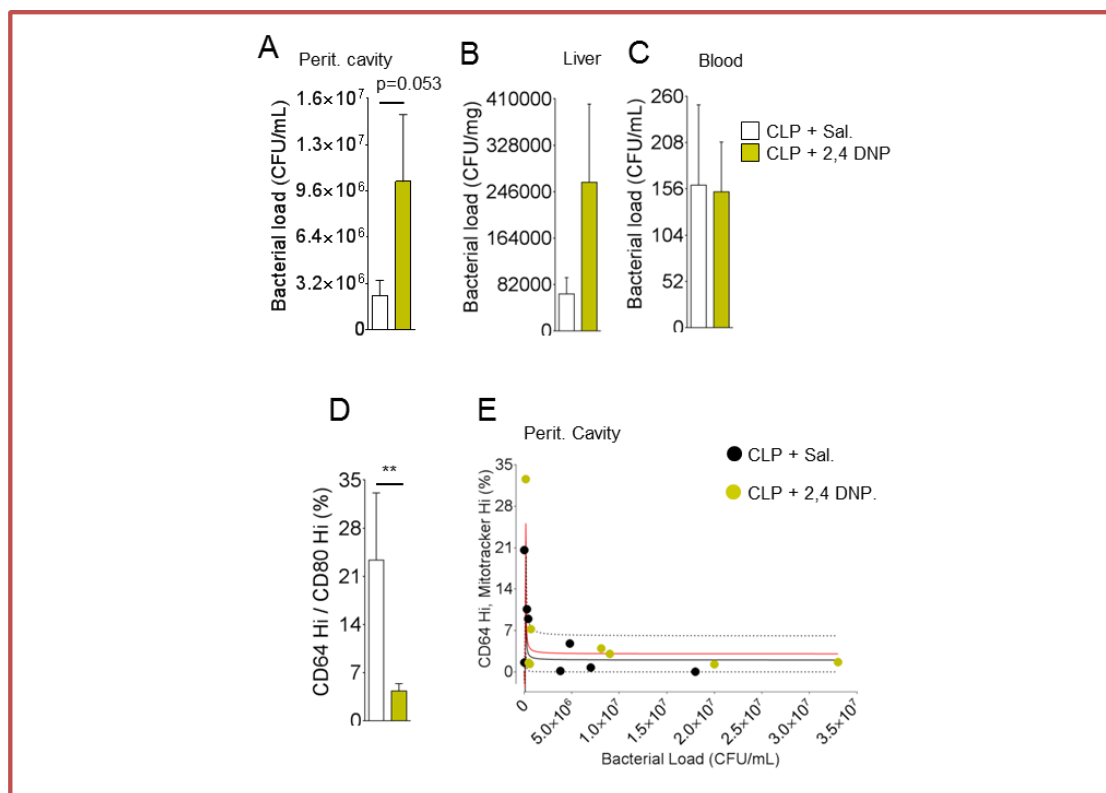
Figure 3.3: Mitophagy inhibition is critical for bacterial clearance
C57BL6/J mice were pre-treated for 24h with 2,4-DNP (10mg/Kg) or (15mg/Kg) or saline (Sal.) and then underwent CLP. Peritoneal fluid was collected 24h after CLP surgery (A-E) to assess bacterial load (A) and macrophage activation by flow cytometry (D). Liver and blood samples were collected 24h after CLP surgery to assess bacterial load in the liver (B) and in the blood (C). Correlation between CD64[Hi]Mitotracker[Hi] macrophage subpopulation and peritoneal bacterial load was examined (E).
The data in represent mean ± SEM, n=8 per group (A-E) and significance levels were assessed by Mann-Whitney test (A-D); *p <0.05, **p <0.01 or ***p <0.001.
Correlation analysis was carried out with the parametric Pearson test (E).

We also assessed the effect of mitophagy induction on the survival of mice in response to LPS injection. For survival studies, C57BL6/J mice received intraperitoneal injection of 2,4-DNP (10 mg.Kg^{-1}) or saline. After 24 hours of 2,4-DNP injection, mice received an injection of LPS (15 mg.Kg^{-1}) or saline and survival of animals was followed upto 7 days.

We observed that mice injected with 2,4-DNP and LPS died more and faster as compared to saline- and LPS-injected mice. On day 7 the mortality reached up to 70 % in 2,4-DNP and LPS injected group whereas in LPS alone injected group it reached up to 40% (Figure 3.1.F). We could have expected an improvement in survival due to a potential decreased in the plasma levels of inflammatory cytokines following treatment with mitophagy inducers. Several studies have reported that LPS increases intestinal tight junction permeability and increases the bacterial translocation from gut to the peritoneal cavity and systemic circulation (Guo et al., 2013; Guo et al., 2015). Therefore, we can assume that the higher mortality in LPS-injected mice pre-treated with LPS is due to a higher bacterial translocation. Unfortunately, the bacterial burden was not assessed in this experiment. This hypothesis would need to be experimentally validated.

3.2 Mitophagy modulation effects on inflammatory cytokines induction in response to LPS

To further assess the impact of the stimulation of mitophagy on the LPS-induced inflammatory response, we next investigated the effect of mitophagy inducer (i.e. CCCP) on cytokine release. We used a lower dose of LPS to avoid the lethal effect of LPS and bacterial translocation. C57BL6/J mice received an intraperitoneal injection of CCCP (5 mg.Kg^{-1}) or saline. After 24 hours, CCCP- or saline-injected mice received the second injection of either low dose of LPS (0.5 mg.Kg^{-1}) or saline. Blood samples were collected at 1, 3 and 24 hours after the LPS injection and plasma cytokines were measured (Figure 3.4.A-D). LPS injection produced significant induction of plasma cytokines including inflammatory cytokines, IL-6, IL-12p70 and TNFα as well as cytokine IL-10, at early time point (1 hour). Interestingly, a significant reduction in the levels of IL-6, IL-12p70 as well as IL-10 was observed in plasma from mice, which received prior-injection of CCCP. Significant differences in levels of cytokines (IL-6, IL-12p70 and IL-10, but not TNFα) were visible after 24 hours of LPS injection between both groups, CCCP- and saline-injected (Figure 3.4.A-D (insets)).
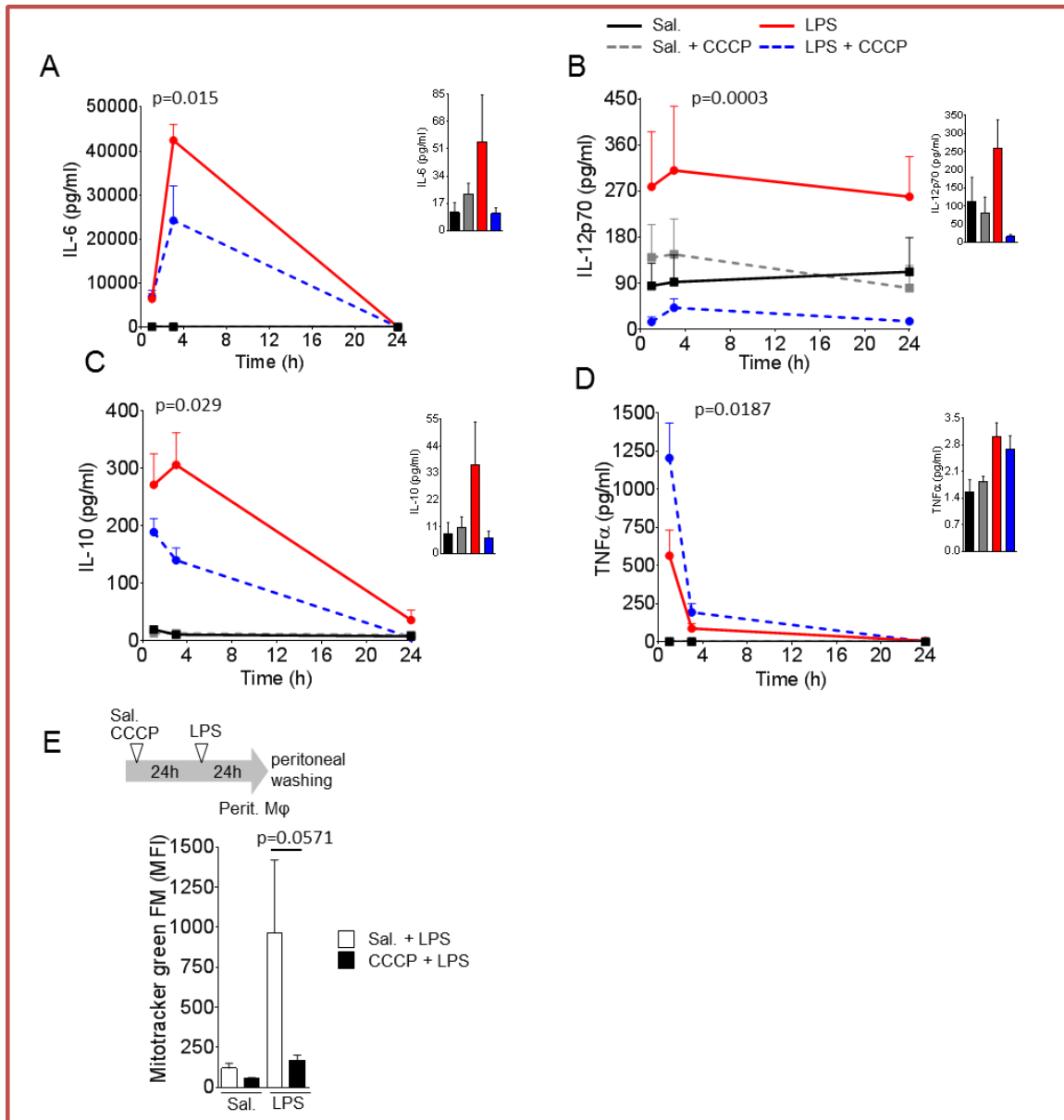
Figure 3.4: Mitophagy modulation impacts on inflammatory cytokine release in response to LPS

(A-E) C57BL6/J mice were pre-treated for 24h with *carbonyl cyanide 3-chlorophenylhydrazone* (CCCP, 5mg/kg) or saline (Sal.) and then received an intraperitoneal injection of LPS (0.5mg/kg). Plasma levels of IL-6 (A), IL-10 (B), IL-12p70 (C) and TNFα(D) were measured at indicated time points. Insets represent plasma levels of IL-6 (A), IL-10 (B), IL-12p70 (C) and TNFα(D) 24h after intraperitoneal LPS injection. (E) Mitochondrial density was assessed by flow cytometry in peritoneal macrophages. Peritoneal fluids were collected 24h after LPS injection.

The data in represent mean ± SEM, n=5 per group (A-E).

For cytokines analysis p values were obtained by running two way ANOVA between LPS vs LPS+DNP injected groups (A-D)

For mitochondrial density p value was obtained by Mann-Whitney test (E).

When we assessed the mitochondrial density in peritoneal macrophages, we observed that peritoneal macrophages from LPS-injected mice exhibited significantly higher mitochondrial density as compared to saline injected. In contrast, mice injected with both CCCP and LPS showed significant reduction in mitochondrial density in peritoneal macrophages as compared to mice injected with LPS only, indicating that CCCP reduced the effect of LPS on mitophagy inhibition in macrophages (in vivo) (Figure 3.4.E). These results, in accordance with previous observations, indicate that rescuing mitophagy in macrophages could lead to decreased inflammatory cytokine release and decreased inflammatory response.

3.4 Stimulation of mitophagy prevents macrophage activation and bactericidal activity

We observed that the induction of mitophagy (*in vivo*) reduces the inflammatory cytokine release, bactericidal activity as well as survival in the context of sepsis. In order to evaluate whether these effects were due to myeloid cells, we assessed the effect of pharmacological modulation of mitophagy in cultured macrophages *in vitro*. Raw 264.7 macrophages were treated with LPS /IFNγ in the presence or absence of CCCP (500 nM) for 24 hours. Impact on macrophage activation and inflammatory markers was examined. As expected, it was observed that LPS/IFNγ-treated macrophages showed higher levels of M1 markers (CD64 and CD80), as assessed by flow cytometry (Figure 3.5.A). Conversely, these LPS/IFNγ-induced M1 markers were significantly reduced in macrophages co-treated with CCCP (Figure 3.5.A). Moreover, the release of inflammatory cytokines in medium from Raw 264.7 macrophages was induced by LPS/IFNγ. At the opposite, this LPS/IFNγ-mediated cytokine release was drastically reduced in macrophages co-treated with CCCP (Figure 3.5.B). Furthermore, gene expression of inflammatory markers, IL-6, iNOS, as well as CD80 was induced by LPS/IFNγ whereas the induction was significantly reduced in macrophages co-treated with CCCP (Figure 3.5.C). We did not observe any significant difference in TNF-α mRNA levels between LPS/IFNγ alone and CCCP-co-treated macrophages (Figure 3.5.D).
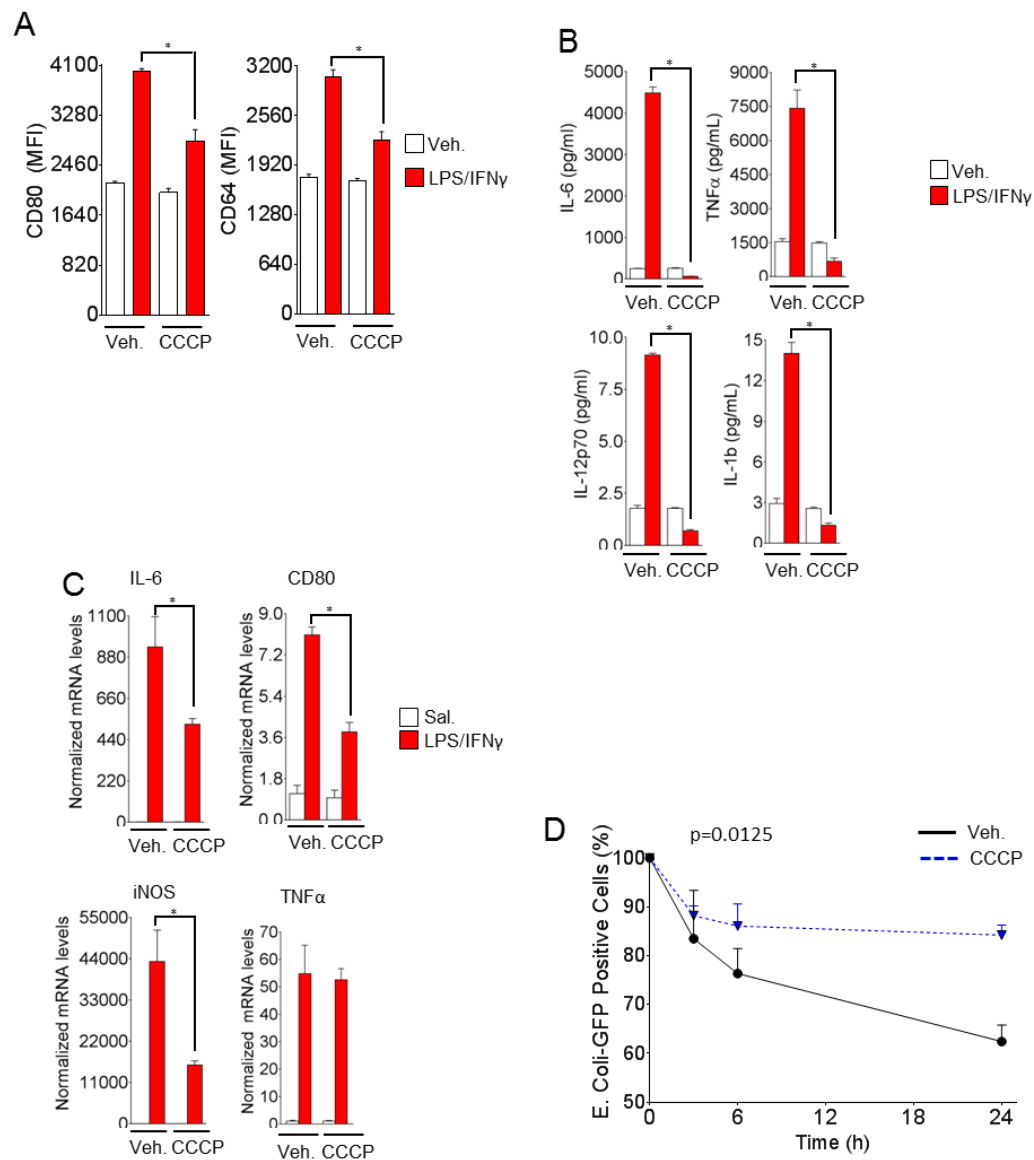
Figure 3.5 : Stimulation of mitophagy prevents macrophage activation and bactericidal activity
 (A-C). Raw 264.7 macrophages were treated for 24h with LPS (100ng.mL^{-1}) or LPS/IFNγ (100/20ng.mL^{-1}) alone or in combination with *carbonyl cyanide 3-chlorophenylhydrazone* (CCCP, 500nM). Macrophage activation was assessed by flow cytometry (A), by measuring cytokines release (B) or inflammatory markers expression levels (C). (E) Bactericidal activity of Raw 264.7 macrophages pre-treated for 24h with CCCP (500nM) or vehicle (Veh. DMSO) against *Escherichia coli-GFP* was determined by gentamycin protection assay.
Data represents mean ±SEM, n=3 per group (A-D) and significance levels were assessed by t test (A-C) or two-way ANOVA (D); *p <0.05, **p <0.01 or ***p <0.001.
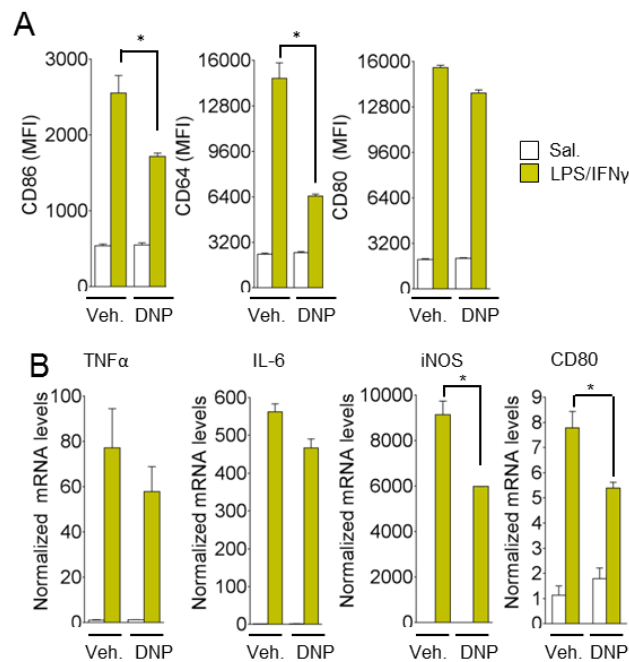
Figure 3.6 : Stimulation of mitophagy prevents macrophage activation in response to LPS/IFNγ
(A-B) Raw 264.7 macrophages were treated for 24h with LPS/IFNγ (100/20ng.mL^{-1}) alone or in combination with *2,4 dinitrophenol* (2,4-DNP, 1μM) (A-B). Inflamatory markers were measured by flow cytometry (A) and by qPCR (B).
Data represents mean ±SEM, n=3 per group and significance levels were assessed by t test; *p <0.05, **p <0.01 or ***p <0.001.

We also assessed the effect of mitophagy stimulation with 2,4-DNP (1μM) on LPS/IFNγ-induced macrophage activation and regulation of inflammatory cytokines at mRNA levels. Similar to CCCP, 2,4-DNP-mediated mitophagy induction reduced the effect of LPS/IFNγ on macrophage activation markers as well as mRNA levels of inflammatory markers (Figure 3.6.B).

Next, we investigated the effect of mitophagy stimulation on bactericidal activity of Raw 264.7 macrophages. Gentamycin protection assay was adapted to quantify the bactericidal activity by flow cytometry. Raw 264.7 macrophages were pretreated with CCCP (500nM) for 24 hours and were infected with *E.coli*-GFP (MOI: 10 bacteria per macrophage) for 2, 6 and 24 hours. Change in GFP fluorescence intensity measured by flow cytometry was used as an indicator of bactericidal activity. We observed that mitophagy stimulation with CCCP significantly reduced the bactericidal activity of macrophages (Figure 3.5.D). Altogether these results show that mitophagy stimulation prevented LPS/IFNγ-mediated switching of macrophages towards

inflammatory and bactericidal phenotype (M1 phenotype). These results suggest that inhibition of mitophagy contributes to activation and functions of M1 macrophage.

Conclusion Part I

Our data demonstrate that, in the context of Gram-negative bacterial infection and endotoxemia, myeloid cells (namely monocytes, macrophages, and neutrophils) exhibit increased mitochondrial density. We have identified a new population of macrophages which express CD64 and are associated with higher mitochondrial density (CD64^{Hi} Mitotracker^{Hi}). This population increases in the context of sepsis or infection as well as in *in vitro* model of macrophages. Furthermore, CD64^{+} macrophages exhibited higher mitochondrial density even at quiescent state.

We have proven *in vitro* and *in vivo* that this increased mitochondrial density in myeloid cells is due to inhibition of mitophagy. Inhibition of mitophagy was evidenced by increased mitochondrial density, increased tubular mitochondrial network, mitophagy assessment with mitokeima probe and downregulation of key mitophagy-related proteins.

To the best of our knowledge, the present study is the first to show modulation of mitophagy in myeloid cells *in vivo* by using pharmacological agents. Furthermore, we were able to mimic the effect of LPS or infection on macrophages *in vitro* as well as *in vivo* by pharmacological inhibitors of mitophagy. Accordingly, we have shown *in vivo* and *in vitro* that mitophagy induction by using the mitochondrial uncouplers could repress the inflammatory response as well as bactericidal activity.

Therefore, inhibition of mitophagy in myeloid cells acts as a protective mechanism and is a prerequisite for survival against bacterial infection.

PART II

Inhibition of mitophagy triggers macrophage activation in a ROS dependent manner

Introduction:

The mROS contributes to the immune response via activating different signaling pathways namely NLRP3, HIF1α and NFκB (Asehnoune et al., 2004; Mills et al., 2016; Tannahill et al., 2013; Zhou et al., 2011). Recent studies have suggested that mROS also contribute to bactericidal activity (Garaude et al., 2016; West et al., 2011a). M1 macrophages are associated with glycolysis whereas M2 phenotype relies on oxidative phosphorylation (Biswas and Mantovani, 2012; Galván-Peña and O'Neill, 2014). The metabolic switch in M1 macrophages allows them to fulfill their energy demand by glycolysis whereas sparing mitochondria from ATP generation and repurposing it to mROS production (Mills et al., 2016; Mills et al., 2017). However, different sources of mROS have been proposed (Mills et al., 2016; West et al., 2011a). One study has reported that the inhibition of complex I leads to increased mROS levels. Nevertheless, these data are debated (Kelly et al., 2015; West et al., 2011a). Increased mitochondrial membrane potential and succinate oxidation have been also reported to contribute to mROS induction (Mills et al., 2016). The source of mROS especially in activated-macrophages needs further investigation. Inhibition mitophagy has been also shown to induce mROS and to activate NLRP3 (Zhou et al., 2011). The contribution of mitophagy inhibition in mROS production and role of mROS in macrophage activation is not known.

4.1 Inhibition of mitophagy induces classical activation with concomitant induction of mROS production

We observed *in vitro* that induction of mitophagy significantly reduced the bactericidal activity of macrophages. We also observed that mice, injected with 2,4-DNP, failed to survive to bacterial infection and presented higher bacterial load. These results suggest that increased bacterial load in the peritoneal cavity in 2,4-DNP-injected mice after CLP could be a consequence of decreased bactericidal activity and activation of macrophages. It was also reported that mitochondria contribute to the bactericidal activity of macrophages via ROS production (Garaude et al., 2016; West et al., 2011a). In order to check the role of mitophagy inhibition in macrophage activation, functionality and its contribution to mROS production, we used different pharmacological inhibitors of mitophagy and checked the impact of mitophagy inhibition on macrophage activation, inflammatory response, mROS production and bactericidal activity.

a) Inhibition of mitophagy triggers macrophage activation

First, to check the impact of mitophagy inhibition on macrophage activation, Raw 264.7 macrophages were treated with 3-MA (1mM), Mdivi1 (50 µM), TBB (100 µM) and apigenin (50 µM) for 24 hours and macrophage activation was assessed by flow cytometry. Inhibition of mitophagy with inhibitors (3-MA, Mdivi1, TBB and Apigenin) induced activation of macrophages as evident by increased expression of the M1 markers CD64 and CD80 as compared to their control counterparts (Figure 4.1.C-F). Moreover, the CD64^{Hi} CD80^{Hi} macrophage subpopulation was increased after 24 hours of treatment with 3-MA and Mdivi1. Furthermore, the impact was more prominent with Mdivi1 (Figure 4.1.A). These results indicated that mitophagy inhibition mimics the effect of LPS/IFNγ on macrophage activation.

Figure 4.1: Inhibition of mitophagy triggers macrophage activation
(A-F) Raw 264.7 macrophages were treated for 24h with the mitophagy inhibitors *3-methyl adenine* (3-MA, 1mM,) (A) or *mitochondrial division inhibitor-1* (Mdivi-1, 50µM) (B), *4,5,6,7-tetrabromobenzotriazole* (TBB, 100 µM) and *apigenin* (50 µM) Macrophage activation was assessed by flow cytometry (A-F).
Data represents mean ±SEM, n=3 per group and significance levels were assessed by t test (A-F); *p <0.05, **p <0.01 or ***p <0.001.

Further, to assess whether pharmacological inhibition of mitophagy mimics the LPS/IFNγ-mediated phenotype of macrophages, we checked the regulation of inflammatory markers at mRNA levels. We treated Raw 264.7 macrophages with the same two mitophagy inhibitors, 3-MA and Mdivi1, for 24 hours. The mRNA levels of inflammatory cytokines (TNFα and IL-6) and iNOS, an enzyme responsible for NO production, were assessed by RT-qPCR. Interestingly, the mRNA levels were significantly higher in treated (with both 3-MA and Mdivi1) macrophages as compared to untreated controls (Figure 4.2.A-B).

We also checked the impact of mitophagy inhibition on the release of inflammatory cytokines. Raw 264.7 macrophages were treated with 3-MA (1 mM) for 24 hours and culture medium was recovered to measure cytokines release. As expected, the levels of inflammatory cytokines (IL-6, TNF-α, IL-12p70 and IL-1B) were significantly higher in 3-MA-treated macrophages as compared to untreated controls (Figure 4.3 A). Next, we assessed the impact of mitophagy inhibition on functional aspects of macrophages by looking at phagocytosis of latex beads. Such beads have

been used in various studies and represent as good strategy to study phagocytosis in different immune cells (Blander and Medzhitov, 2004, 2006). Raw 264.7 macrophages were incubated with fluorescent latex beads in the presence or absence of 3-MA (500 and 1000 µM) for 24 hours. Cells were washed and analyzed by flow cytometry. The fluorescence intensity of beads was used as an indicator of phagocytosis. Interestingly, we observed that inhibition of mitophagy with 3-MA, dose-dependently, boosted the phagocytosis of latex beads in Raw 264.7 macrophages (Figure 4.3.B).

Figure 4.2: Inhibition of mitophagy in macrophages induces inflammatory markers
(A-B) Raw 264.7 macrophages were treated for 24h with the mitophagy inhibitors *3-methyl adenine* (3-MA, 1mM) or *mitochondrial division inhibitor-1* (Mdivi-1, 50µM). Inflammatory markers were assessed at mRNA levels (A-B),
Data represents mean ±SEM, n=3 per group and significance levels were assessed by t test (A-B) ; *p <0.05, **p <0.01 or ***p <0.001.

M1 macrophages are endowed with the ability to kill bacteria (Biswas et al., 2012; Mege et al., 2011). In order to check the effect of mitophagy inhibition on bactericidal activity of macrophages, we used the gentamycin protection assay. Raw 264.7 macrophages were infected with *E. Coli*-GFP (MOI=10 bacteria) in cells pre-treated with mitophagy inhibitors, 3-MA (1mM) or Mdivi1 (50µM) (drugs were not present during exposure to bacteria). Cells were recovered and analyzed by cytometry. The decrease in fluorescence intensity of GFP was used as an indicator of the bactericidal activity of macrophages. We observed that inhibition of mitophagy

with both compounds induced bactericidal activity of macrophages at all time points as compared to their respective controls (Figure 4.4.A-B).
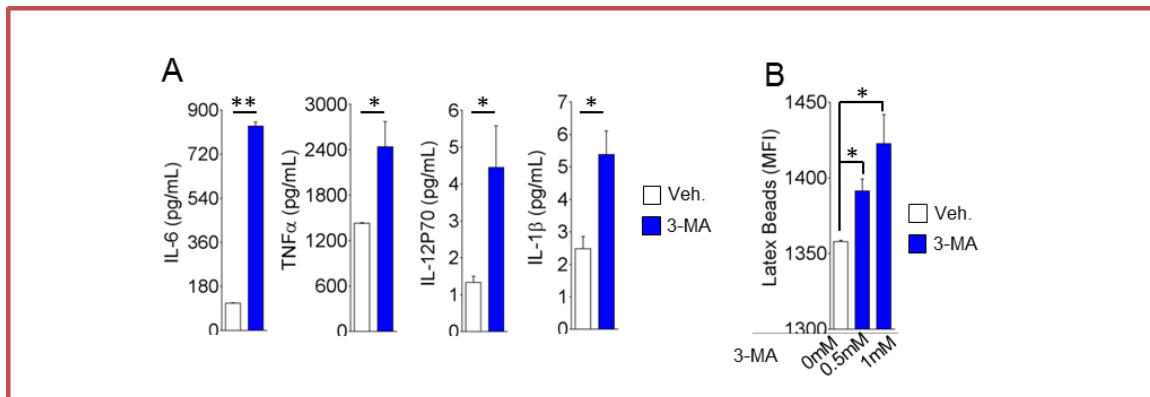
Figure 4.3: Inhibition of mitophagy in macrophages induces release of inflammatory cytokines and enhances phagocytic activity
(A-D) Raw 264.7 macrophages were treated for 24h with *3-methyl adenine* (3-MA, 0.5 or 1mM). Macrophage activation was assessed by measuring cytokines release (3-MA, 1mM) (A) and fluorescent latex beads phagocytosis (3-MA, 0.5 or 1mM) (B).
Data represents mean ±SEM, n=3 per group and significance levels were assessed by t test (A-B); *p <0.05, **p <0.01 or ***p <0.001.
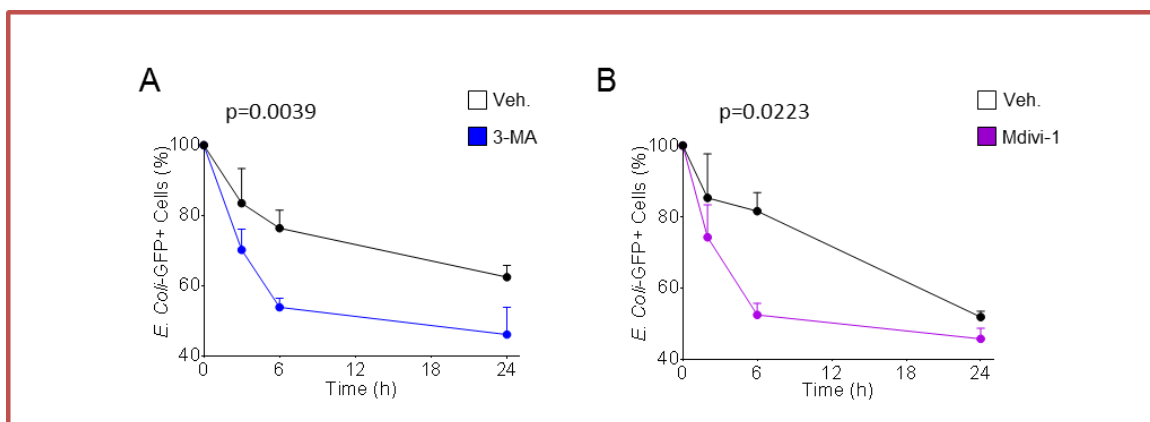
Figure 4.4 Inhibition of mitophagy induces bactericidal activity of macrophages
(A-D) Raw 264.7 macrophages were treated for 24h with the mitophagy inhibitors *3-methyl adenine* (3-MA, 1mM) or *mitochondrial division inhibitor-1* (Mdivi-1, 50µM). Macrophage bactericidal activity was assessed by gentamycin protection assay (A-B).
Data represents mean ±SEM, n=3 per group and significance levels were assessed by two way ANOVA (A-B); *p <0.05, **p <0.01 or ***p <0.001.

Together, these results demonstrate that the mitophagy inhibition plays an important role in switching macrophages towards inflammatory phenotype and enhanced their phagocytic and bactericidal activity.

b) Inhibition of mitophagy in macrophages induce mROS production

Recently it was reported that mROS contribute to the bactericidal activity of macrophages (Garaude et al., 2016; West et al., 2011a). But the exact mechanism of ROS production remained unanswered. It was also reported that inhibition of mitophagy can contribute to higher mROS (Zhou et al., 2011). In order to check the contribution of mitophagy arrest in mROS production, we treated Raw 264.7 macrophages with 3-MA, Mdivi1, TBB and Apigenin for 24 hours. Cells were stained with mitosox red and analyzed by flow cytometry (Figure 4.5.A-D). Mitosox red is a dye which is specifically oxidized by superoxide anions, but not by other ROS or RNS, and produces red fluorescence. As expected, we observed that all mitophagy inhibitors significantly enhanced the mROS production in macrophages. These results indicate that mROS production induced by mitophagy arrest might play role in bactericidal activity and activation of macrophages.
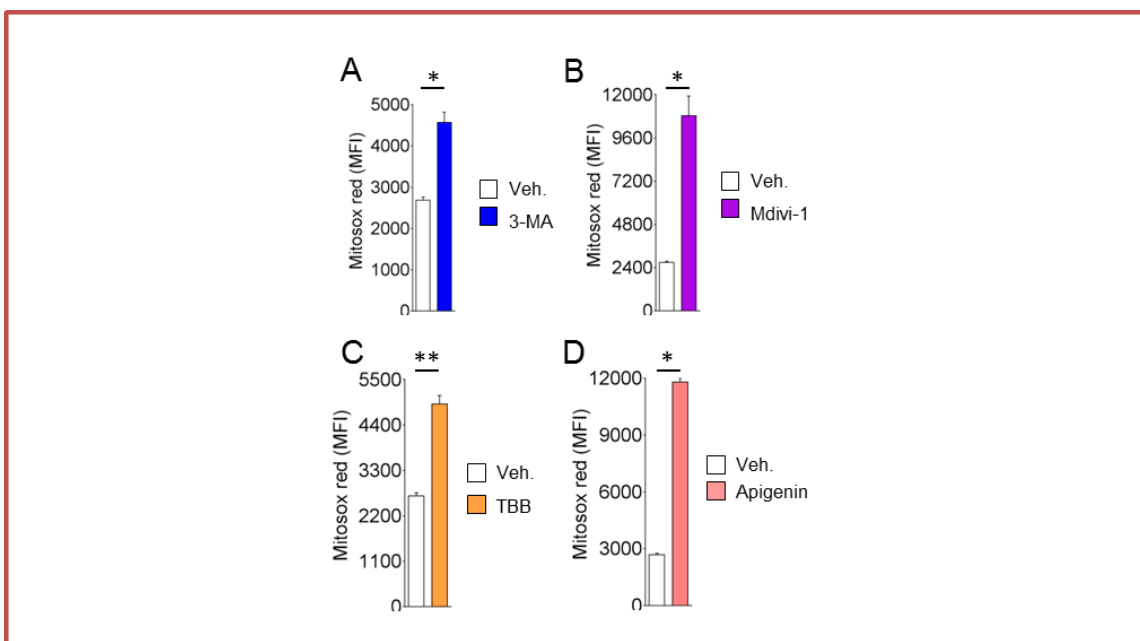
Figure 4.5: Inhibition of mitophagy induces mitochondrial ROS production in macrophages
(A-D) Raw 264.7 macrophages were treated for 24h with the mitophagy inhibitors *3-methyl adenine* (3-MA, 1mM) (A), *mitochondrial division inhibitor-1* (Mdivi-1, 50μM) (B), *4,5,6,7-tetrabromobenzotriazole* (TBB, 50 μM) (C) or *apigenin* (50 μM) (D) . Mitochondrial ROS production was assessed by flow cytometry (A-D) .
Data represents mean ±SEM, n=3 per group and significance levels were assessed by t test (A-D); *p <0.05, **p <0.01 or ***p <0.001.

4.2 Classical activation of macrophages induces mitochondrial ROS production

It was reported that stimulation of different TLRs, including TLR4 with LPS, leads to the increased mROS production in macrophages (West et al., 2011a). When we tested different TLR agonists on Raw 264.7 macrophages, we also observed increased mROS production (Figure 4.6). However, few discrepancies were observed between our results and those reported by West *et al.* (West et al., 2011a). Interestingly, LPS-stimulated macrophages showed increased mROS production in a dose- and time-dependent manner (Figure 4.7.A-B). Furthermore, the combination of LPS with IFNγ potentiated the effect on mROS production, indicating the existence of synergistic effect between two ligands (Figure 4.7.C). Both ligands (LPS and IFNγ) produced similar pattern of effects on mitophagy inhibition in same cell line (presented earlier in this document). Altogether these results indicate that mROS production in macrophages is linked to the inhibition of mitophagy.

Figure 4.6: TLRs stimulation augments mitochondrial ROS production in macrophages
Raw 264.7 macrophages were exposed to various concentration of PAMPs (Pam3CSK4: 1-100ng/mL; Pam2CSK4: 1-100ng/mL; Poly(I:C): 0.1-10μg/mL; R848: 1-5010μg/mL; CpG: 10-1000nmol/L; LTA: 10-1000ng/mL; LPS: 100-500ng/mL) for 24h and mitochondrial ROS was assessed by cytometry.
Data represents mean ±SEM, n=3 per group and one-way ANOVA followed by post hoc Bonferroni's test; *p <0.05, **p <0.01 or ***p <0.001.

Figure 4.7: Classically activated macrophages exhibit increased mitochondrial ROS production
Raw 264.7 macrophages were exposed to various concentration LPS for 24h treatment (A) or LPS (100 ng.mL^{-1}) at indicated time (B) or LPS and IFNγ alone or in combination for 24h (C) Mitochondrial ROS production was assessed by flow cytometry (A-C).
(D) Mitochondrial lipid oxidation was measured by GC-MS/MS in Raw 264.7 macrophages treated with LPS (100ng.mL^{-1}) or LPS/IFNγ (100/20ng.mL^{-1}) at indicated time points.
Data represents mean ±SEM (A-D), n=3 per group (A-D) and significance levels were assessed by one-way ANOVA followed by post hoc Bonferroni's test (A-D); *p <0.05, **p <0.01 or ***p <0.001.

In order to obtain additional evidences that mROS production was induced by LPS/IFNγ, we measured the mitochondrial lipid peroxidation in macrophages. Raw 264.7 macrophages were stimulated with LPS alone or in combination with IFNγ for 1 h and 24 hour time points. Mitochondria were isolated and mitochondrial HODEs (hydroxyoctadecadienoic acids) were measured by gas chromatography-mass spectrometry (GC-MS). Values were normalized to total cardiolipin content. Cardiolipin are phospholipids exclusively present in mitochondrial inner membrane (Scheffler, 2011). As expected, the HODEs were significantly increased in LPS/IFNγ-treated macrophages at 24 hours time point (Figure 4.7.D). This suggests that mROS is induced

by LPS/IFNγ, which ultimately leads to the oxidation of the lipids of mitochondrial membrane (Figure 4.7.D). Altogether these results strengthen our hypothesis that activated macrophages exhibit inhibition of mitophagy which contributes to mROS production.

4.3 Mitochondrial Functions in classically activated macrophages

In order to further assess our hypothesis, we checked the effect of LPS and IFNγ on mitochondrial membrane potential and activities of RCCs. Mitochondrial membrane potential is known to play important role in mitophagy regulation (Greene et al., 2012; Jin et al., 2010). The decrease in mitochondrial membrane potential leads to stabilization of PINK1 on mitochondria and initiation of mitophagy. In contrast, stable mitochondrial membrane potential mediates processing of PINK1 and inhibition of mitophagy (Greene et al., 2012; Jin et al., 2010; Lin and Kang, 2008).

In order to assess the impact of activation of macrophages on mitochondrial membrane potential, we treated Raw 264.7 cells with LPS/IFNγ for 24 hours. Cells were stained with tetramethylrhodamine methyl ester perchlorate (TMRM) and analyzed by flow cytometry. TMRM, is a cationic red-orange fluorescent dye, which gets accumulated in mitochondria depending on membrane potential. We observed that LPS/IFNγ-activated macrophages were associated with higher mitochondrial membrane potential as compared to untreated control (Figure 4.8.A). We next carried out the detailed time course of LPS/IFNγ treatment on macrophages and assessed membrane potential by JC-1. JC-1 is a cationic dye that accumulates in mitochondria as monomers and forms aggregates depending on membrane potential. Monomers exhibit green emission whereas aggregates exhibit red fluorescence. This fluorescence shift makes JC-1 as an ideal probe to measure population with differential membrane potential and mass. The ratio between red and green fluorescence can be used as indicator of membrane potential whereas green fluorescence of monomers can be used to measure mitochondrial density. Raw 264.7 macrophages were treated with LPS/IFNγ for different time points; cells were stained with JC-1 and analyzed by flow cytometry. In accordance with the results obtained from TMRM, the mitochondrial membrane potential was increased with LPS/IFNγ treatment (Figure 4.8.B). The percentage of cells with higher red and green fluorescence increased in a time-dependent manner with LPS/IFNγ treatment, indicating

LPS/IFNγ-activated macrophages exhibit higher mitochondrial density and higher mitochondrial membrane potential (Figure 4.8.B). A similar increase in red and green fluorescence was observed in LPS/IFNγ-treated macrophages compared to control when analyzed by fluorescence microscopy (Figure 4.8.C). These results further strengthen our observation that LPS/IFNγ induces inhibition of mitophagy.

Figure 4.8: Mitochondrial functions in classically activated macrophages
(A-C) Raw 264.7 macrophages were treated with LPs/IFNγ (100/20 ng.mL^{-1}) for 24 hours (A) or indicated time points(B-C) and mitochondria membrane potential was measured by flow cytometry using mitochondrial probes TMRM (A) or JC-1 (B) or Mitochondrial activity was measured by fluorescent microscopy using mitochondrial probes JC-1(C)
Data represents mean ±SEM, n=3 per group and significance levels were assessed by t test (A) or one-way ANOVA followed by post hoc Bonferroni's test (B); *p <0.05, **p <0.01 or ***p <0.001. Microscopy images are representative of at least 3 independent experiments (C).

RCCs are known as the source of mROS and inhibition of complexes are reported to be associated with increased mROS production. During oxidative phosphorylation, there is a leakage of electrons from RCCs into mitochondrial matrix where they react with molecular oxygen and

generate ROS. Inhibitions of complexes are known to induce mROS generation (Koopman et al., 2010; West et al., 2011a). Therefore, we checked the effect of LPS/IFNγ on the activities of respiratory chain complexes. Interestingly, LPS/IFNγ-treated macrophages exhibited a reduction in activities of Complex I, III, and IV in a time-dependent manner (Figure 4.9.A). Next, we assessed the effect on macrophage activation on oxygen consumption by using Clark electrodes. As expected, we observed that LPS/IFNγ-treated macrophages presented with decreased oxygen consumption as compared to untreated control (Figure 4.9.B). These observations are in accordance with other reports in which classically activated macrophages exhibited metabolic switch towards glycolysis and decreased oxygen consumption (Biswas and Mantovani, 2012; Galván-Peña and O'Neill, 2014; Mills et al., 2016; Tannahill et al., 2013).

Figure 4.9: Effects of LPS/IFNγ on mitochondrial functions in macrophages
Raw 264.7 macrophages were treated with LPS/IFNγ (100/20ng.mL^{-1}) for indicated time duration (A) or 24 hours (B). RCCs activity (A) and oxygen consumption (B) were measured.
Data represents mean ±SEM, n=3 per group and significance levels were assessed by one-way ANOVA followed by post hoc Bonferroni's test (A) or by t test (B); *p <0.05, **p <0.01 or ***p <0.001.

4.5 Mitochondrial ROS induction in macrophages contributes to macrophage activation

We observed that LPS/IFNγ boosted mROS production in macrophages in a dose- and time-dependent manner. But how this enhanced ROS production contributes to inflammatory form of macrophages is not well understood yet. We also observed that activities of RCCs were reduced in a time-dependent manner with LPS/IFNγ in Raw 264.7 macrophages. Inhibition of complexes of RCCs is also reported to increase ROS production (Koopman et al., 2010; West et al., 2011a).

Figure 4.10: ROS induction contributes to macrophage activation
(A-B). Raw 264.7 macrophages were treated with a dose of rotenone (1, 5 and 10 μM, for 24h) (A) or antimycin A (20, 40 and 60 μg.mL^{-1}, for 6h) (B) in combination or not with *N-acetylcysteine* (NAC, 5mM), mitochondrial ROS production was assessed by flow cytometry.
(C-D) Raw 264.7 macrophages were treated with the respiratory chain complex inhibitors rotenone (CI inhibitor, 24h, 5 μM) (C) or antimycin A (CIII inhibitor, 6h, 20, 40 and 60 μg.mL^{-1}) (C-D). Macrophage activation was assessed by flow cytometry (C-D) and quantification of inflammatory cytokines release in response of antimycin A (40 μg.mL^{-1}) (E).
Data represents mean ±SEM, n=3 per group and significance levels were assessed by one-way ANOVA followed by post hoc Bonferroni's test (A, B, D) or by t test (E) ; *p <0.05, **p <0.01 or ***p <0.001.

To assess the role of mROS in macrophage activation we pharmacologically induced mROS with RCCs inhibitors; antimycin A (inhibitor of Complex III) and rotenone (inhibitor of Compkex I) (Koopman et al., 2010). Raw 264.7 macrophages were treated with antimycin A or rotenone in the absence or presence of N-acetyl cysteine (5 mM) to assess the effect on mROS production. We observed that both molecules induce mROS-production in a dose-dependent manner in Raw 264.7 macrophages. mROS were scavenged by NAC. Moreover, complex III inhibition more efficiently promotes mROS prodcution as compared to complex I inhibition (Figure 4.10.A-B). Next we assessed the levels of the M1 activation marker, CD64, in macrophages treated with CI or CIII inhibitors. Interestingly, antimycin A exhibited higher induction of CD64 expression as

compared to rotenone (Figure 4.10.C). These results suggest that mROS from complex III could be involved in M1 activation.

In addition, we observed a dose-dependent effect of complex III inhibition on CD64 and CD80 expression (Figure 4.10.D). In accordance with macrophage activation, antimycin A also induced the release of inflammatory cytokines (IL1b, IL-6, TNFα and IL-12P70) in Raw 264.7 macrophages whereas anti-inflammatory cytokine (IL-10) remained unaffected (Figure 4.10.E). Altogether these results suggest that mROS play an important role in classical activation and inflammatory phenotype of macrophages.

4.6 Mitochondrial ROS play important role in maintaining M1 phenotype in response to classical stimulants

We observed that the pharmacological inhibition of complexes (especially complex III) induced mROS production and macrophage activation. We also observed that LPS/IFNγ-stimulated macrophages were associated with increased mROS production and exhibited decreased activity of RCCs. Next we wanted to assess how this increased mROS production in response to LPS/IFNγ contributes to macrophage activation and inflammatory phenotype. To assess this, we treated Raw 26.7 macrophages with LPS/IFNγ in the presence or in the absence of increasing doses (1-5 mM) of N-acetyl cysteine (NAC). Interestingly, we observed that the levels of the macrophage activation markers, CD64 and CD80, induced by LPS/IFNγ were dose-dependently decreased in NAC-co-treated macrophages (Figure 4.11 .A). Furthermore, when we checked the cytokine release in Raw 264.7 macrophage stimulated with LPS alone or in combination with IFNγ and/or NAC, a synergistic effect on the release of inflammatory cytokines (TNFα, IL-1β, IL-6 and IL-12P70) induced by LPS was observed in the presence of IFNγ (Figure 4.11.B). The LPS- and LPS/IFNγ-induced release of inflammatory cytokines were reduced in the presence of NAC whereas no effect was seen on IL-10 with LPS alone or in combination with IFNγ and/or NAC (Figure 4.11.B).

The effect of ROS scavenging on phagocytosis of fluorescent latex beads was also assessed in Raw 264.7 macrophages treated with LPS/IFNγ in combination with NAC or vehicle. As shown on Figure 4.11.C, we observed that the phagocytosis of latex beads was significantly reduced in the presence of NAC. In order to more specifically investigate the contribution of mROS, we used

mitoTEMPOL, a specific mROS scavenger. We treated Raw 264.7 cells with LPS/IFNγ in the presence or absence of increasing dose of mitoTEMPOL (Figure 4.11.D). Interestingly, mROS scavenging drastically reduced the effect of LPS and IFNγ on macrophage activation (Figure 4.11.D). Together, these results demonstrate that classically activated macrophages exhibit higher production of mROS, which play critical role in their activation.

Figure 4.11: Mitochondrial ROS contribute to LPS/IFNγ-mediated activation of macrophages
(A-C) Raw 264.7 macrophages treated for 24h with LPS and IFNγ alone or in combination with *N-acetylcysteine* (NAC, 1 and/or 5 mM). Macrophage activation was assessed by flow cytometry (A), quantification of inflammatory cytokines release (B) or fluorescent latex beads phagocytosis (C). (D) Macrophage activation was assessed by flow cytometry in Raw 264.7 treated with LPS/IFNγ ($100/20ng.mL^{-1}$) alone or in combination with a dose of mitoTEMPOL (50 and 250 μM). The data represent mean ±SEM, n=3 per group and significance levels were assessed by t test (A-D); *p <0.05, **p <0.01 or ***p <0.001.

4.7 Mitochondrial ROS contributes to macrophage activation via NFKB and HIF1α pathway

Mitochondrial ROS have been reported to play a role in the activation of NFkB, NLRP3 as well as HIF1α signaling pathways (Asehnoune et al., 2004; Mills et al., 2016; Tannahill et al., 2013; Tschopp and Schroder, 2010; Zhou et al., 2011). Therefore, we used a gene silencing strategy to

study the involvement of HIF1α, NFkB, and NLRP3 in mROS-mediated activation of macrophage. Raw 264.7 macrophages were transfected with siRNA targeting HIF1α, NFkB, and NLRP3 or with control siRNA. After 24 hours of transfection, macrophages were stimulated with LPS/IFNγ.

Figure 4.12: Mitochondrial ROS contribute to macrophage activation via NFkB and HIF1α signaling pathway
(A-B) Macrophages activation was assessed by flow cytometry in Raw 264.7 macrophages transfected with indicated siRNA and treated with LPS/IFNγ (100/20ng.mL^{-1}, 24h) (A) or *mitochondrial division inhibitor-1* (Mdivi-1, 50μ, 24h) or *antimycin A* (40μg/mL, 6h) (B).
The data represent mean ±SEM, n=3 per group and significance levels were assessed by t test (A-B) by comparing the each values from treated/untereated conditions in different siRNA transfected conditions with control siRNA transfected conditions;
*p <0.05, **p <0.01 or ***p <0.001; Red = LPS/IFNγ, Purple = Mdivi-1, Green = Antimycin A.

LPS/IFNγ-induced expression of CD80 and CD64 was significantly reduced by NFκB invalidation and more modestly with HIF-1α invalidation. By contrast, no reduction was observed with NLRP3 invalidation (Figure 4.12.A). Concomitantly, we treated Raw 264.7 macrophages with Mdivi1 (24h) and Antimycin A (6h) to promote mROS production. We noticed that the impact of mROS on macrophage activation was significantly reduced by HIF1a and NFκB invalidation, similarly to the observation made with LPS/IFNγ treatment (Figure 4.12.A). In order to further investigate the

contribution of HIF1α in activation of macrophages, Raw 264.7 macrophages were treated for 24 hours either with LPS/IFNγ, Mdivi1 or Antimycin A in the presence or absence of increasing concentrations of echinomycin, a pharmacological inhibitor of HIF1α (Kong et al., 2005). Pharmacological inhibition of HIF1α produced a dose-dependent reduction in the expression of CD64 and CD80 in response to LPS/IFNγ as well as with mROS-stimulating drugs (Figure 4.13.C). Therefore, these results indicated that LPS/IFNγ-mediated inhibition of mitophagy contributes to macrophage activation through mROS-dependent activation of NFkB and HIF1α pathways.

Figure 4.13: Mitochondrial ROS contribute to macrophage activation through HIF1α signaling pathway

(A-C) Macrophages activation was assessed by flow cytometry in Raw 264.7 macrophages treated with LPS/IFNγ (100/20ng.mL^{-1}, 24h) (A) or *mitochondrial division inhibitor-1* (Mdivi-1, 50μM, 24h) (B) or *antimycin A* (40μg/mL, 6h) (C) alone or in combination with a dose of *echinomycin* (Echino, 1-5nM, 24h).

The data represent mean ± SEM, n=3 per group and significance levels were assessed by one-way ANOVA followed by post hoc Bonferroni's test by comparing treated groups (LPS/IFNγ / Mdivi-1 / Antimycin A) with echinomycin co-treated groups (A-C); *p <0.05, **p <0.01 or ***p <0.001.

Conclusion Part II

Our data show that inhibition of mitophagy contributes to LPS/IFNγ-mediated macrophage activation and mROS production. Furthermore, we have demonstrated here that classically activated macrophages are associated with the inhibition of different complexes of respiratory chain, increased mitochondrial membrane potential as well as increased mitochondrial density, which ultimately contribute to mROS production. This increased mROS production in turn can contribute to macrophage activation via HIF1α and NFκB signaling pathway. Therefore, these *in vitro* results suggest that *in vivo* effect observed with CLP can be linked to LPS/IFNγ-mediated inhibition of mitophagy in macrophage and other phagocytes such as neutrophils.

PART III

Signaling pathways involved in LPS/IFNγ-mediated inhibition of mitophagy in macrophages

Introduction

In our study we have observed that classically activated macrophages exhibited inhibition of mitophagy, as evidenced by increased mitochondrial density, increased mitochondrial network, down regulation of key proteins regulating mitophagy, and mitophagy inhibition assessed by the use of mitokeima expression vector. Classically activated macrophages are reported to be activated by LPS and IFNγ (Biswas et al., 2012). LPS is known as a ligand for TLR4 but recent reports have suggested caspase 4/11 as an intracellular sensor of LPS (Chow et al., 1999; Kayagaki et al., 2011). LPS recognition by TLR4 leads to the activation of downstream signaling cascade including IRAK4, TRAF6, IRF3 and ends up with the activation of different transcription factors (NFκB, IRF3 and AP1). This in turn regulates the inflammatory response (Needham and Trent, 2013). Activation of IFNGRs leads to recruitment of signal transducer and activator of transcription 1 (STAT1). STAT1 is a transcription factor primarily involved in IFNγ signaling pathway. STAT1 is recruited on the tyrosine 440 phosphorylated residue of IFNGRs through its SH2 domain (Boehm et al., 1997; Igarashi et al., 1994). STAT1 is phosphorylated on tyrosine residue (Y701), forms homodimer and is translocated to the nucleus where it binds to gamma-associated sequence (GAS) element and initiates transcription of IFNγ responsive genes (Aaronson and Horvath, 2002; Boehm et al., 1997; Darnell, 1997; Stark et al., 1998). Phosphorylation of STAT1 at serine (s727) is known to synergize the transcriptional activity of STAT1 (Wen et al., 1995). STAT1 plays important role in immune response against infection. However the role of IFNGR and STAT1 in mitophagy regulation in the context of infection and macrophages is not known yet. Furthermore, STAT1 is also known to regulate caspase 4/11 at transcriptional level (Kayagaki et al., 2011; Schauvliege et al., 2002). Caspase 4/11 lies under the category of inflammatory caspases and is known to play role in the activation of NLRP3 inflammasome activation, release of IL-1β and IL-18 as well as in pyroptosis (He et al., 2016; Kayagaki et al., 2011). To understand the underlying molecular mechanism we checked the role of key actors of both signaling pathway as well as caspase 4/11 in inhibition mitophagy.

5.1 LPS- and IFNγ-mediated inhibition of mitophagy in macrophages relies on IFNGRs signaling Pathway

In order to unravel the molecular mechanism contributing to the inhibition of mitophagy in classically activated macrophages, we used siRNA approach to silence key actors of TLR4 and IFNγ signaling pathway. Raw 264.7 macrophages treated with LPS alone exhibited significant reduction of LPS-mediated inhibition of mitophagy with TLR4 invalidation (Figure 5.1.A). In contrast, macrophages stimulated with LPS/IFNγ did not exhibit this reduction in mitophagy inhibition subsequent to TLR4 invalidation (Figure 5.1.B). In a second step, the downstream TLR4 signaling cascade including IRAK4, TRAF6, IRF3 and NFkB was invalidated with siRNA. Cells were stimulated with LPS/IFNγ and mitochondrial density was determined by flow cytometry.

Similarly to TLR4 invalidation, the invalidation of the main contributors of TLR4 signaling pathway revealed no significant decrease in LPS/IFNγ-mediated inhibition of mitophagy as compared to siRNA control (Figure 5.1.C). We did not observe any effect of TLR4 invalidation on expression of CD64 and CD80 in response to LPS/IFNγ-mediated stimulation of macrophages (Figure 5.1.D) whereas mRNA levels of inflammatory cytokines (TNFα, IL-6 and IL-1β) were significantly reduced by TLR4 invalidation in LPS/IFNγ-stimulated macrophages, as compared to siRNA control (Figure 5.1.E). These results demonstrated that TLR4 pathway was efficiently silenced by TLR4 siRNA and that strikingly this pathway might not be pivotal in the control of the expression of CD64 and CD80.

Next, we blocked TLR4 signaling by using pharmacological inhibitors. Raw 264.7 macrophages were treated with LPS/IFNγ in the presence or absence of increasing dose of either of LPS-RS (a competitive inhibitor of LPS) or CLI-095 (inhibitor of TLR4 signaling pathway) for 24 hours. Cells were stained with mitotracker green FM followed by analyses with flow cytometry. In agreement with the results obtained from TLR4 silencing, we did not observe any decrease in LPS/IFNγ-mediated inhibition of mitophagy in macrophages treated with TLR4 antagonists (Figure 5.1.F-G).

In contrast, invalidation of IFNGR signaling pathway resulted in significant reduction in inhibition of mitophagy on stimulation of macrophages either with LPS alone or in combination with IFNγ (Figure 5.2.A-B).

Altogether, these results demonstrate that inhibition of mitophagy in LPS/IFNγ-stimulated macrophages mainly relies on IFNγ signaling pathway. We can assume that the effect of LPS alone on the inhibition of mitophagy might be indirect as it is known that LPS-treated macrophages have an increased release of IFNγ. Therefore, LPS may act on mitophagy by activating IFNGRs through TLR4-mediated induction of IFNγ release.

Figure 5.1: LPS- and IFNγ-mediated inhibition of mitophagy in macrophages does not seem to rely on TLR4 signaling pathway
(A-E) TLR4 signaling pathway was invalidated at different level by siRNA in Raw 264.7 macrophages treated with LPS (100ng.mL^{-1}) or LPS/IFNγ (100/20ng.mL^{-1}) for 24h. Mitophagy(A-C) and macrophages activation (D) was assessed by flow cytometry and inflammatory cytokine were assessed by qPCR (E)
(F-G) Mitophagy was assessed by flow cytometry in Raw 264.7 macrophages treated with LPS/IFNγ (100/20ng.mL^{-1}) for 24h alone or in combination with a dose TLR4 inhibitors CLI-095 (0.5, 1, 2, 3 µM) (F) or LPS-RS (0.01, 0.1, 0.25, 0.5, 1 and 10 µg.mL^{-1}) (G).
The data represent mean ± SEM, n=3 per group, significance levels were assessed by t test (A-G); *p <0.05, **p <0.01 or ***p <0.001.

Figure 5.2: LPS- and IFNγ-mediated inhibition of mitophagy relies on IFNG signaling pathway
(A-B) IFNGR signaling pathway were invalidated siRNA in Raw 264.7 macrophages treated with LPS (100ng.mL^{-1}) (A) or LPS/IFNγ (100/20ng.mL^{-1}) (B) for 24h. Mitophagy was assessed by flow cytometry (A-B).
The data represent mean ± SEM, n=3 per group, significance levels were assessed by t test (A-B); *p <0.05, **p <0.01 or ***p <0.001.

5.2 LPS and IFNγ mediated inhibition of mitophagy in activated macrophages relies on STAT1

Figure 5.3: LPS- and IFNγ-mediated inhibition of mitophagy in activated macrophages is dependent on STAT1
(A-B) Mitophagy and activation was assessed in Raw 264.7 macrophages invalidated siRNA STAT1 and treated with LPS/IFNγ (100/20ng.mL^{-1}) for 24h.
The data represent mean ± SEM, n=3 per group, significance levels were assessed by t test (A-B); *p <0.05, **p <0.01 or ***p <0.001.
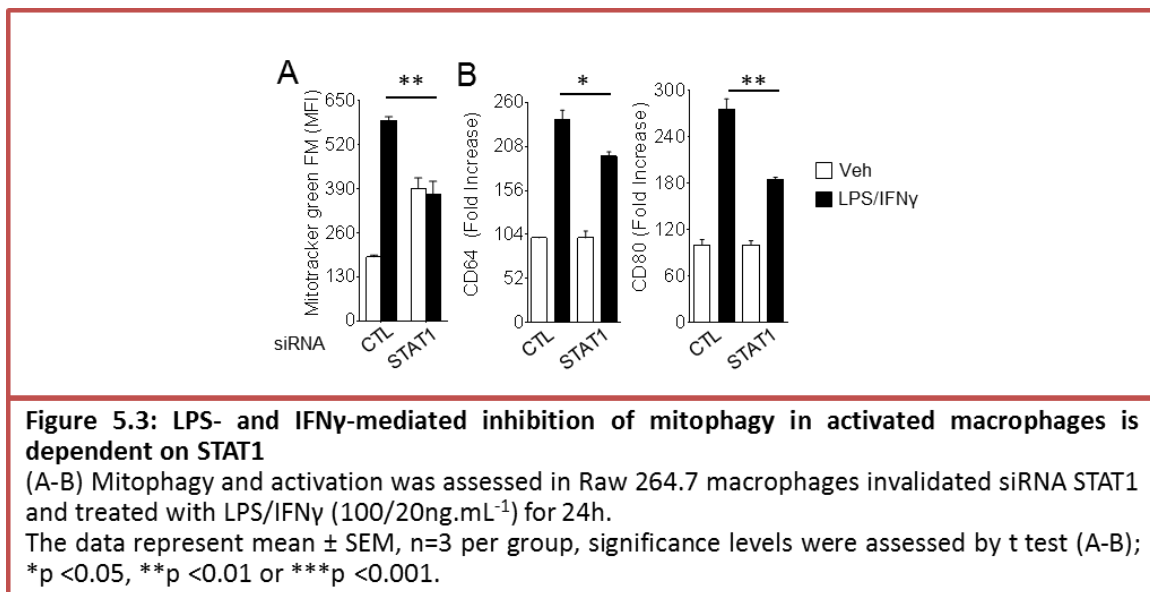
Binding of IFNγ to IFNG receptor leads to the activation of STAT1 signaling. Therefore, we next assessed the impact of STAT1 invalidation on mitophagy inhibition and macrophage activation in Raw 264.7 macrophages by flow cytometry. Strikingly, STAT1 invalidation resulted in dramatic loss of the effect of LPS and IFNγ on mitopagy inhibition (Figure 5.3.A). These results marked STAT1 as a key actor responsible for inhibition of mitophagy in LPS/IFNγ-stimulated

macrophages. In parallel to this, STAT1 invalidation also resulted in significant reduction of LPS/IFNγ-mediated activation of macrophages, as illustrated by decrease levels of CD64 and CD80 (Figure 5.3.B).

5.3 LPS and IFNγ induce mitochondrial ROS production in macrophage in a STAT1-dependent manner

We have demonstrated above that mROS have a central role in mitophagy inhibition-mediated activation of macrophages. Therefore, we assessed mROS production in STAT1-silenced Raw 264.7 macrophages in response to LPS/IFNγ. In agreement with our hypothesis, we observed that invalidation of STAT1 drastically reduced mROS production in LPS/IFNγ-activated macrophages (Figure 5.4).

Figure 5.4: LPS and IFNγ induce mROS production in macrophages in a STAT1-dependent manner
Mitochondrial ROS production was assessed in Raw 264.7 macrophages invalidated siRNA STAT1 and treated with LPS/IFNγ (100/20ng.mL^{-1}) for 24h followed by staining with Mitosox Red and analyzed by flow cytometry
The data represent mean ± SEM, n=3 per group, significance levels were assessed by t test;
*p <0.05, **p <0.01 or ***p <0.001.

5.4 Mitochondrial functions are modulated by LPS and IFNγ in a STAT1-dependent manner

We demonstrated above that LPS/IFNγ-activated macrophages were associated with increased mitochondrial membrane potential and decreased activity of RCCs (Figure 4.9). In order to assess if modulation of these mitochondrial functions in LPS/IFNγ-stimulated macrophages were mediated through STAT1, we checked the impact of STAT1 invalidation on these features in Raw

264.7 macrophages. Mitochondrial membrane potential was assessed by flow cytometry using TMRM. As expected, a significant loss of effect LPS/IFNγ on mitochondrial membrane potential was seen in response to STAT1 invalidation in macrophages (Figure 5.5.A).

Figure 5.5: Mitochondrial functions are modulated in response to LPS and IFNγ in a STAT1-dependent manner
(A-B) Mitochondrial activity was assessed in Raw 264.7 macrophages invalidated for STAT1 gene expression by siRNA and treated with LPS/IFNγ (100/20ng.mL^{-1}) by measuring mitochondrial membrane potential by flow cytometry using TMRM mitochondrial probes (A), or mitochondrial respiratory chain complexes activity (B). Macrophages were treated with LPS/IFNγ for 24 hour for TMRM (A) or 16 and 24hours for RCCs activity (B)
The data represent mean ± SEM, n=3 per group, significance levels were assessed by t test;
*p <0.05, **p <0.01 or ***p <0.001.

We next checked the impact of STAT1 invalidation on the activity of RCCs. We noticed that in Raw 264.7 macrophages transfected with control siRNA, LPS/IFNγ treatment triggered a significant decrease in the activity of CI, CIII and CIV in a dose-dependent manner. This contributes to explain increased mROS production as well as drastic reduction of oxygen consumption in activated macrophages. Moreover, we observed that LPS/IFNγ-mediated reduction in CIII and CIV activity was significantly less pronounced when STAT1 was invalidated. These observations further confirmed that STAT1 pathway play a key role in LPS/IFNγ-mediated inhibition of mitophagy as well as mitochondrial features (Figure 5.5.B).

5.5 STAT1 regulate mitophagy in monocyte and macrophages *in vivo* in response to CLP surgery or LPS

Figure 5.6: STAT1 regulates mitophagy in monocytes and macrophages *in vivo* in response to CLP and endotoxemia

(A-D) Mitophagy was assessed by flow cytometry in peritoneal macrophages (Perit. Mφ) (C) or blood monocytes (D) from wild-type or STAT1 knock-out mice 2h after CLP or sham-surgery. (C-D) Assessment of mitophagy by flow cytometry in peritoneal macrophages (C) and blood monocytes (D) from wild-type or STAT1 knock-out mice 24h after the intraperitoneal injection of LPS (0.5mg/Kg). (E) Present the percentage of population with differential levels of expression of CD64 and CD80 fro from F4/80 Hi CD11b Hi

The data represent mean ± SEM, n=9 per group (A-B), n=7 per group (C-E), significance levels were assessed by t test; *p <0.05, **p <0.01 or ***p <0.001.

We demonstrated *in vitro* that STAT1 is a key component of LPS/IFNγ-mediated inhibition of mitophagy. We next investigated the role of STAT1 *in vivo* by submitting STAT1-knock-out (STAT1$^{-/-}$) or wild-type (STAT1$^{+/+}$) mice (129SV) to CLP surgery or intraperitoneal injection of LPS (0.5mg.kg^{-1}). Blood and peritoneal fluid were collected 2 hours after CLP or sham surgery or 24h after intraperitoneal injection. In accordance with data obtained in C57BL6/J mice, we observed that the CD64^{Hi} Mitotracker^{Hi} subpopulation of peritoneal macrophages was dramatically increased by both CLP surgery and LPS injection (Figure 5.6.A & C). Moreover, analysis of blood monocytes also revealed a significant increase in mitochondrial density after CLP or endotoxin

injection (Figure 5.6.B & D). In line with *in vitro* data, infection-mediated inhibition of mitophagy was blunted in STAT1$^{-/-}$ mice (Figure 5.6.B & D). Interestingly, we observed that modulation of mitophagy in peritoneal macrophages paralleled the impact of LPS on subpopulation of peritoneal macrophages. Indeed, both CD64^{Hl} CD80^{Lo} and CD64^{Hi} CD80^{Hi} macrophage subpopulations were greatly enhanced after LPS injection whereas this effect was fully abrogated in STAT1$^{-/-}$ mice (Figure 5.6.E). This further reinforced *in vivo* our assumption that inhibition of mitophagy induces macrophage activation (especially CD64 positive macrophages) in a STAT1-dependent manner.

5.6 LPS/IFNγ impact on PINK1-dependent mitophagy in a STAT1-dependent manner

We observed that LPS/IFNγ-mediated inhibition of mitophagy in BMDMs and Raw 264.7 macrophages was associated with a reduction of the actors of PINK1-dependent mitophagy. In order to investigate the underlying molecular mechanism, we assessed the effect of STAT1 invalidation on LPS/IFNγ-mediated diminution of proteins regulating mitophagy in macrophages. This was tested in Raw 264.7 macrophages silenced for STAT1 mRNA as well as in peritoneal macrophages from wild-type or STAT1$^{-/-}$ mice. LPS/IFNγ-treated macrophages showed decreased protein levels of PINK1, Parkin, DJ-1 as well as DRP1 in a time-dependent manner. In agreement with data obtained on mitochondrial density, mROS and RCC activity, this effect of LPS/IFNγ on diminution of proteins (PINK1, DJ-1, Drp1) was abrogated in macrophages invalidated for STAT1 (Figure 5.7.A-B). Unexpectedly, for Parkin we observed some discrepancies between both types of macrophages. Diminution of Parkin protein level with LPS/IFNγ was independent on STAT1 in Raw 264.7 macrophages but was dependent on STAT1 in peritoneal macrophages (Figure 5.7.A-B).

Furthermore, significant reduction in gene expression levels, PINK1, DJ-1 and Drp1, was seen with LPS/IFNγ treatment in peritoneal macrophages from both WT and STAT1$^{-/-}$ mice. This suggests that the downregulation of this key protein in STAT1-dependent manner does not occur at transcriptional level (Figure 5.7.C).

Figure 5.7: LPS/IFNγ impact on PINK1-dependent mitophagy in a STAT1-dependent manner
(A-B) Immunoblots of indicated proteins on whole protein lysates from Raw 264.7 macrophages invalidated with siRNA CTL or STAT1 (A) and peritoneal macrophages from wild-type or STAT1 knock-out mice (B)
(C) Gene expression levels in peritoneal macrophages from wild-type or STAT1 knock-out mice. The data represent mean ± SEM, n=3 per group and significance levels were assessed by t test (C); *p <0.05, **p <0.01 or ***p <0.001.

PINK1 is a key actor of Parkin/PINK1-dependent mitophagy. Recruitment of Parkin to the mitochondria relies of stabilization and kinase activity of PINK1 (Chen and Dorn, 2013; Matsuda et al., 2010; Okatsu et al., 2012). Next we assessed the localization of PINK1 of mitochondria in peritoneal macrophages isolated from wild-type and STAT1$^{-/-}$ mice by fluorescence microcopy. In wild-type macrophages, PINK1 was mainly localized on mitochondria (co-localization with Tom20). Once treated with LPS/IFNγ we observed that PINK1-Tom20 colocalization was decreased. We could suspect that it could be due to a cleavage of mitochondrial PINK1 and release of cleaved PINK1 to the cytosol. Conversely, no differences were observed in treated and untreated STAT1$^{-/-}$ macrophages (Figure 5.8). These results suggest that STAT1 invalidation, in

addition to impacting on PINK1 protein levels, also affects its subcellular localization both in basal condition and after LPS/IFNγ exposure.

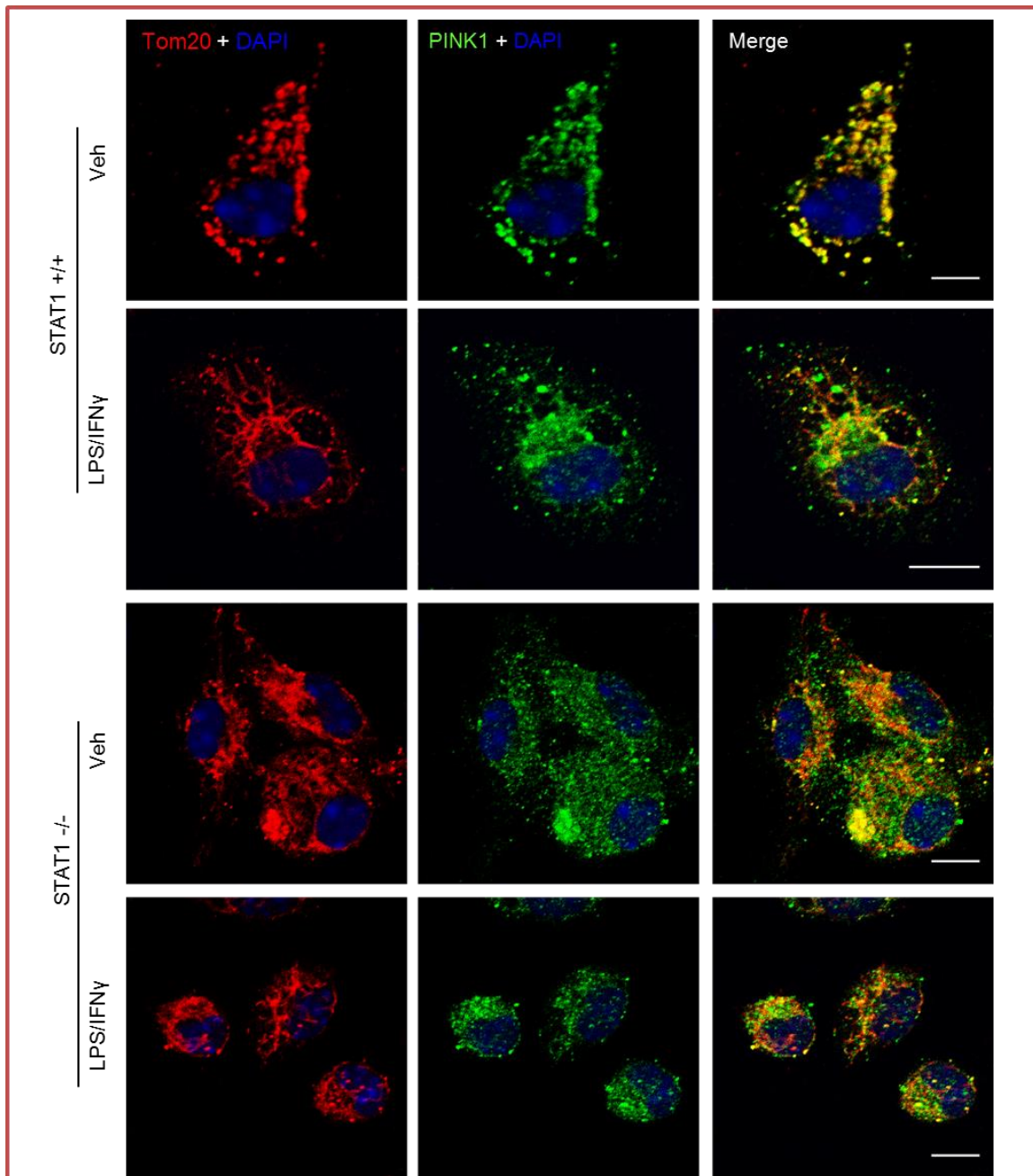**Figure 5.8: LPS/IFNγ impacts on mitochondrial localization of PINK1**
Subcellular localization of PINK1 was assessed by confocal microscopy in peritoneal macrophages from wild-type and STAT1 knock-out mice treated for 24h with LPS/IFNγ (100/20ng.mL^{-1}), immuno-stained for mitochondrial Tom 20 (red) or PINK1 (green).
Confocal microscopy images are representative of at least 3 independent experiments.

5.7 LPS/IFNγ-mediated inhibition of mitophagy regulated through STAT1 and Caspase 4/11

We observed that mitophagy inhibition in macrophages mainly relies on STAT1 and was only partially dependent on TLR4 signaling pathway. Recent studies have reported caspase 4/11 as intracellular sensor of LPS (Hagar et al., 2013; Kayagaki et al., 2011; Kayagaki et al., 2013). Therefore, we hypothesized that the intracellular LPS sensor caspase 4/11 could be involved in LPS/IFNγ-mediated inhibition of mitophagy in macrophages. This can be achieved only if LPS is present in the cytosol. We checked the internalization of LPS in Raw 264.7 cells using Bodipy-labeled LPS coupled to flow cytometry analysis. Results were compared to those obtained in peritoneal macrophages using similar experimental setting. Raw 264.7 and peritoneal macrophages were treated with LPS-Bodipy and IFNγ for 24 hours and analyzed by flow cytometry. Peritoneal macrophages exhibited significantly lower LPS-bodipy uptake as compared to Raw264.7 macrophages (Figure 5.9.A). Interestingly, the extent of mitophagy inhibition in peritoneal macrophages was drastically less pronounced than in Raw 264.7 macrophages. This parallels the level of LPS uptake which is strinkingly lower in peritoneal macrophages as compared to raw 264.7 macrophages (Figure 5.9.B). Therefore, we might speculate that caspase 4/11 is activated in a higher extent in Raw 264.7 macrophages. This could contribute to explain the more pronounced inhibition of mitophagy seen in LPS/IFNγ-treated Raw 264.7 macrophages.

STAT1 was reported as a regulator of caspase 4/11 expression levels (Schauvliege et al., 2002). Therefore, we checked the regulation of caspase 4/11 in STAT1-invalidated Raw 264.7 macrophages and peritoneal macrophages from STAT1$^{-/-}$ mice. LPS/IFNγ dramatically induced caspase 4/11 gene expression in Raw 264.7 macrophages as well as peritoneal macrophages whereas the effect was significantly reduced in STAT1-deficient macrophages (Figure 5.10.A-B). Furthermore, protein levels of Caspase 4/11 were also augmented in response to LPS/IFNγ whereas the effect was blunted with STAT1 invalidation (Figure 5.10.C). These results argue in favor to the involvement of caspase 4/11 in LPS/IFNγ-mediated inhibition of mitophagy.
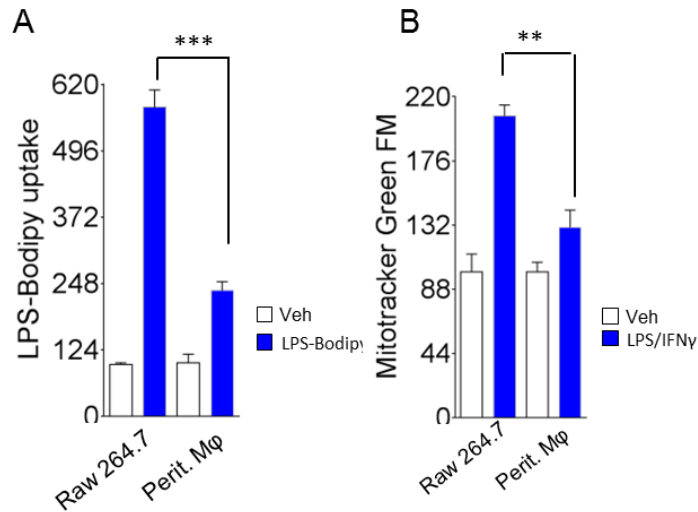
Figure 5.9: LPS/IFNγ-mediated inhibition of mitophagy involves intracellular sensing of LPS
(A) Uptake of LPS-Bodipy was analyzed by flow cytometry in Raw 264.7 macrophages and C57BL6/J peritoneal macrophages treated for 24h with LPS-Bodipy (100ng/mL) along with IFNγ (20ng/mL). (B) Mitophagy was analyzed by flow cytometry in Raw 264.7 macrophages and C57BL6/J peritoneal macrophages treated for 24h with LPS/IFNγ (100/20ng.mL^{-1}).
The data represent mean ± SEM, n=3 per group and significance levels were assessed by t test; *p <0.05, **p <0.01 or ***p <0.001.
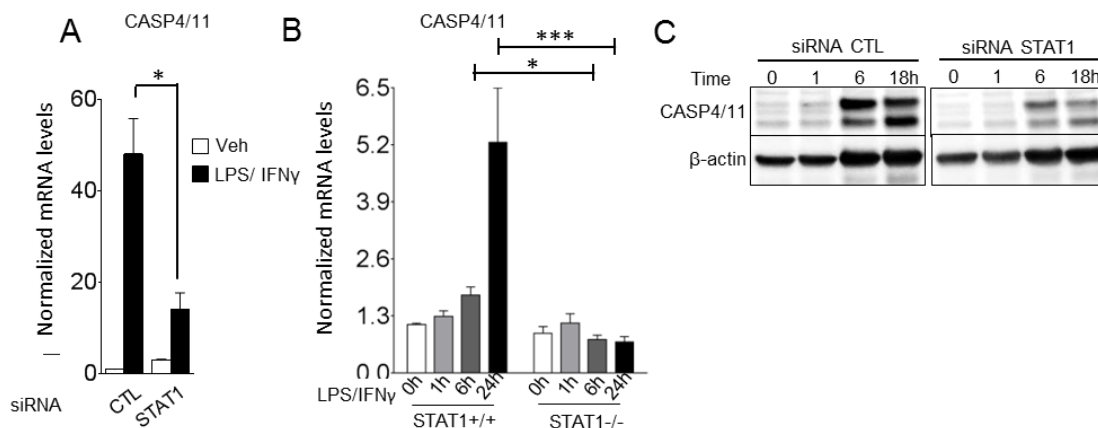
Figure 5.10: STAT1 regulates Caspase 4/11 in LPS and IFNγ stimulated macrophages
(A-C) Casp4/11 expression levels in Raw 264..7 macrophages invalidated with siRNA CTL or siRNA STAT1 at mRNA levels (A) and protein levels (C) or mRNA levels in peritoneal macrophages from wild-type or STAT1 knock-out mice (B)
The data represent mean ± SEM, n=3 per group and significance levels were assessed by t test (A-B); *p <0.05, **p <0.01 or ***p <0.001.
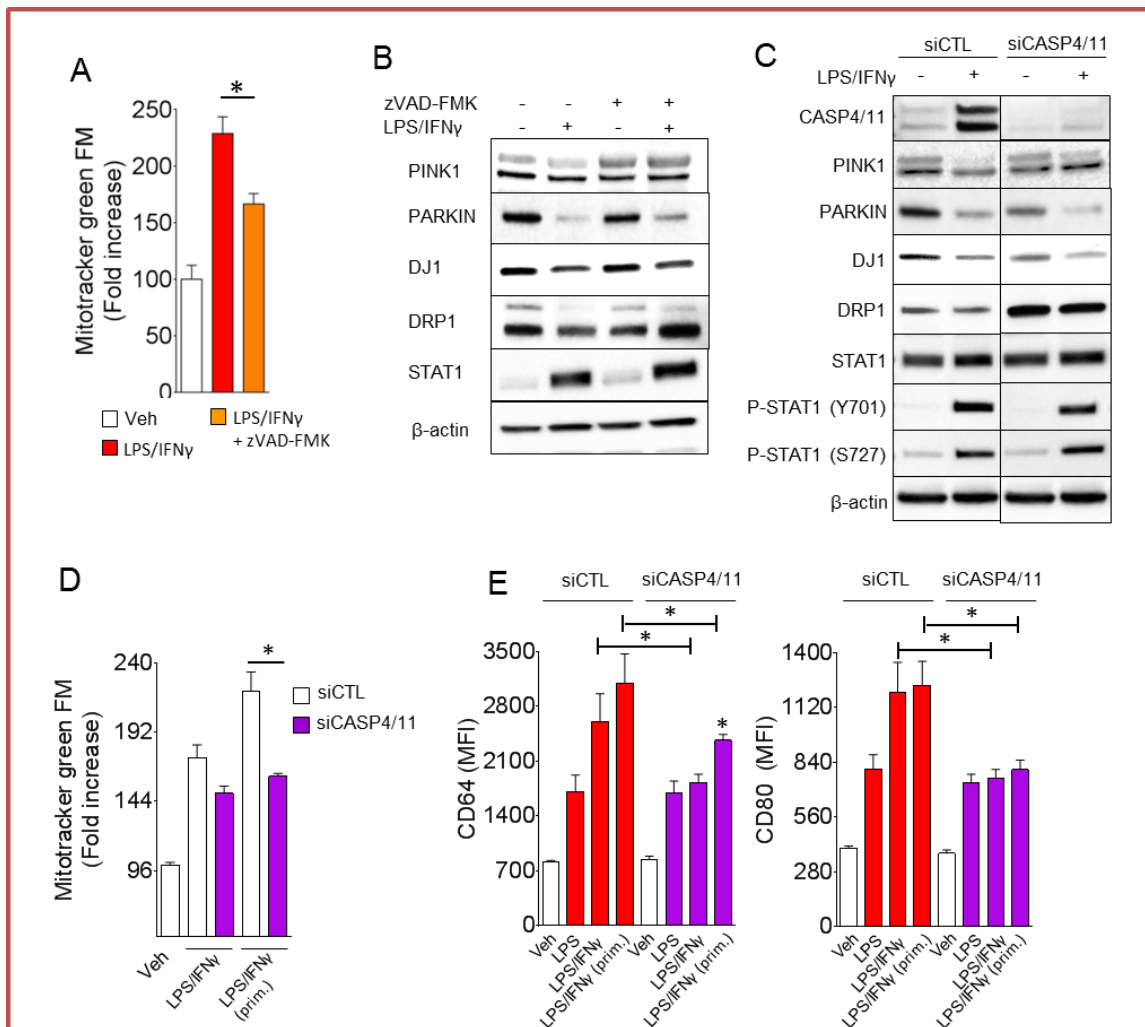
Figure 5.11: LPS/IFNγ-mediated inhibition of mitophagy is regulated through STAT1 and Caspase-4/11

(A) Mitophagy was assessed by flow cytometry in Raw 264.7 macrophages which were pretreated with zVAD-FMK (50 μM) or vehicle for 1h or treated with LPS/IFNγ (100/20ng.mL^{-1}) for 24h. (B-C) Immunoblots of indicated proteins on whole protein lysates from Raw264.7 macrophages pretreated with zVAD-FMK or vehicle for 1h (B) or invalidated for Casp4/11 by siRNA (C) or not (C) or. Cells were treated with LPS/IFNγ (100/20ng.mL^{-1}) for 18h (B-C). (D-E) Mitophagy (D) and activation was assessed by flow cytometry in Raw 264.7 macrophages invalidated for Casp4/11 by siRNA treated with LPS/IFNγ (100/20ng.mL^{-1}) for 24h with or without 24h priming with IFNγ (prim.,5 ng.mL^{-1}) (J). (K) Macrophages activation was assessed by flow cytometry in Raw 264.7 macrophages invalidated for Casp4/11 by siRNA and with LPS (100ng.mL^{-1}) or LPS/IFNγ (100/20ng.mL^{-1}) for 24h with or without 24h priming with IFNγ (prim.,5 ng.mL^{-1}). Flow cytometry data represent mean ± SEM, n=3 per group and significance levels were assessed by t test (A, D-E); *p <0.05, **p <0.01 or ***p <0.001.

To further assess this hypothesis, macrophages we treated pan-caspase inhibitor ZVAD FMK or invalidated for caspase 4/11 using siRNA. Raw 264.7 macrophages were pretreated with ZVAD FMK or vehicle (DMSO) for 1 hour and then stimulated with LPS/IFNγ for 24 hours. Pretreatment

of macrophages with ZVAD FMK significantly reduced the impact of LPS/IFNγ on mitophagy inhibition in macrophages (Figure 5.11.A). The impact of caspase inhibition on regulation of proteins involved in mitophagy was then assessed. As expected, we observed that the diminution of PINK1, Parkin, DJ-1 and DRP1 mediated by LPS and IFNγ was less pronounced in macrophages pre-exposed to the pan-caspase inhibitor (Figure 5.11.B). Therefore, this strengthen the assumption of a caspase-mediated effect.

The impact of caspase 4/11 invalidation in the regulation of proteins responsible for mitophagy and mitochondrial dynamics was assessed by western blotting. Interestingly, we observed that caspase 4/11 invalidation reduced the effect of LPS/IFNγ on key proteins regulating mitophagy and dynamics, especially PINK1 and DRP1 (Figure 5.11.C). As caspase 4/11 is downstream of STAT1, we checked the levels of total and phosphorylated form of STAT1, which were increased after LPS/IFNγ treatment. This indicates that STAT1 pathway was still active and not affected by caspase 4/11 invalidation (Figure 5.11.C).
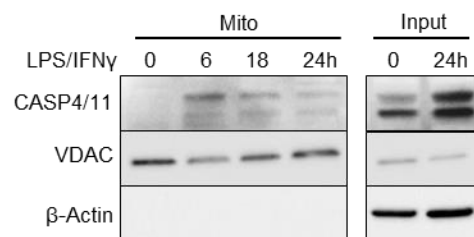
Figure 5.12: Caspase 4/11 translocates to mitochondria in response to LPS/IFNγ
Immunoblots of Caspase 4/11 and VADC on mitochondrial protein or whole protein lysates from Raw264.7 macrophages treated with LPS/IFNγ (100/20ng.mL^{-1}) at indicated time points.

Next we checked the impact of caspase 4/11 invalidation on the inhibition of mitophagy by flow cytometry. Different studies have suggested that priming of macrophages, either of the following ligands including LPS, Poly(I:C), IFNβ or IFNγ, enhances the protein levels of caspase 4/11 (Aachoui et al., 2013; Broz et al., 2012; Hagar et al., 2013; Schauvliege et al., 2002). Here in our study we primed macrophages with IFNγ (5 ng.mL^{-1}) for 24 hours. Raw 264.7 macrophages were transfected with siRNA control and caspase 4/11 and cells were treated with LPS/IFNγ for 24

hours with or without IFNγ priming. For priming IFNγ was added to cells at the time of transfection. We observed that priming further enhanced the effect of LPS/IFNγ on mitophagy inhibition in macrophages. The effect of LPS/IFNγ on inhibition of mitophagy was significantly reduced with caspase 4/11 invalidation (Figure 5.11.D). The decrease in the inhibition of mitophagy in caspase 4/11-invalidated macrophages was more prominent in conditions of priming. Noteworthy, in addition to impacting on mitophagy flux, invalidation of caspase 4/11 also reduces LPS/IFNγ-mediated increase in CD64 and CD80 (Figure 5.11.E). This suggests that caspase 4/11 might impacts on macrophage polarization through the modulation of mitophagy.

We isolated mitochondria from LPS/IFNγ-treated macrophages. Interestingly we observed that caspase 4/11 appeared in the mitochondrial fraction in LPS/IFNγ-activated macrophages (Figure 5.12). VDAC and β-actin levels were checked to assess the purity of mitochondrial fraction whereas whole cells lysates were also blotted as positive control for caspase 4/11-detection (Figure 5.12). We could speculate that caspase 4/11 directly interacts with PINK1 in the mitochondria to ultimately cleave it or activate a protease that will subsequently cleave PINK1 as well as other mitophagy-regulating protein. This hypothesis will require complementary investigations.

Conclusion Part III

The data demonstrate that LPS/IFNγ-mediated inhibition of mitophagy and mROS production in macrophages relies on IFNGR and STAT1 signaling pathway. Our *in vivo* and *in vitro* data show that STAT1 play a key role in inhibition of mitophagy in myeloid cells. Furthermore, we demonstrate that STAT1-dependent inhibition of mitophagy in LPS/IFNγ-activated macrophages also involves caspase 4/11 that is likely activated by intracellular LPS.

Discussion

Discussion

The unique contribution of mitochondria to the innate and adaptive immunity led the researchers to name mitochondria as "powerhouse of the immunity" or "central hub of immunity" (Arnoult et al., 2011; Mills et al., 2017; Weinberg et al., 2015; West et al., 2011b). The recognition of mtDNA by TLR9, due to the presence of CpG motif, and activation of the NLRP3 inflammasome by mtDNA are only a few examples of the wide contribution of mitochondria to innate immunity (Nakahira et al., 2011; Shimada et al., 2012). Recent studies have also highlighted the role of mROS in bactericidal activity of macrophages (Garaude et al., 2016; West et al., 2011a). The contribution of mROS in the activation of NLRP3 inflammasome has also been reported (Zhou et al., 2011). Several sources of ROS are known in cells. Inhibition of mitophagy has also been reported to be associated with an increased mROS production (Zhou et al., 2011). The link between mitophagy inhibition and mROS production and its effect on macrophages activity and phenotype is not known.

Macrophages are immune cells able of functional plasticity which contributes to eradicating infectious agents. This event is usually associated with a two phase process comprising an inflammatory phase followed by an anti-inflammatory period and tissue repair function. These phases rely on the switch of macrophages to an M1 (inflammatory) followed by an M2 (anti-inflammatory) phenotype of the macrophages (Biswas et al., 2012; Mantovani et al., 2013; Mege et al., 2011). Metabolic reprogramming in macrophages plays an important role in their activation and phenotype. M1 macrophages display increased glycolysis whereas M2 phenotype relies on OXPHOS. The inhibition of glycolysis with 2-deoxyglucose inhibits the release of the inflammatory cytokine IL-1β in response to LPS. Inhibition of OXPHOS with etomoxir inhibits M2 polarization in response to IL-4 (Huang et al., 2014). Here in our study, we have shown that in response to LPS or infection, macrophages exhibit an inhibition of mitophagy and are associated with higher mitochondrial mass (Figure 1.1-3). The results were consistent in peritoneal macrophages, blood monocytes and neutrophils in an *in vivo* model of sepsis (CLP) as well as in a model of endotoxemia (Figure 1.4-8). This inhibition of mitophagy assists macrophages in their activation and functionality. To our knowledge, there is no prior study which has reported the inhibition of mitophagy in activated macrophages. Kasahara *et al.* reported that normal

mitochondrial density is important for macrophage response to LPS. They treated Raw 264.7 macrophages with ethidium bromide to establish a cell line depleted of mtDNA termed as ρ^o cells. In comparison to normal Raw 264.7 macrophages, ρ^o cells exhibit lower mitochondrial density, lower mtDNA content, and reduced respiratory chain activity. They showed that ρ^o cells have a decreased response to LPS as compared to normal Raw 264.7 macrophages. The LPS-mediated release of cytokines was significantly lower in ρ^o cells as compared to normal Raw 264.7 macrophages. This study suggested that normal mitochondrial density in macrophages is critically important for mROS and inflammatory cytokine release in response to LPS (Kasahara et al., 2011). However, they did not investigate any effect of LPS on mitochondrial morphology and density in macrophages. Furthermore, the impact of macrophage activation on dynamics and mitophagy was also not reported.

Mitophagy is a selective form of autophagy. It was also reported that autophagy is important in monocyte differentiation to macrophages in response to M-CSF (Jacquel et al., 2012). Pharmacological inhibition of autophagy in monocytes abrogated the effect of M-CSF on monocytes differentiation into macrophages (Jacquel et al., 2012). Induction of autophagy in macrophages has also been reported (Delgado et al., 2008; Xu et al., 2007). Different studies have shown the regulation of autophagy by TLR4. Enhanced autophagy in these cells plays an important role in the regulation of inflammatory response and pathogen clearance (Delgado et al., 2008; Xu et al., 2007). Autophagy also plays an important role in the removal of intracellular pathogens and this selective form of autophagy is referred as xenophagy (Bauckman et al., 2015). LPS-treated macrophages showed higher entrapment of mycobacterium tuberculosis inside autophagosome as compared to untreated controls (Xu et al., 2007). LPS-mediated induction of autophagy in Raw264.7 macrophages was reported to take place in a TLR4- and TRIF-dependent manner (Myd88 independent pathway) (Xu et al., 2007). Other PAMPs and cytokines, including IFNγ, were also shown to induce autophagy (Delgado et al., 2008). In accordance with these studies, we also observed that autophagy was induced in LPS/IFNγ-stimulated macrophages (Figure 2.2). There are numbers of studies about autophagy in immune cells but the role of mitophagy in macrophage activation and function has not been reported. We used mitokeima protein to check the impact of stimulation of macrophages with LPS/IFNγ on mitophagy in

macrophages. We found that mitophagy was decreased in LPS/IFNγ-activated Raw 264.7 macrophages (Figure 2.2). These results were in accordance with our hypothesis that mitophagy is inhibited in activated macrophages.

Mitophagy is known to be regulated by three key proteins PINK1, Parkin and DJ-1, which are also reported to form an ubiquitin ligase complex (Kazlauskaite et al., 2014; Shiba-Fukushima et al., 2014; Xiong et al., 2009). The mutation of these three key proteins (Parkin, PINK1, DJ-1) is known to be associated with the autosomal recessive form of Parkinson's disease (Dodson and Guo, 2007). Parkinson's disease is a neurodegenerative disease characterized by motor dysfunction, tremors and rigidity, caused by degeneration of dopaminergic neurons in substantia nigra (Jankovic, 2008). Although its etiology remains obscure, inflammation has been identified as a major risk factor in the pathogenesis of neurodegenerative disease including Parkinson's disease and Alzheimer's disease (McGeer and McGeer, 2004; Tufekci et al., 2012). Interestingly, intra-striatal injection of LPS is considered as a model of Parkinson's disease. LPS injection was associated with degeneration of dopaminergic neurons in the substantia nigra, depletion of dopamine and induction of signs and symptoms of Parkinson's disease (Hunter et al., 2009). The symptoms were alleviated by L-Dopa, a known drug used for Parkinson's disease (Hunter et al., 2009). With regards to our data, we could speculate that in that settings, intra-striatal injection of LPS leads to inhibition of mitophagy in neurons and/or microglial cells that contributes to trigger Parkinson's disease-like symptoms. LPS- and TNFα-treated BV2 microglia, primary microglia as well as peritoneal macrophages were reported to be associated with decreased mRNA and protein levels of Parkin in a NFκB-dependent manner (Tran et al., 2011). The authors reported that NFκB negatively regulates the expression of Parkin (Tran et al., 2011). LPS-treated peritoneal macrophages from Parkin-knock-out mice showed higher mRNA levels of inflammatory markers, TNFα, IL-1β, and iNOS, as compared to wild-type macrophages (Tran et al., 2011). Freshly prepared brain slices from PINK1-knock-out mice presented higher levels of pro-inflammatory cytokines, IL-1β, IL-6 and TNFα, as compared to wild-type (Kim et al., 2013). Interestingly, PINK1$^{+/-}$ mice were more susceptible to a lethal dose of LPS (Mannam et al., 2014), illustrating the important role of this protein and mitophagy in host protection against endotoxemia. Recent studies have reported the link between PINK1/Parkin-mediated mitophagy

and mitochondrial antigen presentation (Matheoud et al., 2016). They reported that Parkin and PINK1 negatively regulated presentation of mitochondrial antigen in macrophages and dendritic cells thereby suggesting a link between immunity and mitophagy (Matheoud et al., 2016). Altogether, these studies highlight a link between mitophagy and inflammation as well as link between mitophagy proteins involved in PD and inflammation.

PINK1 is the key protein responsible for the initiation of mitophagy. PINK1 is a serine/threonine kinase enzyme which is continuously recruited to mitochondria and surveys the mitochondrial health (Nguyen et al., 2016). On the detection of any damage or decreased mitochondrial membrane potential, it is stabilized and initiates mitophagy via its kinase activity (Nguyen et al., 2016). PINK1 phosphorylates and recruits Parkin to the damaged mitochondria to initiate mitophagy (Nguyen et al., 2016). Hence, the mitophagy regulation mainly relies on PINK1 stabilization and recruitment of Parkin to mitochondria. We checked the levels of these proteins in mitochondrial fractions and we observed that in the mitochondrial fraction from LPS/IFNγ-treated Raw 264.7 macrophages, Parkin and PINK1 were reduced after 18 hour treatment (Figure 2.5). Furthermore, the recruitment of PINK1 and Parkin to the mitochondria reciprocally relies on mitochondrial membrane potential (Jin et al., 2010; Narendra et al., 2008). PINK1 is cleaved by mitochondrial membrane protease when the mitochondrial membrane potential is intact (Deas et al., 2011; Greene et al., 2012; Jin et al., 2010; Meissner et al., 2011). Cleavage and translocation of PINK1 back to the cytosol leads to either degradation of PINK1 by protease or binding of PINK1 to the cytosolic Parkin (Fedorowicz et al., 2014). Both conditions lead to the inhibition of mitophagy. In contrast, the dissipation of mitochondrial membrane potential leads to the stabilization of PINK1 onto mitochondria and induction of mitophagy (Deas et al., 2011; Greene et al., 2012; Jin et al., 2010; Meissner et al., 2011). In our model, we observed that LPS/IFNγ-treated macrophages were associated with higher mitochondrial membrane potential as observed by TMRM and JC1 probes (Figure 4.8). We also observed that PINK1 and Parkin were downregulated in mitochondrial fraction from Raw 264.7 macrophages, as well as in total protein lysates from Raw 264.7 macrophages, BMDMs and peritoneal macrophages with LPS/IFNγ treatment, in a time-dependent manner (Figures 2.4, 2.5, 5.7). This might give an answer to the observation that the decrease in PINK1 in all three cell lines could be due to increased cleavage

of mitochondrial PINK1 and subsequent degradation mediated by cytosolic proteasomes. This ultimately leads to the inhibition of mitophagy in macrophages. Moreover, dissipation of mitochondrial membrane potential by mitochondrial uncouplers and mitophagy inducers abrogated the effect of LPS/IFNγ on the diminution of PINK1, Parkin and DJ-1 in Raw 264.7 macrophages (Figure 2.4). To our knowledge, no study has shown a link between mitophagy and macrophage activation. This is the first time any study uses mitochondrial uncouplers *in vivo* and *in vitro* to induce mitophagy in myeloid cells in the context of sepsis and activated macrophages. Mitochondrial dynamics and membrane potential are closely related processes. Mitochondrial depolarization was reported to induce mitochondrial fragmentation (Legros et al., 2002) and inhibition of fusion (Meeusen et al., 2004). However, Parkin translocation to mitochondria depends on membrane potential, independent of mitochondrial fragmentation (Narendra et al., 2008). CCCP-induced translocation and accumulation of Parkin was seen in the elongated mitochondrial network in cells expressing negative-mutant of Drp1 protein, suggesting that Parkin translocation to mitochondria depends on depolarization, independent of mitochondrial fission (Narendra et al., 2008).

Mitophagy is a continuous process and occurs at a basal level. Continuous mitophagy flux allows cells to maintain homeostasis by removing damaged part of mitochondria (Ashrafi and Schwarz, 2013; Stotland and Gottlieb, 2015). Mitochondrial fission is believed to be a mandatory step of mitophagy. The normal size of mitochondria varies and can reach up to 5 μm whereas the diameter of autophagosome is approximately 1 μm (Cereghetti and Scorrano, 2006). This makes the fragmentation of mitochondrial network mandatory process prior to entrapment by the autophagosomal assembly. In the condition of starvation Drp1 translocation to the mitochondria was inhibited that resulted in elongation of mitochondrial network (Gomes et al., 2011; Rambold et al., 2011). Decreased mitochondrial fission ultimately leads to higher mitochondrial fusion. This mitochondrial fusion helps the mildly affected mitochondria to form a network with viable mitochondria to maintain the membrane potential and fulfill energy demands. This increased mitochondrial network also acts as a protective mechanism against autophagy induced under the condition of starvation (Gomes et al., 2011; Rambold et al., 2011). In our model of study, electron and fluorescence microscopy results showed that the LPS/IFNγ-stimulated Raw 264.7

macrophages were associated with elongated mitochondrial network (Figure 2.3). When we assessed the mitochondrial density and mitochondrial morphology by confocal microscopy, we observed that LPS/IFNγ-treated macrophages showed higher mitochondrial network in Raw 267.4 and peritoneal macrophages (Figure 2.3). We also observed that Drp1 was also down regulated in all three types of macrophages with LPS/IFNγ treatment. This Drp1 downregulation with LPS/IFNγ treatment in Raw 264.7 macrophages was rescued in the presence of mitophagy inducers, CCCP and DNP (Figures 2.4, 5.7).

Recent studies have shown a clear link between DJ-1 and inflammation. Peritoneal cells from DJ-1^{-/-} mice after CLP showed higher mRNA levels of CD80 and iNOS and higher phagocytic activity as compared to WT (Amatullah et al., 2016). BMDMs from DJ-1^{-/-} mice showed higher bactericidal activity (Amatullah et al., 2016). DJ-1^{-/-} mice were more resistant to the CLP as well as to the intraperitoneal injection of bacteria as compared to WT counterparts (Amatullah et al., 2016). BMDMs from DJ-1^{-/-} mice showed higher levels of inflammatory cytokines in response to LPS as compared to WT (Amatullah et al., 2016). The authors reported that high concentration of LPS (1 µg.mL^{-1}) treatment resulted in up regulation of DJ-1 at mRNA and protein levels in BMDMs (Amatullah et al., 2016). However, in our study, we observed that DJ-1 was down-regulated in LPS/IFNγ-treated Raw 264.7 macrophages, BMDM, as well as peritoneal macrophages (Figures 2.4, 2.5, 5.7).

The role of DJ-1 in the regulation of mitophagy is still ambiguous. An interaction and the formation a complex with Parkin, PINK1 and DJ-1 have been reported (Xiong et al., 2009). Furthermore, DJ-1 is also reported to be involved in the stabilization of PINK1 onto mitochondria (Tang et al., 2006). This is an initial step in the regulation of Parkin/PINK1-mediated mitophagy. Therefore, downregulation of DJ-1 in LPS/IFNγ-treated macrophages might further contribute negatively to PINK1 recruitment to the mitochondria and mitophagy (Figures 2.4, 2.5, 5.7).

In the context of sepsis, a study conducted on peripheral blood mononuclear cells obtained from septic patients showed decreased activity of respiratory chain complex, CI, CIII, and CIV, as compared to non-septic control samples (Garrabou et al., 2012). PBMCs from septic patients were also associated with decreased oxygen consumption rate (Garrabou et al., 2012). Furthermore, plasma from septic patients showed significantly higher levels of mtDNA as

compared to control (Garrabou et al., 2012). Blood monocytes from septic patients were associated with decreased ATP synthesis as well as activity of respiratory chain complexes (Japiassu et al., 2011) . M1 macrophages are known to be associated with decreased oxygen consumption and rely on anaerobic glycolysis even in the presence of oxygen. This phenomenon can be related to the Warburg effect observed in cancer cells. LPS stimulated macrophages showed upregulation of genes involved in glycolysis (Tannahill et al., 2013). BMDMs stimulated with LPS were shown to be associated with decreased oxygen consumption, decreased ATP/ADP ratio and decreased ATP synthesis by oxidative phosphorylation (Mills et al., 2016). We also assessed the oxygen consumption in LPS/IFNγ-activated macrophages and observed that activated macrophages were associated with decreased oxygen consumption rate (Figure 4.9). Furthermore, we also observed that the activities of respiratory chain complexes were significantly reduced in LPS/IFNγ-treated macrophages (Figure 4.9). This was in accordance with the previously reported studies that the activated macrophages are associated with the metabolic switch from oxidative phosphorylation to glycolysis (Galván-Peña and O'Neill, 2014; Mills et al., 2016). LPS-stimulated BMDMs were shown to exhibit higher mitochondrial membrane potential (Mills et al., 2016). We also observed that in LPS/IFNγ-stimulated Raw 264.7 macrophages mitochondrial membrane potential was increased in a time-dependent manner. Increased mitochondrial membrane potential in activated macrophages could be due to decreased utilization of proton gradient to run ATP synthase assembly to generate ATP, as in the case of oxidative phosphorylation.

In mouse hepatocytes, treatment with LPS resulted in decreased mitochondrial density at early time point (8 hours) whereas density was recovered to normal between 24 to 48 hours of LPS treatment (Carchman et al., 2013). mRNA levels of TFAM, PGC1α and NRF1 were increased in hepatocytes at 8 hours of LPS treatment (Carchman et al., 2013). These studies suggested that mitochondrial biogenesis was increased to maintain the mitochondrial pool back to the normal. In the condition of sepsis, some other studies have also reported an increase in mitochondrial biogenesis in different tissues (Carchman et al., 2013; Carré et al., 2010) whereas others found no changes in mitochondrial biogenesis (Vanhorebeek et al., 2012). Modulation of mitochondrial homeostasis was also observed in lung and endothelial cells in the model of sepsis (Mannam et

al., 2014). A study Mannam and colleagues showed that MKK3$^{-/-}$ mice were more resistant to injection of LPS and bacteria (*E.coli*) as well as to CLP as compared to their control littermates (Mannam et al., 2014). The authors proposed that MKK3-deficient mice maintain the healthy mitochondrial pool by a higher rate of mitochondrial biogenesis as well as increased mitophagy (Mannam et al., 2014). But the mechanism how mitophagy contributes to the sepsis and inflammation was not investigated. In our study, we have shown here that mitophagy acts as a protective mechanism against bacterial infection and is a feature of activated macrophages.

Sepsis is characterized by an uncontrolled inflammatory response in which macrophages, especially inflammatory macrophages, play an important role. Therefore, we investigated the contribution of the mitophagy inhibition to the switch of macrophages toward an inflammatory phenotype (M1 polarization). We showed that inhibiting the mitophagy with pharmacological mitophagy inhibitors was sufficient to mimic the effect of LPS/IFNγ on macrophage activation. Alternatively, the treatment of macrophages with LPS/IFNγ in the presence of mitophagy inducers as well as injection of mitophagy inducers to mice prior to LPS injection or CLP, reduced the activation of macrophages (Figure 2.7). CLP-induced inflammatory cytokines were also decreased with a prior injection of mitophagy inducers (Figure 3.2). This contributes to explain the higher death rate and lower anti-bacterial defense (Figure 3.1). These observations indicate that mitophagy inhibition in myeloid cells plays an important role in bactericidal activity and acts as a protective mechanism for the host. Moreover, inhibition of mitophagy is protective but if maintained for prolong period, it might be harmful due to increased inflammation and ROS production. This might ultimately lead to tissue damage and organ failure. We have not investigated mitophagy in other tissues, but it might be interesting to investigate these novel findings in other tissues, especially in the heart and the muscle that are known to be affected in the context of sepsis. Prolonged inhibition of mitophagy leads to feedback mechanism either leading to mitochondrial biogenesis which may explain the observed results in other studies, or initiate Parkin/PINK1-independent mitophagy which further needs to be investigated.

West et *al.* reported that in macrophages the stimulation of cell surface (TLRs, TLR1, TLR2 and TLR4) lead to increased mROS production, whereas no mROS induction was observed by stimulation of endosomal TLRs (TLR3, TLR7, TLR8 and TLR9) (West et al., 2011a). In our

experimental settings, we observed that mROS was induced by stimulation of cell surface TLRs (TLR 1/2/4) as well as some endosomal TLRs including TLR3 and TLR7/8 stimulation. Our results show that mROS production in response to different TLRs stimulation is not limited to only cell surface TLRs. This area should be further investigated and the underlying molecular mechanism needs to be delineated. We observed that stimulation of Raw 264.7 macrophages with LPS and IFNγ induced mROS production in a dose- and time-dependent manner (Figure 4.7). The induction of mROS in response to LPS in macrophages gave a similar pattern to that of mitophagy inhibition (Figure 4.7 vs 2.3). Studies have reported that mROS contributes to the bactericidal activity of macrophages. Here in our study, we have shown that macrophage activation and function relies on mROS via inhibition of mitophagy. By using two known ROS scavenger, NAC and Mitotempol, we observed that both of them reduced the protein levels of M1 markers, CD80 and CD64, induced by LPS/IFNγ (Figure 4.11). West et *al.* suggested that TLRs-stimulated macrophages exhibit enhanced mROS production through complex I in an ECSIT- and TRAF6-dependent pathway (West et al., 2011a). They proposed that TRAF6 is recruited to mitochondria in response to TLR 1/2/4 stimulation and interacts with ECSIT. ECSIT is polyubiquitinated and degraded by E3-ubiquitin ligase activity of TRAF6, which ultimately leads to destabilization of complex I and increased mROS production. They assessed the polyubiquitination of ECSIT in HEK 293 cells and macrophages. TRAF6-knock-out macrophages represented impaired mROS and H_2O_2 induction upon TLR 1/2/4 stimulation. A similar decrease in mROS production was reported for ECSIT-depleted macrophages (West et al., 2011a). In contrast, another study has reported that inhibition of complex I with rotenone and metformin reduces the mROS production and decreases the production of pro-IL-1β in macrophages in response to LPS (Kelly et al., 2015). The contribution of complex I inhibition in mROS production needs to be further characterized. In our model, we saw the higher induction of mROS with complex III inhibition. Inhibition of compkex III contributed to macrophage activation. It was also reported that inhibition of autophagy/mitophagy by 3-MA causes an increase in mROS production in THP1 macrophages (Zhou et al., 2011). mROS act as a signaling molecule for the processing and release of IL-1β in a NLRP3- and ASC-dependent manner (Zhou et al., 2011). In our study, we have shown that inhibition of mitophagy in macrophages with 3-MA leads to release of different inflammatory

cytokines, including IL-6, TNF-α, IL-12P70 as well as IL-1β (Figure 4.3). Inflammatory markers including iNOS, TNFα and IL-6 were upregulated at mRNA levels after mitophagy inhibition with 3-MA and Mdivi1 (Figure 4.2). Inhibition of mitophagy in macrophages mimicked the effect of LPS/IFNγ on macrophage activation markers, including CD64 and CD80 (Figure 4.1). These results clearly show that mROS produced subsequently to the inhibition in mitophagy have effects that are not only restricted to the activation of the NRLP3 inflammasome. Interestingly, we observed that NLRP3 invalidation does not impact on mROS-induced macrophage activation. ROS have been reported to induce stabilization of HIF1α *via* inactivation of prolyl hydroxylase (PHD) (Lee et al., 2016) and activation of NFκB (Asehnoune et al., 2004). It was also reported that stabilization of HIF1-α is mediated by ROS after stimulation with LPS (Mills et al., 2016; Tannahill et al., 2013). Conversely, the pretreatment of BMDMs with NAC reduced the effect of LPS on HIF1α stabilization in macrophages (Tannahill et al., 2013). The notion should be made that to our knowledge, no study has reported the link between inhibition of mitophagy and HIF1α stabilization. Here we have shown that increased mROS in response to the inhibition of mitophagy contributes to macrophage activation partly through HIF1α. Raw 264.7 macrophages invalidated for HIF1α and NFκB showed a significant reduction in M1 markers in response to mitophagy inhibitor as well as ROS inducers (Figure 4.12). Furthermore, M1 activation markers were significantly reduced in response to LPS/IFNγ, Mdivi1 as well as antimycin A in the presence of echinomycin, an inhibitor of HIF1α (Kong et al., 2005). HIF1α is also known to induce inflammatory cytokines (Corcoran and O'Neill, 2016). These results further emphasized the fact that the inhibition of mitophagy mimics the effect of LPS/IFNγ on macrophage activation.

Dissection of underlying molecular mechanisms *in vitro* and *in vivo* highlighted a key role of the transcription factor STAT1 in LPS-mediated inhibition of mitophagy. STAT1 is a major component of IFNγ signaling pathway. In response to IFNγ, STAT1 undergoes activation via phosphorylation at tyrosine 701 and serine 727 which forms a homodimer and is translocates to the nucleus to regulate gene expression (Darnell et al., 1994; Platanias and Fish, 1999). To our knowledge, our data demonstrate for the first time a link between mitophagy and STAT1 in immune cells upon bacterial infection. In the context of cardiac ischemia-reperfusion injuries, STAT1 was suggested to be involved in the regulation of autophagy. In an *ex vivo* model of ischemia reperfusion, STAT1-

$^{/-}$ mice showed decreased infarct size as compared to wild-type. Inhibition of autophagy in STAT1$^-$$^{/-}$ mice abrogated this protective effect whereas induction of autophagy by pretreatment with rapamycin reduced infarct size and produced protective effect. This suggests that STAT1 acts as a negative regulator of autophagy and leads to worsening of condition after ischemia reperfusion (McCormick et al., 2012). Furthermore, autophagy markers, LC3-II were higher in STAT1$^{-/-}$ mice as compared to wild-type after *ex vivo* ischemia-reperfusion (McCormick et al., 2012). IFNγ treatment of cardiomyocytes showed STAT1 phosphorylation and reduced LC3-II levels (McCormick et al., 2012). It has also been reported that STAT1 translocates to the mitochondria but the role of STAT1 in mitochondria is not yet clear (Boengler et al., 2010). Furthermore, increased mitochondrial biogenesis, mitochondrial mass and PGC1α mRNA levels were reported in the livers of STAT1$^{-/-}$ mice as compared to STAT1$^{+/+}$. This suggests that STAT1 could act as a negative regulator of mitochondrial biogenesis (Sisler et al., 2015). STAT1-deficient mice were reported to be resistant to CLP as well as LPS injection (Herzig et al., 2012; Kamezaki et al., 2004). CLP-operated STAT1$^{-/-}$ mice presented lower plasma levels of IL-6, MIP-2, CXCL10, and IFNα, as compared to wild-type mice (Herzig et al., 2012). This confirms that STAT1 activation plays a critical role in the pathogenesis of septic shock and organ injury (Herzig et al., 2012). We have shown here that mitophagy was inhibited in macrophages and monocytes after CLP surgery or LPS injection in STAT1-dependent manner. This link between STAT1 signaling pathway and mitophagy is completely new. We also observed that LPS-mediated mitophagy inhibition partially relies on TLR4 as LPS-treated macrophages showed a reduction in mitophagy inhibition with TLR4 invalidation (Figure 5.1). A similar reduction was also observed with invalidation of IFNGR signaling pathway when macrophages were stimulated with LPS alone (Figure 5.2). This suggests that TLR4 might contribute to mitophagy inhibition via indirect activation of IFNGR signaling pathway by inducing the release of IFNγ. It was also reported that caspase 4/11 is transcriptionally regulated by NFkB and STAT1 in response to LPS and IFNγ, respectively (Schauvliege et al., 2002). Accordingly, we observed that peritoneal macrophages from STAT1$^{-/-}$ mice showed loss of induction of caspase 4/11 at mRNA levels in response to LPS/IFNγ (Figure 5.10). We also observed marked reduction of LPS/IFNγ-mediated induction of caspase 11/4 expression at mRNA and protein levels in Raw 264.7 macrophages invalidated for STAT1 (Figure

5.10). Several recent studies highlighted that caspase 4/11 is an intracellular receptor for the bacterial LPS (Kayagaki et al., 2011). Inhibition of mitophagy, downregulation of mitophagy proteins as well as expression of M1 markers in response to LPS/IFNγ were reduced in caspase 4/11-dependent manner. To conclude, we have shown in this study that inhibition of mitophagy in macrophages *in vitro* and *in vivo* drives macrophage activation towards M1 phenotype, which acts as a protective mechanism against Gram-negative bacterial infection and bactericidal activity in a ROS-dependent manner. Furthermore, this inhibition of mitophagy is driven by the STAT1-caspase-11/4 signaling pathway. This inhibition of mitophagy is a hallmark of the M1 phenotype.

Conclusion and Perspectives

Conclusion and Future Perspectives

This study unravels a previously unknown contribution of mitochondrial quality control and dynamics to innate immunity. In the context of sepsis and endotoxemia myeloid cells present increased mitochondrial density due to an inhibition of mitophagy. This acts as a protective mechanism and may contribute to survival against bacterial infection. Investigations of mitophagy regulation in other tissues especially in the context of sepsis will help to better understand the link between mitochondrial dysfunction and multi-organ failure associated with sepsis. It may ultimately lead to discovering better diagnostic and therapeutic strategy for sepsis and inflammation.

We have established a new flow cytometry strategy to assess mitophagy on fresh white blood cells from the whole organism. We have reported a new population of macrophages that express high levels of CD64 and exhibit higher mitochondrial density. This population increases in the context of infection and endotoxemia, as evidenced by *in vivo* and *in vitro* observations. This new population can present a new diagnostic criterion in the context of different inflammatory diseases for future investigations.

This study shows that activation of macrophages is tightly linked to mitophagy and mitochondrial dynamics. Mitophagy inhibition plays a vital role in macrophage activation, inflammatory cytokines release, phagocytosis and bactericidal activity. Pharmacological modulation of mitophagy (*in vivo* and *in vitro*) showed modulation of inflammatory response. This is the first time that a study shows that mitophagy can be modulated *in vivo* by using uncouplers or mitochondrial fission inhibitors. We demonstrated that classically activated macrophages exhibit inhibition of mitophagy, increased mitochondrial density, increased mitochondrial membrane potential and inhibition of RCCs, which ultimately contributes to increased mROS production. This increased mROS helps macrophages in the acquisition of their inflammatory phenotype via NFκB and HIF1α. This inhibition of mitophagy in macrophages relies on IFNγ and STAT1 signaling pathway with the contribution of the intracellular LPS sensor caspase 4/11. The link between STAT1 and mitophagy inhibition as well as macrophage activation has never been shown. Furthermore, the link between caspase 4/11 and STAT1 in mitophagy inhibition is also novel. We
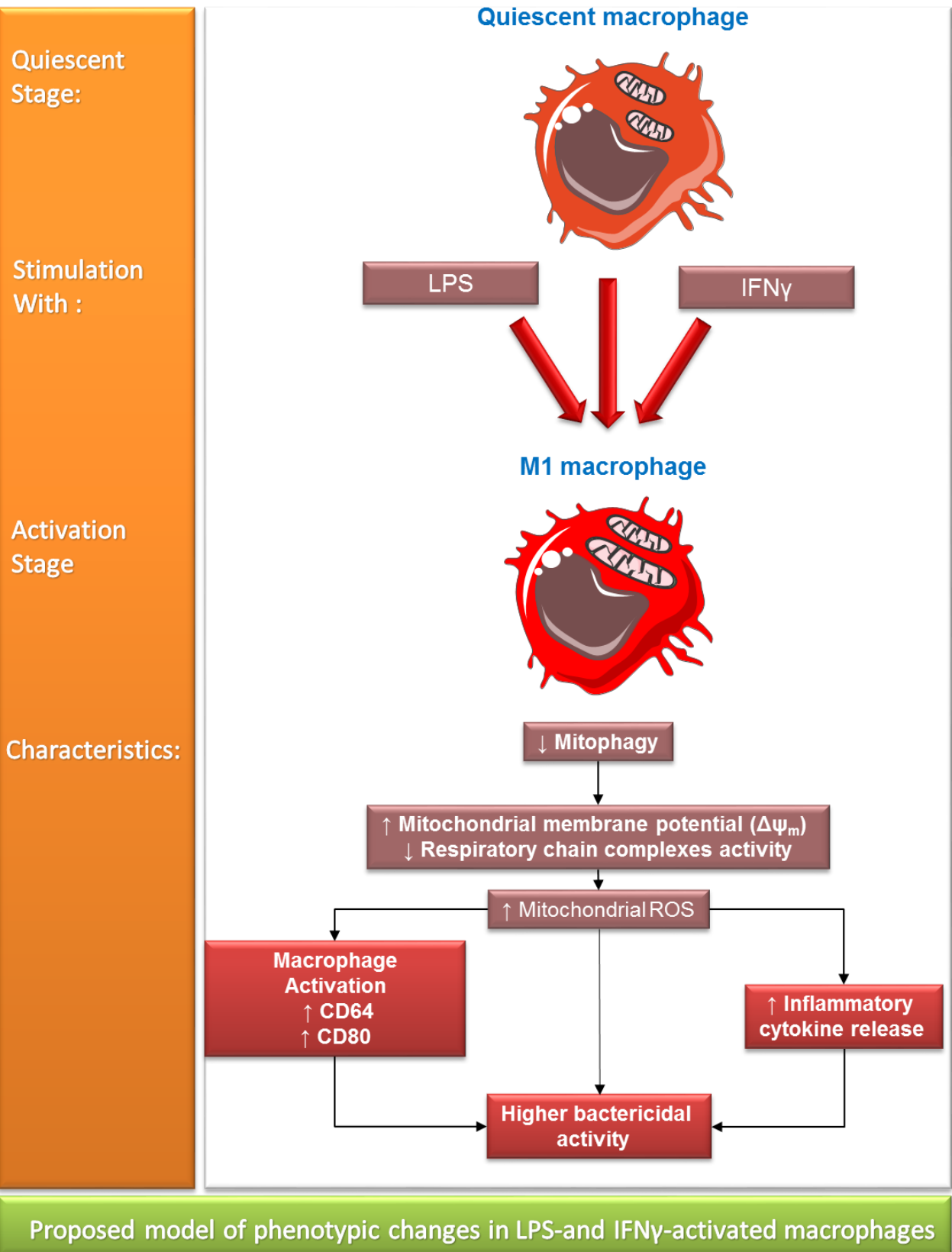
have shown here that STAT1 and caspase 4/11 are involved in regulation of mitophagy in LPS/IFNγ-activated macrophages. To further dissect molecular mechanism, it will be good to investigate the role of caspase 4/11 and STAT1 in the downregulation of key proteins-regulating mitophagy. Caspase 1 has been reported to cleave Parkin (Kahns et al., 2003; Yu et al., 2014). PINK1 cleavage in LPS/IFNγ-activated macrophages may require either direct interaction with inflammatory caspase namely caspase 4/11. Alternatively, in LPS/IFNγ-activated macrophages, caspase 4/11 might activate proteases that subsequently cleaves PINK1 to trigger its degradation by the proteasome. Deciphering this pathway will help to better understand the mitophagy regulation in LPS-treated macrophages.

Neutrophils are the most abundant and most motile innate immune cells which respond faster and reach the site of infection or injury. We also observed increased mitochondrial density in neutrophils. It will be worthwhile to further investigate the regulation of mitophagy in other immune cells especially lymphocytes.

It will be worth to investigate the modulation of mitophagy in macrophages and other immune cells in the context of atherosclerosis, diabetes as well as other cardiovascular and metabolic diseases.

Overall, modulation of mitophagy may represent a new therapeutic approach in the context of inflammatory conditions like sepsis or chronic inflammatory diseases where uncontrolled inflammatory response can be lethal or highly deleterious. Creating new pharmacological agents to selectively target specific immune cells to modulate mitophagy could represent a good strategy to control the inflammatory response and to improve therapeutic outcomes in different pathophysiological conditions. Additionally, it would be worth investigating the effect of different pharmacological drugs, such as anti-inflammatory agents and antibiotics, on mitophagy in different immune cells. This may help to improve the therapeutic outcomes and to better understand the side effects of currently used medicines.

To conclude, this study has opened a new window in the field of immunometabolism and should contribute to a better understanding of the role of mitochondria immunity.

Quiescent macrophage

Quiescent
Stage:

Stimulation
With :

LPS   IFNγ

M1 macrophage

Activation
Stage

Characteristics:

↓ Mitophagy

↑ Mitochondrial membrane potential ($\Delta\psi_m$)
↓ Respiratory chain complexes activity

↑ Mitochondrial ROS

Macrophage
Activation
↑ CD64
↑ CD80

↑ Inflammatory
cytokine release

Higher bactericidal
activity

Proposed model of phenotypic changes in LPS-and IFNγ-activated macrophages

Steps:
1. LPS mediated stimulation of TLR4.
2. Endogenous or exogenous IFNγ-mediated activation of IFNGRs.
3. Activation of STAT1
4. Transcriptional induction of pro-caspase 4/11
5. Activation of caspase 4/11
6. Caspase 4/11 contributes to the downregulation of PINK1, Parkin, DJ-1, and Drp1.
7. Increase in mitochondrial density (Inhibition of Mitophagy).
8. Increased mROS production.
9. mROS contribute to the activation of NFκB.
10. mROS contributes to activation of HIF1α.
11. Classical activation of macrophages

Proposed mechanism of LPS- and IFNγ-mediated inhibition of mitophagy in macrophages

Bibliography

(1982). Mitochondrial N-formylmethionyl proteins as chemoattractants for neutrophils. The Journal of Experimental Medicine *155*, 264-275.

Aachoui, Y., Leaf, I.A., Hagar, J.A., Fontana, M.F., Campos, C.G., Zak, D.E., Tan, M.H., Cotter, P.A., Vance, R.E., and Aderem, A. (2013). Caspase-11 protects against bacteria that escape the vacuole. Science *339*, 975-978.

Aaronson, D.S., and Horvath, C.M. (2002). A road map for those who don't know JAK-STAT. Science *296*, 1653-1655.

Abbas, A.K., Lichtman, A.H., and Pillai, S. (2014). Basic immunology: functions and disorders of the immune system (Elsevier Health Sciences).

Adrie, C., Alberti, C., Chaix-Couturier, C., Azoulay, É., de Lassence, A., Cohen, Y., Meshaka, P., Cheval, C., Thuong, M., and Troché, G. (2005). Epidemiology and economic evaluation of severe sepsis in France: age, severity, infection site, and place of acquisition (community, hospital, or intensive care unit) as determinants of workload and cost. Journal of critical care *20*, 46-58.

Adrie, C., Bachelet, M., Vayssier-Taussat, M., Russo-Marie, F., Bouchaert, I., Adib-Conquy, M., Cavaillon, J.M., Pinsky, M.R., Dhainaut, J.F., and Polla, B.S. (2001). Mitochondrial membrane potential and apoptosis peripheral blood monocytes in severe human sepsis. Am J Respir Crit Care Med *164*, 389-395.

Aguirre, E., López-Bernardo, E., and Cadenas, S. (2012). Functional evidence for nitric oxide production by skeletal-muscle mitochondria from lipopolysaccharide-treated mice. Mitochondrion *12*, 126-131.

Akhter, A., Caution, K., Khweek, A.A., Tazi, M., Abdulrahman, B.A., Abdelaziz, D.H., Voss, O.H., Doseff, A.I., Hassan, H., and Azad, A.K. (2012). Caspase-11 promotes the fusion of phagosomes harboring pathogenic bacteria with lysosomes by modulating actin polymerization. Immunity *37*, 35-47.

Akira, S., Uematsu, S., and Takeuchi, O. (2006). Pathogen recognition and innate immunity. Cell *124*, 783-801.

Alexander, C., Votruba, M., Pesch, U.E., Thiselton, D.L., Mayer, S., Moore, A., Rodriguez, M., Kellner, U., Leo-Kottler, B., and Auburger, G. (2000). OPA1, encoding a dynamin-related GTPase,

is mutated in autosomal dominant optic atrophy linked to chromosome 3q28. Nature genetics *26*, 211-215.

Amar, J., Burcelin, R., Ruidavets, J.B., Cani, P.D., Fauvel, J., Alessi, M.C., Chamontin, B., and Ferrieres, J. (2008). Energy intake is associated with endotoxemia in apparently healthy men. The American journal of clinical nutrition *87*, 1219-1223.

Amatullah, H., Shan, Y., Beauchamp, B.L., Gali, P.L., Gupta, S., Maron-Gutierrez, T., Speck, E.R., Fox-Robichaud, A.E., Tsang, J.L., Mei, S.H.*, et al.* (2016). DJ-1/PARK7 Impairs Bacterial Clearance in Sepsis. Am J Respir Crit Care Med.

Angus, D.C., Linde-Zwirble, W.T., Lidicker, J., Clermont, G., Carcillo, J., and Pinsky, M.R. (2001). Epidemiology of severe sepsis in the United States: analysis of incidence, outcome, and associated costs of care. Critical Care Medicine-Baltimore- *29*, 1303-1310.

Arnoult, D., Soares, F., Tattoli, I., and Girardin, S.E. (2011). Mitochondria in innate immunity. EMBO reports *12*, 901-910.

Asehnoune, K., Strassheim, D., Mitra, S., Kim, J.Y., and Abraham, E. (2004). Involvement of reactive oxygen species in Toll-like receptor 4-dependent activation of NF-kappa B. Journal of immunology (Baltimore, Md : 1950) *172*, 2522-2529.

Ashrafi, G., and Schwarz, T.L. (2013). The pathways of mitophagy for quality control and clearance of mitochondria. Cell death and differentiation *20*, 31-42.

Barrientos, A. (2002). In vivo and in organello assessment of OXPHOS activities. Methods *26*, 307-316.

Barth, S., Glick, D., and Macleod, K.F. (2010). Autophagy: assays and artifacts. The Journal of pathology *221*, 117-124.

Bauckman, K.A., Owusu-Boaitey, N., and Mysorekar, I.U. (2015). Selective Autophagy: Xenophagy. Methods (San Diego, Calif) *75*, 120-127.

Bauernfeind, F.G., Horvath, G., Stutz, A., Alnemri, E.S., MacDonald, K., Speert, D., Fernandes-Alnemri, T., Wu, J., Monks, B.G., Fitzgerald, K.A.*, et al.* (2009). Cutting edge: NF-kappaB activating pattern recognition and cytokine receptors license NLRP3 inflammasome activation by regulating NLRP3 expression. Journal of immunology (Baltimore, Md : 1950) *183*, 787-791.

Becker, D., Richter, J., Tocilescu, M.A., Przedborski, S., and Voos, W. (2012). Pink1 kinase and its membrane potential (Deltapsi)-dependent cleavage product both localize to outer mitochondrial membrane by unique targeting mode. The Journal of biological chemistry *287*, 22969-22987.

Beltran, B., Mathur, A., Duchen, M.R., Erusalimsky, J.D., and Moncada, S. (2000). The effect of nitric oxide on cell respiration: A key to understanding its role in cell survival or death. Proceedings of the National Academy of Sciences of the United States of America *97*, 14602-14607.

Biswas, S.K., Chittezhath, M., Shalova, I.N., and Lim, J.Y. (2012). Macrophage polarization and plasticity in health and disease. Immunologic research *53*, 11-24.

Biswas, S.K., and Mantovani, A. (2010). Macrophage plasticity and interaction with lymphocyte subsets: cancer as a paradigm. Nat Immunol *11*, 889-896.

Biswas, S.K., and Mantovani, A. (2012). Orchestration of metabolism by macrophages. Cell metabolism *15*, 432-437.

Blackinton, J., Lakshminarasimhan, M., Thomas, K.J., Ahmad, R., Greggio, E., Raza, A.S., Cookson, M.R., and Wilson, M.A. (2009). Formation of a Stabilized Cysteine Sulfinic Acid Is Critical for the Mitochondrial Function of the Parkinsonism Protein DJ-1. The Journal of biological chemistry *284*, 6476-6485.

Blander, J.M., and Medzhitov, R. (2004). Regulation of phagosome maturation by signals from toll-like receptors. Science *304*, 1014-1018.

Blander, J.M., and Medzhitov, R. (2006). On regulation of phagosome maturation and antigen presentation. Nat Immunol *7*, 1029-1035.

Boehm, U., Klamp, T., Groot, M., and Howard, J.C. (1997). Cellular responses to interferon-gamma. Annu Rev Immunol *15*, 749-795.

Boengler, K., Hilfiker-Kleiner, D., Heusch, G., and Schulz, R. (2010). Inhibition of permeability transition pore opening by mitochondrial STAT3 and its role in myocardial ischemia/reperfusion. Basic Research in Cardiology *105*, 771-785.

Bone, R.C., Balk, R.A., Cerra, F.B., Dellinger, R.P., Fein, A.M., Knaus, W.A., Schein, R.M.H., and Sibbald, W.J. (1992). Definitions for Sepsis and Organ Failure and Guidelines for the Use of Innovative Therapies in Sepsis. Chest *101*, 1644-1655.

Bonifati, V., Rizzu, P., van Baren, M.J., Schaap, O., Breedveld, G.J., Krieger, E., Dekker, M.C., Squitieri, F., Ibanez, P., Joosse, M., *et al.* (2003). Mutations in the DJ-1 gene associated with autosomal recessive early-onset parkinsonism. Science *299*, 256-259.

Bosenberg, A.T., Brock-Utne, J.G., Gaffin, S.L., Wells, M.T., and Blake, G.T. (1988). Strenuous exercise causes systemic endotoxemia. Journal of applied physiology (Bethesda, Md : 1985) *65*, 106-108.

Bowie, A., and O'Neill, L.A. (2000). The interleukin-1 receptor/Toll-like receptor superfamily: signal generators for pro-inflammatory interleukins and microbial products. Journal of leukocyte biology *67*, 508-514.

Boya, P., Reggiori, F., and Codogno, P. (2013). Emerging regulation and functions of autophagy. Nature cell biology *15*, 713-720.

Brackett, D.J., Schaefer, C.F., Tompkins, P., Fagraeus, L., Peters, L.J., and Wilson, M.F. (1985). Evaluation of cardiac output, total peripheral vascular resistance, and plasma concentrations of vasopressin in the conscious, unrestrained rat during endotoxemia. Circulatory shock *17*, 273-284.

Briscoe, J., Rogers, N.C., Witthuhn, B.A., Watling, D., Harpur, A.G., Wilks, A.F., Stark, G.R., Ihle, J.N., and Kerr, I.M. (1996). Kinase-negative mutants of JAK1 can sustain interferon-gamma-inducible gene expression but not an antiviral state. The EMBO journal *15*, 799-809.

Brock-Utne, J.G., Gaffin, S.L., Wells, M.T., Gathiram, P., Sohar, E., James, M.F., Morrell, D.F., and Norman, R.J. (1988). Endotoxaemia in exhausted runners after a long-distance race. South African medical journal = Suid-Afrikaanse tydskrif vir geneeskunde *73*, 533-536.

Brown, G.D., and Gordon, S. (2005). Immune recognition of fungal β-glucans. Cellular microbiology *7*, 471-479.

Broz, P., Ruby, T., Belhocine, K., Bouley, D.M., Kayagaki, N., Dixit, V.M., and Monack, D.M. (2012). Caspase-11 increases susceptibility to Salmonella infection in the absence of caspase-1. Nature *490*, 288-291.

Broz, P., von Moltke, J., Jones, J.W., Vance, R.E., and Monack, D.M. (2010). Differential requirement for Caspase-1 autoproteolysis in pathogen-induced cell death and cytokine processing. Cell host & microbe *8*, 471-483.

Buras, J.A., Holzmann, B., and Sitkovsky, M. (2005). Animal Models of sepsis: setting the stage. Nat Rev Drug Discov *4*, 854-865.

Canet-Avilés, R.M., Wilson, M.A., Miller, D.W., Ahmad, R., McLendon, C., Bandyopadhyay, S., Baptista, M.J., Ringe, D., Petsko, G.A., and Cookson, M.R. (2004). The Parkinson's disease protein DJ-1 is neuroprotective due to cysteine-sulfinic acid-driven mitochondrial localization. Proceedings of the National Academy of Sciences of the United States of America *101*, 9103-9108.

Cantó, C., Gerhart-Hines, Z., Feige, J.N., Lagouge, M., Noriega, L., Milne, J.C., Elliott, P.J., Puigserver, P., and Auwerx, J. (2009). AMPK regulates energy expenditure by modulating NAD(+) metabolism and SIRT1 activity. Nature *458*, 1056-1060.

Caradonna, L., Amati, L., Magrone, T., Pellegrino, N.M., Jirillo, E., and Caccavo, D. (2000). Enteric bacteria, lipopolysaccharides and related cytokines in inflammatory bowel disease: biological and clinical significance. Journal of endotoxin research *6*, 205-214.

Carchman, E.H., Whelan, S., Loughran, P., Mollen, K., Stratamirovic, S., Shiva, S., Rosengart, M.R., and Zuckerbraun, B.S. (2013). Experimental sepsis-induced mitochondrial biogenesis is dependent on autophagy, TLR4, and TLR9 signaling in liver. The FASEB Journal *27*, 4703-4711.

Carré, J.E., Orban, J.-C., Re, L., Felsmann, K., Iffert, W., Bauer, M., Suliman, H.B., Piantadosi, C.A., Mayhew, T.M., and Breen, P. (2010). Survival in critical illness is associated with early activation of mitochondrial biogenesis. American journal of respiratory and critical care medicine *182*, 745-751.

Case, C.L., Kohler, L.J., Lima, J.B., Strowig, T., De Zoete, M.R., Flavell, R.A., Zamboni, D.S., and Roy, C.R. (2013). Caspase-11 stimulates rapid flagellin-independent pyroptosis in response to Legionella pneumophila. Proceedings of the National Academy of Sciences *110*, 1851-1856.

Cassidy-Stone, A., Chipuk, J.E., Ingerman, E., Song, C., Yoo, C., Kuwana, T., Kurth, M.J., Shaw, J.T., Hinshaw, J.E., Green, D.R.*, et al.* (2008). Chemical inhibition of the mitochondrial division dynamin reveals its role in Bax/Bak-dependent mitochondrial outer membrane permeabilization. Developmental cell *14*, 193-204.

Cereghetti, G.M., and Scorrano, L. (2006). The many shapes of mitochondrial death. Oncogene *25*, 4717-4724.

Chamaillard, M., Hashimoto, M., Horie, Y., Masumoto, J., Qiu, S., Saab, L., Ogura, Y., Kawasaki, A., Fukase, K., Kusumoto, S*., et al.* (2003). An essential role for NOD1 in host recognition of bacterial peptidoglycan containing diaminopimelic acid. Nat Immunol *4*, 702-707.

Chan, N.C., Salazar, A.M., Pham, A.H., Sweredoski, M.J., Kolawa, N.J., Graham, R.L., Hess, S., and Chan, D.C. (2011). Broad activation of the ubiquitin-proteasome system by Parkin is critical for mitophagy. Human molecular genetics *20*, 1726-1737.

Chang, L., and Karin, M. (2001). Mammalian MAP kinase signalling cascades. Nature *410*, 37-40.

Chen, G.Y., and Nuñez, G. (2010a). Sterile inflammation: sensing and reacting to damage. Nat Rev Immunol *10*, 826-837.

Chen, G.Y., and Nuñez, G. (2010b). Sterile inflammation: sensing and reacting to damage. Nature Reviews Immunology *10*, 826-837.

Chen, H., Chomyn, A., and Chan, D.C. (2005). Disruption of fusion results in mitochondrial heterogeneity and dysfunction. The Journal of biological chemistry *280*, 26185-26192.

Chen, H., Detmer, S.A., Ewald, A.J., Griffin, E.E., Fraser, S.E., and Chan, D.C. (2003). Mitofusins Mfn1 and Mfn2 coordinately regulate mitochondrial fusion and are essential for embryonic development. The Journal of cell biology *160*, 189-200.

Chen, P., Stanojcic, M., and Jeschke, M.G. (2014). Differences between murine and human sepsis. Surgical Clinics of North America *94*, 1135-1149.

Chen, Y., and Dorn, G.W., 2nd (2013). PINK1-phosphorylated mitofusin 2 is a Parkin receptor for culling damaged mitochondria. Science *340*, 471-475.

Chow, J.C., Young, D.W., Golenbock, D.T., Christ, W.J., and Gusovsky, F. (1999). Toll-like receptor-4 mediates lipopolysaccharide-induced signal transduction. The Journal of biological chemistry *274*, 10689-10692.

Cipolat, S., de Brito, O.M., Dal Zilio, B., and Scorrano, L. (2004). OPA1 requires mitofusin 1 to promote mitochondrial fusion. Proceedings of the National Academy of Sciences of the United States of America *101*, 15927-15932.

Cipolat, S., Rudka, T., Hartmann, D., Costa, V., Serneels, L., Craessaerts, K., Metzger, K., Frezza, C., Annaert, W., D'Adamio, L*., et al.* Mitochondrial Rhomboid PARL Regulates Cytochrome c Release during Apoptosis via OPA1-Dependent Cristae Remodeling. Cell *126*, 163-175.

Collins, L.V., Hajizadeh, S., Holme, E., Jonsson, I.M., and Tarkowski, A. (2004). Endogenously oxidized mitochondrial DNA induces in vivo and in vitro inflammatory responses. Journal of leukocyte biology *75*, 995-1000.

Corcoran, S.E., and O'Neill, L.A.J. (2016). HIF1α and metabolic reprogramming in inflammation. The Journal of Clinical Investigation *126*, 3699-3707.

Corraliza, I.M., Soler, G., Eichmann, K., and Modolell, M. (1995). Arginase induction by suppressors of nitric oxide synthesis (IL-4, IL-10 and PGE2) in murine bone-marrow-derived macrophages. Biochemical and biophysical research communications *206*, 667-673.

Crompton, M. (1999). The mitochondrial permeability transition pore and its role in cell death. Biochemical Journal *341*, 233-249.

da Silva Correia, J., Soldau, K., Christen, U., Tobias, P.S., and Ulevitch, R.J. (2001). Lipopolysaccharide is in close proximity to each of the proteins in its membrane receptor complex. transfer from CD14 to TLR4 and MD-2. The Journal of biological chemistry *276*, 21129-21135.

Dagda, R.K., Cherra, S.J., Kulich, S.M., Tandon, A., Park, D., and Chu, C.T. (2009). Loss of PINK1 Function Promotes Mitophagy through Effects on Oxidative Stress and Mitochondrial Fission. The Journal of biological chemistry *284*, 13843-13855.

Danial, N.N., and Korsmeyer, S.J. (2004). Cell death: critical control points. Cell *116*, 205-219.

Darnell, J., Kerr, I., and Stark, G. (1994). Jak-STAT pathways and transcriptional activation in response to IFNs and other extracellular signaling proteins. Science *264*, 1415-1421.

Darnell, J.E., Jr. (1997). STATs and gene regulation. Science *277*, 1630-1635.

Deas, E., Plun-Favreau, H., Gandhi, S., Desmond, H., Kjaer, S., Loh, S.H., Renton, A.E., Harvey, R.J., Whitworth, A.J., Martins, L.M.*, et al.* (2011). PINK1 cleavage at position A103 by the mitochondrial protease PARL. Human molecular genetics *20*, 867-879.

Deb, D.K., Sassano, A., Lekmine, F., Majchrzak, B., Verma, A., Kambhampati, S., Uddin, S., Rahman, A., Fish, E.N., and Platanias, L.C. (2003). Activation of protein kinase C delta by IFN-gamma. Journal of immunology (Baltimore, Md : 1950) *171*, 267-273.

Delettre, C., Griffoin, J.M., Kaplan, J., Dollfus, H., Lorenz, B., Faivre, L., Lenaers, G., Belenguer, P., and Hamel, C.P. (2001). Mutation spectrum and splicing variants in the OPA1 gene. Human genetics *109*, 584-591.

Delettre, C., Lenaers, G., Griffoin, J.M., Gigarel, N., Lorenzo, C., Belenguer, P., Pelloquin, L., Grosgeorge, J., Turc-Carel, C., Perret, E.*, et al.* (2000). Nuclear gene OPA1, encoding a mitochondrial dynamin-related protein, is mutated in dominant optic atrophy. Nature genetics *26*, 207-210.

Delgado, M.A., Elmaoued, R.A., Davis, A.S., Kyei, G., and Deretic, V. (2008). Toll-like receptors control autophagy. The EMBO journal *27*, 1110-1121.

Di Meo, S., Reed, T.T., Venditti, P., and Victor, V.M. (2016). Role of ROS and RNS Sources in Physiological and Pathological Conditions. Oxidative Medicine and Cellular Longevity *2016*, 1245049.

Dodson, M.W., and Guo, M. (2007). Pink1, Parkin, DJ-1 and mitochondrial dysfunction in Parkinson's disease. Current opinion in neurobiology *17*, 331-337.

Dominy, J.E., and Puigserver, P. (2013). Mitochondrial Biogenesis through Activation of Nuclear Signaling Proteins. Cold Spring Harbor Perspectives in Biology *5*, a015008.

Drose, S., and Brandt, U. (2012). Molecular mechanisms of superoxide production by the mitochondrial respiratory chain. Advances in experimental medicine and biology *748*, 145-169.

Erridge, C. (2010). Endogenous ligands of TLR2 and TLR4: agonists or assistants? Journal of leukocyte biology *87*, 989-999.

Exner, N., Lutz, A.K., Haass, C., and Winklhofer, K.F. (2012). Mitochondrial dysfunction in Parkinson's disease: molecular mechanisms and pathophysiological consequences. The EMBO journal *31*, 3038-3062.

Faustin, B., Lartigue, L., Bruey, J.M., Luciano, F., Sergienko, E., Bailly-Maitre, B., Volkmann, N., Hanein, D., Rouiller, I., and Reed, J.C. (2007). Reconstituted NALP1 inflammasome reveals two-step mechanism of caspase-1 activation. Molecular cell *25*, 713-724.

Fedorowicz, M.A., de Vries-Schneider, R.L., Rub, C., Becker, D., Huang, Y., Zhou, C., Alessi Wolken, D.M., Voos, W., Liu, Y., and Przedborski, S. (2014). Cytosolic cleaved PINK1 represses Parkin translocation to mitochondria and mitophagy. EMBO reports *15*, 86-93.

Fink, M.P., and Heard, S.O. (1990). Laboratory models of sepsis and septic shock. Journal of Surgical Research *49*, 186-196.

Fink, M.P., Morrissey, P.E., Stein, K.L., Clement, R.E., Fiallo, V., and Gardiner, W.M. (1988). Systemic and regional hemodynamic effects of cyclo-oxygenase and thromboxane synthetase inhibition in normal and hyperdynamic endotoxemic rabbits. Circulatory shock *26*, 41-57.

Fish, R.E., and Spitzer, J.A. (1984). Continuous infusion of endotoxin from an osmotic pump in the conscious, unrestrained rat: a unique model of chronic endotoxemia. Circulatory shock *12*, 135-149.

Fitzgerald, K.A., McWhirter, S.M., Faia, K.L., Rowe, D.C., Latz, E., Golenbock, D.T., Coyle, A.J., Liao, S.M., and Maniatis, T. (2003). IKKepsilon and TBK1 are essential components of the IRF3 signaling pathway. Nat Immunol *4*, 491-496.

Fox, E.S., Brower, J.S., Bellezzo, J.M., and Leingang, K.A. (1997). N-acetylcysteine and alpha-tocopherol reverse the inflammatory response in activated rat Kupffer cells. Journal of immunology (Baltimore, Md : 1950) *158*, 5418-5423.

Galanos, C., and Freudenberg, M.A. (1993). Mechanisms of endotoxin shock and endotoxin hypersensitivity. Immunobiology *187*, 346-356.

Galván-Peña, S., and O'Neill, L.A.J. (2014). Metabolic Reprograming in Macrophage Polarization. Frontiers in immunology *5*, 420.

Garaude, J., Acin-Perez, R., Martinez-Cano, S., Enamorado, M., Ugolini, M., Nistal-Villan, E., Hervas-Stubbs, S., and Pelegrin, P. (2016). Mitochondrial respiratory-chain adaptations in macrophages contribute to antibacterial host defense. *17*, 1037-1045.

Garrabou, G., Moren, C., Lopez, S., Tobias, E., Cardellach, F., Miro, O., and Casademont, J. (2012). The effects of sepsis on mitochondria. The Journal of infectious diseases *205*, 392-400.

Gegg, M.E., Cooper, J.M., Chau, K.Y., Rojo, M., Schapira, A.H., and Taanman, J.W. (2010). Mitofusin 1 and mitofusin 2 are ubiquitinated in a PINK1/parkin-dependent manner upon induction of mitophagy. Human molecular genetics *19*, 4861-4870.

Geisler, S., Holmstrom, K.M., Skujat, D., Fiesel, F.C., Rothfuss, O.C., Kahle, P.J., and Springer, W. (2010). PINK1/Parkin-mediated mitophagy is dependent on VDAC1 and p62/SQSTM1. Nature cell biology *12*, 119-131.

Geissmann, F., Manz, M.G., Jung, S., Sieweke, M.H., Merad, M., and Ley, K. (2010). Development of monocytes, macrophages, and dendritic cells. Science *327*, 656-661.

Georgakopoulos, N.D., Wells, G., and Campanella, M. (2017). The pharmacological regulation of cellular mitophagy. Nature Chemical Biology *13*, 136-146.

Giaime, E., Yamaguchi, H., Gautier, C.A., Kitada, T., and Shen, J. (2012). Loss of DJ-1 Does Not Affect Mitochondrial Respiration but Increases ROS Production and Mitochondrial Permeability Transition Pore Opening. PloS one *7*, e40501.

Girardin, S.E., Boneca, I.G., Carneiro, L.A.M., Antignac, A., Jéhanno, M., Viala, J., Tedin, K., Taha, M.-K., Labigne, A., Zäthringer, U.*, et al.* (2003). Nod1 Detects a Unique Muropeptide from Gram-Negative Bacterial Peptidoglycan. Science *300*, 1584-1587.

Gitlin, L., Barchet, W., Gilfillan, S., Cella, M., Beutler, B., Flavell, R.A., Diamond, M.S., and Colonna, M. (2006). Essential role of mda-5 in type I IFN responses to polyriboinosinic:polyribocytidylic acid and encephalomyocarditis picornavirus. Proceedings of the National Academy of Sciences of the United States of America *103*, 8459-8464.

Glauser, L., Sonnay, S., Stafa, K., and Moore, D.J. (2011). Parkin promotes the ubiquitination and degradation of the mitochondrial fusion factor mitofusin 1. Journal of neurochemistry *118*, 636-645.

Glick, D., Barth, S., and Macleod, K.F. (2010). Autophagy: cellular and molecular mechanisms. The Journal of pathology *221*, 3-12.

Gohda, J., Matsumura, T., and Inoue, J. (2004). Cutting edge: TNFR-associated factor (TRAF) 6 is essential for MyD88-dependent pathway but not toll/IL-1 receptor domain-containing adaptor-inducing IFN-beta (TRIF)-dependent pathway in TLR signaling. Journal of immunology (Baltimore, Md : 1950) *173*, 2913-2917.

Gomes, L.C., Benedetto, G.D., and Scorrano, L. (2011). During autophagy mitochondria elongate, are spared from degradation and sustain cell viability. Nature cell biology *13*, 589-598.

Gordon, S., and Taylor, P.R. (2005). Monocyte and macrophage heterogeneity. Nat Rev Immunol *5*, 953-964.

Gough, D.J., Levy, D.E., Johnstone, R.W., and Clarke, C.J. (2008). IFNγ signaling—Does it mean JAK–STAT? Cytokine & growth factor reviews *19*, 383-394.

Greene, A.W., Grenier, K., Aguileta, M.A., Muise, S., Farazifard, R., Haque, M.E., McBride, H.M., Park, D.S., and Fon, E.A. (2012). Mitochondrial processing peptidase regulates PINK1 processing, import and Parkin recruitment. EMBO reports *13*, 378-385.

Greenfield, L.J., Jackson, R.H., Elkins, R.C., Coalson, J.J., and Hinshaw, L.B. (1974). Cardiopulmonary effects of volume loading of primates in endotoxin shock (DTIC Document).

Guo, B., and Cheng, G. (2007). Modulation of the interferon antiviral response by the TBK1/IKKi adaptor protein TANK. The Journal of biological chemistry *282*, 11817-11826.

Guo, S., Al-Sadi, R., Said, H.M., and Ma, T.Y. (2013). Lipopolysaccharide Causes an Increase in Intestinal Tight Junction Permeability in Vitro and in Vivo by Inducing Enterocyte Membrane Expression and Localization of TLR-4 and CD14. The American Journal of Pathology *182*, 375-387.

Guo, S., Nighot, M., Al-Sadi, R., Alhmoud, T., Nighot, P., and Ma, T.Y. (2015). Lipopolysaccharide Regulation of Intestinal Tight Junction Permeability Is Mediated by TLR4 Signal Transduction Pathway Activation of FAK and MyD88. Journal of immunology (Baltimore, Md : 1950) *195*, 4999-5010.

Hagar, J.A., Powell, D.A., Aachoui, Y., Ernst, R.K., and Miao, E.A. (2013). Cytoplasmic LPS activates caspase-11: implications in TLR4-independent endotoxic shock. Science *341*, 1250-1253.

Hales, K.G., and Fuller, M.T. (1997). Developmentally regulated mitochondrial fusion mediated by a conserved, novel, predicted GTPase. Cell *90*, 121-129.

Halestrap, A.P., and Brenner, C. (2003). The adenine nucleotide translocase: a central component of the mitochondrial permeability transition pore and key player in cell death. Current medicinal chemistry *10*, 1507-1525.

Halle, A., Hornung, V., Petzold, G.C., Stewart, C.R., Monks, B.G., Reinheckel, T., Fitzgerald, K.A., Latz, E., Moore, K.J., and Golenbock, D.T. (2008). The NALP3 inflammasome is involved in the innate immune response to amyloid-beta. Nat Immunol *9*, 857-865.

Hardie, D.G. (2007). AMP-activated/SNF1 protein kinases: conserved guardians of cellular energy. Nature reviews Molecular cell biology *8*, 774-785.

Haschemi, A., Kosma, P., Gille, L., Evans, C.R., Burant, C.F., Starkl, P., Knapp, B., Haas, R., Schmid, J.A., Jandl, C., *et al.* (2012). The sedoheptulose kinase CARKL directs macrophage polarization through control of glucose metabolism. Cell metabolism *15*, 813-826.

Hattori, N., and Mizuno, Y. (2004). Pathogenetic mechanisms of parkin in Parkinson's disease. Lancet (London, England) *364*, 722-724.

He, Y., Hara, H., and Núñez, G. (2016). Mechanism and Regulation of NLRP3 Inflammasome Activation. Trends in biochemical sciences *41*, 1012-1021.

Hellman, J., Loiselle, P.M., Tehan, M.M., Allaire, J.E., Boyle, L.A., Kurnick, J.T., Andrews, D.M., Sik Kim, K., and Warren, H.S. (2000). Outer Membrane Protein A, Peptidoglycan-Associated Lipoprotein, and Murein Lipoprotein Are Released by Escherichia coli Bacteria into Serum. Infection and Immunity *68*, 2566-2572.

Hemmi, H., Takeuchi, O., Sato, S., Yamamoto, M., Kaisho, T., Sanjo, H., Kawai, T., Hoshino, K., Takeda, K., and Akira, S. (2004). The roles of two IkappaB kinase-related kinases in lipopolysaccharide and double stranded RNA signaling and viral infection. J Exp Med *199*, 1641-1650.

Herzig, D., Fang, G., Toliver-Kinsky, T.E., Guo, Y., Bohannon, J., and Sherwood, E.R. (2012). STAT1-deficient Mice are Resistant to CLP-induced Septic Shock. Shock (Augusta, Ga) *38*, 395-402.

Hoppins, S., Lackner, L., and Nunnari, J. (2007). The machines that divide and fuse mitochondria. Annu Rev Biochem *76*, 751-780.

Horner, S.M., Liu, H.M., Park, H.S., Briley, J., and Gale, M. (2011). Mitochondrial-associated endoplasmic reticulum membranes (MAM) form innate immune synapses and are targeted by hepatitis C virus. Proceedings of the National Academy of Sciences of the United States of America *108*, 14590-14595.

Hu, X., Chakravarty, S.D., and Ivashkiv, L.B. (2008). Regulation of IFN and TLR Signaling During Macrophage Activation by Opposing Feedforward and Feedback Inhibition Mechanisms. Immunological reviews *226*, 41-56.

Hu, X., Herrero, C., Li, W.-P., Antoniv, T.T., Falck-Pedersen, E., Koch, A.E., Woods, J.M., Haines, G.K., and Ivashkiv, L.B. (2002). Sensitization of IFN-[gamma] Jak-STAT signaling during macrophage activation. Nat Immunol *3*, 859-866.

Huang, S.C., Everts, B., Ivanova, Y., O'Sullivan, D., Nascimento, M., Smith, A.M., Beatty, W., Love-Gregory, L., Lam, W.Y., O'Neill, C.M.*, et al.* (2014). Cell-intrinsic lysosomal lipolysis is essential for alternative activation of macrophages. Nat Immunol *15*, 846-855.

Hunter, R.L., Cheng, B., Choi, D.Y., Liu, M., Liu, S., Cass, W.A., and Bing, G. (2009). Intrastriatal lipopolysaccharide injection induces parkinsonism in C57/B6 mice. Journal of neuroscience research *87*, 1913-1921.

Igarashi, K., Garotta, G., Ozmen, L., Ziemiecki, A., Wilks, A.F., Harpur, A.G., Larner, A.C., and Finbloom, D.S. (1994). Interferon-gamma induces tyrosine phosphorylation of interferon-gamma receptor and regulated association of protein tyrosine kinases, Jak1 and Jak2, with its receptor. The Journal of biological chemistry *269*, 14333-14336.

Ingersoll, M.A., Platt, A.M., Potteaux, S., and Randolph, G.J. (2011). Monocyte trafficking in acute and chronic inflammation. Trends in immunology *32*, 470-477.

Irrcher, I., Aleyasin, H., Seifert, E., Hewitt, S., Chhabra, S., Phillips, M., Lutz, A., Rousseaux, M., Bevilacqua, L., and Jahani-Asl, A. (2010). Loss of the Parkinson's disease-linked gene DJ-1 perturbs mitochondrial dynamics. Human molecular genetics *19*, 3734-3746.

Ishihara, N., Fujita, Y., Oka, T., and Mihara, K. (2006). Regulation of mitochondrial morphology through proteolytic cleavage of OPA1. The EMBO journal *25*, 2966-2977.

Ivaska, J., Bosca, L., and Parker, P.J. (2003). PKCepsilon is a permissive link in integrin-dependent IFN-gamma signalling that facilitates JAK phosphorylation of STAT1. Nature cell biology *5*, 363-369.

Jacobson, J., and Duchen, M.R. (2004). Interplay between mitochondria and cellular calcium signalling. Molecular and cellular biochemistry *256-257*, 209-218.

Jacquel, A., Obba, S., Boyer, L., Dufies, M., Robert, G., Gounon, P., Lemichez, E., Luciano, F., Solary, E., and Auberger, P. (2012). Autophagy is required for CSF-1–induced macrophagic differentiation and acquisition of phagocytic functions. Blood *119*, 4527-4531.

Jager, S., Handschin, C., St-Pierre, J., and Spiegelman, B.M. (2007). AMP-activated protein kinase (AMPK) action in skeletal muscle via direct phosphorylation of PGC-1alpha. Proceedings of the National Academy of Sciences of the United States of America *104*, 12017-12022.

Jankovic, J. (2008). Parkinson's disease: clinical features and diagnosis. Journal of neurology, neurosurgery, and psychiatry *79*, 368-376.

Janssen, A.J., Trijbels, F.J., Sengers, R.C., Smeitink, J.A., van den Heuvel, L.P., Wintjes, L.T., Stoltenborg-Hogenkamp, B.J., and Rodenburg, R.J. (2007). Spectrophotometric assay for complex

I of the respiratory chain in tissue samples and cultured fibroblasts. Clinical chemistry *53*, 729-734.

Japiassu, A.M., Santiago, A.P., d'Avila, J.C., Garcia-Souza, L.F., Galina, A., Castro Faria-Neto, H.C., Bozza, F.A., and Oliveira, M.F. (2011). Bioenergetic failure of human peripheral blood monocytes in patients with septic shock is mediated by reduced F1Fo adenosine-5'-triphosphate synthase activity. Crit Care Med *39*, 1056-1063.

Jin, S.M., Lazarou, M., Wang, C., Kane, L.A., Narendra, D.P., and Youle, R.J. (2010). Mitochondrial membrane potential regulates PINK1 import and proteolytic destabilization by PARL. The Journal of cell biology *191*, 933-942.

Jin, Z., Wei, W., Yang, M., Du, Y., and Wan, Y. (2014). Mitochondrial complex I activity suppresses inflammation and enhances bone resorption by shifting macrophage-osteoclast polarization. Cell metabolism *20*, 483-498.

John, G.B., Shang, Y., Li, L., Renken, C., Mannella, C.A., Selker, J.M.L., Rangell, L., Bennett, M.J., and Zha, J. (2005). The Mitochondrial Inner Membrane Protein Mitofilin Controls Cristae Morphology. Molecular Biology of the Cell *16*, 1543-1554.

Joselin, A.P., Hewitt, S.J., Callaghan, S.M., Kim, R.H., Chung, Y.H., Mak, T.W., Shen, J., Slack, R.S., and Park, D.S. (2012). ROS-dependent regulation of Parkin and DJ-1 localization during oxidative stress in neurons. Human molecular genetics *21*, 4888-4903.

Kahns, S., Kalai, M., Jakobsen, L.D., Clark, B.F., Vandenabeele, P., and Jensen, P.H. (2003). Caspase-1 and caspase-8 cleave and inactivate cellular parkin. Journal of Biological Chemistry *278*, 23376-23380.

Kamezaki, K., Shimoda, K., Numata, A., Matsuda, T., Nakayama, K., and Harada, M. (2004). The role of Tyk2, Stat1 and Stat4 in LPS-induced endotoxin signals. International immunology *16*, 1173-1179.

Kang, R., Zeng, L., Xie, Y., Yan, Z., Zhou, B., Cao, L., Klionsky, D.J., Tracey, K.J., Li, J., and Wang, H. (2016). A novel PINK1-and PARK2-dependent protective neuroimmune pathway in lethal sepsis. Autophagy, 1-12.

Kanki, T., Kurihara, Y., Jin, X., Goda, T., Ono, Y., Aihara, M., Hirota, Y., Saigusa, T., Aoki, Y., Uchiumi, T., *et al.* (2013). Casein kinase 2 is essential for mitophagy. EMBO reports *14*, 788-794.

Kanki, T., Wang, K., Cao, Y., Baba, M., and Klionsky, D.J. (2009). Atg32 is a mitochondrial protein that confers selectivity during mitophagy. Developmental cell *17*, 98-109.

Kasahara, E., Sekiyama, A., Hori, M., Hara, K., Takahashi, N., Konishi, M., Sato, E.F., Matsumoto, S., Okamura, H., and Inoue, M. (2011). Mitochondrial density contributes to the immune response of macrophages to lipopolysaccharide via the MAPK pathway. FEBS letters *585*, 2263-2268.

Katayama, H., Kogure, T., Mizushima, N., Yoshimori, T., and Miyawaki, A. (2011). A sensitive and quantitative technique for detecting autophagic events based on lysosomal delivery. Chemistry & biology *18*, 1042-1052.

Kato, H., Takeuchi, O., Mikamo-Satoh, E., Hirai, R., Kawai, T., Matsushita, K., Hiiragi, A., Dermody, T.S., Fujita, T., and Akira, S. (2008). Length-dependent recognition of double-stranded ribonucleic acids by retinoic acid-inducible gene-I and melanoma differentiation-associated gene 5. J Exp Med *205*, 1601-1610.

Kato, H., Takeuchi, O., Sato, S., Yoneyama, M., Yamamoto, M., Matsui, K., Uematsu, S., Jung, A., Kawai, T., Ishii, K.J.*, et al.* (2006). Differential roles of MDA5 and RIG-I helicases in the recognition of RNA viruses. Nature *441*, 101-105.

Kawai, T., Adachi, O., Ogawa, T., Takeda, K., and Akira, S. (1999). Unresponsiveness of MyD88-deficient mice to endotoxin. Immunity *11*, 115-122.

Kawai, T., and Akira, S. (2010). The role of pattern-recognition receptors in innate immunity: update on Toll-like receptors. Nat Immunol *11*, 373-384.

Kayagaki, N., Stowe, I.B., Lee, B.L., O/'Rourke, K., Anderson, K., Warming, S., Cuellar, T., Haley, B., Roose-Girma, M., Phung, Q.T.*, et al.* (2015). Caspase-11 cleaves gasdermin D for non-canonical inflammasome signalling. Nature *526*, 666-671.

Kayagaki, N., Warming, S., Lamkanfi, M., Walle, L.V., Louie, S., Dong, J., Newton, K., Qu, Y., Liu, J., and Heldens, S. (2011). Non-canonical inflammasome activation targets caspase-11. Nature *479*, 117-121.

Kayagaki, N., Wong, M.T., Stowe, I.B., Ramani, S.R., Gonzalez, L.C., Akashi-Takamura, S., Miyake, K., Zhang, J., Lee, W.P., and Muszyński, A. (2013). Noncanonical inflammasome activation by intracellular LPS independent of TLR4. Science *341*, 1246-1249.

Kazlauskaite, A., Kondapalli, C., Gourlay, R., Campbell, D.G., Ritorto, M.S., Hofmann, K., Alessi, D.R., Knebel, A., Trost, M., and Muqit, M.M. (2014). Parkin is activated by PINK1-dependent phosphorylation of ubiquitin at Ser65. The Biochemical journal *460*, 127-139.

Kelly, B., Tannahill, G.M., Murphy, M.P., and O'Neill, L.A. (2015). Metformin Inhibits the Production of Reactive Oxygen Species from NADH:Ubiquinone Oxidoreductase to Limit Induction of Interleukin-1beta (IL-1beta) and Boosts Interleukin-10 (IL-10) in Lipopolysaccharide (LPS)-activated Macrophages. The Journal of biological chemistry *290*, 20348-20359.

Kim, J., Byun, J.W., Choi, I., Kim, B., Jeong, H.K., Jou, I., and Joe, E. (2013). PINK1 Deficiency Enhances Inflammatory Cytokine Release from Acutely Prepared Brain Slices. Experimental neurobiology *22*, 38-44.

Kim, P.K., Hailey, D.W., Mullen, R.T., and Lippincott-Schwartz, J. (2008). Ubiquitin signals autophagic degradation of cytosolic proteins and peroxisomes. Proceedings of the National Academy of Sciences of the United States of America *105*, 20567-20574.

Kitada, T., Asakawa, S., Hattori, N., Matsumine, H., Yamamura, Y., Minoshima, S., Yokochi, M., Mizuno, Y., and Shimizu, N. (1998). Mutations in the parkin gene cause autosomal recessive juvenile parkinsonism. Nature *392*, 605-608.

Komatsu, M., and Ichimura, Y. (2010). Selective autophagy regulates various cellular functions. Genes to cells : devoted to molecular & cellular mechanisms *15*, 923-933.

Komatsu, M., Ueno, T., Waguri, S., Uchiyama, Y., Kominami, E., and Tanaka, K. (2007). Constitutive autophagy: vital role in clearance of unfavorable proteins in neurons. Cell death and differentiation *14*, 887-894.

Kondapalli, C., Kazlauskaite, A., Zhang, N., Woodroof, H.I., Campbell, D.G., Gourlay, R., Burchell, L., Walden, H., Macartney, T.J., Deak, M.*, et al.* (2012). PINK1 is activated by mitochondrial membrane potential depolarization and stimulates Parkin E3 ligase activity by phosphorylating Serine 65. Open biology *2*, 120080.

Kong, D., Park, E.J., Stephen, A.G., Calvani, M., Cardellina, J.H., Monks, A., Fisher, R.J., Shoemaker, R.H., and Melillo, G. (2005). Echinomycin, a small-molecule inhibitor of hypoxia-inducible factor-1 DNA-binding activity. Cancer research *65*, 9047-9055.

Koopman, W.J., Nijtmans, L.G., Dieteren, C.E., Roestenberg, P., Valsecchi, F., Smeitink, J.A., and Willems, P.H. (2010). Mammalian mitochondrial complex I: biogenesis, regulation, and reactive oxygen species generation. Antioxidants & redox signaling *12*, 1431-1470.

Kotas, M.E., and Medzhitov, R. (2015). Homeostasis, inflammation, and disease susceptibility. Cell *160*, 816-827.

Kubli, D.A., and Gustafsson, Å.B. (2012). Mitochondria and mitophagy the yin and yang of cell death control. Circulation research *111*, 1208-1221.

Kuma, A., Hatano, M., Matsui, M., Yamamoto, A., Nakaya, H., Yoshimori, T., Ohsumi, Y., Tokuhisa, T., and Mizushima, N. (2004). The role of autophagy during the early neonatal starvation period. Nature *432*, 1032-1036.

Kumar, H., Kawai, T., and Akira, S. (2009). Pathogen recognition in the innate immune response. The Biochemical journal *420*, 1-16.

Labrousse, A.M., Zappaterra, M.D., Rube, D.A., and van der Bliek, A.M. (1999). C. elegans dynamin-related protein DRP-1 controls severing of the mitochondrial outer membrane. Molecular cell *4*, 815-826.

Law, W.R., and Ferguson, J.L. (1988). Naloxone alters organ perfusion during endotoxin shock in conscious rats. American Journal of Physiology - Heart and Circulatory Physiology *255*, H1106-H1113.

Lazarou, M., Jin, S.M., Kane, L.A., and Youle, R.J. (2012). Role of PINK1 binding to the TOM complex and alternate intracellular membranes in recruitment and activation of the E3 ligase Parkin. Developmental cell *22*, 320-333.

Lazarou, M., Sliter, D.A., Kane, L.A., Sarraf, S.A., Wang, C., Burman, J.L., Sideris, D.P., Fogel, A.I., and Youle, R.J. (2015). The ubiquitin kinase PINK1 recruits autophagy receptors to induce mitophagy. Nature *524*, 309-314.

Lee, G., Won, H.-S., Lee, Y.-M., Choi, J.-W., Oh, T.-I., Jang, J.-H., Choi, D.-K., Lim, B.-O., Kim, Y.J., Park, J.-W.*, et al.* (2016). Oxidative Dimerization of PHD2 is Responsible for its Inactivation and Contributes to Metabolic Reprogramming via HIF-1α Activation. Scientific Reports *6*, 18928.

Legros, F., Lombès, A., Frachon, P., and Rojo, M. (2002). Mitochondrial fusion in human cells is efficient, requires the inner membrane potential, and is mediated by mitofusins. Molecular biology of the cell *13*, 4343-4354.

Levine, B., and Kroemer, G. (2008). Autophagy in the pathogenesis of disease. Cell *132*, 27-42.

Levy, M.M., Fink, M.P., Marshall, J.C., Abraham, E., Angus, D., Cook, D., Cohen, J., Opal, S.M., Vincent, J.-L., and Ramsay, G. (2003). 2001 sccm/esicm/accp/ats/sis international sepsis definitions conference. Intensive care medicine *29*, 530-538.

Lin, W., and Kang, U.J. (2008). Characterization of PINK1 processing, stability, and subcellular localization. Journal of neurochemistry *106*, 464-474.

Lira, F.S., Rosa, J.C., Pimentel, G.D., Souza, H.A., Caperuto, E.C., Carnevali, L.C., Jr., Seelaender, M., Damaso, A.R., Oyama, L.M., de Mello, M.T.*, et al.* (2010). Endotoxin levels correlate positively with a sedentary lifestyle and negatively with highly trained subjects. Lipids in health and disease *9*, 82.

Liu, L., Feng, D., Chen, G., Chen, M., Zheng, Q., Song, P., Ma, Q., Zhu, C., Wang, R., Qi, W.*, et al.* (2012). Mitochondrial outer-membrane protein FUNDC1 mediates hypoxia-induced mitophagy in mammalian cells. Nature cell biology *14*, 177-185.

Lomaga, M.A., Yeh, W.C., Sarosi, I., Duncan, G.S., Furlonger, C., Ho, A., Morony, S., Capparelli, C., Van, G., Kaufman, S.*, et al.* (1999). TRAF6 deficiency results in osteopetrosis and defective interleukin-1, CD40, and LPS signaling. Genes & development *13*, 1015-1024.

Loo, Y.M., Fornek, J., Crochet, N., Bajwa, G., Perwitasari, O., Martinez-Sobrido, L., Akira, S., Gill, M.A., Garcia-Sastre, A., Katze, M.G.*, et al.* (2008). Distinct RIG-I and MDA5 signaling by RNA viruses in innate immunity. Journal of virology *82*, 335-345.

Lu, Y.C., Yeh, W.C., and Ohashi, P.S. (2008). LPS/TLR4 signal transduction pathway. Cytokine *42*, 145-151.

Lugtenberg, B., and Van Alphen, L. (1983). Molecular architecture and functioning of the outer membrane of Escherichia coli and other gram-negative bacteria. Biochimica et biophysica acta *737*, 51-115.

Lye, E., Mirtsos, C., Suzuki, N., Suzuki, S., and Yeh, W.C. (2004). The role of interleukin 1 receptor-associated kinase-4 (IRAK-4) kinase activity in IRAK-4-mediated signaling. The Journal of biological chemistry *279*, 40653-40658.

Macdonald, J., Galley, H.F., and Webster, N.R. (2003). Oxidative stress and gene expression in sepsis. British journal of anaesthesia *90*, 221-232.

MacMicking, J.D. (2004). IFN-inducible GTPases and immunity to intracellular pathogens. Trends in immunology *25*, 601-609.

Maier, S., Traeger, T., Entleutner, M., Westerholt, A., Kleist, B., Hüser, N., Holzmann, B., Stier, A., Pfeffer, K., and Heidecke, C.-D. (2004). Cecal ligation and puncture versus colon ascendens stent peritonitis: two distinct animal models for polymicrobial sepsis. Shock *21*, 505-512.

Mannam, P., Shinn, A.S., Srivastava, A., Neamu, R.F., Walker, W.E., Bohanon, M., Merkel, J., Kang, M.J., Dela Cruz, C.S., Ahasic, A.M*., et al.* (2014). MKK3 regulates mitochondrial biogenesis and mitophagy in sepsis-induced lung injury. American journal of physiology Lung cellular and molecular physiology *306*, L604-619.

Mantovani, A., Biswas, S.K., Galdiero, M.R., Sica, A., and Locati, M. (2013). Macrophage plasticity and polarization in tissue repair and remodelling. The Journal of pathology *229*, 176-185.

Mantovani, A., Sica, A., Sozzani, S., Allavena, P., Vecchi, A., and Locati, M. (2004). The chemokine system in diverse forms of macrophage activation and polarization. Trends in immunology *25*, 677-686.

Martinez, F.O., and Gordon, S. (2014). The M1 and M2 paradigm of macrophage activation: time for reassessment. F1000prime reports *6*, 13.

Martinon, F., Mayor, A., and Tschopp, J. (2009). The inflammasomes: guardians of the body. Annu Rev Immunol *27*, 229-265.

Martinon, F., Petrilli, V., Mayor, A., Tardivel, A., and Tschopp, J. (2006). Gout-associated uric acid crystals activate the NALP3 inflammasome. Nature *440*, 237-241.

Martinon, F., and Tschopp, J. (2004). Inflammatory caspases: linking an intracellular innate immune system to autoinflammatory diseases. Cell *117*, 561-574.

Matheoud, D., Sugiura, A., Bellemare-Pelletier, A., Laplante, A., Rondeau, C., Chemali, M., Fazel, A., Bergeron, J.J., Trudeau, L.E., Burelle, Y.*, et al.* (2016). Parkinson's Disease-Related Proteins PINK1 and Parkin Repress Mitochondrial Antigen Presentation. Cell *166*, 314-327.

Matsuda, N., Sato, S., Shiba, K., Okatsu, K., Saisho, K., Gautier, C.A., Sou, Y.S., Saiki, S., Kawajiri, S., Sato, F.*, et al.* (2010). PINK1 stabilized by mitochondrial depolarization recruits Parkin to damaged mitochondria and activates latent Parkin for mitophagy. The Journal of cell biology *189*, 211-221.

McCormick, J., Suleman, N., Scarabelli, T.M., Knight, R.A., Latchman, D.S., and Stephanou, A. (2012). STAT1 deficiency in the heart protects against myocardial infarction by enhancing autophagy. Journal of cellular and molecular medicine *16*, 386-393.

McGeer, P.L., and McGeer, E.G. (2004). Inflammation and neurodegeneration in Parkinson's disease. Parkinsonism & related disorders *10 Suppl 1*, S3-7.

McNab, F., Mayer-Barber, K., Sher, A., Wack, A., and O'Garra, A. (2015). Type I interferons in infectious disease. Nat Rev Immunol *15*, 87-103.

Medzhitov, R. (2008). Origin and physiological roles of inflammation. Nature *454*, 428-435.

Meeusen, S., McCaffery, J.M., and Nunnari, J. (2004). Mitochondrial fusion intermediates revealed in vitro. Science *305*, 1747-1752.

Mege, J.L., Mehraj, V., and Capo, C. (2011). Macrophage polarization and bacterial infections. Current opinion in infectious diseases *24*, 230-234.

Meissner, C., Lorenz, H., Weihofen, A., Selkoe, D.J., and Lemberg, M.K. (2011). The mitochondrial intramembrane protease PARL cleaves human Pink1 to regulate Pink1 trafficking. Journal of neurochemistry *117*, 856-867.

Meraz, M.A., White, J.M., Sheehan, K.C., Bach, E.A., Rodig, S.J., Dighe, A.S., Kaplan, D.H., Riley, J.K., Greenlund, A.C., Campbell, D.*, et al.* (1996). Targeted disruption of the Stat1 gene in mice reveals unexpected physiologic specificity in the JAK-STAT signaling pathway. Cell *84*, 431-442.

Merx, M.W., Liehn, E.A., Janssens, U., Lutticken, R., Schrader, J., Hanrath, P., and Weber, C. (2004). HMG-CoA reductase inhibitor simvastatin profoundly improves survival in a murine model of sepsis. Circulation *109*, 2560-2565.

Meunier, E., Dick, M.S., Dreier, R.F., Schurmann, N., Broz, D.K., Warming, S., Roose-Girma, M., Bumann, D., Kayagaki, N., Takeda, K*., et al.* (2014). Caspase-11 activation requires lysis of pathogen-containing vacuoles by IFN-induced GTPases. Nature *509*, 366-370.

Mills, E.L., Kelly, B., Logan, A., Costa, A.S., Varma, M., Bryant, C.E., Tourlomousis, P., Dabritz, J.H., Gottlieb, E., Latorre, I*., et al.* (2016). Succinate Dehydrogenase Supports Metabolic Repurposing of Mitochondria to Drive Inflammatory Macrophages. Cell *167*, 457-470.e413.

Mills, E.L., Kelly, B., and O'Neill, L.A.J. (2017). Mitochondria are the powerhouses of immunity. Nat Immunol *18*, 488-498.

Mizushima, N., Levine, B., Cuervo, A.M., and Klionsky, D.J. (2008). Autophagy fights disease through cellular self-digestion. Nature *451*, 1069-1075.

Mogensen, T.H. (2009). Pathogen recognition and inflammatory signaling in innate immune defenses. Clin Microbiol Rev *22*, 240-273, Table of Contents.

Morrison, D.C., and Ryan, J.L. (1987). Endotoxins and disease mechanisms. Annu Rev Med *38*, 417-432.

Munder, M., Eichmann, K., and Modolell, M. (1998). Alternative metabolic states in murine macrophages reflected by the nitric oxide synthase/arginase balance: competitive regulation by CD4+ T cells correlates with Th1/Th2 phenotype. Journal of immunology (Baltimore, Md : 1950) *160*, 5347-5354.

Murakawa, T., Yamaguchi, O., Hashimoto, A., Hikoso, S., Takeda, T., Oka, T., Yasui, H., Ueda, H., Akazawa, Y., Nakayama, H*., et al.* (2015). Bcl-2-like protein 13 is a mammalian Atg32 homologue that mediates mitophagy and mitochondrial fragmentation. Nature communications *6*, 7527.

Murray, P.J., and Wynn, T.A. (2011). Protective and pathogenic functions of macrophage subsets. Nat Rev Immunol *11*, 723-737.

Nagai, Y., Akashi, S., Nagafuku, M., Ogata, M., Iwakura, Y., Akira, S., Kitamura, T., Kosugi, A., Kimoto, M., and Miyake, K. (2002). Essential role of MD-2 in LPS responsiveness and TLR4 distribution. Nat Immunol *3*, 667-672.

Nakahira, K., and Choi, A.M.K. (2013). Autophagy: a potential therapeutic target in lung diseases. American Journal of Physiology - Lung Cellular and Molecular Physiology *305*, L93-L107.

Nakahira, K., Haspel, J.A., Rathinam, V.A., Lee, S.J., Dolinay, T., Lam, H.C., Englert, J.A., Rabinovitch, M., Cernadas, M., Kim, H.P., *et al.* (2011). Autophagy proteins regulate innate immune responses by inhibiting the release of mitochondrial DNA mediated by the NALP3 inflammasome. Nat Immunol *12*, 222-230.

Narendra, D., Tanaka, A., Suen, D.-F., and Youle, R.J. (2008). Parkin is recruited selectively to impaired mitochondria and promotes their autophagy. The Journal of cell biology *183*, 795-803.

Narendra, D.P., Jin, S.M., Tanaka, A., Suen, D.-F., Gautier, C.A., Shen, J., Cookson, M.R., and Youle, R.J. (2010). PINK1 Is Selectively Stabilized on Impaired Mitochondria to Activate Parkin. PLoS Biology *8*, e1000298.

Nathan, C.F., Murray, H.W., Wiebe, M.E., and Rubin, B.Y. (1983). Identification of interferon-gamma as the lymphokine that activates human macrophage oxidative metabolism and antimicrobial activity. J Exp Med *158*, 670-689.

Nathan, C.F., Prendergast, T.J., Wiebe, M.E., Stanley, E.R., Platzer, E., Remold, H.G., Welte, K., Rubin, B.Y., and Murray, H.W. (1984). Activation of human macrophages. Comparison of other cytokines with interferon-gamma. J Exp Med *160*, 600-605.

Nauseef, W.M. (2004). Assembly of the phagocyte NADPH oxidase. Histochemistry and cell biology *122*, 277-291.

Needham, B.D., and Trent, M.S. (2013). Fortifying the barrier: the impact of lipid A remodelling on bacterial pathogenesis. Nature reviews Microbiology *11*, 467-481.

Nguyen, T.N., Padman, B.S., and Lazarou, M. (2016). Deciphering the Molecular Signals of PINK1/Parkin Mitophagy. Trends in Cell Biology.

Novak, I., and Dikic, I. (2011). Autophagy receptors in developmental clearance of mitochondria. Autophagy *7*, 301-303.

Okamoto, K., Kondo-Okamoto, N., and Ohsumi, Y. (2009). Mitochondria-anchored receptor Atg32 mediates degradation of mitochondria via selective autophagy. Developmental cell *17*, 87-97.

Okatsu, K., Koyano, F., Kimura, M., Kosako, H., Saeki, Y., Tanaka, K., and Matsuda, N. (2015). Phosphorylated ubiquitin chain is the genuine Parkin receptor. The Journal of cell biology *209*, 111-128.

Okatsu, K., Oka, T., Iguchi, M., Imamura, K., Kosako, H., Tani, N., Kimura, M., Go, E., Koyano, F., Funayama, M*., et al.* (2012). PINK1 autophosphorylation upon membrane potential dissipation is essential for Parkin recruitment to damaged mitochondria. Nature communications *3*, 1016.

Olichon, A., Baricault, L., Gas, N., Guillou, E., Valette, A., Belenguer, P., and Lenaers, G. (2003). Loss of OPA1 perturbates the mitochondrial inner membrane structure and integrity, leading to cytochrome c release and apoptosis. The Journal of biological chemistry *278*, 7743-7746.

Opal, S.M., Garber, G.E., LaRosa, S.P., Maki, D.G., Freebairn, R.C., Kinasewitz, G.T., Dhainaut, J.F., Yan, S.B., Williams, M.D., Graham, D.E*., et al.* (2003). Systemic host responses in severe sepsis analyzed by causative microorganism and treatment effects of drotrecogin alfa (activated). Clinical infectious diseases : an official publication of the Infectious Diseases Society of America *37*, 50-58.

Ordureau, A., Sarraf, S.A., Duda, D.M., Heo, J.M., Jedrychowski, M.P., Sviderskiy, V.O., Olszewski, J.L., Koerber, J.T., Xie, T., Beausoleil, S.A*., et al.* (2014). Quantitative proteomics reveal a feedforward mechanism for mitochondrial PARKIN translocation and ubiquitin chain synthesis. Molecular cell *56*, 360-375.

Orvedahl, A., MacPherson, S., Sumpter, R., Jr., Talloczy, Z., Zou, Z., and Levine, B. (2010). Autophagy protects against Sindbis virus infection of the central nervous system. Cell Host Microbe *7*, 115-127.

Osellame, L.D., Blacker, T.S., and Duchen, M.R. (2012). Cellular and molecular mechanisms of mitochondrial function. Best Practice & Research Clinical Endocrinology & Metabolism *26*, 711-723.

Palikaras, K., and Tavernarakis, N. (2014). Mitochondrial homeostasis: the interplay between mitophagy and mitochondrial biogenesis. Experimental gerontology *56*, 182-188.

Pålsson-McDermott, E.M., and O'Neill, L.A.J. (2004). Signal transduction by the lipopolysaccharide receptor, Toll-like receptor-4. Immunology *113*, 153-162.

Pappova, E., Urbaschek, B., Heitmann, L., Oroz, M., Streit, E., Lemeunier, A., and Lundsgaard-Hansen, P. (1971). Energy-rich phosphates and glucose metabolism in early endotoxin shock. Journal of Surgical Research *11*, 506-512.

Parker, S.J., and Watkins, P.E. (2001). Experimental models of Gram-negative sepsis. British Journal of Surgery *88*, 22-30.

Parrillo, J.E., Parker, M.M., Natanson, C., Suffredini, A.F., Danner, R.L., Cunnion, R.E., and Ognibene, F.P. (1990). Septic shock in humans. Advances in the understanding of pathogenesis, cardiovascular dysfunction, and therapy. Annals of internal medicine *113*, 227-242.

Pestka, S., Kotenko, S.V., Muthukumaran, G., Izotova, L.S., Cook, J.R., and Garotta, G. (1997). The interferon gamma (IFN-γ) receptor: a paradigm for the multichain cytokine receptor. Cytokine & growth factor reviews *8*, 189-206.

Pestka, S., Krause, C.D., and Walter, M.R. (2004). Interferons, interferon-like cytokines, and their receptors. Immunological reviews *202*, 8-32.

Pilla, D.M., Hagar, J.A., Haldar, A.K., Mason, A.K., Degrandi, D., Pfeffer, K., Ernst, R.K., Yamamoto, M., Miao, E.A., and Coers, J. (2014). Guanylate binding proteins promote caspase-11-dependent pyroptosis in response to cytoplasmic LPS. Proceedings of the National Academy of Sciences of the United States of America *111*, 6046-6051.

Platanias, L.C. (2005). Mechanisms of type-I-and type-II-interferon-mediated signalling. Nature Reviews Immunology *5*, 375-386.

Platanias, L.C., and Fish, E.N. (1999). Signaling pathways activated by interferons. Experimental hematology *27*, 1583-1592.

Poeze, M., Ramsay, G., Gerlach, H., Rubulotta, F., and Levy, M. (2004). An international sepsis survey: a study of doctors' knowledge and perception about sepsis. Critical Care *8*, 1.

Poltorak, A., He, X., Smirnova, I., Liu, M.Y., Van Huffel, C., Du, X., Birdwell, D., Alejos, E., Silva, M., Galanos, C.*, et al.* (1998a). Defective LPS signaling in C3H/HeJ and C57BL/10ScCr mice: mutations in Tlr4 gene. Science *282*, 2085-2088.

Poltorak, A., Smirnova, I., He, X., Liu, M.Y., Van Huffel, C., McNally, O., Birdwell, D., Alejos, E., Silva, M., Du, X.*, et al.* (1998b). Genetic and physical mapping of the Lps locus: identification of the toll-4 receptor as a candidate gene in the critical region. Blood cells, molecules & diseases *24*, 340-355.

Poole, A.C., Thomas, R.E., Andrews, L.A., McBride, H.M., Whitworth, A.J., and Pallanck, L.J. (2008). The PINK1/Parkin pathway regulates mitochondrial morphology. Proceedings of the National Academy of Sciences of the United States of America *105*, 1638-1643.

Poole, A.C., Thomas, R.E., Yu, S., Vincow, E.S., and Pallanck, L. (2010). The mitochondrial fusion-promoting factor mitofusin is a substrate of the PINK1/parkin pathway. PloS one *5*, e10054.

Rabiet, M.J., Huet, E., and Boulay, F. (2007). The N-formyl peptide receptors and the anaphylatoxin C5a receptors: an overview. Biochimie *89*, 1089-1106.

Raetz, C.R. (1990). Biochemistry of endotoxins. Annual review of biochemistry *59*, 129-170.

Ramachandran, G. (2014). Gram-positive and gram-negative bacterial toxins in sepsis: a brief review. Virulence *5*, 213-218.

Rambold, A.S., Kostelecky, B., Elia, N., and Lippincott-Schwartz, J. (2011). Tubular network formation protects mitochondria from autophagosomal degradation during nutrient starvation. Proceedings of the National Academy of Sciences of the United States of America *108*, 10190-10195.

Ray, P.D., Huang, B.-W., and Tsuji, Y. (2012). Reactive oxygen species (ROS) homeostasis and redox regulation in cellular signaling. Cellular signalling *24*, 981-990.

Reid, D.M., Montoya, M., Taylor, P.R., Borrow, P., Gordon, S., Brown, G.D., and Wong, S.Y. (2004). Expression of the β-glucan receptor, Dectin-1, on murine leukocytes in situ correlates with its function in pathogen recognition and reveals potential roles in leukocyte interactions. Journal of leukocyte biology *76*, 86-94.

Remick, D.G., and Ward, P.A. (2005). Evaluation of endotoxin models for the study of sepsis. Shock *24*, 7-11.

REYNOLDS, D.G. (1972). Blood flow to the liver and spleen during endotoxin shock in the baboon. Surgery *72*, 388-394.

Rietschel, E.T., Kirikae, T., Schade, F.U., Mamat, U., Schmidt, G., Loppnow, H., Ulmer, A.J., Zahringer, U., Seydel, U., Di Padova, F.*, et al.* (1994). Bacterial endotoxin: molecular relationships of structure to activity and function. FASEB journal : official publication of the Federation of American Societies for Experimental Biology *8*, 217-225.

Rittirsch, D., Huber-Lang, M.S., Flierl, M.A., and Ward, P.A. (2008). Immunodesign of experimental sepsis by cecal ligation and puncture. Nat Protocols *4*, 31-36.

Rodriguez-Prados, J.C., Traves, P.G., Cuenca, J., Rico, D., Aragones, J., Martin-Sanz, P., Cascante, M., and Bosca, L. (2010). Substrate fate in activated macrophages: a comparison between innate, classic, and alternative activation. Journal of immunology (Baltimore, Md : 1950) *185*, 605-614.

Rogers, N.C., Slack, E.C., Edwards, A.D., Nolte, M.A., Schulz, O., Schweighoffer, E., Williams, D.L., Gordon, S., Tybulewicz, V.L., Brown, G.D.*, et al.* (2005). Syk-dependent cytokine induction by Dectin-1 reveals a novel pattern recognition pathway for C type lectins. Immunity *22*, 507-517.

Ross, R. (1999). Atherosclerosis--an inflammatory disease. The New England journal of medicine *340*, 115-126.

Rubartelli, A., Lotze, M., Latz, E., and Manfredi, A. (2013). Mechanisms of sterile.

Ruzzene, M., Penzo, D., and Pinna, L.A. (2002). Protein kinase CK2 inhibitor 4,5,6,7-tetrabromobenzotriazole (TBB) induces apoptosis and caspase-dependent degradation of haematopoietic lineage cell-specific protein 1 (HS1) in Jurkat cells. The Biochemical journal *364*, 41-47.

Sadik, C.D., Kim, N.D., and Luster, A.D. (2011). Neutrophils cascading their way to inflammation. Trends in immunology *32*, 452-460.

Saitoh, T., Fujita, N., Jang, M.H., Uematsu, S., Yang, B.G., Satoh, T., Omori, H., Noda, T., Yamamoto, N., Komatsu, M.*, et al.* (2008). Loss of the autophagy protein Atg16L1 enhances endotoxin-induced IL-1beta production. Nature *456*, 264-268.

Santos, S.S., Carmo, A.M., Brunialti, M.K.C., Machado, F.R., Azevedo, L.C., Assunção, M., Trevelin, S.C., Cunha, F.Q., and Salomao, R. (2016). Modulation of monocytes in septic patients: preserved phagocytic activity, increased ROS and NO generation, and decreased production of inflammatory cytokines. Intensive Care Medicine Experimental *4*.

Sato, K., Yang, X.L., Yudate, T., Chung, J.S., Wu, J., Luby-Phelps, K., Kimberly, R.P., Underhill, D., Cruz, P.D., Jr., and Ariizumi, K. (2006). Dectin-2 is a pattern recognition receptor for fungi that couples with the Fc receptor gamma chain to induce innate immune responses. The Journal of biological chemistry *281*, 38854-38866.

Sato, S., Sanjo, H., Takeda, K., Ninomiya-Tsuji, J., Yamamoto, M., Kawai, T., Matsumoto, K., Takeuchi, O., and Akira, S. (2005). Essential function for the kinase TAK1 in innate and adaptive immune responses. Nat Immunol *6*, 1087-1095.

Scarpulla, R.C. (2008). Transcriptional paradigms in mammalian mitochondrial biogenesis and function. Physiological reviews *88*, 611-638.

Schauvliege, R., Vanrobaeys, J., Schotte, P., and Beyaert, R. (2002). Caspase-11 gene expression in response to lipopolysaccharide and interferon-γ requires nuclear factor-κB and signal transducer and activator of transcription (STAT) 1. Journal of Biological Chemistry *277*, 41624-41630.

Scheffler, I.E. (2011). Mitochondria (John Wiley & Sons).

Scherz-Shouval, R., and Elazar, Z. (2011). Regulation of autophagy by ROS: physiology and pathology. Trends in biochemical sciences *36*, 30-38.

Schletter, J., Heine, H., Ulmer, A.J., and Rietschel, E.T. (1995). Molecular mechanisms of endotoxin activity. Archives of microbiology *164*, 383-389.

Schneider, J.L., and Cuervo, A.M. (2014). Liver autophagy: much more than just taking out the trash. Nature reviews Gastroenterology & hepatology *11*, 187-200.

Schroder, K., Hertzog, P.J., Ravasi, T., and Hume, D.A. (2004). Interferon-gamma: an overview of signals, mechanisms and functions. Journal of leukocyte biology *75*, 163-189.

Schroder, K., and Tschopp, J. (2010). The inflammasomes. Cell *140*, 821-832.

Schumann, R.R., Leong, S.R., Flaggs, G.W., Gray, P.W., Wright, S.D., Mathison, J.C., Tobias, P.S., and Ulevitch, R.J. (1990). Structure and function of lipopolysaccharide binding protein. Science *249*, 1429-1431.

Schweers, R.L., Zhang, J., Randall, M.S., Loyd, M.R., Li, W., Dorsey, F.C., Kundu, M., Opferman, J.T., Cleveland, J.L., Miller, J.L.*, et al.* (2007). NIX is required for programmed mitochondrial clearance during reticulocyte maturation. Proceedings of the National Academy of Sciences of the United States of America *104*, 19500-19505.

Seglen, P.O., and Gordon, P.B. (1982). 3-Methyladenine: specific inhibitor of autophagic/lysosomal protein degradation in isolated rat hepatocytes. Proceedings of the National Academy of Sciences of the United States of America *79*, 1889-1892.

Sekimoto, T., Imamoto, N., Nakajima, K., Hirano, T., and Yoneda, Y. (1997). Extracellular signal-dependent nuclear import of Stat1 is mediated by nuclear pore-targeting complex formation with NPI-1, but not Rch1. The EMBO journal *16*, 7067-7077.

Sharon, N., and Lis, H. (1972). Lectins: Cell-Agglutinating and Sugar-Specific Proteins. Science *177*, 949-959.

Shi, J., Zhao, Y., Wang, K., Shi, X., Wang, Y., Huang, H., Zhuang, Y., Cai, T., Wang, F., and Shao, F. (2015). Cleavage of GSDMD by inflammatory caspases determines pyroptotic cell death. Nature *526*, 660-665.

Shi, J., Zhao, Y., Wang, Y., Gao, W., Ding, J., Li, P., Hu, L., and Shao, F. (2014a). Inflammatory caspases are innate immune receptors for intracellular LPS. Nature *514*, 187-192.

Shi, J., Zhao, Y., Wang, Y., Gao, W., Ding, J., Li, P., Hu, L., and Shao, F. (2014b). Inflammatory caspases are innate immune receptors for intracellular LPS. Nature *514*, 187-192.

Shiba-Fukushima, K., Arano, T., Matsumoto, G., Inoshita, T., Yoshida, S., Ishihama, Y., Ryu, K.Y., Nukina, N., Hattori, N., and Imai, Y. (2014). Phosphorylation of mitochondrial polyubiquitin by PINK1 promotes Parkin mitochondrial tethering. PLoS genetics *10*, e1004861.

Shiba-Fukushima, K., Imai, Y., Yoshida, S., Ishihama, Y., Kanao, T., Sato, S., and Hattori, N. (2012). PINK1-mediated phosphorylation of the Parkin ubiquitin-like domain primes mitochondrial translocation of Parkin and regulates mitophagy. Sci Rep *2*, 1002.

Shimada, K., Crother, T.R., Karlin, J., Dagvadorj, J., Chiba, N., Chen, S., Ramanujan, V.K., Wolf, A.J., Vergnes, L., Ojcius, D.M.*, et al.* (2012). Oxidized mitochondrial DNA activates the NLRP3 inflammasome during apoptosis. Immunity *36*, 401-414.

Shimazu, R., Akashi, S., Ogata, H., Nagai, Y., Fukudome, K., Miyake, K., and Kimoto, M. (1999). MD-2, a molecule that confers lipopolysaccharide responsiveness on Toll-like receptor 4. J Exp Med *189*, 1777-1782.

Shimobayashi, M., and Hall, M.N. (2014). Making new contacts: the mTOR network in metabolism and signalling crosstalk. Nature reviews Molecular cell biology *15*, 155-162.

Shoshan-Barmatz, V., Israelson, A., Brdiczka, D., and Sheu, S.S. (2006). The voltage-dependent anion channel (VDAC): function in intracellular signalling, cell life and cell death. Current pharmaceutical design *12*, 2249-2270.

Shuai, K., Horvath, C.M., Huang, L.H., Qureshi, S.A., Cowburn, D., and Darnell, J.E., Jr. (1994). Interferon activation of the transcription factor Stat91 involves dimerization through SH2-phosphotyrosyl peptide interactions. Cell *76*, 821-828.

Sisler, J.D., Morgan, M., Raje, V., Grande, R.C., Derecka, M., Meier, J., Cantwell, M., Szczepanek, K., Korzun, W.J., Lesnefsky, E.J.*, et al.* (2015). The Signal Transducer and Activator of Transcription 1 (STAT1) Inhibits Mitochondrial Biogenesis in Liver and Fatty Acid Oxidation in Adipocytes. PloS one *10*, e0144444.

Sjövall, F., Morota, S., Hansson, M.J., Friberg, H., Gnaiger, E., and Elmér, E. (2010). Temporal increase of platelet mitochondrial respiration is negatively associated with clinical outcome in patients with sepsis. Critical Care *14*, 1.

Sjövall, F., Morota, S., Persson, J., Hansson, M.J., and Elmér, E. (2013). Patients with sepsis exhibit increased mitochondrial respiratory capacity in peripheral blood immune cells. Critical Care *17*, 1.

Smirnova, E., Griparic, L., Shurland, D.L., and van der Bliek, A.M. (2001). Dynamin-related protein Drp1 is required for mitochondrial division in mammalian cells. Mol Biol Cell *12*, 2245-2256.

Sparwasser, T., Miethke, T., Lipford, G., Erdmann, A., Häcker, H., Heeg, K., and Wagner, H. (1997). Macrophages sense pathogens via DNA motifs: induction of tumor necrosis factor-α-mediated shock. European journal of immunology *27*, 1671-1679.

Speakman, J.R. (2003). Oxidative phosphorylation, mitochondrial proton cycling, free-radical production and aging. Advances in Cell Aging and Gerontology *14*, 35-68.

Spelbrink, J.N. (2010). Functional organization of mammalian mitochondrial DNA in nucleoids: history, recent developments, and future challenges. IUBMB life *62*, 19-32.

Stark, G.R., Kerr, I.M., Williams, B.R., Silverman, R.H., and Schreiber, R.D. (1998). How cells respond to interferons. Annu Rev Biochem *67*, 227-264.

Stein, M., Keshav, S., Harris, N., and Gordon, S. (1992). Interleukin 4 potently enhances murine macrophage mannose receptor activity: a marker of alternative immunologic macrophage activation. J Exp Med *176*, 287-292.

Stojanovski, D., Koutsopoulos, O.S., Okamoto, K., and Ryan, M.T. (2004). Levels of human Fis1 at the mitochondrial outer membrane regulate mitochondrial morphology. Journal of cell science *117*, 1201-1210.

Stotland, A., and Gottlieb, R.A. (2015). Mitochondrial quality control: Easy come, easy go. Biochimica et biophysica acta *1853*, 2802-2811.

Stowe, I., Lee, B., and Kayagaki, N. (2015). Caspase-11: arming the guards against bacterial infection. Immunol Rev *265*, 75-84.

Sunderkotter, C., Nikolic, T., Dillon, M.J., Van Rooijen, N., Stehling, M., Drevets, D.A., and Leenen, P.J. (2004). Subpopulations of mouse blood monocytes differ in maturation stage and inflammatory response. Journal of immunology (Baltimore, Md : 1950) *172*, 4410-4417.

Suzuki, N., Suzuki, S., Duncan, G.S., Millar, D.G., Wada, T., Mirtsos, C., Takada, H., Wakeham, A., Itie, A., Li, S.*, et al.* (2002). Severe impairment of interleukin-1 and Toll-like receptor signalling in mice lacking IRAK-4. Nature *416*, 750-756.

Swan, K., and Jacobson, E. (1967). Hemodynamics of endotoxin shock in the conscious animal. Surgery, gynecology & obstetrics *125*, 1041.

Swantek, J.L., Tsen, M.F., Cobb, M.H., and Thomas, J.A. (2000). IL-1 receptor-associated kinase modulates host responsiveness to endotoxin. Journal of immunology (Baltimore, Md : 1950) *164*, 4301-4306.

Tacke, F., and Randolph, G.J. (2006). Migratory fate and differentiation of blood monocyte subsets. Immunobiology *211*, 609-618.

Tanaka, A., Cleland, M.M., Xu, S., Narendra, D.P., Suen, D.F., Karbowski, M., and Youle, R.J. (2010). Proteasome and p97 mediate mitophagy and degradation of mitofusins induced by Parkin. The Journal of cell biology *191*, 1367-1380.

Tang, B., Xiong, H., Sun, P., Zhang, Y., Wang, D., Hu, Z., Zhu, Z., Ma, H., Pan, Q., Xia, J.H.*, et al.* (2006). Association of PINK1 and DJ-1 confers digenic inheritance of early-onset Parkinson's disease. Human molecular genetics *15*, 1816-1825.

Tannahill, G.M., Curtis, A.M., Adamik, J., Palsson-McDermott, E.M., McGettrick, A.F., Goel, G., Frezza, C., Bernard, N.J., Kelly, B., Foley, N.H.*, et al.* (2013). Succinate is an inflammatory signal that induces IL-1beta through HIF-1alpha. Nature *496*, 238-242.

Taylor, C.T., Doherty, G., Fallon, P.G., and Cummins, E.P. (2016). Hypoxia-dependent regulation of inflammatory pathways in immune cells. Journal of Clinical Investigation *126*, 3716.

Thomas, K.J., McCoy, M.K., Blackinton, J., Beilina, A., van der Brug, M., Sandebring, A., Miller, D., Maric, D., Cedazo-Minguez, A., and Cookson, M.R. (2011). DJ-1 acts in parallel to the PINK1/parkin pathway to control mitochondrial function and autophagy. Human molecular genetics *20*, 40-50.

Thornberry, N.A. (1999). Caspases: a decade of death research. Cell death and differentiation *6*, 1023-1027.

Thornberry, N.A., Bull, H.G., Calaycay, J.R., Chapman, K.T., Howard, A.D., Kostura, M.J., Miller, D.K., Molineaux, S.M., Weidner, J.R., Aunins, J.*, et al.* (1992). A novel heterodimeric cysteine protease is required for interleukin-1 beta processing in monocytes. Nature *356*, 768-774.

Thurston, T.L., Ryzhakov, G., Bloor, S., von Muhlinen, N., and Randow, F. (2009). The TBK1 adaptor and autophagy receptor NDP52 restricts the proliferation of ubiquitin-coated bacteria. Nat Immunol *10*, 1215-1221.

Ting, J.P.-Y., Lovering, R.C., Alnemri, E.S.P.D., Bertin, J., Boss, J.M., Davis, B., Flavell, R.A., Girardin, S.E., Godzik, A., and Harton, J.A. (2008). The NLR gene family: an official nomenclature. Immunity *28*, 285.

Tobias, P.S., Soldau, K., Gegner, J.A., Mintz, D., and Ulevitch, R.J. (1995). Lipopolysaccharide binding protein-mediated complexation of lipopolysaccharide with soluble CD14. The Journal of biological chemistry *270*, 10482-10488.

Traeger, T., Koerner, P., Kessler, W., Cziupka, K., Diedrich, S., Busemann, A., Heidecke, C.D., and Maier, S. (2010). Colon Ascendens Stent Peritonitis (CASP) - a Standardized Model for Polymicrobial Abdominal Sepsis. Journal of Visualized Experiments : JoVE.

Tran, T.A., Nguyen, A.D., Chang, J., Goldberg, M.S., Lee, J.-K., and Tansey, M.G. (2011). Lipopolysaccharide and tumor necrosis factor regulate Parkin expression via nuclear factor-kappa B. PloS one *6*, e23660.

Trempe, J.F., and Fon, E.A. (2013). Structure and Function of Parkin, PINK1, and DJ-1, the Three Musketeers of Neuroprotection. Frontiers in neurology *4*, 38.

Tschopp, J., and Schroder, K. (2010). NLRP3 inflammasome activation: the convergence of multiple signalling pathways on ROS production? Nat Rev Immunol *10*, 210-215.

Tsukada, M., and Ohsumi, Y. (1993). Isolation and characterization of autophagy-defective mutants of Saccharomyces cerevisiae. FEBS letters *333*, 169-174.

Tufekci, K.U., Meuwissen, R., Genc, S., and Genc, K. (2012). Inflammation in Parkinson's disease. Advances in protein chemistry and structural biology *88*, 69-132.

Turrens, J.F. (2003). Mitochondrial formation of reactive oxygen species. The Journal of Physiology *552*, 335-344.

Twig, G., Elorza, A., Molina, A.J., Mohamed, H., Wikstrom, J.D., Walzer, G., Stiles, L., Haigh, S.E., Katz, S., Las, G.*, et al.* (2008). Fission and selective fusion govern mitochondrial segregation and elimination by autophagy. The EMBO journal *27*, 433-446.

Twig, G., and Shirihai, O.S. (2011). The interplay between mitochondrial dynamics and mitophagy. Antioxidants & redox signaling *14*, 1939-1951.

Uddin, S., Sassano, A., Deb, D.K., Verma, A., Majchrzak, B., Rahman, A., Malik, A.B., Fish, E.N., and Platanias, L.C. (2002). Protein kinase C-delta (PKC-delta) is activated by type I interferons and mediates phosphorylation of Stat1 on serine 727. The Journal of biological chemistry *277*, 14408-14416.

Ulevitch, R., and Tobias, P. (1995). Receptor-dependent mechanisms of cell stimulation by bacterial endotoxin. Annual review of immunology *13*, 437-457.

Valente, E.M., Abou-Sleiman, P.M., Caputo, V., Muqit, M.M., Harvey, K., Gispert, S., Ali, Z., Del Turco, D., Bentivoglio, A.R., Healy, D.G.*, et al.* (2004). Hereditary early-onset Parkinson's disease caused by mutations in PINK1. Science *304*, 1158-1160.

Van Amersfoort, E.S., Van Berkel, T.J.C., and Kuiper, J. (2003). Receptors, Mediators, and Mechanisms Involved in Bacterial Sepsis and Septic Shock. Clinical Microbiology Reviews *16*, 379-414.

Van den Bossche, J., O'Neill, L.A., and Menon, D. (2017). Macrophage immunometabolism: where are we (going)? Trends in immunology.

van Furth, R., and Cohn, Z.A. (1968). The origin and kinetics of mononuclear phagocytes. The Journal of experimental medicine *128*, 415-435.

Vanaja, S.K., Russo, A.J., Behl, B., Banerjee, I., Yankova, M., Deshmukh, S.D., and Rathinam, V.A. (2016). Bacterial Outer Membrane Vesicles Mediate Cytosolic Localization of LPS and Caspase-11 Activation. Cell *165*, 1106-1119.

Vanhorebeek, I., Gunst, J., Derde, S., Derese, I., Boussemaere, M., D'Hoore, A., Wouters, P.J., and Van den Berghe, G. (2012). Mitochondrial fusion, fission, and biogenesis in prolonged critically ill patients. The Journal of clinical endocrinology and metabolism *97*, E59-64.

Vats, D., Mukundan, L., Odegaard, J.I., Zhang, L., Smith, K.L., Morel, C.R., Wagner, R.A., Greaves, D.R., Murray, P.J., and Chawla, A. (2006). Oxidative metabolism and PGC-1beta attenuate macrophage-mediated inflammation. Cell metabolism *4*, 13-24.

Venkataraman, T., Valdes, M., Elsby, R., Kakuta, S., Caceres, G., Saijo, S., Iwakura, Y., and Barber, G.N. (2007). Loss of DExD/H box RNA helicase LGP2 manifests disparate antiviral responses. Journal of immunology (Baltimore, Md : 1950) *178*, 6444-6455.

Vogelpoel, L.T., Baeten, D.L., de Jong, E.C., and den Dunnen, J. (2015). Control of cytokine production by human fc gamma receptors: implications for pathogen defense and autoimmunity. Frontiers in immunology *6*, 79.

Wang, X., Winter, D., Ashrafi, G., Schlehe, J., Wong, Y.L., Selkoe, D., Rice, S., Steen, J., LaVoie, M.J., and Schwarz, T.L. (2011). PINK1 and Parkin target Miro for phosphorylation and degradation to arrest mitochondrial motility. Cell *147*, 893-906.

Ward, N.S., Casserly, B., and Ayala, A. (2008). The Compensatory Anti-inflammatory Response syndrome (CARS) in Critically ill patients. Clinics in chest medicine *29*, 617-viii.

Weinberg, S.E., Sena, L.A., and Chandel, N.S. (2015). Mitochondria in the regulation of innate and adaptive immunity. Immunity *42*, 406-417.

Weischenfeldt, J., and Porse, B. (2008). Bone Marrow-Derived Macrophages (BMM): Isolation and Applications. CSH protocols *2008*, pdb.prot5080.

Wen, Z., Zhong, Z., and Darnell, J.E., Jr. (1995). Maximal activation of transcription by Stat1 and Stat3 requires both tyrosine and serine phosphorylation. Cell *82*, 241-250.

West, A.P., Brodsky, I.E., Rahner, C., Woo, D.K., Erdjument-Bromage, H., Tempst, P., Walsh, M.C., Choi, Y., Shadel, G.S., and Ghosh, S. (2011a). TLR signalling augments macrophage bactericidal activity through mitochondrial ROS. Nature *472*, 476-480.

West, A.P., Shadel, G.S., and Ghosh, S. (2011b). Mitochondria in innate immune responses. Nat Rev Immunol *11*, 389-402.

Wichterman, K.A., Baue, A.E., and Chaudry, I.H. (1980). Sepsis and septic shock—a review of laboratory models and a proposal. Journal of Surgical Research *29*, 189-201.

Willerson, J.T., Trelstad, R.L., Pincus, T., Levy, S.B., and Wolff, S.M. (1970). Subcellular localization of Salmonella enteritidis endotoxin in liver and spleen of mice and rats. Infection and immunity *1*, 440-445.

Wright, D.C., Geiger, P.C., Han, D.H., Jones, T.E., and Holloszy, J.O. (2007). Calcium induces increases in peroxisome proliferator-activated receptor gamma coactivator-1alpha and mitochondrial biogenesis by a pathway leading to p38 mitogen-activated protein kinase activation. The Journal of biological chemistry *282*, 18793-18799.

Wu, H., Kanatous, S.B., Thurmond, F.A., Gallardo, T., Isotani, E., Bassel-Duby, R., and Williams, R.S. (2002). Regulation of mitochondrial biogenesis in skeletal muscle by CaMK. Science *296*, 349-352.

Wyler, F., Neutze, J., and Rudolph, A. (1970). Effects of endotoxin on distribution of cardiac output in unanesthetized rabbits. American Journal of Physiology -- Legacy Content *219*, 246-251.

Xiong, H., Wang, D., Chen, L., Choo, Y.S., Ma, H., Tang, C., Xia, K., Jiang, W., Ronai, Z., Zhuang, X., *et al.* (2009). Parkin, PINK1, and DJ-1 form a ubiquitin E3 ligase complex promoting unfolded protein degradation. J Clin Invest *119*, 650-660.

Xu, Y., Jagannath, C., Liu, X.-D., Sharafkhaneh, A., Kolodziejska, K.E., and Eissa, N.T. (2007). Toll-like receptor 4 is a sensor for autophagy associated with innate immunity. Immunity *27*, 135-144.

Yamano, K., and Youle, R.J. (2013). PINK1 is degraded through the N-end rule pathway. Autophagy *9*, 1758-1769.

Yan, M.H., Wang, X., and Zhu, X. (2013). Mitochondrial defects and oxidative stress in Alzheimer disease and Parkinson disease. Free radical biology & medicine *62*, 90-101.

Yang, J., Zhang, L., Yu, C., Yang, X.-F., and Wang, H. (2014). Monocyte and macrophage differentiation: circulation inflammatory monocyte as biomarker for inflammatory diseases. Biomarker research *2*, 1.

Yoneyama, M., Kikuchi, M., Natsukawa, T., Shinobu, N., Imaizumi, T., Miyagishi, M., Taira, K., Akira, S., and Fujita, T. (2004). The RNA helicase RIG-I has an essential function in double-stranded RNA-induced innate antiviral responses. Nat Immunol *5*, 730-737.

Yoon, Y., Krueger, E.W., Oswald, B.J., and McNiven, M.A. (2003). The mitochondrial protein hFis1 regulates mitochondrial fission in mammalian cells through an interaction with the dynamin-like protein DLP1. Molecular and cellular biology *23*, 5409-5420.

Yu, J., Nagasu, H., Murakami, T., Hoang, H., Broderick, L., Hoffman, H.M., and Horng, T. (2014). Inflammasome activation leads to Caspase-1–dependent mitochondrial damage and block of mitophagy. Proceedings of the National Academy of Sciences *111*, 15514-15519.

Zantl, N., Uebe, A., Neumann, B., Wagner, H., Siewert, J.-R., Holzmann, B., Heidecke, C.-D., and Pfeffer, K. (1998). Essential role of gamma interferon in survival of colon ascendens stent peritonitis, a novel murine model of abdominal sepsis. Infection and immunity *66*, 2300-2309.

Zelensky, A.N., and Gready, J.E. (2005). The C-type lectin-like domain superfamily. The FEBS journal *272*, 6179-6217.

Zhang, H., Spapen, H., Nguyen, D.N., Benlabed, M., Buurman, W.A., and Vincent, J.L. (1994). Protective effects of N-acetyl-L-cysteine in endotoxemia. The American journal of physiology *266*, H1746-1754.

Zhang, Q., Itagaki, K., and Hauser, C.J. (2010a). Mitochondrial DNA is released by shock and activates neutrophils via p38 map kinase. Shock *34*, 55-59.

Zhang, Q., Raoof, M., Chen, Y., Sumi, Y., Sursal, T., Junger, W., Brohi, K., Itagaki, K., and Hauser, C.J. (2010b). Circulating mitochondrial DAMPs cause inflammatory responses to injury. Nature *464*, 104-107.

Zhong, Z., Umemura, A., Sanchez-Lopez, E., Liang, S., Shalapour, S., Wong, J., He, F., Boassa, D., Perkins, G., Ali, S.R.*, et al.* (2016). NF-kappaB Restricts Inflammasome Activation via Elimination of Damaged Mitochondria. Cell *164*, 896-910.

Zhou, R., YAZDI, A.S., MENU, P., and TSCHOPP, J. (2011). A role for mitochondria in NLRP3 inflammasome activation. Nature *469*, 221-225.